FZK-161-2
5 JANUARY 1963

INVESTIGATION OF COMBINED EFFECTS OF RADIATION AND VACUUM AND OF RADIATION AND CRYO-TEMPERATURES ON ENGINEERING MATERIALS

Annual Report
9 November 1961 through 8 November 1962

Volume II: Radiation-Cryotemperature Tests

N63 21332

E. T. SMITH

Prepared for
George C. Marshall Space Flight Center
Huntsville, Alabama

Contract No. NAS8-2450
Request No. TP85-468

NUCLEAR AEROSPACE RESEARCH FACILITY

GENERAL DYNAMICS | FORT WORTH

FZK-161-2
5 JANUARY 1963

INVESTIGATION OF COMBINED EFFECTS OF RADIATION AND VACUUM AND OF RADIATION AND CRYO-TEMPERATURES ON ENGINEERING MATERIALS

Annual Report
9 November 1961 through 8 November 1962

Volume II: Radiation-Cryotemperature Tests

N63 21332

E. T. SMITH

Prepared for
George C. Marshall Space Flight Center
Huntsville, Alabama

XEROX $
MICROFILM $

Contract No. NAS8-2450
Request No. TP85-468

NUCLEAR AEROSPACE RESEARCH FACILITY

operated by

GENERAL DYNAMICS | FORT WORTH

FZK-161-2
5 JANUARY 1963

GD

CA

NUCLEAR AEROSPACE RESEARCH FACILITY

INVESTIGATION OF COMBINED EFFECTS OF RADIATION AND VACUUM AND OF RADIATION AND CRYO-TEMPERATURES ON ENGINEERING MATERIALS

Annual Report
9 November 1961 ~~through~~ 8 November 1962

Volume II: Radiation-Cryotemperature Tests

E. T. SMITH Jan 5, 1963 261 p

Prepared for
George C. Marshall Space Flight Center
Huntsville, Alabama

NASA Contract ~~No.~~ NAS8-2450
Request No. TP85-468

(NASA CR-; FZK-)

$8.03

GENERAL DYNAMICS | FORT WORTH, Tex.

This report was prepared by General Dynamics/Fort Worth under Contract No. NAS8-2450, Investigation of Combined Effects of Radiation and Vacuum and of Radiation and Cryotemperatures on Engineering Materials, for the George C. Marshall Space Flight Center of the National Aeronautics and Space Administration. The work was administered under the technical direction of the Propulsion and Vehicle Engineering Division, Engineering Materials Branch of the George C. Marshall Space Flight Center with Eugene C. McKannan acting as project manager.

ABSTRACT

21332

A series of tests was performed to measure the combined effects of nuclear radiation and cryotemperatures on a group of nonmetallic spacecraft materials. This group consisted of materials classified as adhesives, seals, thermal insulations, electrical insulations, structural laminates, and thermal-control coatings. Typical tests performed on specimens prepared from the materials included lap-shear strength, ultimate tensile strength, ultimate elongation, stress-strain characteristics, and compressive strength. Special test equipment to submerge the specimens in liquid nitrogen or liquid hydrogen during irradiation and to subsequently perform the above tests was designed and built at General Dynamics/Fort Worth.

Measured properties of the materials as a function of integrated neutron flux and gamma dose are reported and recommendations for use of the various materials in nuclear-powered spacecraft are made.

REPORT SUMMARY

Previous work in the field of radiation effects has shown that drastic changes are induced in various engineering properties of nonmetallic materials by incident nuclear radiation. The successful development of a nuclear-powered spacecraft will therefore depend, to a large extent, upon the determination of a series of radiation-resistance dose levels for component materials in the vehicle. These levels will have to be established for both fast-neutron and gamma radiation and will vary with different kinds of materials, location of the material with respect to the radiation source, and also with different associated environments, such as high vacuum and cryotemperature, or the combination of these two.

The purpose of this particular experimental program (conducted under Modification I to NASA Contract NAS8-2450) was to measure the effects of the combined environment of nuclear radiation and cryotemperature on the engineering properties of a selection of nonmetallic materials. The materials selected for testing were representative of those most likely to be used in spacecraft of this type and consisted of two materials from each of the categories of adhesives, seals, thermal insulations, electrical insulations, structural laminates, and thermal-control coatings. Representative tests included those sufficient to measure ultimate tensile strength, ultimate elongation, breaking factor, tensile-shear strength, compressive strength, stress-strain in tension, stress-

strain in compression, and spectral reflectivity. The radiation source for the experiment was the Ground Test Reactor (GTR) located at the Nuclear Aerospace Research Facility (NARF), General Dynamics Corporation, Fort Worth, Texas.

The procedure for the cryotemperature tests was to position the test specimens in the cryogen chamber of the experimental assemblies and locate the assemblies next to the reactor face. The irradiation run was carried out with the specimens submerged in cryogen fluid. Operation of the reactor was terminated after the required radiation dose was achieved, and the specimens were then pulled in tension and compression without intervening warmup. Nine data points were recorded during each test on each material. These included those obtainable from all combinations of three radiation doses (zero, low, and high) and three temperatures (ambient, -320°F, and -423°F). Ambient-temperature irradiations were conducted in an air environment with specimen temperatures ranging from 110°F to 143°F, and the subsequent tensile and compression tests were performed with an Instron test machine in the Irradiated Materials Laboratory.

A brief resume of the results of the tests on each material, along with recommendations for its use, is given below:

Adhesives

Hexcel 1252. This material demonstrated increased tensile-shear strength after irradiation at room temperature. At cryotemperatures, the strength before irradiation was considerably higher than the room-temperature value. Radiation then served to reduce this strength somewhat, but the value still remained higher than the room-temperature/no-irradiation level. The material is therefore highly recommended for use in this combination environment, up to the tested dose level of $5x10^{10}$ ergs/gm(C) of gamma-type radiation.

Metlbond 406. This adhesive suffered severe degradation in tensile-shear strength at all temperatures after irradiation to a dose level of about $3x10^{10}$ ergs/gm(C). It is not recommended for use under these environmental conditions.

Seals

Teflon TFE. This material was tested at ambient temperature in air only. After a relatively low dose of radiation under these conditions the test specimens crumbled to powder. Further testing is needed before recommendations can be made.

Kel-F-81. This fluorocarbon plastic was tested under all conditions. Its properties were excellent under no-irradiation conditions, but relatively small doses of gamma and neutron radiation were sufficient to cause significant degradation in tensile strength and severe embrittlement. It is not recommended for use in a radiation environment at any temperature.

Thermal Insulations

Stafoam AA402 and Styrofoam 22. Results of tests were similar for both of these materials. Their compressive strength at cryotemperatures increased with incident radiation up to a gamma dose of about $5x10^9$ ergs/gm(C). Beyond this dose level, the strength dropped off severely. Irradiation at ambient temperature ($\sim$120°F) served to reduce the compressive strength significantly. Both materials are recommended for use under relatively low radiation environments at cryotemperatures.

Electrical Insulations

DuPont H-Film and Mylar-C. These materials were tested in tension in thin-film form. Contrasting values in tensile strength for different radiation doses and different temperatures were noted. Further testing is needed, and specific recommendations are not possible at this time.

Structural Laminates

Conolon 506 and Paraplex P-43. Tensile properties of these two laminates were measured and found to be similar. The ultimate tensile strength of both materials was higher at cryotemperatures than at room temperature, as could be expected, and remained higher after doses to 5×10^{10} ergs/gm(C). Both materials are recommended for use under a radiation-cryotemperature environment to the above-mentioned dose level.

Thermal-Control Coatings

Skyspar A-423-SA9185 and Sherwin-Williams W-49-BC12. After irradiation at room temperature, the subsequently measured optical properties of these two coatings showed variations as a function of radiation dose. However, after irradiation at cryotemperatures, the properties remained fairly constant as a function of radiation dose. No recommendations are attempted with the data available from these tests, but the data shown in the text is suitable for possible correlation with results from other related tests.

A series of tests to measure the combined effects of nuclear radiation and high vacuum was also conducted at NARF under the same NASA contract. The experiment utilized two vacuum chambers designed to operate in conjunction with the reactor. Tests were performed in air after irradiation in air and in vacuum and air after irradiation in vacuum. The experiment is described in Volume I of this report.

FOREWORD

Work under this contract was performed by the Nuclear Aerospace Research Facility (NARF) at General Dynamics/Fort Worth. It was conducted in two separate sections under NASA Contract No. NAS8-2450. The basic section, an experiment to measure the combined effects of nuclear radiation and high vacuum on materials, was initiated November 9, 1961, and carried out under the direction of E. E. Kerlin. The work is described in Volume I of this report. The second section, an experiment to measure the combined effects of nuclear radiation and cryotemperatures on a selected group of nonmetallic materials, was initiated on July 1, 1962, as Modification I to the original contract. The work was performed under the direction of E. T. Smith and is described in this volume, Volume II, of the report.

The author wishes to acknowledge the valuable services of the following people who have helped make this experiment possible: J. W. Gordon for assistance in material selection and preparation; F. F. Fleming and W. E. Ivie for the nuclear-radiation measurements; E. E. Baggett, D. C. Butson, and E. M. Nelson for assistance in equipment design; R. E. Miller for design and operation of the electronic test instrumentation; and W. M. Brandenburg of GD/Astronautics for conducting the optical measurements on thermal-control coatings.

TABLE OF CONTENTS

Preceding page blank

TABLE OF CONTENTS (cont'd)

TABLE OF CONTENTS (cont'd)

LIST OF FIGURES

LIST OF FIGURES (cont'd)

LIST OF FIGURES (cont'd)

LIST OF FIGURES (cont'd)

LIST OF FIGURES (cont'd)

LIST OF FIGURES (cont'd)

LIST OF FIGURES (cont'd)

LIST OF FIGURES (cont'd)

LIST OF TABLES

LIST OF TABLES (cont'd)

LIST OF TABLES (cont'd)

LIST OF TABLES (cont'd)

LIST OF TABLES (cont'd)

I. INTRODUCTION

Considerable effort has been expended in the past several years toward measuring the effects, individually, of nuclear radiation and of cryotemperatures on various classes of materials, particularly those materials which have been used in or have potential application to space vehicles. Very little data have been accumulated, though, which show the combined effects of these two environments. This has been due, in part, at least, to the difficulty in designing and fabricating equipment suitable for performing tests under these extreme conditions.

During this experimental program, which was designed to provide combined-environment data, tests were performed on six different classes of materials: namely, adhesives, seals, thermal insulations, electrical insulations, structural laminates, and thermal-control coatings. Two materials in each class were tested.

The selection of specific materials for testing was based upon considerations involving the past history of their use in spacecraft, potential use in this application, and knowledge of their properties after separate exposure to radiation and cryotemperatures. Measurements included tensile-shear strength, ultimate tensile strength, ultimate elongation, stress-strain, leakage, compression-deflection, and spectral reflectivity. Tests for each material were performed under nine different conditions, consisting of the possible combinations of three different radiation doses (zero, relatively low, and relatively high) and three different temperatures (ambient, -320°F, and -423°F).

In the low-temperature portions of the experiment, irradiation of the material specimens was carried out with the specimens submerged in liquid nitrogen (LN_2) and, again, in liquid hydrogen (LH_2). Subsequent tests (with the exception of the reflectivity measurements on the thermal-control coatings) were then performed on the materials at these cryotemperatures without an intervening warmup. This factor in the experiment should be emphasized. It points to the fact that any annealing out of radiation-induced defects resulting from warm-up to room temperature prior to testing was minimized, thus providing a measurement of the true conditions that exist in materials which have been exposed to and are to be used in this combined environment.

II. TEST FACILITY AND EQUIPMENT

2.1 Radiation Effects Testing System

The Ground Test Reactor (GTR) is a heterogeneous, highly enriched, thermal reactor which utlizes water as neutron moderator and reflector, as radiation shielding, and as coolant. Maximum power generation is three megawatts. A detailed description of the GTR may be found in Reference 1.

The irradiation pool (Fig. 2.1) is divided into two sections - one north, one south. The south section forms the reactor pool and is filled with water, while the north section is the irradiation cell and is kept dry. The reactor closet in the center of the pool divider extends into the irradiation cell to provide three sides for irradiation. The corresponding irradiation positions - east, north, and west - are clearly visible in Figure 2.1. Also shown in the figure is the reactor in the fully retracted position on the horizontal positioning mechanism.

Adjacent to the north wall of the irradiation cell is the handling area. Equipment permanently installed in the handling area includes a gas-monitoring system, a Davis explosion meter, and environmental conditioning equipment for the Radiation Effects Testing System. The auxiliary equipment necessary for cryogenic experiments was also located in this area. Figure 2.2 is a view, looking south, of the Radiation Effects Testing System. It shows the concrete pool shields, the irradiation pool, the shuttle system, and the handling area.

NPC 17,426
31-6311

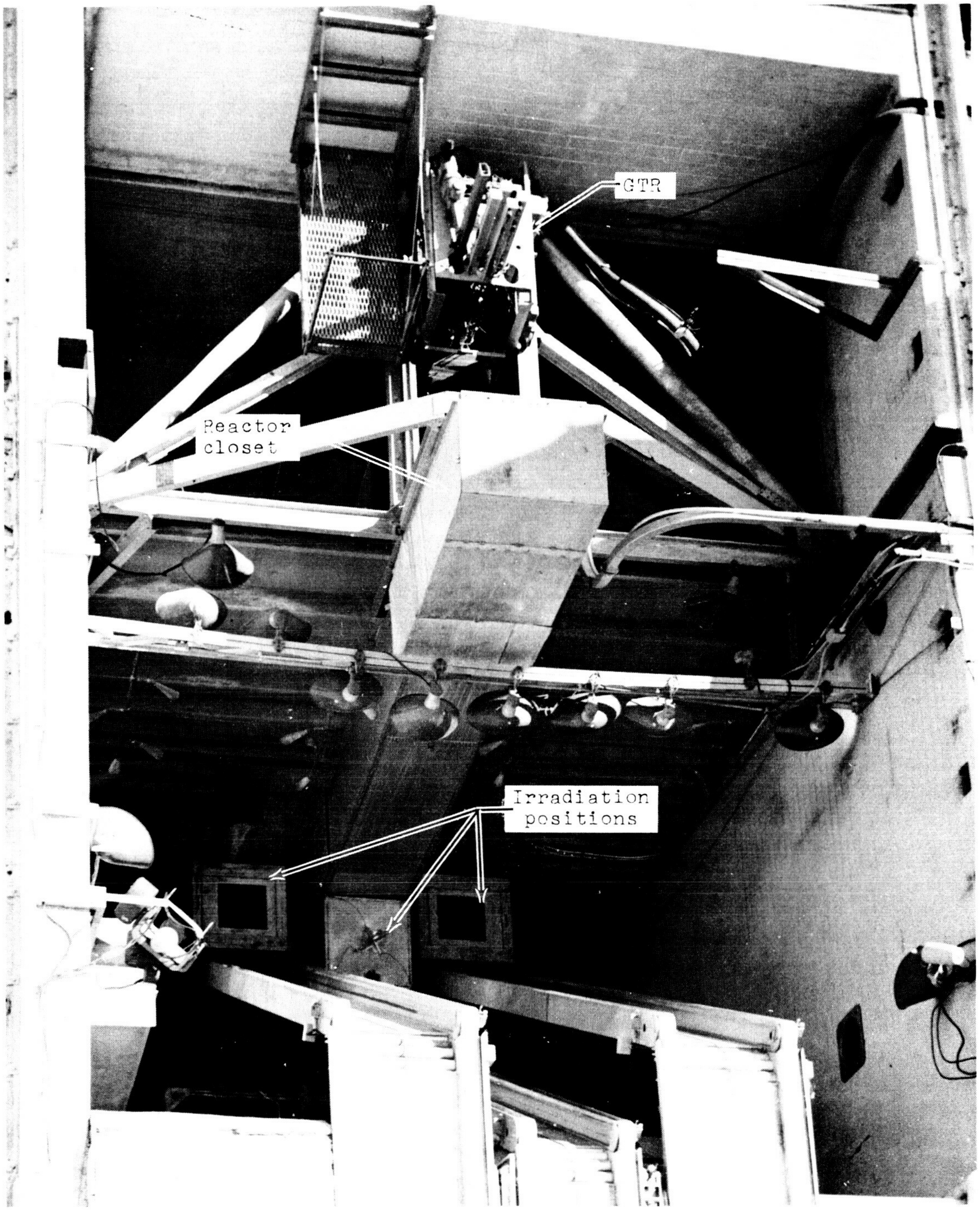

Figure 2.1 Reactor Pool

NPC 17,427
31-6312

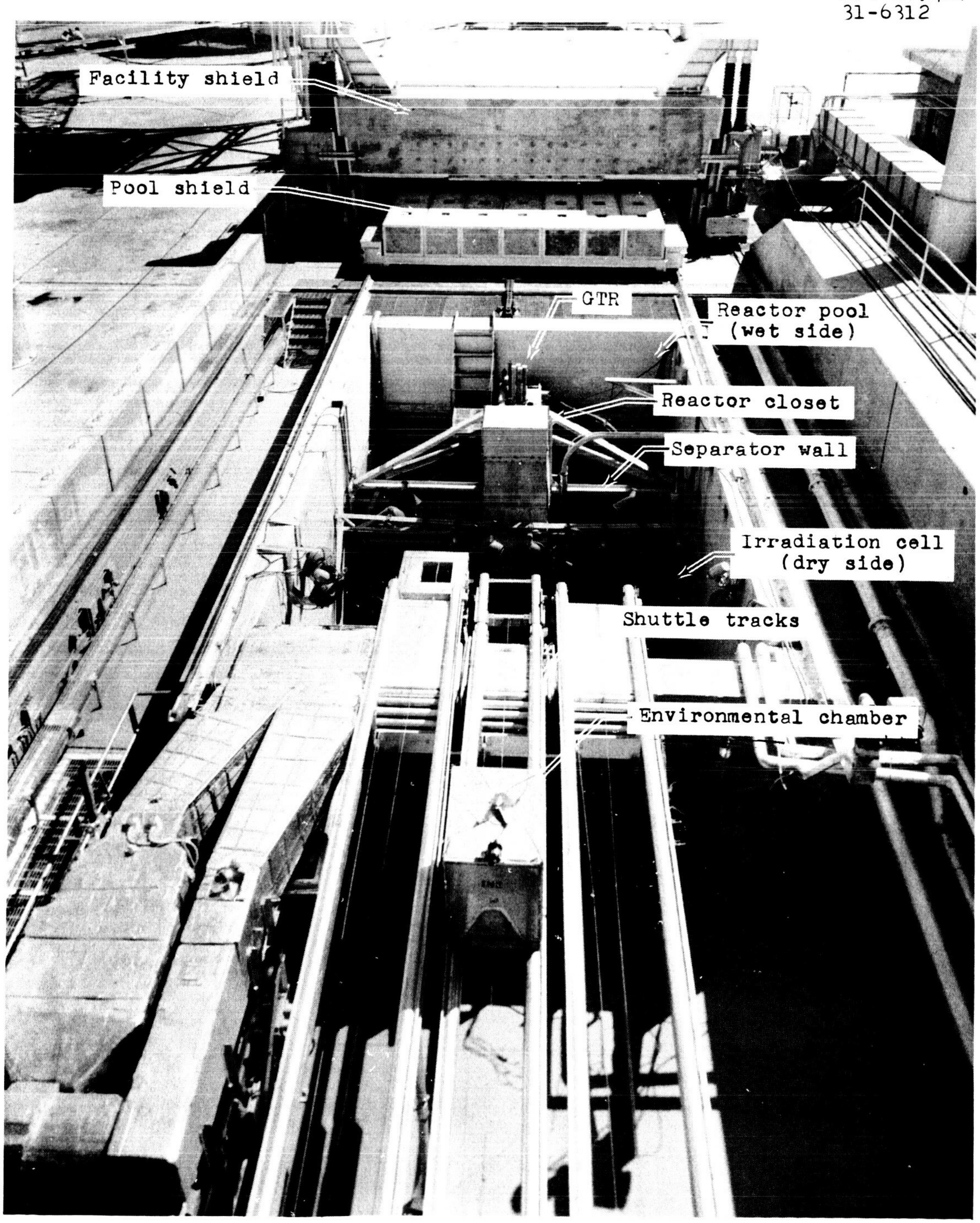

Figure 2.2 Radiation Effects Testing System

The reactor closet is partially covered by $\frac{1}{4}$-in.-thick boral to attenuate thermal neutrons. The boral extends 36 inches east and west along the pool divider from the closet, and 36 inches up and down from the horizontal centerline of the reactor. The centerline is 57 inches above the cell floor.

The reactor, in an aluminum enclosure to facilitate cooling-water flow, is mounted on a horizontal positioning mechanism in the south section. This mechanism enables the reactor to be positioned at any distance from 2 to 90 inches from the north face of the closet.

An integral part of the NARF Radiation Effects Testing Facility is the shuttle system. This system consists of cable-driven dollies mounted on three sets of parallel tracks. The tracks extend from the irradiation positions adjacent to the reactor closet, up an incline to the north wall of the irradiation cell, and to a loading area on the ramp just north of the handling area. The system can be operated from either the control room or the dolly motor-drive shed on the north ramp. Full-coverage televiewing of the entire shuttle system is provided by means of a closed-circuit television system in the control room.

Cryotemperature and ambient-temperature irradiation tests were performed on the east and north irradiation positions. The experimental assemblies and the ambient-temperature irradiation racks were secured on the dollies and lowered into position by means of the shuttle system.

2.2 Cryotemperature Experimental Assemblies

Previous experience of General Dynamics personnel in the use of remotely operated tensile-testing apparatus in conjunction with the Ground Test Reactor contributed significantly to the design of three experimental assemblies constructed for use in this experiment. Prime requirements which were incorporated into the experiment included (1) means for applying tensile and compression forces remotely to material specimens submerged in cryogen fluids and (2) means for measuring the magnitude of these forces and the resulting strain in the specimens. In addition, each assembly was required to handle over 60 specimens in a single loading.

In Figure 2.3 are photographs of the front, side, and back of the complete assembly mounted in a support frame. In actual operation, this frame, with the assembly installed, latches to an escalator system which automatically positions the assembly next to the face of the reactor. Also in Figure 2.3 is an exploded view of the assembly. As shown in this photograph, the assembly consists of two main sections: (1) the upper section, containing ten hydraulic cylinders, the cylinder mounting structure, ten pull rods, specimen-mounting yokes, and ten linear variable differential transformers (LVDT's); and (2) a lower section, or quadruple-walled Dewar, to contain the specimens and the cryogen.

The hydraulic-cylinder mounting framework and specimen-mounting framework are bolted, respectively, to the top and bottom of a flange which, in turn, mates to the top of the Dewar. The [illegible]

[illegible]

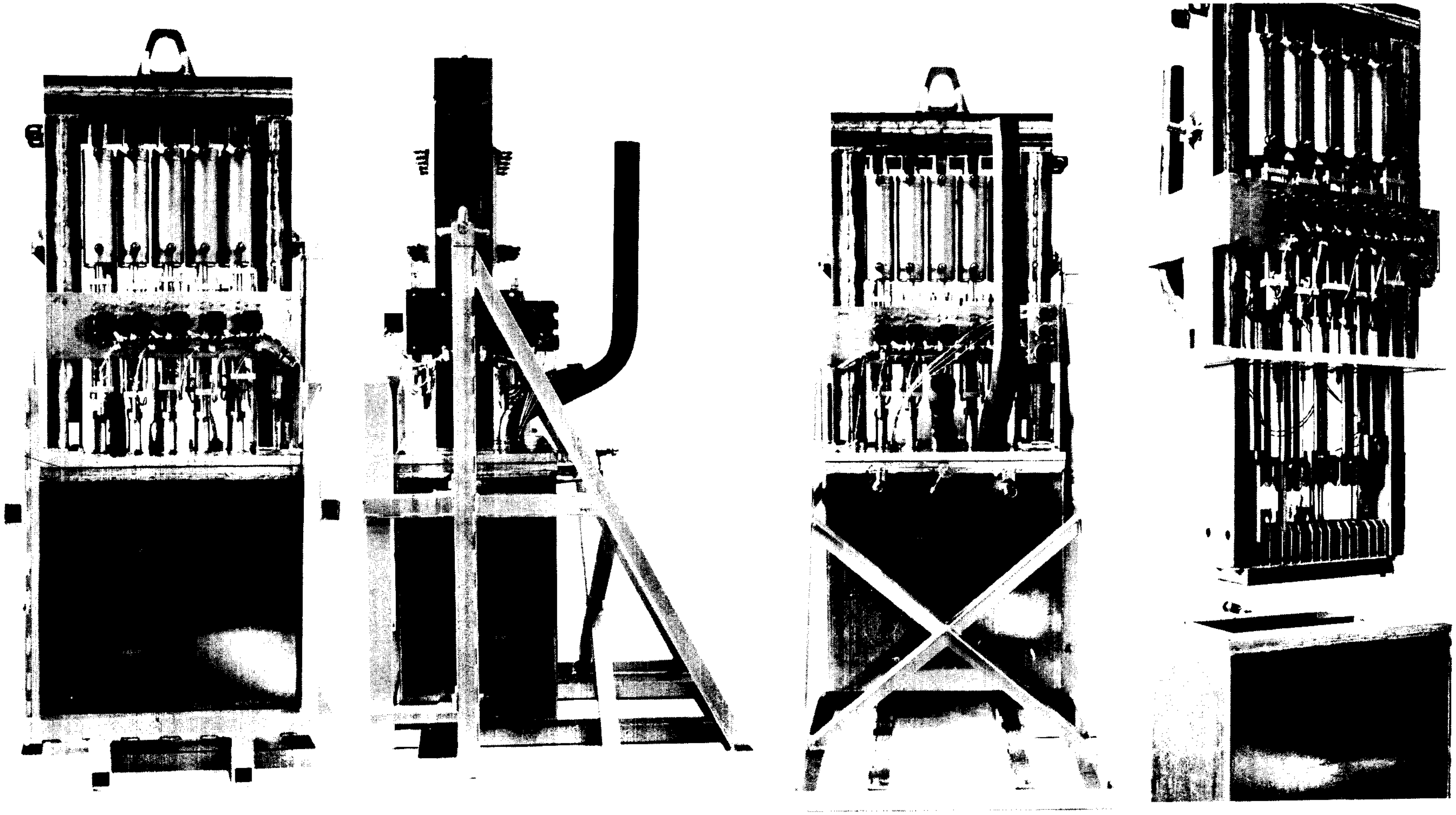

Front View   Side View   Back View   Exploded View

Figure 2.3 Various Views of Experimental Assembly

pull rods operate through tubular risers welded to the top of the flange. These risers contain Teflon shaft seals. Various other drillings and tappings through this top flange contain the cryogen inlet tube, evaporated-cryogen outlet pipe, thermocouple leads, strain-gage leads, pressure transducer, and liquid-level probe. Prior to operation of the system, particularly with LH_2 as the cryogen, all openings to the cryogen chamber are sealed completely to prevent even the minutest of gas leaks.

The Dewar, or cryogen chamber, is a quadruple-walled vessel with an 8 by 24 by 26 in.-deep inner chamber to receive the cryogen, test specimens, and specimen-mounting apparatus. Surrounding this inner chamber on all sides is a $\frac{1}{2}$-in.-thick vacuum chamber which is pumped to a pressure of 5 microns just prior to operation of the assembly. Surrounding the vacuum chamber on all sides is a $\frac{1}{2}$-in.-thick chamber to contain LN_2 when LH_2 is used in the inner chamber. Then, surrounding the LN_2 chamber on all sides is a $1\frac{1}{2}$-in.-thick outer chamber which is filled with Refrasil, an inert SiO_2 thermal-insulation material. Ports for the vacuum and LN_2 insulation chambers are positioned on the back side of the Dewar.

The LVDT's are used to measure movement of the test-specimen pull rods to an accuracy of $\pm$0.001 inch over a linear range of 0.60 inch. The transformer core is fastened rigidly to the pull rod, and the transformer coil is mounted to the upper structure framework through a gear-and-rack unit. A small electric motor is used in conjunction with this unit to reposition the transformer coil over a 4-in. vertical range. This repositioning of the coil is necessary to permit linear measurements of pull-rod movement over a total pull-rod travel of four inches.

One of the three experimental assemblies utilizes five 0- to 1000-lb dynamometers to measure load on the specimens directly, rather than indirectly with an Instron testing machine through the hydraulic servo system. These units are installed in the assembly just below the hydraulic cylinders by breaking and removing a section of the pull rod.

Figures 2.4 and 2.5 are closeups of test-specimen mounting apparatus. The center rod on the front row in Figure 2.4 contains four dumbbell-type specimens of structural-laminate material. Each specimen contains glued-on doublers on both ends. The upper clevis rod passes through a single $\frac{1}{2}$-in.-diam hole in the top of each specimen. The bottom of each specimen contains a $\frac{1}{2}$-in.-wide slot of varying length to permit four specimens to be pulled and broken in tension, sequentially, with one upward movement of the pull rod.

Figure 2.5 shows two thin-film testers on the left and three compression-button testers on the right. Each film tester is arranged to pull four thin films in tension, sequentially, with one upward movement of the pull rod. The ends of the films are wrapped and glued to $\frac{1}{4}$-in.-diam spools which have a milled "flat" on each end. These flats slide in varying-length slots in the lower section of the film tester to permit sequential pulling of each film. In addition, the flats serve to prevent rotation of the spools when the film is in tension.

NPC 17,429
31-6559

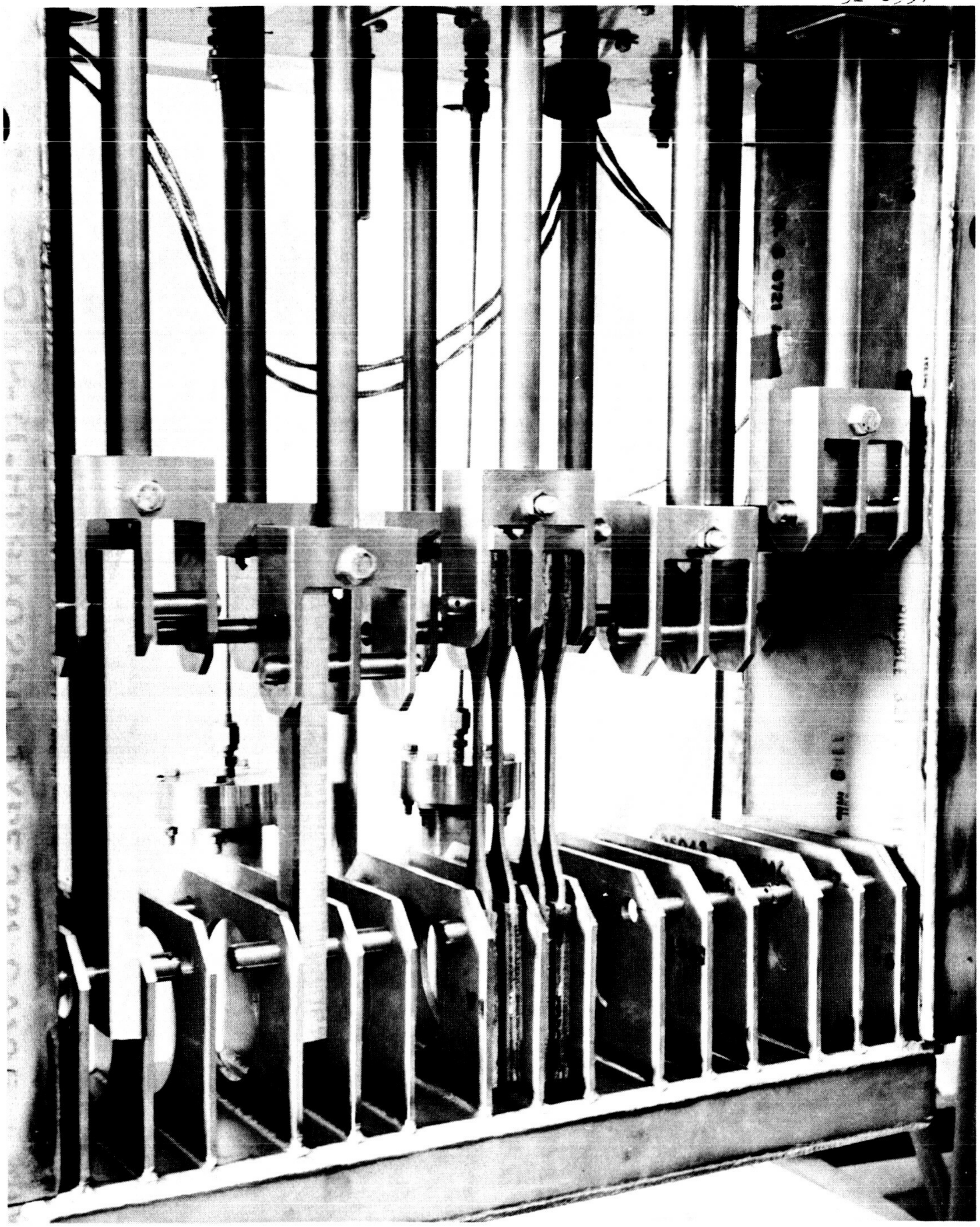

Figure 2.4 Tensile Specimens Mounted in Experimental Assembly

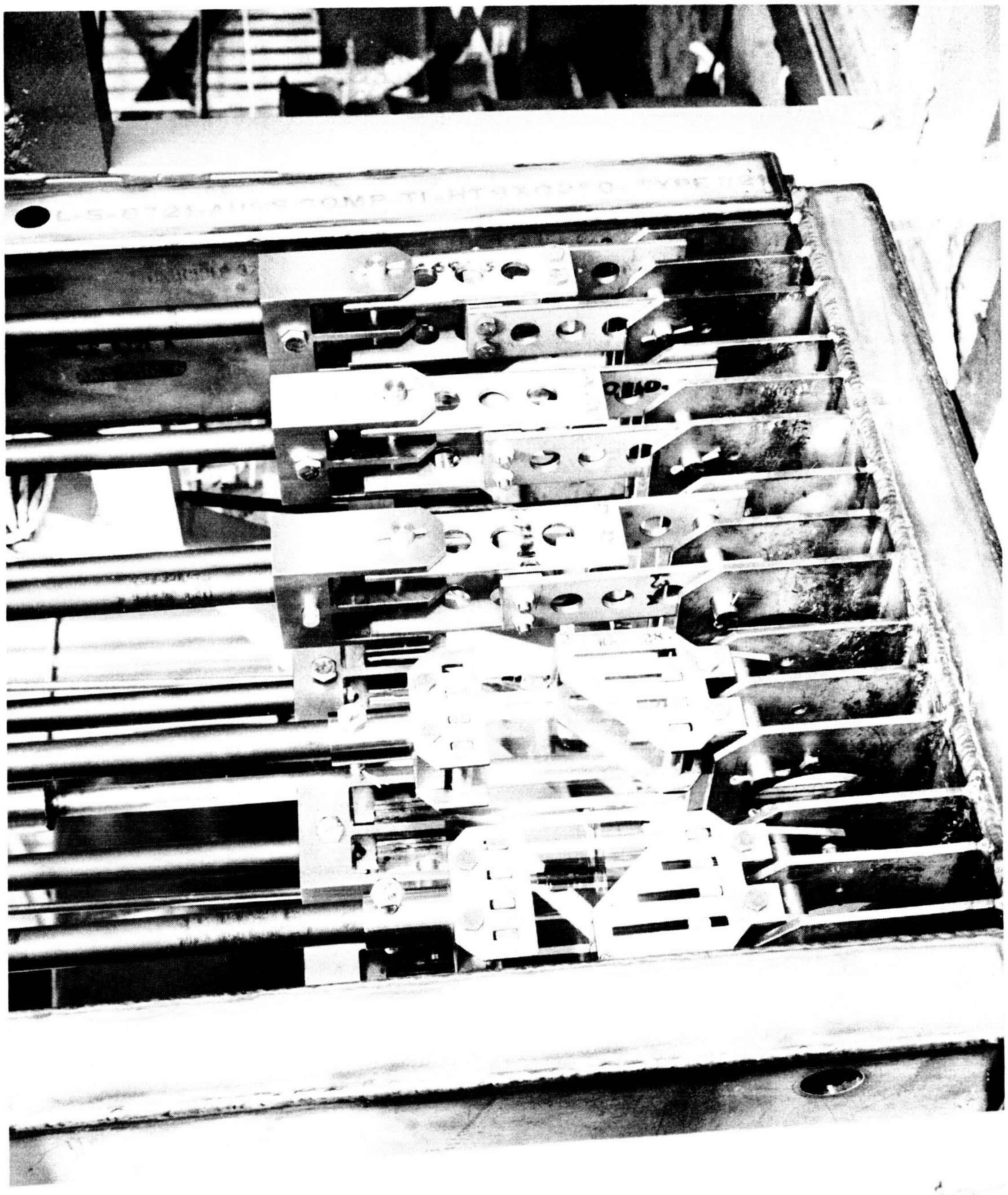

Figure 2.5 Thin-Film and Compression-Button Specimens Mounted in Experimental Assembly

The compression-button testers consist of upper and lower yokes which mount to the standard clevis. The end of each yoke contains a flat plate for compressing the specimen. The specimen rests on the upper-yoke plate and rises with upward pull-rod movement to meet the lower-yoke plate and thus undergo compression.

Figure 2.6 is a closeup of two pressure chambers containing an O-ring seal made from one of the test materials. These chambers are pressurized with helium gas to 50 psi during irradiation. During a test, the supply valve is closed and pressure drops are monitored. Losses in pressure during the test and the results of postirradiation inspection and testing of the O-ring are both considered in evaluating the radiation resistance of the material at cryotemperatures.

The liquid-level probe can be seen hanging vertically along the left-hand edge of Figure 2.6. The cryogen supply tube is located between the two O-ring testers.

The Dewar for the experimental assembly was fabricated completely from type 6061-T6 aluminum. The top flange and hydraulic-cylinder support frame are also 6061-T6 aluminum. The box frame below the top flange, as well as the upper and lower clevises and the specimen-mounting apparatus, is fabricated from type 321 stainless steel.

All design and fabrication work on the experimental assemblies was performed at General Dynamics/Fort Worth.

NPC 17,431
31-6556

Figure 2.6 O-Ring Pressure Test Chambers

2.3 Experimental-Assembly Accessory Equipment

Operation of the experimental-assembly hydraulic cylinder (slave cylinder) is accomplished with a master cylinder connected to the crosshead of an Instron machine (Fig. 2.7). The master cylinder is connected to the slave cylinders by $\frac{1}{4}$-in. soft-copper hydraulic lines. Twenty lines (supply and return to ten cylinders) are routed from each experimental assembly through a selector panel (Fig. 2.8). Forces exerted by the Instron machine are thus transmitted indirectly to the specimens in the experimental assembly. Length of the connecting hydraulic lines is 100 feet. Oronite 8515 hydraulic fluid is used.

The LN_2 supply lines are $\frac{1}{2}$-in. soft-copper tubing insulated with a 1-in. thickness of Armstrong Armaflex insulation. These lines connect to a 3-outlet manifold on the LN_2 supply tanks. The LH_2 supply line is a $\frac{1}{4}$-in. ID x 1-in. OD flexible, bellows-type, stainless-steel line made by The Linde Company. It is vacuum-insulated and requires no outside covering. A 1-inlet, 3-outlet, vacuum-insulated manifold is used in the LH_2 supply-piping system to feed three experimental assemblies simultaneously from one LH_2 supply tank. The manifold contains a solenoid-controlled, air-operated, vacuum-insulated cutoff valve in each outlet line. Evaporated-cryogen lines are $1\frac{1}{2}$-in. flexible metal hose. Provision is made to vent evaporated LH_2 to the atmosphere from a 20-ft-high stack located in a remote end of the reactor area.

NPC 17,432
31-6812

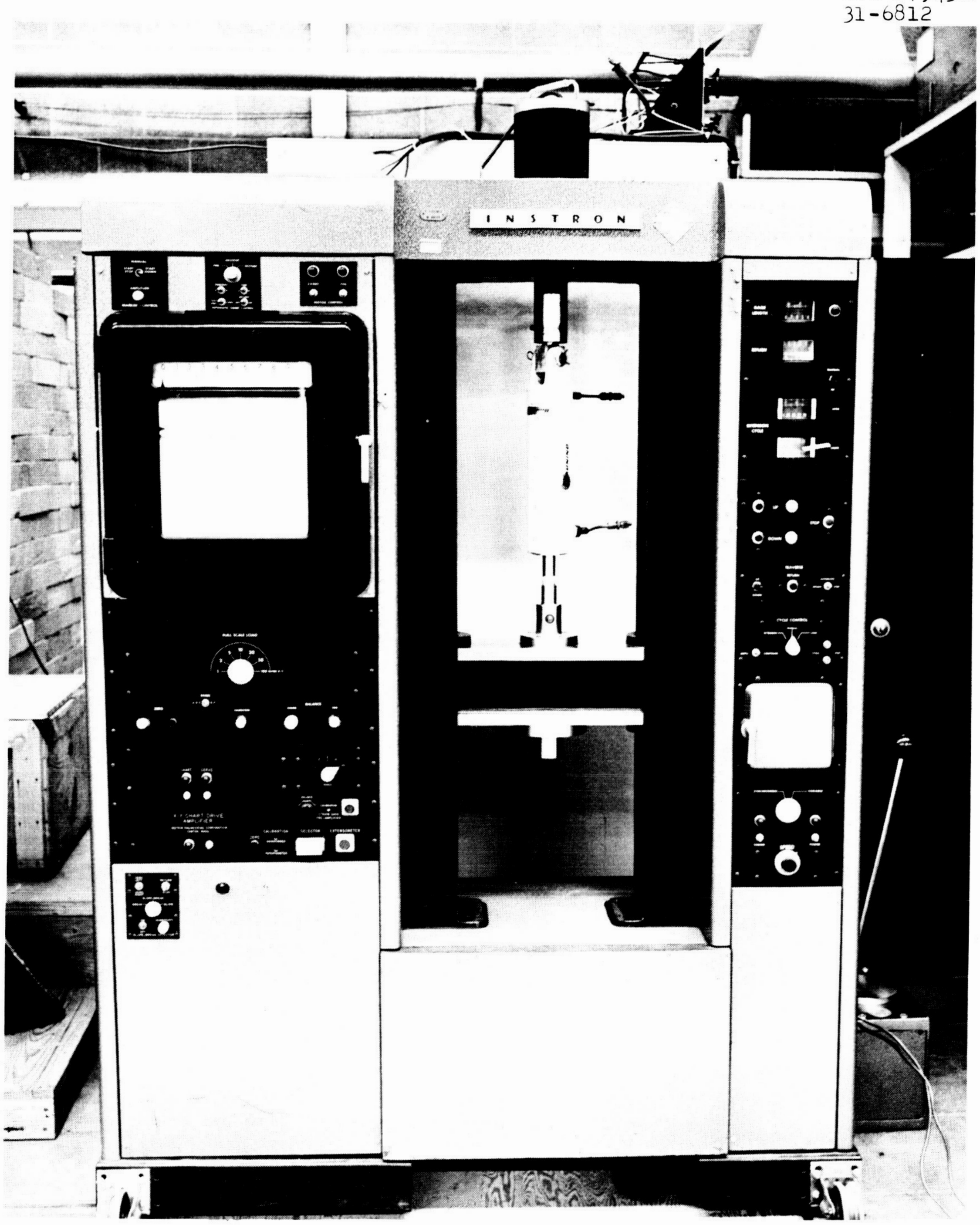

Figure 2.7 **Model TT Instron Machine with Hydraulic Servo-System Master-Cylinder Installed**

NPC 17,433
31-6813

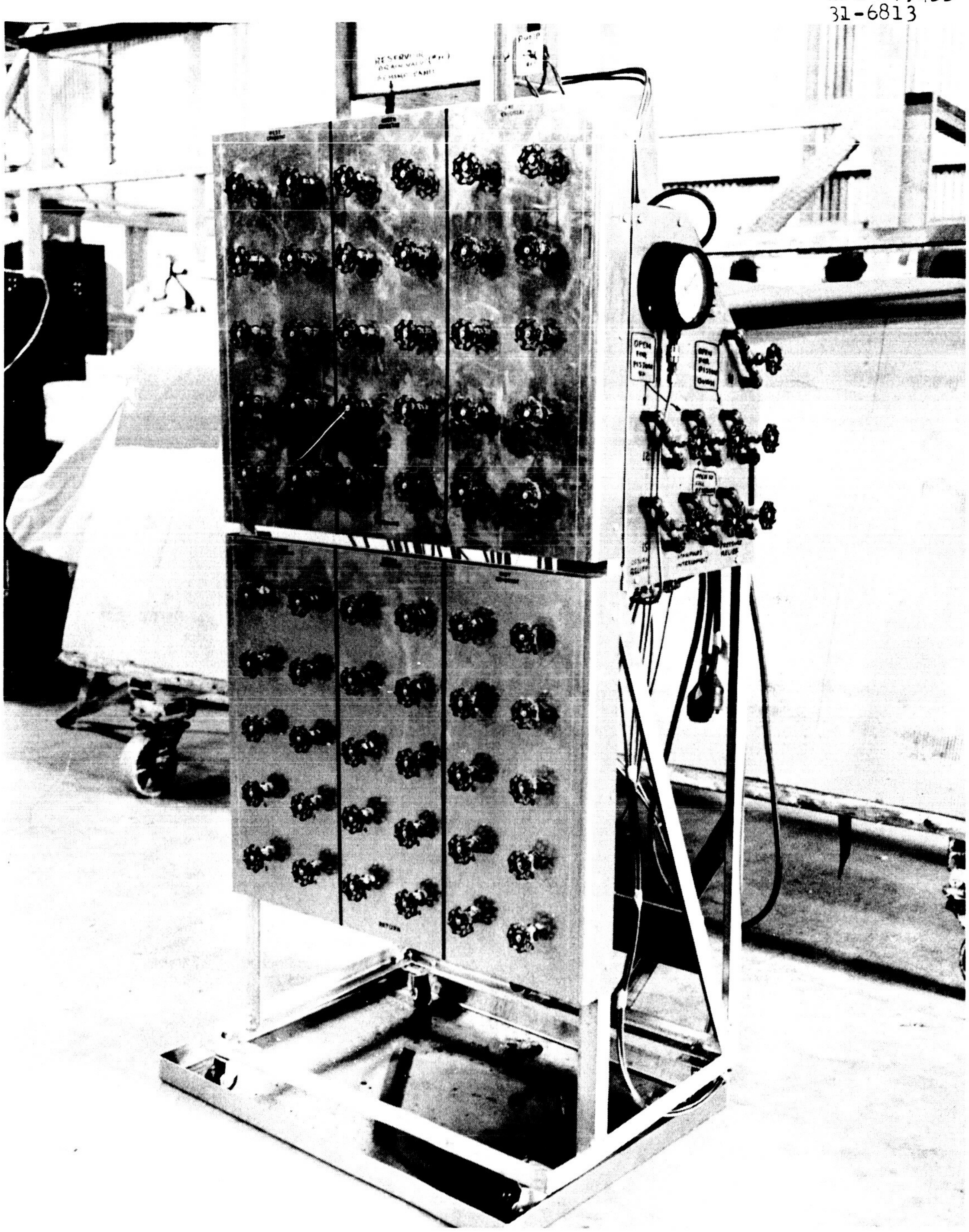

Figure 2.8 Hydraulic Servo-System Slave-Cylinder Selector Panel

Figure 2.9 is a photograph showing two experimental assemblies in irradiation position at the east and north positions. The vacuum-irradiation system is located at the west position. Reference to the photograph shows the bundle of 20 soft-copper hydraulic lines, electrical harness, insulated LN_2 supply line, and flexible-metal evaporated-cryogen outlet line coming from each experimental assembly. Frost around the top flange and on the evaporated cryogen-outlet line of the north assembly indicates that this assembly is partially filled with LN_2. The west escalator pallet is shown in the half-down position.

2.4 Ambient-Temperature Irradiation Equipment

For the ambient-temperature irradiation, an aluminum box frame with slots for expanded-metal trays was used (Fig. 2.10). This frame-work also latches to the escalator pallet for positioning next to the reactor face. Different specimens scheduled to receive the same radiation dose were wired to the expanded-metal trays in a circular arrangement. This was necessary because of the circular pattern of isodose lines that exist in vertical planes out from the reactor face during operation. The trays were placed at various distances from the reactor face to achieve varying doses on different specimens during an irradiation. Specimens irradiated at ambient temperature were subsequently tested at room temperature in the Irradiated Materials Laboratory (IML).

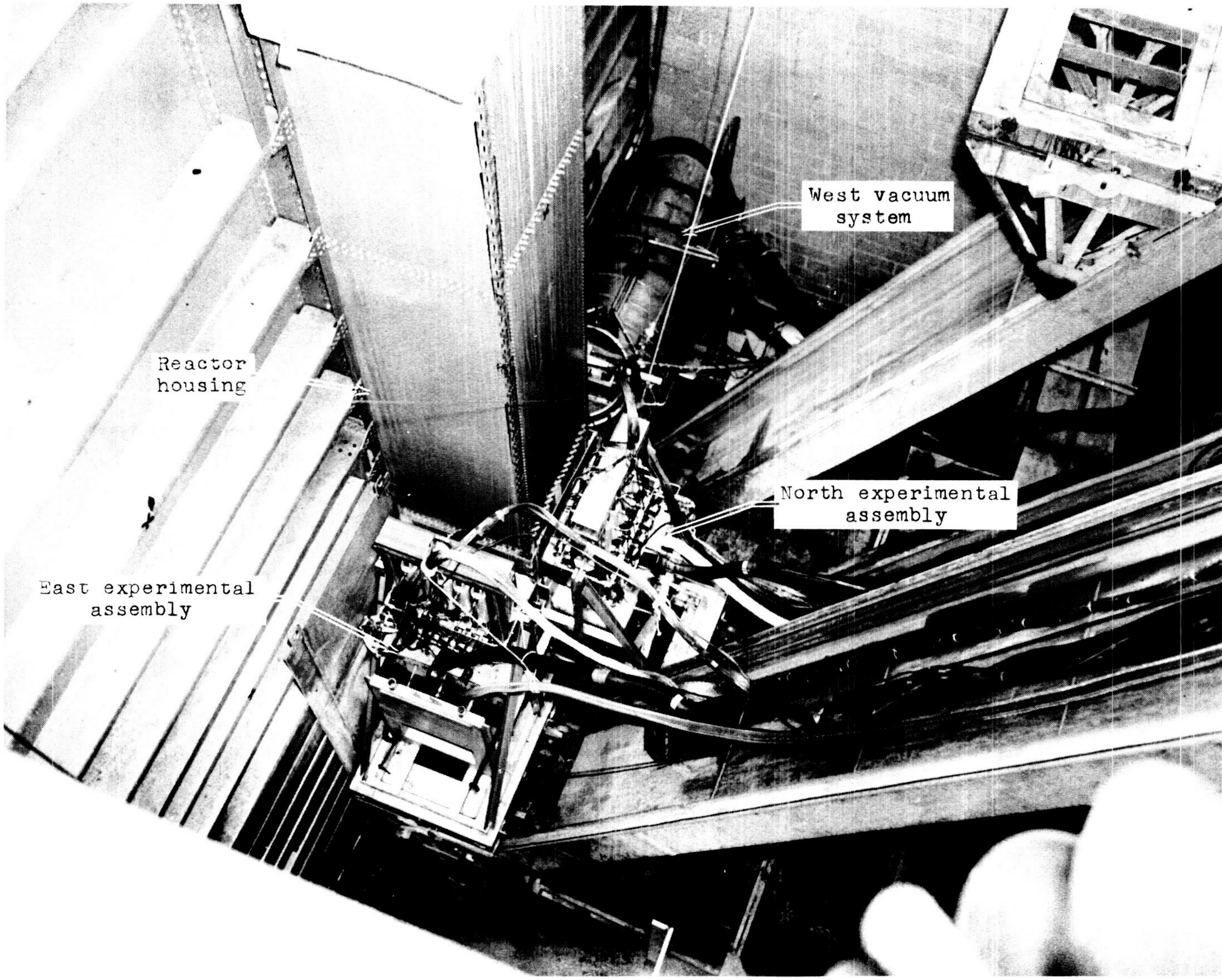

NPC 17,434
31-6718

Figure 2.9 Irradiation Area with Experimental Assemblies Installed

NPC 17,435
31-6562

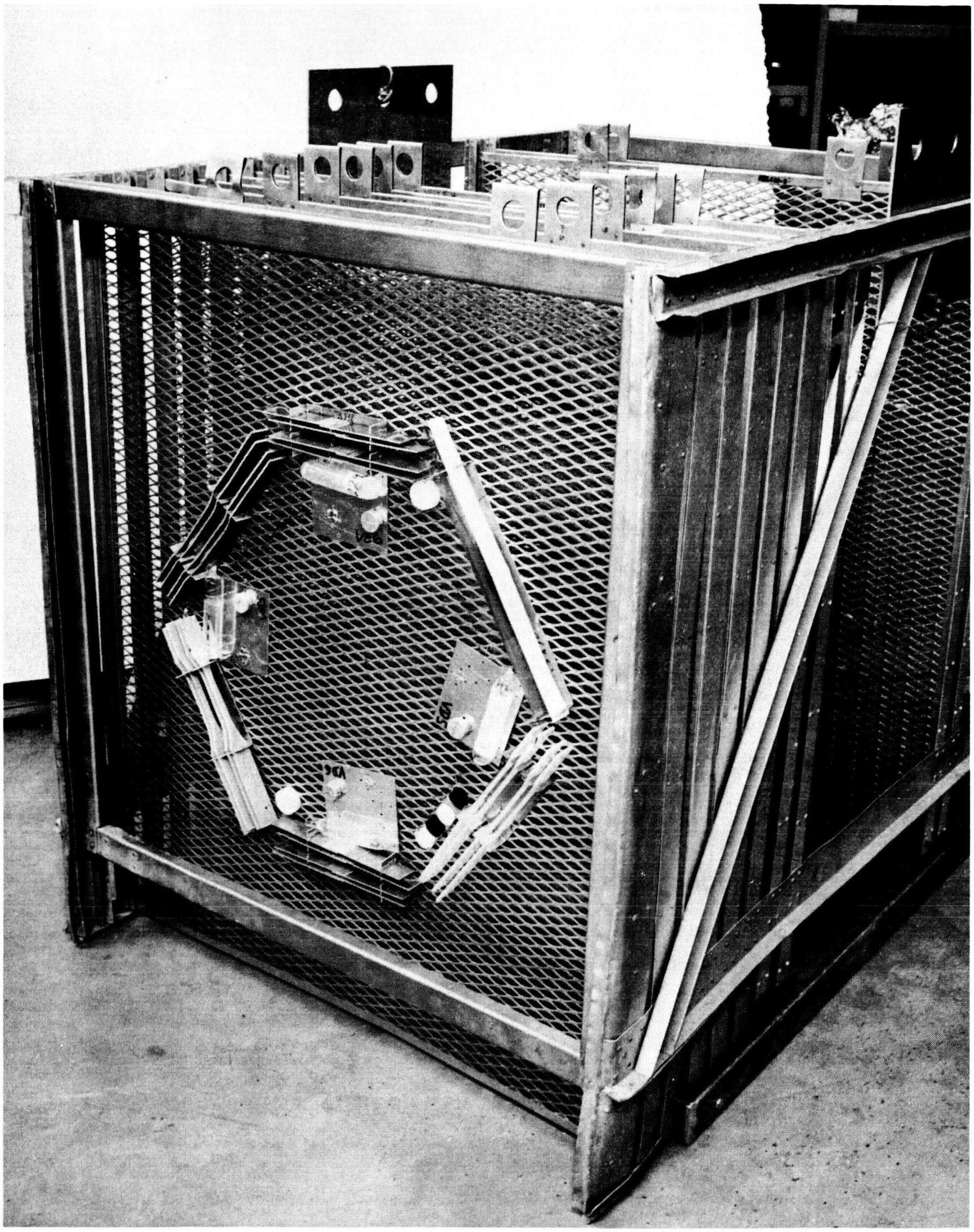

Figure 2.10 **Rack Framework for Ambient Irradiation Showing Typical Material and Dosimetry Packet Arrangement**

2.5 Test Instrumentation

Instrumentation necessary to operate the experimental assemblies and record the required data included the following: (1) standard Instron instrumentation to record stress-strain data; (2) ten-point Honeywell recorders to chart temperatures of specimens during the ambient irradiation, together with temperatures of specimens and cryogen during the LH_2 and LN_2 irradiations; (3) a GD/FW-designed instrument to provide continuous indication of cryogen liquid level during operation with LN_2 and LH_2; and (4) a Model 150 Sanborn oscillograph recording system with a Model 150-100 carrier preamplifier which was used to record (a) stress-strain data as received from the dynamometers and LVDT's and (b) cryogen-chamber pressure signals received from a pressure transducer installed in the top flange of each experimental assembly. The Instron machine is a Model TT. The LVDT's are Schaevitz No. 600ES-L; the dynamometers, Schaevitz No. TDC-4A-1000; and the pressure transducers, Consolidated Electrodynamics No. 4-312. Figure 2.11 is a photograph of the Sanborn equipment and the GD/FW-designed liquid-level indicator control panel.

The liquid-level indicator utilizes a basic balanced-bridge circuit as the principle of operation (Fig. 2.12). The sensing elements are 1000-ohm resistors positioned on approximately 3-in. vertical intervals in the cryogen chamber (Fig. 2.6). The resistance of these sensing resistors when submerged in cryogen changes to approximately 5000 ohms which, during operation, unbalances the

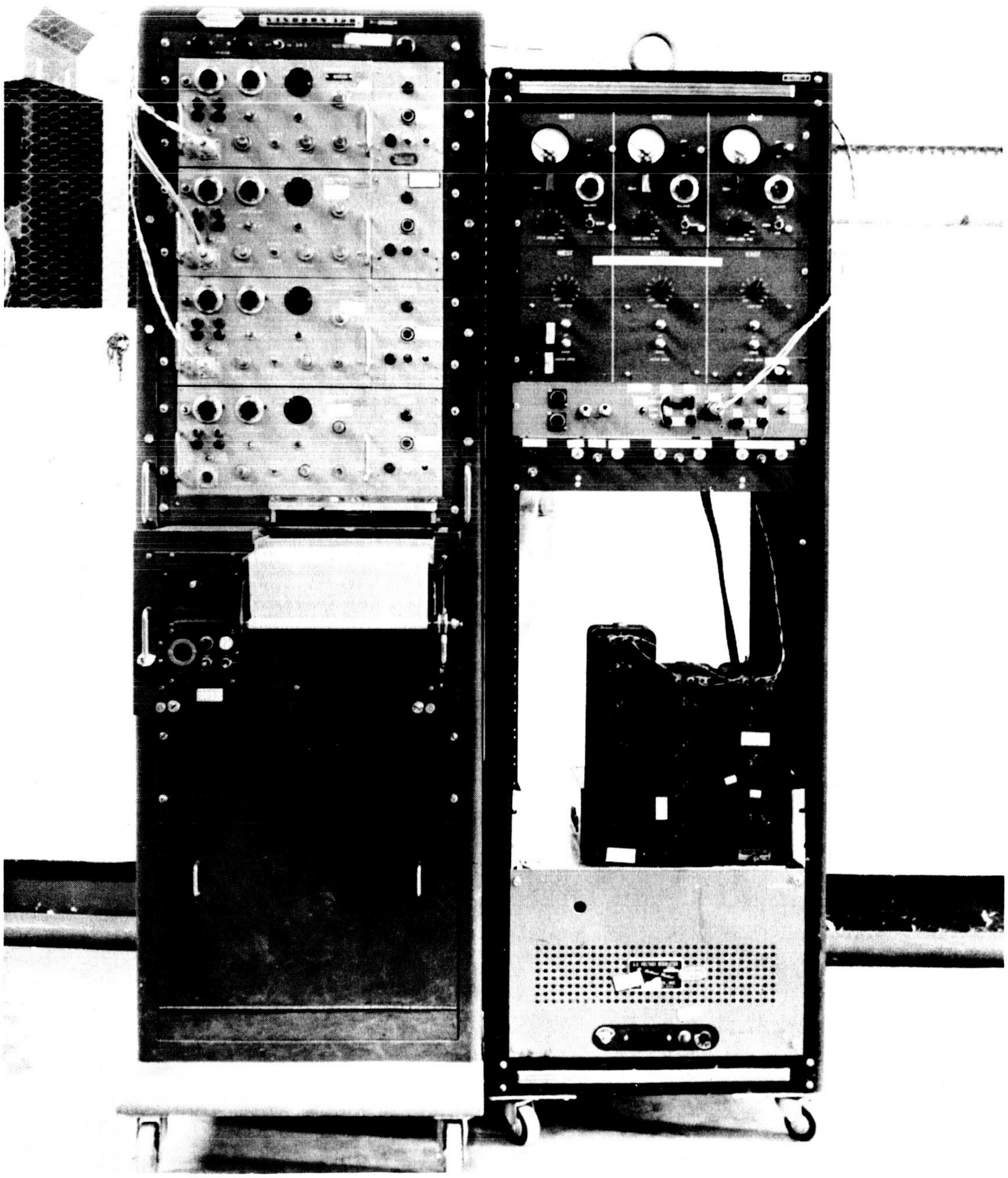

Figure 2.11 Instrumentation for Experimental Assembly

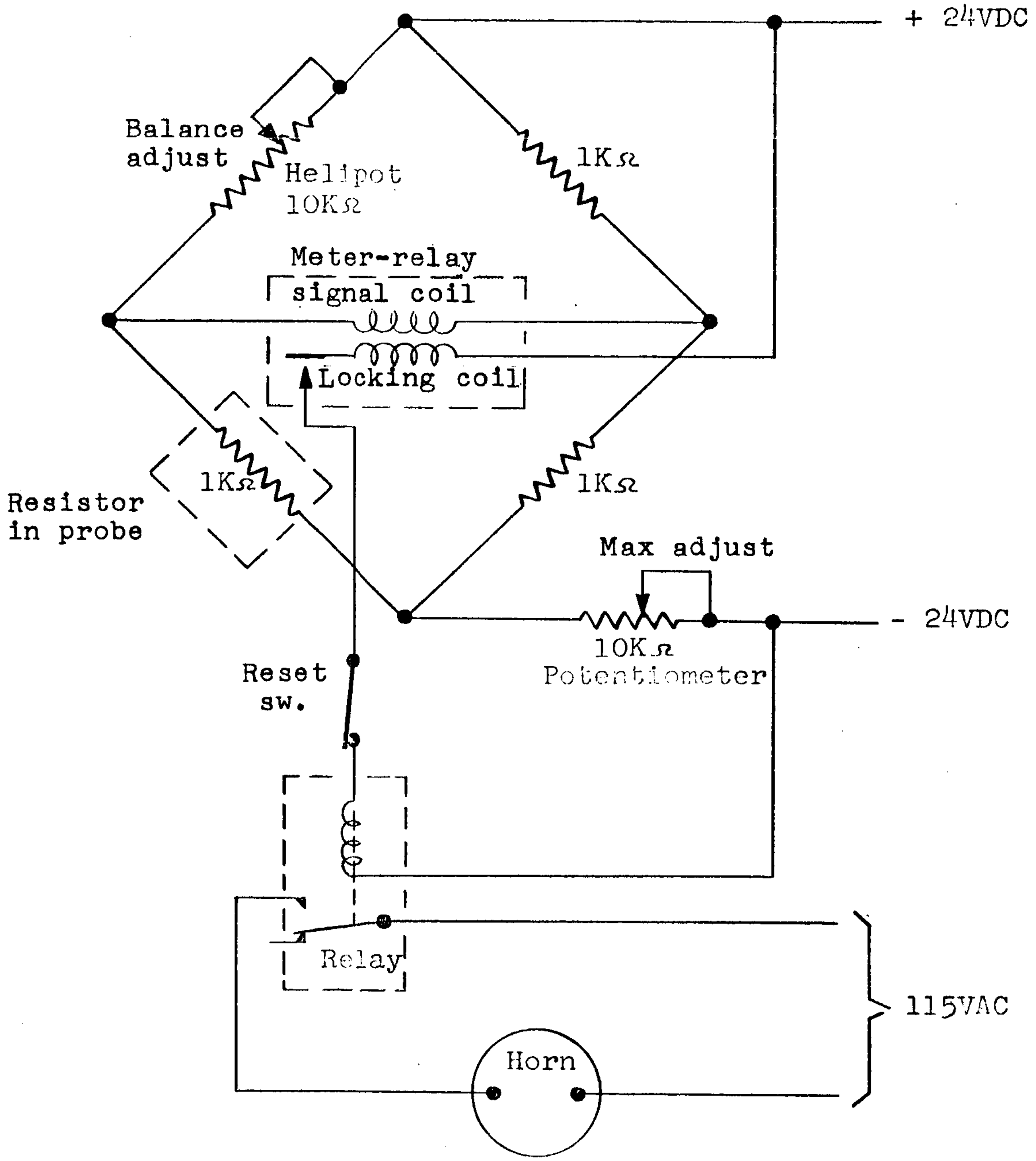

Figure 2.12 Schematic Diagram of Liquid-Level Indicator

bridge circuit and causes current to flow through the meter relay. This current deflects the meter needle until it comes in contact with another preset needle, thus closing contacts which activate the warning-horn circuit.

A meter-polarity-reversal switch and a bridge-adjustment potentiometer are provided on the control panel. Operation of these units provides a warning-horn signal either with a sensing resistor "in-liquid" or "out-of-liquid," thus providing a means of determining whether the liquid level is rising or falling in the chamber and the approximate rate of change.

During an irradiation run, the pressure-transducer recording chart and cryogen-chamber temperature recorders are operated continuously and are visually monitored to guard against any unusual rise in these readings. The allowable limit on pressure for the cryogen chamber is 5 psi. Any rise above this point necessitates closing the cryogen supply valve and checking the evaporated-cryogen outlet pipe for stoppages.

The liquid-level instrumentation is also operated and monitored continuously whenever cryogen is flowing into any assembly. The liquid level is maintained by opening and closing valves in the LN_2 and LH_2 manifolds.

Before data are taken with the LVDT's, dynamometers, and Instron machine, each of these units must be calibrated. This is accomplished by plotting output signals against known loads and deflections.

When actual measurements of a specimen being pulled in tension or compression are taken, the Instron, LVDT, and dynamometer recorders all work in conjunction. As the specimen is pulled, all three recorders are pipped periodically and simultaneously to establish common points on the three curves. The Instron recorder plots the stress seen by the crosshead as a function of the actual crosshead (or master-cylinder) movement. Voltage changes resulting from movement of the LVDT core are plotted and readily translated into inches of pull-rod movement. Similar data are received from the dynamometers and read from the chart as pounds-of-force exerted by the pull rod.

III. RADIATION ENVIRONMENT

3.1 GTR Neutron Spectrum Determination

3.1.1 Analytical GTR Neutron Spectrum

The spectrum (Ref. 2) of the GTR in a water moderator has been measured to be Maxwellian at thermal energies ($E < 0.48$ ev), approximately E^{-1} from about 0.5 ev to 0.1 Mev, and essentially a fission spectrum for higher energies. In Figure 3.1, this spectral shape has been mathematically altered to account for the attenuation of the neutron flux by the boral surrounding the reactor in the dry-pool configuration. The resulting analytical spectrum has been shown to represent the actual spectrum fairly accurately.

Flux measurements have been made in the thermal, epithermal, and fast energy ranges by use of a variety of thermal, resonance, and threshold detectors. Measurements made in the dry side with the boral in place, in the energy range above 2.9 Mev, agree well with those in the wet-pool side. The measured thermal flux is in general agreement with that obtained by integration of the analytical curve shown in Figure 3.1. Measurement of the epithermal flux by use of resonance detectors is very difficult and values differing by as much as a factor of 2 are obtained by the various detectors.

An experiment (Ref. 3) performed for Sandia Corporation mapped the irradiation volumes with plutonium, neptunium, uranium foils, and sulfur pellets of the type used by GD/FW. The foil-counting

Preceding page blank

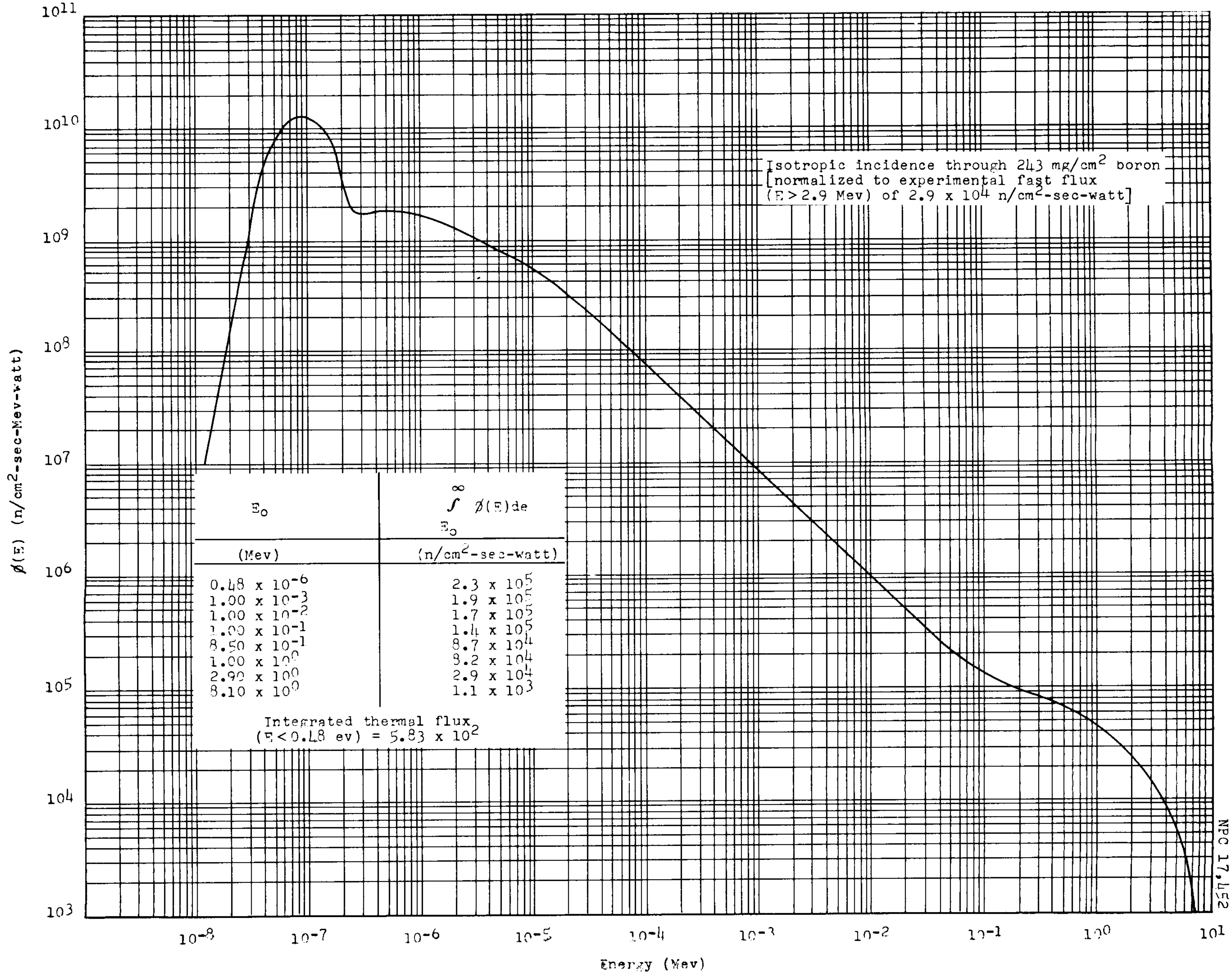

Figure 3.1 Analytical GTR Neutron Spectrum

and data reduction were done by Sandia. The results as reported by Sandia show that Sandia and GD/FW agree within a few percent on sulfur measurements ($E > 2.9$ Mev) and that fission-foil data agree favorably with the analytical spectrum at all locations.

The neutron spectrum above 0.5 Mev has also been determined at one location by means of Ilford neutron plates (type E-1). Integrals of this spectrum agree closely with integrals of the analytical spectrum.

In June 1960, a comprehensive foil-calibration experiment encompassing both GD/FW and Aerojet-General Nucleonics (AGN) foils was conducted (Ref. 4). The results of the two independent counting and data-reduction programs agree within a few percent.

3.1.2 Experimental GTR Neutron Spectrum

Figure 3.2 shows a representative neutron-energy spectrum in the east cryogen chamber at a point midway (front to back) between the center sample positions. This spectrum is normalized to an experimental fast flux $\phi(E > 2.9 \text{ Mev}) = 2.9 \times 10^4$ n/cm^2-sec-watt and shows that, in the energy interval given, the spectrum shape is affected only slightly, if at all, by attenuation through LN_2 or LH_2 (compare with Figure 3.1).

3.2 Nuclear-Measurement Procedures

Determination of the neutron flux and gamma dose inside the experimental assemblies was done according to NARF standard procedures used on all irradiation tests. Radioactivants used for

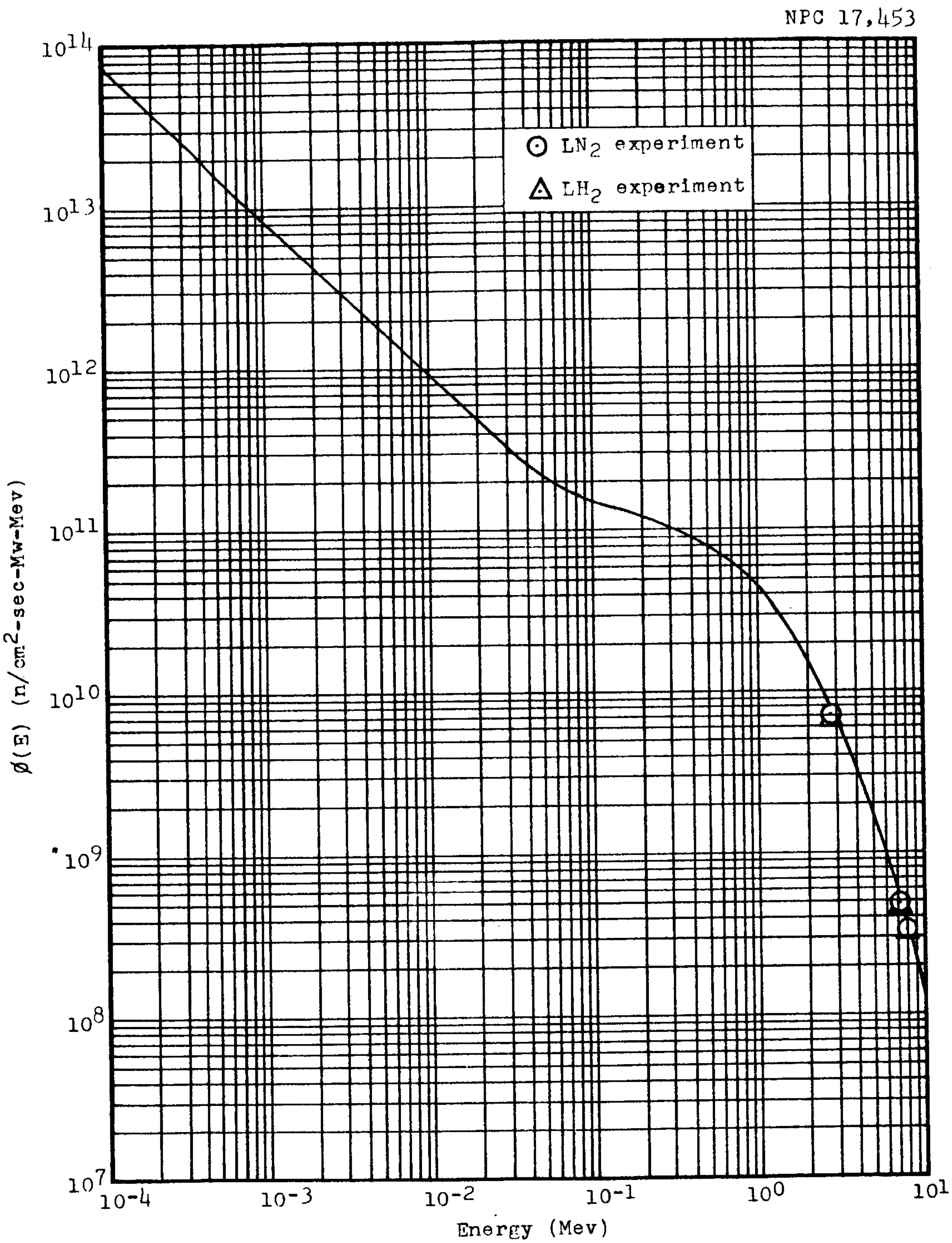

Figure 3.2 Representative Neutron Spectrum in the East Cryogen Chambers Midway Between Front and Back Sample Locations on Vertical Centerline

neutron-flux measurements were standard types and are outlined in the succeeding sections. Gamma-dose levels were monitored with nitrous-oxide and polyethylene plastic dosimeters.

3.2.1 Ambient-Temperature Irradiation

Three racks mounted with the material specimens prescribed for the tests were irradiated in air at ambient temperature($\sim 125^{\circ}F$) on the north pallet position of the GTR at a power level of 1.5 Mw. The rack-mounted materials were to receive integrated gamma doses [ergs/gm(C)] as follows: Rack 1, 5×10^{10}; Rack 2, 1×10^{10}; and Rack 3, 5×10^{9}.

Nuclear measurements were made at strategic locations on each rack with bare and cadmium-covered copper foils for the thermal flux, sulfur pellets for fast-neutron flux ($E > 2.9$ Mev), and nitrous-oxide gamma dosimeters. Figures 3.3, 3.4, and 3.5 show locations of material specimens and nuclear measurement packets on Racks 1, 2, and 3, respectively.

3.2.2 Liquid-Nitrogen Irradiation

Packets containing one each of the neutron radioactivants sulfur, magnesium, aluminum, and bare and cadmium-covered copper were mounted on 0.040-in.-thick expanded-aluminum sheets in an array as shown in Figure 3.6. Locations of nitrous-oxide gamma dosimeters are also shown. Sheets with detectors arranged in this manner were attached to the lower box-frame directly in front of, and directly behind, the test samples in the cryogen chambers of

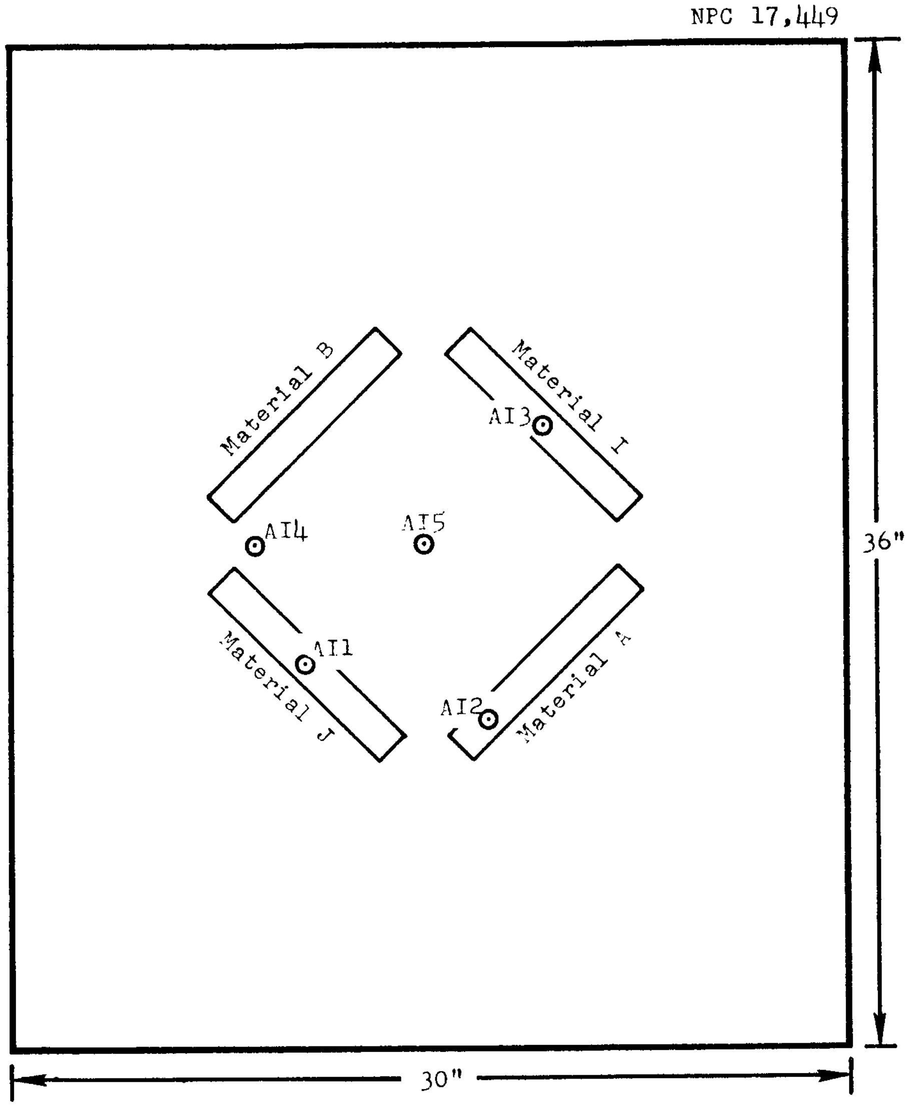

Figure 3.3 Layout of Materials and Dosimetry Packets on Rack 1 for Ambient Irradiation

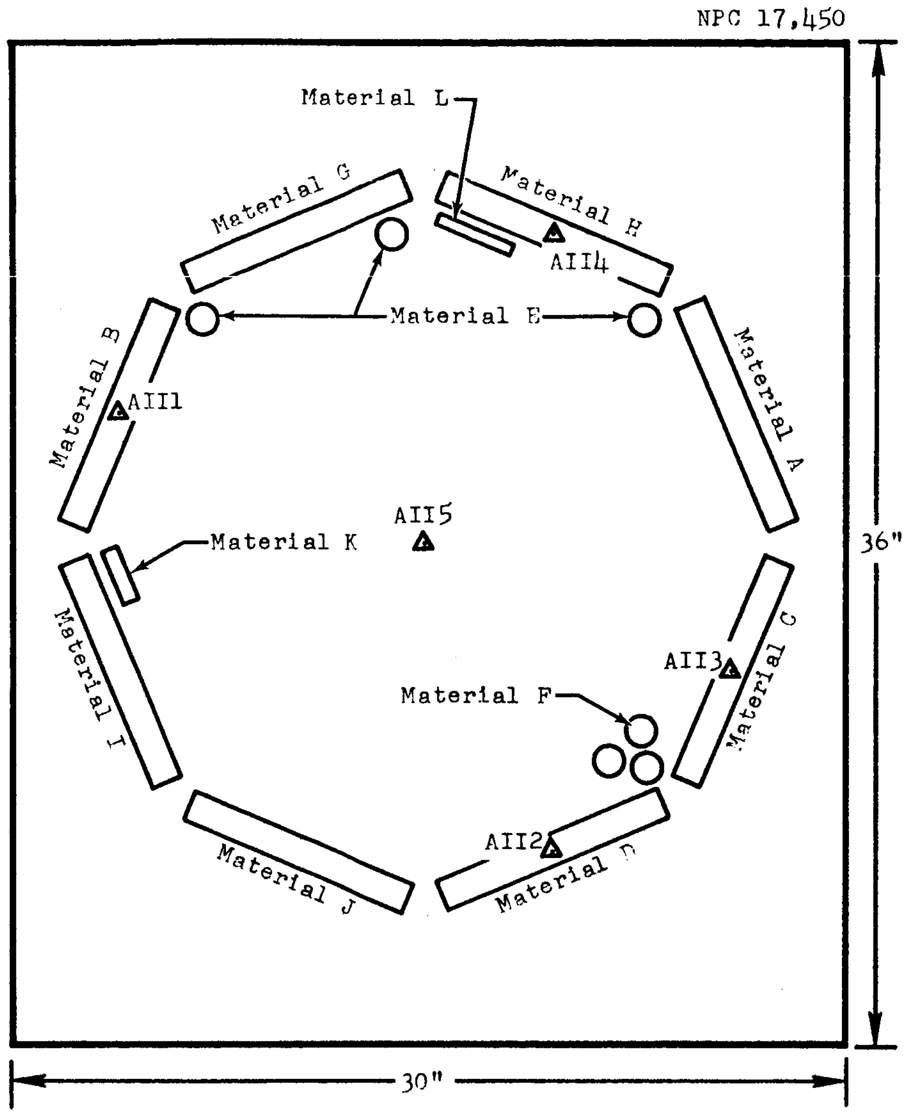

Figure 3.4 Layout of Materials and Dosimetry Packets on Rack 2 for Ambient Irradiation

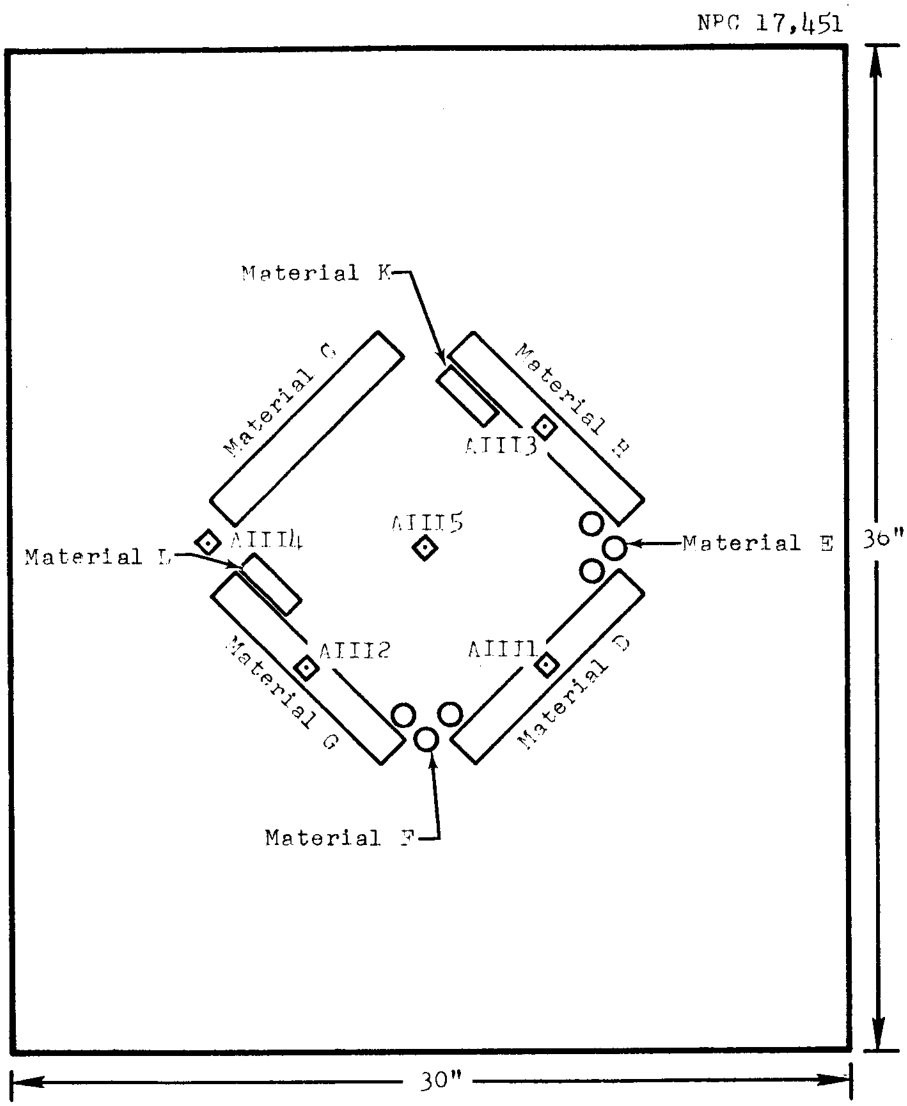

Figure 3.5 **Layout of Materials and Dosimetry Packets on Rack 3 for Ambient Irradiation**

the north and east assemblies. Measurements were made with the detectors submerged in liquid nitrogen.

In addition, a total of six nitrous-oxide gamma dosimeters were located on the outside, front and back, of each of the north and east cryogen chambers during irradiation. They were positioned so as to be on a horizontal plane through the test materials, and were spaced evenly with respect to the pull-rod centerline. (The spacing of these dosimeters across the front and back faces, relative to the pull-rod positions in the cryogen chambers, is indicated by the points on the solid curve shown in Figure 3.10).

3.2.3 Liquid-Hydrogen Irradiation

Packets containing the neutron radioactivants sulfur, magnesium, aluminum, and bare and cadmium-covered phosphorous were mounted on 0.040-inch-thick expanded-aluminum sheets in an array as shown in Figure 3.7. These neutron-detector packets were located in front of and behind the test samples and were irradiated while submerged in liquid hydrogen.

Since there are no calibration data for gamma dosimeters irradiated at liquid-hydrogen temperatures, no gamma-measurement devices were placed inside the experimental assemblies during the LH_2 test. At the present time, investigation is being made of the effects of cryotemperatures upon nitrous-oxide gamma dosimeters, with hopes that they may be used with confidence in future experiments.

NPC 17,454

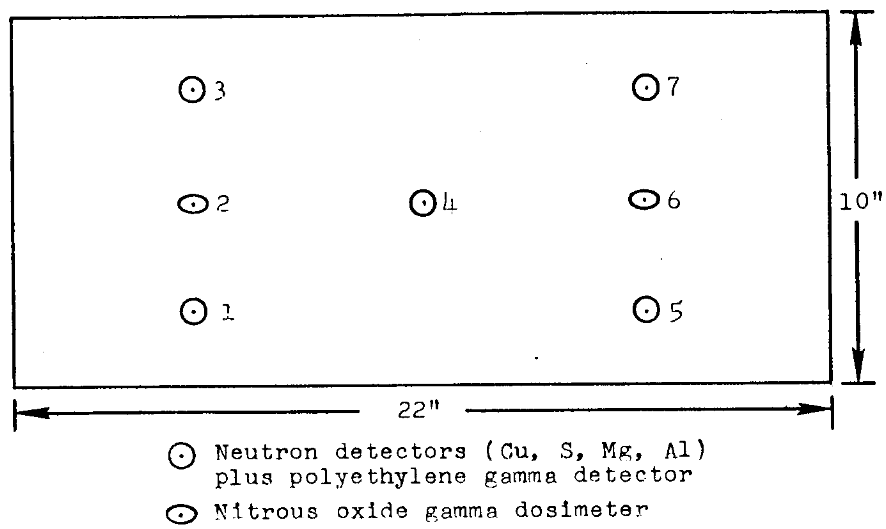

Figure 3.6 **Layout of Dosimetry Packets for LN_2 Irradiation**

NPC 17,455

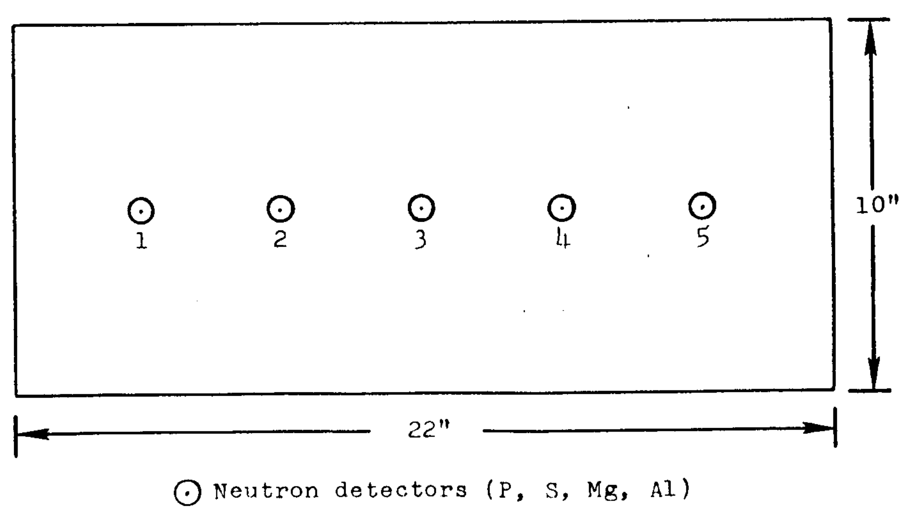

Figure 3.7 **Layout of Dosimetry Packets for LH_2 Irradiation**

A total of eight nitrous-oxide gamma dosimeters were located on the outside, front and back, of each of the north and east cryogen chambers during irradiation. They were positioned so as to be on a horizontal plane through the material specimens. The spacing of these dosimeters across the front and back chamber faces, relative to the pull-rod positions in the cryogen chambers, is indicated by the points on the solid curves shown in Figure 3.13.

3.3 Nuclear Measurement Results

3.3.1 Ambient-Temperature Irradiation Tests

The radiation exposure levels measured during the ambient-temperature irradiations are given in Table 3.1. These radiation measurements show good agreement with previously measured radiation levels made in airat these locations (Ref. 5).

3.3.2 Liquid-Nitrogen Irradiation Tests

There were two factors which contributed to the loss of portions of the required LN_2 data. First, an unexpectedly high radioactivity in the experimental assemblies hampered the manual removal of the neutron foils. This resulted in a loss of some of the foils and an excessively long retrieval time for others. Second, gamma heating during the test resulted in the melting of sections of a lead shield. The molten lead then came in contact with some of the dosimetry and destroyed it.

Average values of the neutron flux midway between the front and back sample rows were obtained by interpolation between flux measurements made with neutron detectors located directly in front

Table 3.1

Radiation Exposure Levels for Ambient Irradiation

Dosimetry Packet Number*	Integrated Neutron Flux		Gamma Dose [ergs/gm(C)]
	Thermal (n/cm^2)	E >2.9 Mev (n/cm^2)	
Rack 1			
AI1	2.2×10^{14}	1.7×10^{16}	6.0×10^{10}
AI2	2.4×10^{14}	1.6×10^{16}	6.0×10^{10}
AI3	4.7×10^{14}	1.7×10^{16}	6.7×10^{10}
AI4	2.3×10^{14}	1.6×10^{16}	4.9×10^{10}
AI5	6.3×10^{14}	1.9×10^{16}	8.8×10^{10}
Rack 2			
AII1	3.7×10^{14}	2.5×10^{15}	1.1×10^{10}
AII2	3.6×10^{14}	2.5×10^{15}	1.0×10^{10}
AII3	3.5×10^{14}	2.6×10^{15}	1.2×10^{10}
AII4	3.2×10^{14}	2.2×10^{15}	7.6×10^{9}
AII5	3.5×10^{14}	2.9×10^{15}	1.1×10^{10}
Rack 3			
AIII1	1.1×10^{14}	1.1×10^{15}	5.5×10^{9}
AIII2	1.0×10^{14}	1.3×10^{15}	4.8×10^{9}
AIII3	9.6×10^{13}	1.3×10^{15}	4.9×10^{9}
AIII4	1.7×10^{14}	1.2×10^{15}	4.6×10^{9}
AIII5	2.2×10^{14}	1.3×10^{15}	4.6×10^{9}

*See Figures 3.3, 3.4 and 3.5 for locations of packets of and behind the sample positions during the irradiation. Figures 3.8 and 3.9 show these values for the east and north chambers, respectively, plotted as the solid lines. The broken lines in the figures show analytical neutron-flux values, the values most likely to be expected in the chambers (see below).

The flux values shown in the figures for both chambers for $E > 2.9$ Mev are in very good agreement with the air-flux values (Ref. 5). However, for the reasons given above, the flux values in the east chamber (Fig. 3.8) for $E > 8.1$ Mev and $E < 0.48$ ev are known to be low, and the $E > 7.5$ Mev flux values are erratic and are not plotted. In the north chamber (Fig. 3.9) the thermal-flux values ($E < 0.48$ ev) are not shown because they too are erratic. In order to determine these missing values, a comparative analysis was made with other reliable measurements, as follows:

The ratio of the neutron flux above 2.9 Mev to that above 8.1 Mev measured during the LH_2 experiments (Sec. 3.3.3) was found to be 25. This value is in good agreement with the accepted value of 26 for the GTR spectrum measured through the boral shroud in previous tests (Fig. 3.1). Multiplying the 2.9-Mev neutron flux, plotted in Figures 3.8 and 3.9 by 1/25 yields the neutron flux for $E > 8.1$ Mev shown as a dashed line.

The neutron flux for $E > 7.5$ Mev was obtained in much the same manner. For the GTR spectrum measured through the boral shroud, where $\phi(E > 2.9 \text{ Mev})/\phi(E > 8.1 \text{ Mev}) = 26$, then $\phi(E > 2.9 \text{ Mev})/\phi(E > 7.5 \text{ Mev}) = 18$. Thus, in the cryogenic experimental assemblies,

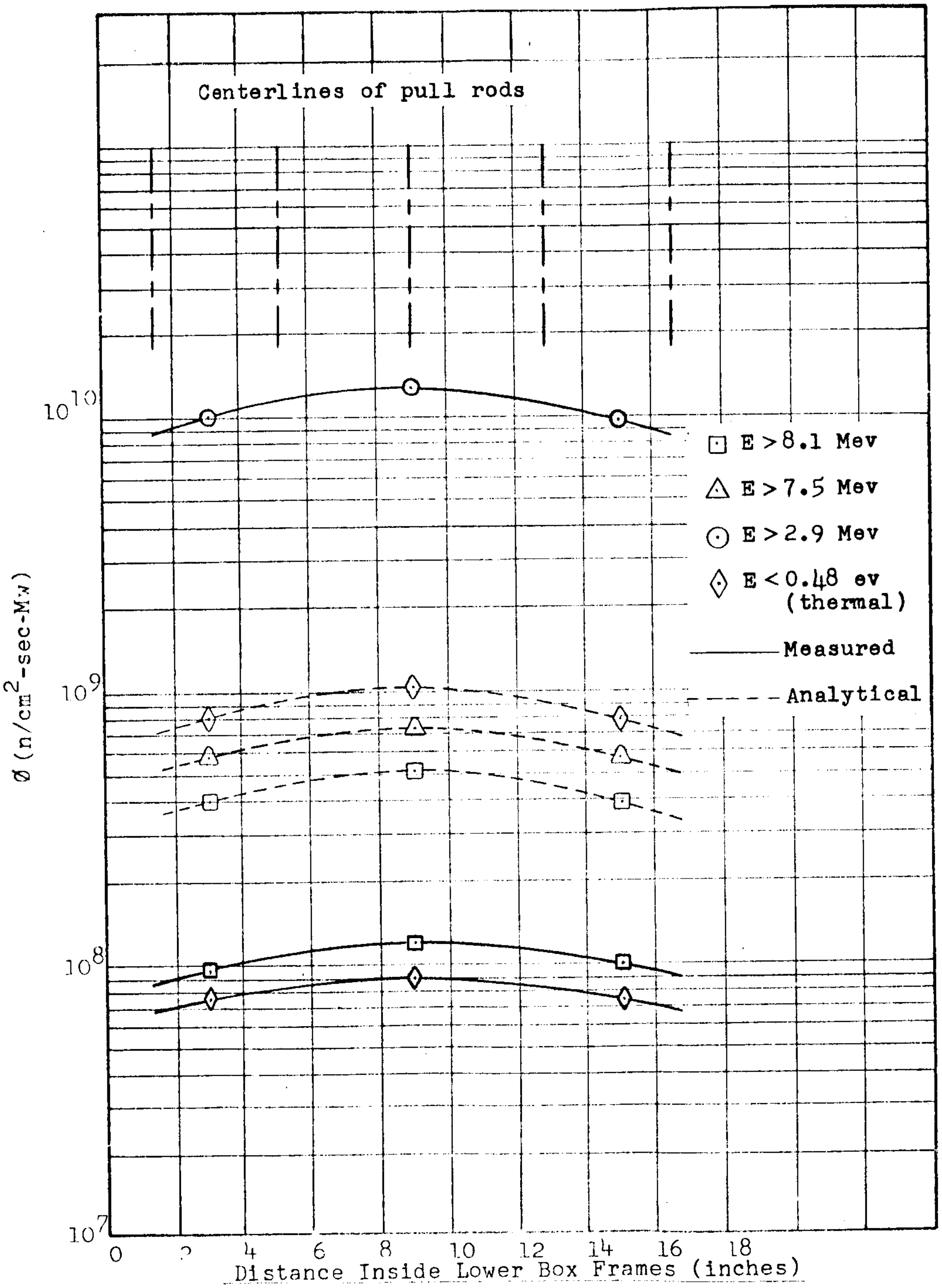

Figure 3.8 **Neutron Flux Midway Between Front and Back Sample Positions: LN$_2$ Irradiation; East Chamber**

NPC 17,457

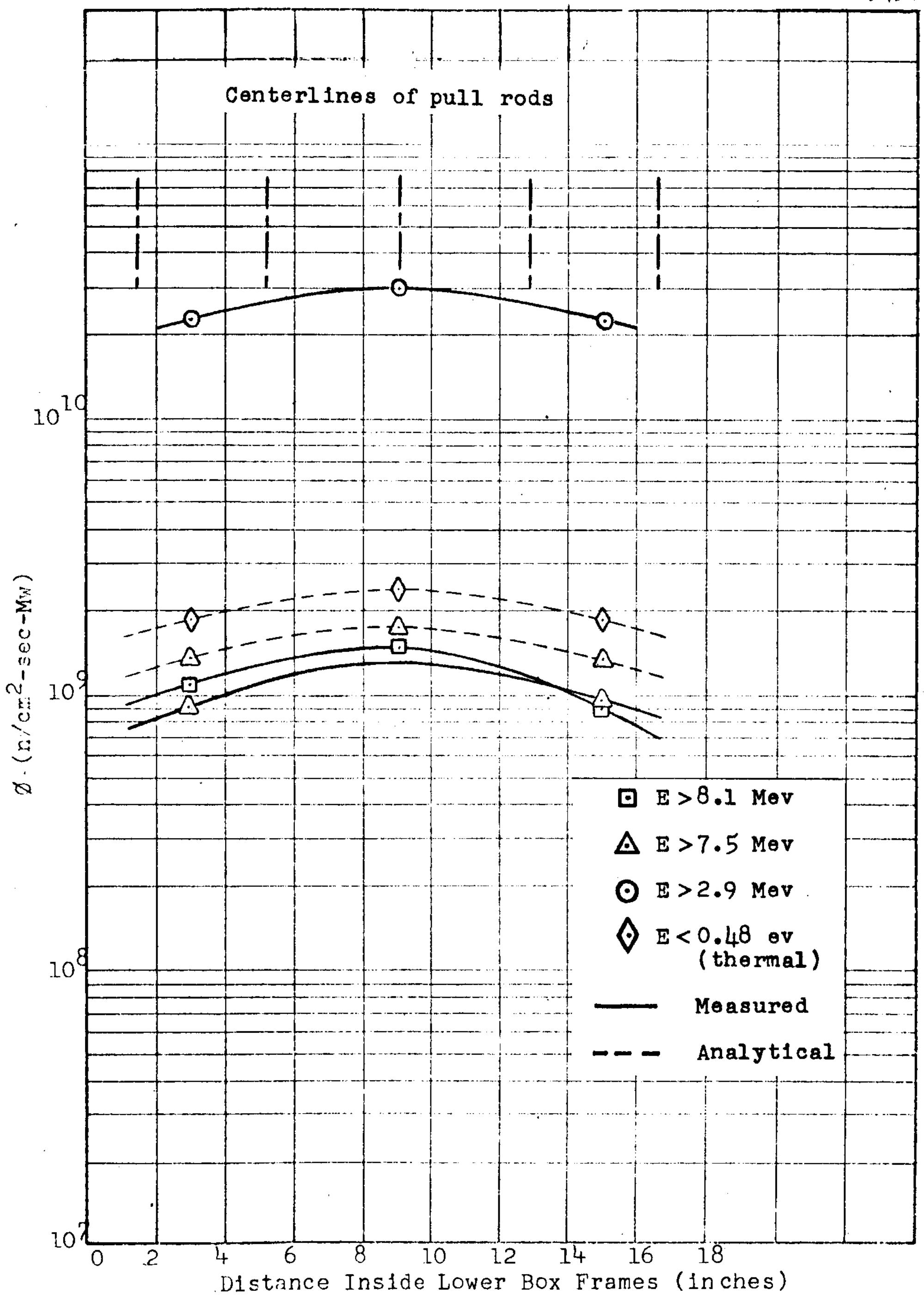

Figure 3.9 **Neutron Flux Midway Between Front and Back Sample Positions: LN_2 Irradiation; North Chamber**

where $\phi(E > 2.9 \text{ Mev})/\phi(E > 8.1 \text{ Mev}) \doteq 25$, it may be assumed that the ratio $\phi(E > 2.9 \text{ Mev})/\phi(E > 7.5 \text{ Mev}) \doteq 17$. Therefore, values for the neutron flux for E >7.5 Mev are determined from the measured sulfur flux (E > 2.9 Mev) by multiplying this flux by 1/17. These values are also shown as dashed lines in Figures 3.8 and 3.9.

The gamma dose-rate values are shown in Figure 3.10 for both the north and east chamber locations. The solid line in Figure 3.10 is the average gamma dose rate along a line midway between the front and back rows of pull rods inside the east experimental assembly. These values were obtained from measurements made with N_2O gamma dosimeters located directly in front of and behind the specimen positions but on the outside of the chamber. The N_2O dosimeters mounted on the outside of the north chamber were accidentally destroyed during manual removal after irradiation.

The dashed lines in Figure 3.10 show the gamma dose rate along a line midway between front and back rows of pull rods inside the east and north assemblies obtained from previous measurements made in air (Ref. 5). These curves are, for reasons given below, considered to be a more reliable representation of the gamma flux in this run.

A considerable difference exists between the two gamma dose-rate curves for the LN_2 and LH_2 runs for the east cryogen chamber (compare Figs. 3.10 and 3.13). This variation can be attributed, in part, to the use of a lead shield on the reactor side of the assembly during the LN_2 run. An area on the front face of the cryo-

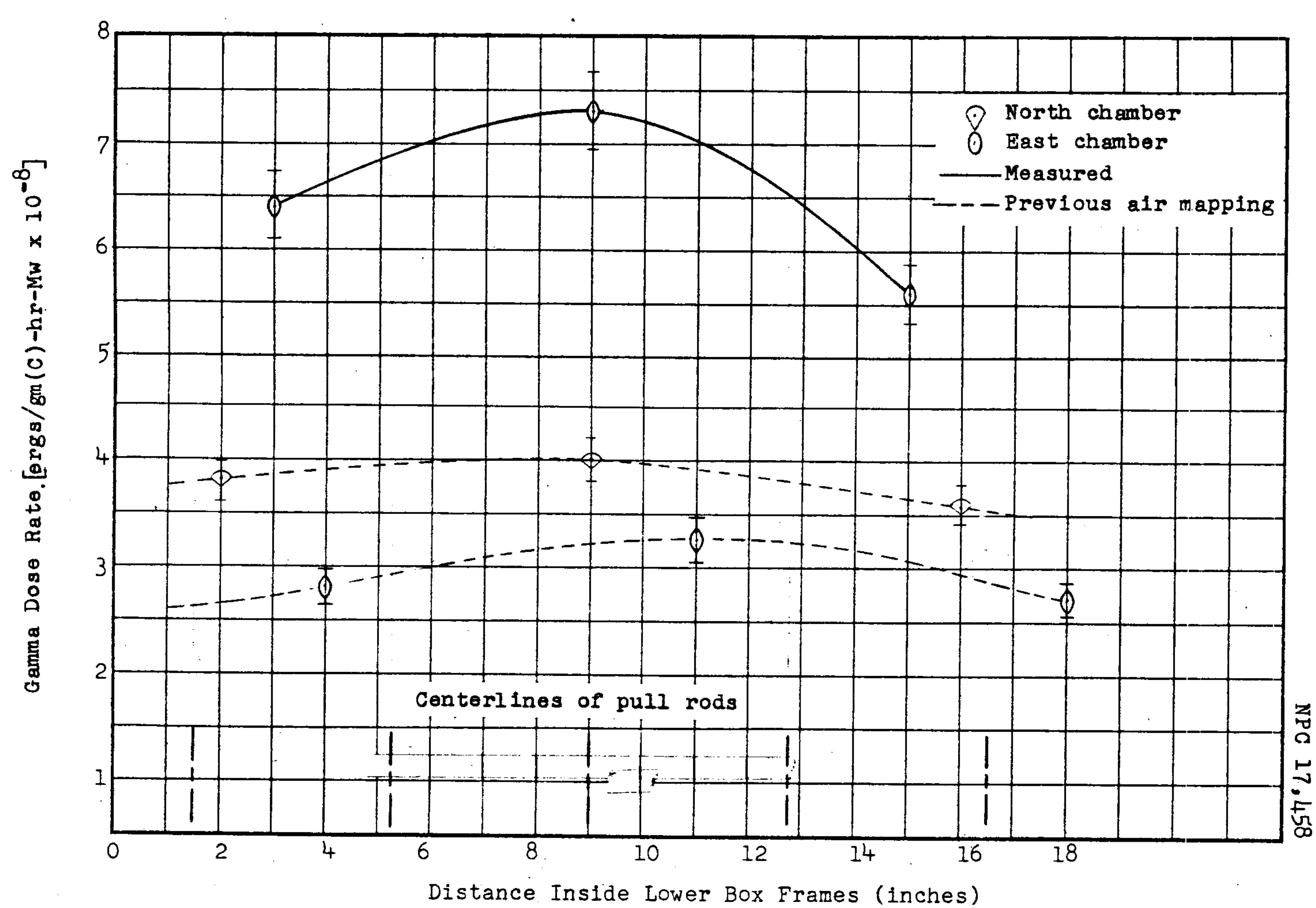

Figure 3.10 **Gamma Dose Rate Midway Between Front and Back Sample Positions: LN_2 Irradiation; East Chamber**

gen chamber sufficient to expose all specimens to a direct beam of radiation from the reactor was provided by a rectangular port in the shield. The dosimetry was then mounted on the exposed surface of the cryogen chamber within the confines of this port, which meant that the gamma dosimeters were in close proximity to the two-inch-thick, steel-enclosed lead. Heat buildup in this shield - estimates of the temperature are $600^{o}F$ to $800^{o}F$ - is thought to have caused the response rate of the nearby nitrous-oxide dosimeters to increase, resulting in erroneously high dose readings for the LN_2 run.

Nitrous-oxide dosimeters irradiated while submerged in liquid nitrogen in the north and east chambers were analyzed, but, because the results appeared somewhat erratic, they were considered not to be representative of actual gamma-dose levels. These values are given in Table 3.2 for information only.

Most of the polyethylene plastic dosimeters irradiated during this test were overexposed. The useful range of this type of dosimeter is from 1×10^8 to 1.5×10^9 ergs/gm(C). The results of post-irradiation processing of the polyethylene dosimeters indicated, however, that the integrated gamma doses at the north-front, north-back, and east-front positions were equal to or greater than 1.5×10^9 ergs/gm(C). Those dosimeters located at the east-back position showed an integrated dose of approximately 1.4×10^9 ergs/gm(C).

Table 3.2

Results from Nitrous-Oxide Gamma Dosimeters Irradiated in Liquid Nitrogen		
Positions	ergs/gm(C)	ergs/gm(C)-hr-Mw
	North Chamber	
Front 2	1.75×10^{11}	1.46×10^{9}
Front 6	1.7×10^{11}	1.42×10^{9}
Back 2	6.5×10^{10}	5.4×10^{8}
Back 6	(broken)	
	East Chamber	
Front 2	(not exposed)	
Front 6	(not exposed)	
Back 2	7.4×10^{9}	1.9×10^{8}
Back 6	8.3×10^{9}	2.1×10^{8}

3.3.3 Liquid-Hydrogen Irradiation Tests

Figures 3.11 and 3.12 show an average and analytical neutron flux determined in the same manner as that shown in Figures 3.8 and 3.9. Table 3.3 shows average values of the neutron flux above the given thresholds as a function of the neutron flux for $E > 2.9$ Mev. The data indicate that reliable measurements were obtained from the sulfur ($E > 2.9$ Mev) and aluminum ($E > 8.1$ Mev) threshold detectors.

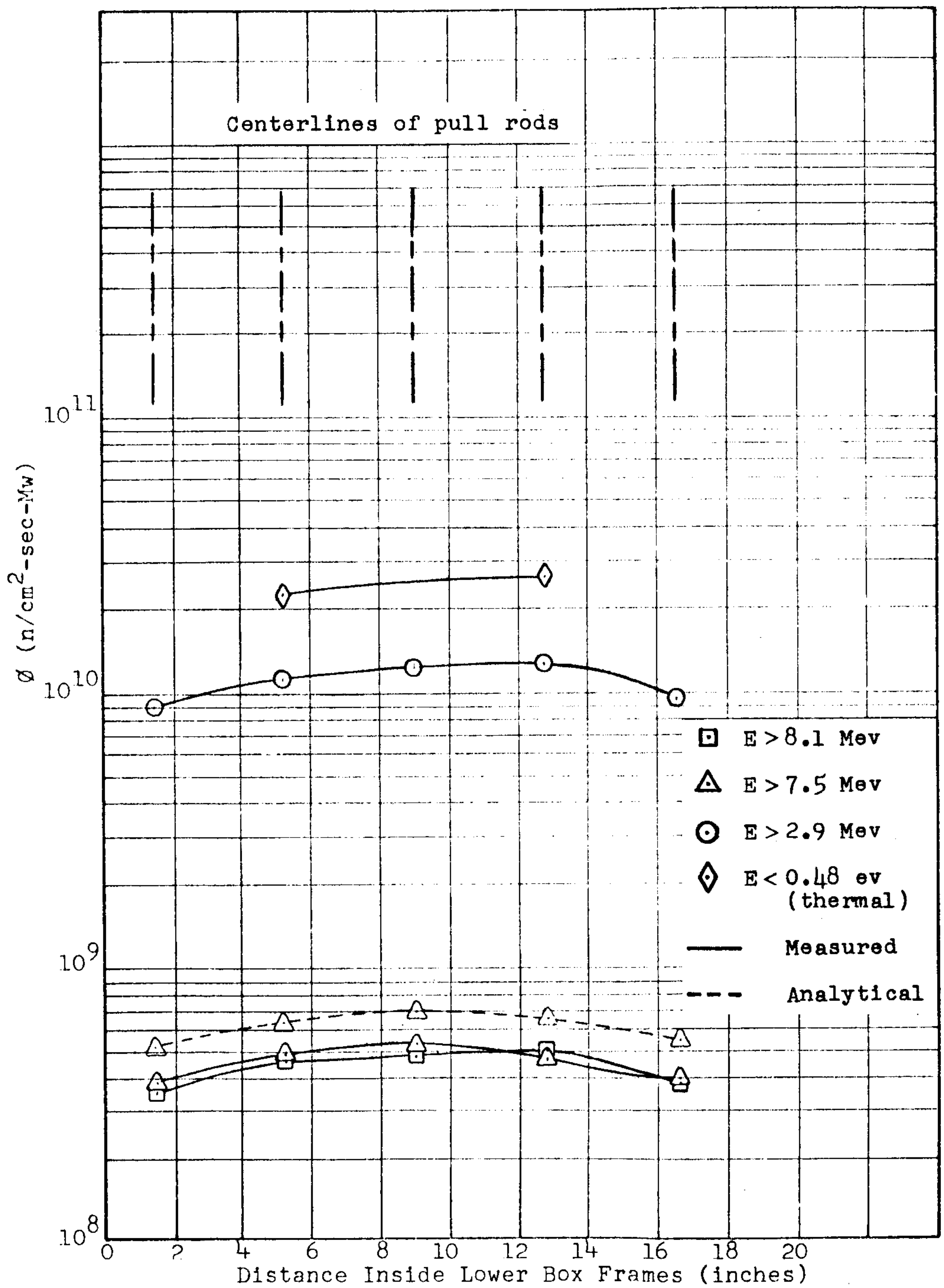

Figure 3.11 Neutron Flux Midway Between Front and Back Sample Positions: LH_2 Irradiation; East Chamber

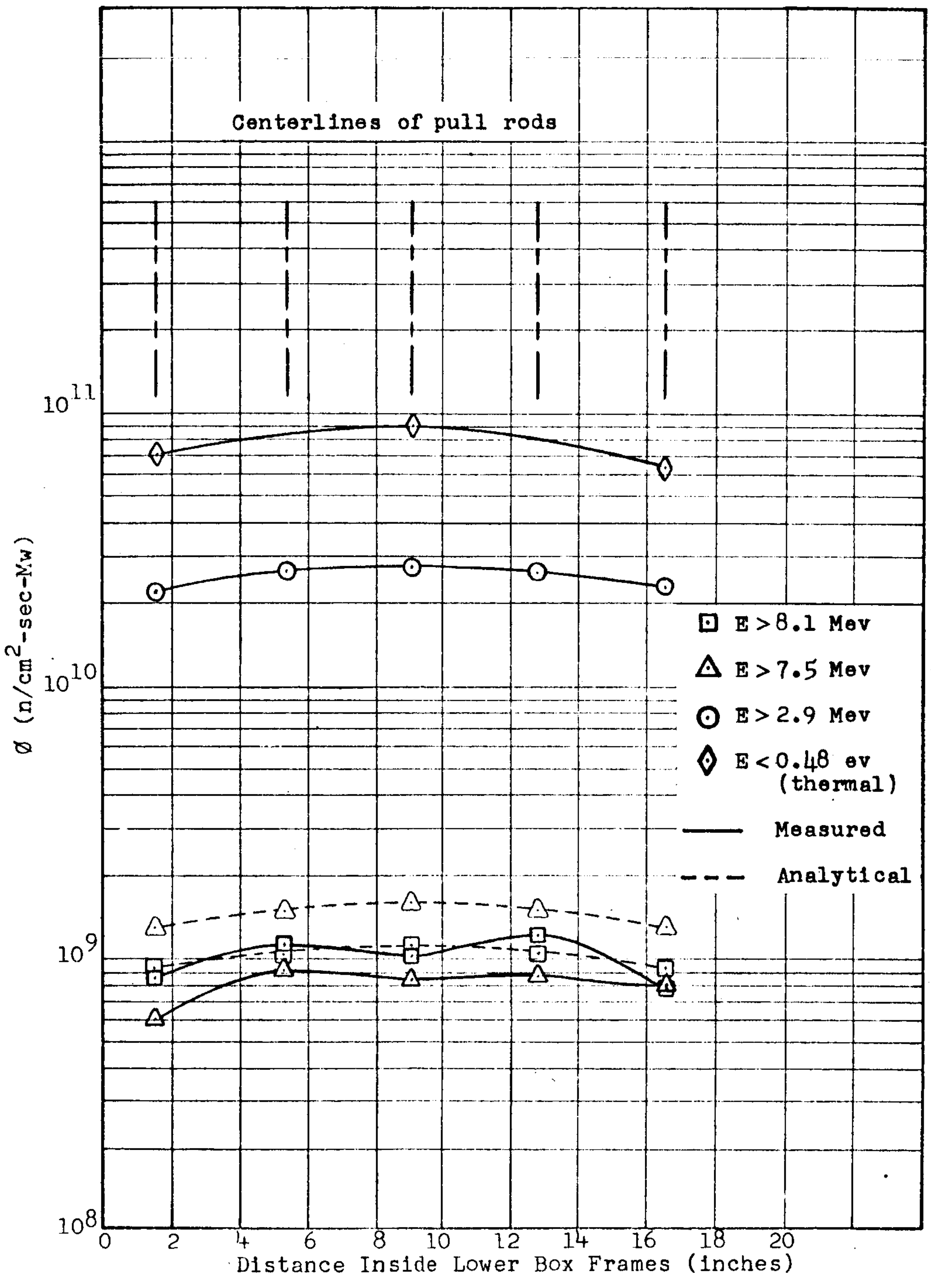

Figure 3.12 Neutron Flux Midway Between Front and Back Sample Positions: LH_2 Irradiation; North Chamber

Table 3.3

Neutron-Flux Ratios in East and North Cryogen Chambers			
Chamber	ϕ>2.9 Mev/$\phi_{o(Th)}$	ϕ>2.9 Mev/ϕ>7.5 Mev	ϕ 2.9>Mev/ϕ>8.1 Mev
East	0.45	24	25
North	0.35	31	25

Thermal-flux values in LH_2 are higher than those measured in air (Ref. 5), which is about as expected. Data on the thermal-neutron flux presented here are based on an ambient-temperature determination and do not reflect a conversion factor for the cryotemperature in the chamber. Use of a temperature correction factor to determine the true thermal flux involves two rather broad assumptions: (1) the neutrons are in thermal equilibrium with the surroundings, and (2) the energy distribution of the neutrons is indeed Maxwellian. Since neither of these assumptions may be substantiated, all thermal-flux values throughout this section are based on an ambient-temperature determination.

The average gamma dose rates along a line midway between the front and back pull rods in the east and north chambers are given in Figure 3.13. These values are shown as the solid lines. They were obtained from nitrous-oxide dosimeters placed directly in front of and behind specimen locations, but on the outside of the

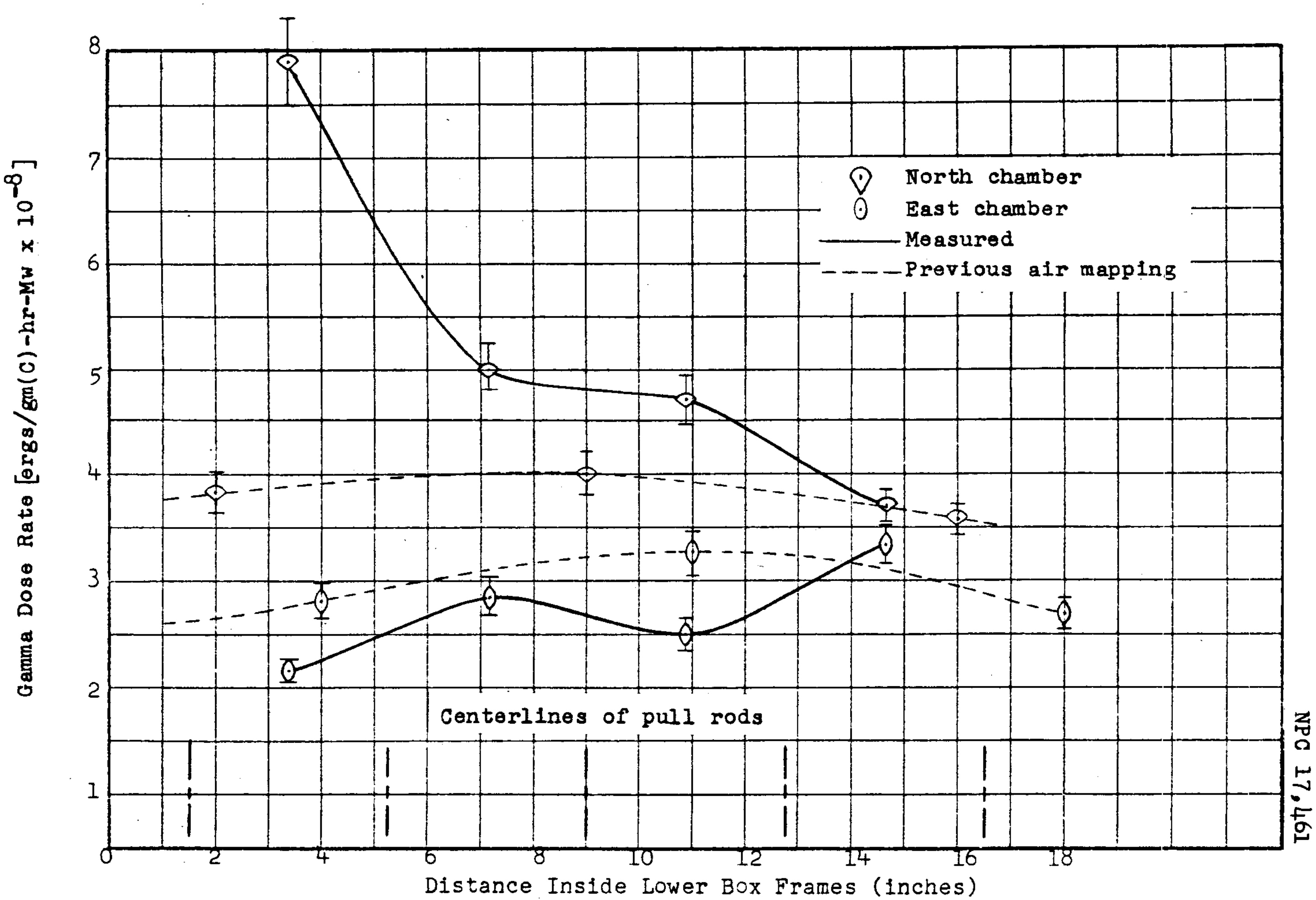

Figure 3.13 Gamma Dose Rate Midway Between Front and Back Sample Positions: LH_2 Irradiation; North and East Chambers

cryogen chambers. The broken lines are the gamma dose rates along the line just described and are obtained from previous measurements made in air (Ref. 5).

IV. TESTING PROCEDURES

The materials tested and the test plan for each are given in Table 4.1. In all tests, the ASTM procedure that was most applicable was followed as closely as possible. However, some modifications were required because of the environment involved and the use of remote control to operate the equipment. Shapes and dimensions of the test specimens were held very close to ASTM dictates, although some deviation was necessary where doublers, rod holes, and slots were needed, as in the dumbbell-type specimens of materials D, I, and J.

All tests were performed according to the test plan, with a few minor exceptions (which will be discussed individually) and one major exception. The major exception was concerned with the LH_2 high-dose tests for materials A, B, I, and J. A small fire of undetermined origin occurred in the area of the electrical and tubing harness of one experimental assembly after 20 hours operation in the LH_2 irradiation, resulting in termination of the test at this point. The harness was destroyed over a small section, which prevented the taking of any data on materials requiring the highest scheduled dose in the LH_2 run. This is reflected in the data and demonstrated in photographs of the tested specimens.

Temperatures of specimens during the ambient irradiation ranged from 110°F for those in the tray farthest from the reactor to 143°F for those nearest the face of the reactor.

Table 4.1

Materials Test Plan for Radiation-Cryotemperature Tests

Material Application	Material Designation	Chemical Class	Trade Name	Manufacturer	Tests Performed	Test Method	Type of Specimen	No. of Specimens Tested Per Data Point	Planned Value of Gamma Dose [ergs/gm(C)]	
									Low Dose	High Dose
Adhesive	A	Polyurethane	Hexcel 1252	Hexcel Products Inc.	Tensile-shear strength	ASTM-D-1002-53T (modified)	Lap-shear	4	1(10)*	5(10)
	B	Epoxy-polyamid	Metlbond 406	Normco Materials Div.	Tensile-shear strength	ASTM-D-1002-53T (modified)	Lap-shear	4	1(10)	5(10)
Seal	C	Tetra-fluoro-ethylene	Teflon TFE	E.I. du Pont de Nemours & Co.	Ult. tensile strength Ult. elongation Stress-Strain	ASTM-D-882-61T (modified)	Thin film (10 mil)	4	5(9)	1(10)
	D	Fluorocarbon	Kel-F-81	Minnesota Mining & Mfg. Co.	Ult. tensile strength Ult. elongation Stress-Strain	ASTM-D-638-61T (modified)	Dumbbell & O-ring	4	5(9)	1(10)
Thermal Insulation	E	Polyurethane	Stafoam AA402	American Latex Products Co.	Compression-Deflection	ASTM-D-1565-59T (modified)	1.129 in. diam. x 0.50 in. thick Compr. button	1	5(9)	1(10)
	F	Polystyrene	Styrofoam 22	Dow Chemical Co.	Compression-Deflection	ASTM-D-1565-59T (modified)	1.219 in. diam. x 0.50 in. thick Compr. button	1	5(9)	1(10)

*Read 1(10) as 1×10^{10}

Table 4.1 (cont'd)

Material Application	Material Designation	Chemical Class	Trade Name	Manufacturer	Tests Performed	Test Method	Type of Specimen	No. of Specimens Tested Per Data Point	Planned Value of Gamma Dose [ergs/gm(C)]	
									Low Dose	High Dose
Electrical Insulation	G	Polyimid	H-Film	DuPont	Ult. tensile strength Ult. elongation Stress-Strain	ASTM-D-822-61T (modified)	Thin film (2.5 mil)	4	5(9)	1(10)
	H	Polyester	Mylar-C	DuPont	Ult. tensile strength Ult. elongation Stress-Strain	ASTM-D-822-61T (modified)	Thin film (1 mil)	4	5(9)	1(10)
Structural Laminate	I	Phenolic	Conolon 506	GD/FW (Normco Materials Div.)	Ult. tensile strength Ult. elongation Stress-Strain	ASTM-D-638-61T (modified)	Dumbbell	4	1(10)	5(10)
	J	Polyester	Paraplex P-43	NASA (Rohm & Haas)	Ult. tensile strength Ult. elongation Stress-Strain	ASTM-D-638-61T (modified)	Dumbbell	4	1(10)	5(10)
Thermal-Control Coating	K	Epoxy	Skyspar A423	Andrew Brown Co.	α/ϵ ratio	Test performed by GD/Astro	Wafer	3	5(9)	1(10)
	L	Acrylic	W-49-BC-12	Sherwin Williams	α/ϵ ratio	Test performed by GD/Astro	Wafer	3	5(9)	1(10)

4.1 Material A: Hexcel 1252

The samples for testing this adhesive were prepared by the laboratories at the George C. Marshall Space Flight Center, Huntsville, Alabama. The adhesive was applied in a ½-in.-wide strip across the ends of 6-in.-wide, 1/16-in.-thick aluminum sheets. The 2024 aluminum sheets were cleaned chemically by standard procedures before application of the adhesive. One hundred grams of the adhesive (1252) was thoroughly mixed with 5 mg of a catalyst (1252C) and this mixture applied to the bond area of each aluminum sheet. After air-drying for 30 minutes, a thin coat of the adhesive was applied to one of the sheets making up the sample and the two sheets placed together so that the ½-in. bond areas overlapped. Reduction of the glue area was at first considered necessary because the pulling forces obtainable on the pull rods through the hydraulic servosystem reached a maximum of about 3000 lb (instead of the desired capability of 10,000 lb) at Instron crosshead speeds below 0.10 in./min. Apparently, small leaks past piston seals and through fitting joints developed at hydraulic pressures of around 300 psi (or 3000 lb total force). The transmission rate of fluid from the Instron master cylinder to the slave cylinder at these slow speeds was then less than the leak rate, which resulted in a gradual slowing-down and an ultimate stop in pull-rod movement at these pressures.

The problem of testing materials under these conditions existed with Materials B, I, and J, as well as A. It was partially solved by reducing the glue area on Material A and, later on, during the tests, by raising the crosshead speed to the point of surpassing the leak rate for tests on the other materials. This increase in crosshead speed provided higher pull-rod forces, but pull-rod rates remained on the low side and, in some cases, amounted to only one-tenth of that called for in the test plan.

Some Material A specimens failed in the doublers, but most were tested satisfactorily. The data for Material A are tabulated in Table A-1, and a photograph of representative specimens which were tested under all nine conditions is shown in Figure 4.1. The conditions were as follows: no-irradiation (No IRR.); irradiated, low dose (IRR., L.D.), and irradiated, high dose (IRR., H.D.) at each of three temperatures. A standard untested specimen is shown at the top of the figure.

4.2 Material B: Metlbond 406

This material was also furnished by the George C. Marshall Space Flight Center. Aluminum sheets (2023-T3), 4 by 6 by 1/8 in., were degreased by wiping with toluene and soaking in warm water containing Alconox detergent. After thorough rinsing and air-drying, the bond areas were cleaned by a solution containing 330 gm of sodium dichromate 2H 20, 2740 ml of distilled water, and 525 ml of 95% sulphuric acid. This solution was kept at from 150° to 160°F for 20 minutes before using. The test pieces were rinsed and air-dried. The bond area of all pieces was coated with liquid Metlbond 408, applied with a brush. This coat was air-dried a minimum of two hours.

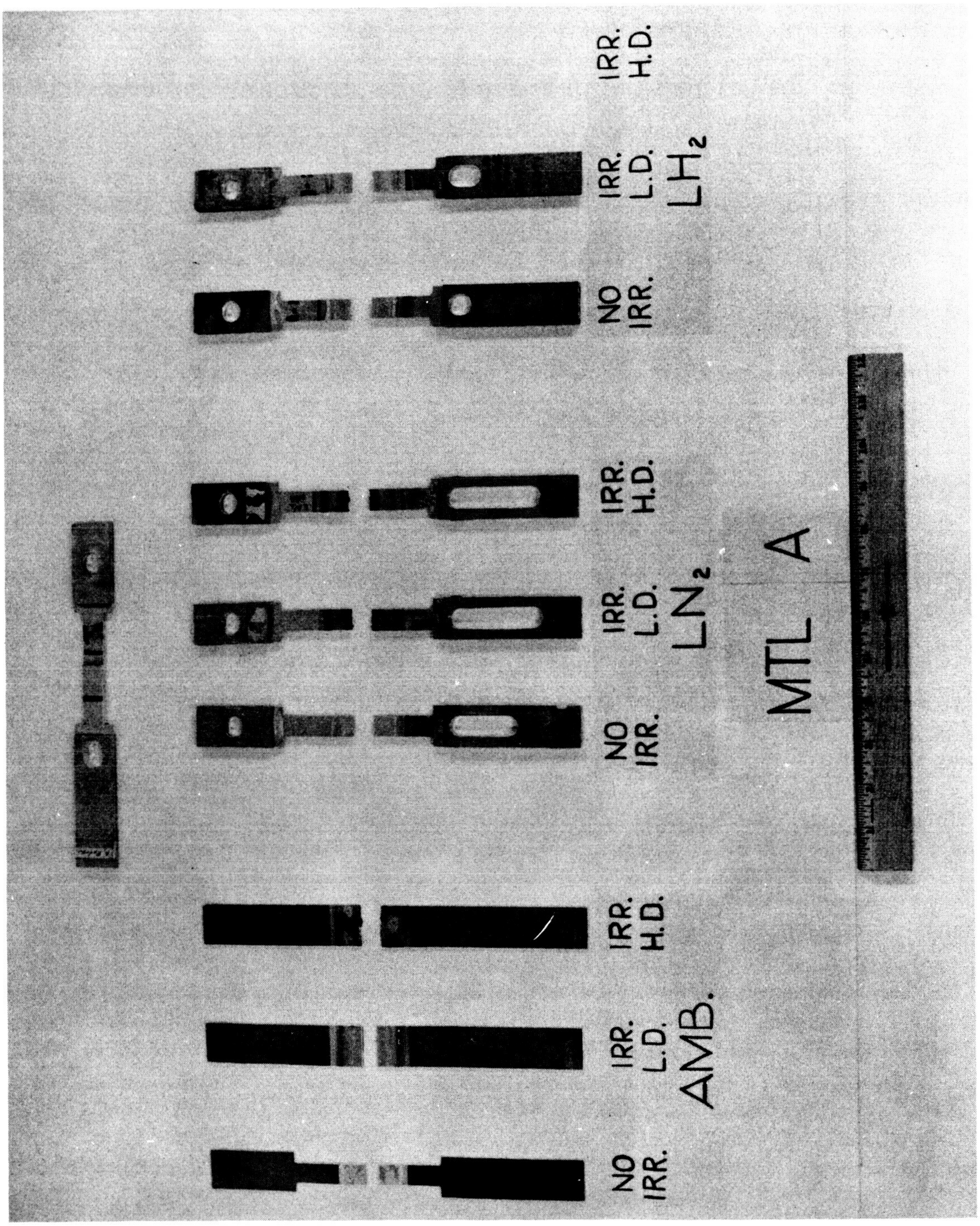

Figure 4.1 Material A Specimens

A strip of the Metlbond 408 was applied to one side of the test sample and placed in a hot-air oven at 105°C for one hour. This piece was used with a primed-air-dried half and was overlapped $\frac{1}{2}$ inch. The excess adhesive film was removed and the sample was placed in a modified Carver press at about 5 psi for 5 minutes at 300°F. The pressure was released for about 30 seconds and the sample cured for one hour. The sample was removed and a 3/8-in. strip cut from its side and discarded. The remainder of the sample was cut to 1-in.-wide strips for test specimens. The excess adhesive was removed from all bond edges and the bond area was measured to ±0.005 inch. The cure was for one hour at 350°F at 25 psi.

The glue area of these specimens was 1 by $\frac{1}{2}$ in. Most of the test specimens pulled satisfactorily, with very few showing breaks in the doublers. The doublers, in the case of both A and B materials, were made from 1/16-in.-thick aluminum sheet and were glued and riveted to both sides and both ends of each specimen.

Data for Material B are tabulated in Table A-2. Figure 4.2 is a photograph of representative specimens which were tested under the nine conditions.

4.3 Material C: Teflon TFE

This material was tested for stress-strain, tensile strength, and ultimate elongation at the ambient-temperature, no-irradiation condition only. It was irradiated to the low and high doses at ambient temperature in air, but the specimens crumbled while being removed from the mounting trays. The specimens were in thin-film

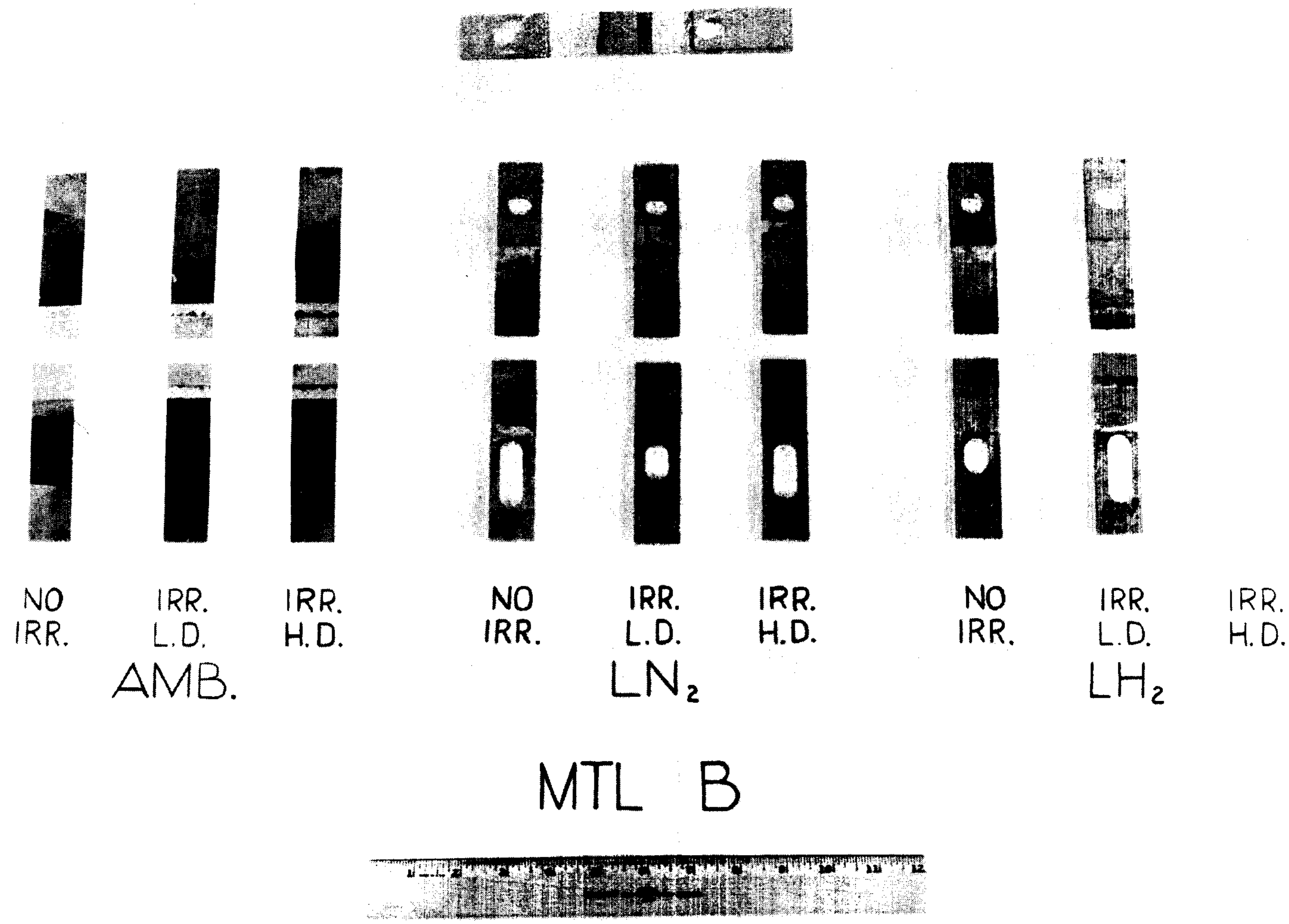

Figure 4.2 Material B Specimens

form (10-mil thickness), but all attempts to glue them to the thin-film-tester spools used for low-temperature tests in the experimental assemblies failed.

The data for this material are tabulated in Table A-3. Figure 4.3 is a photograph of the specimens.

4.4 <u>Material D: Kel-F-81</u>

This material was tested in the form of a dumbbell tensile specimen and as an O-ring. Doublers for the tensile specimens were made from aluminum sheet and were glued and riveted on. About 20% of these specimens, upon inspection, were found to be broken in the doubler area. Analysis of the data, however, indicated that most of these probably broke in the narrowed section of the specimen first.

The normal procedure for testing dumbbell-type specimens in tension is, of course, to attach an extensometer to a 2-in. gage length in the center of the narrowed section of the specimen and to measure the resulting strain over this gage length as the specimen is pulled. However, no provision was made for any kind of remotely operated extensometer to be used with specimens submerged in cryogen in the experimental assemblies. Instead, only the extension between clevis rods was measured. This approximates the crosshead extension, or extension between clamping jaws, of a specimen tested in a standard tensile machine.

The ambient-temperature dumbbell-type specimens, however, were tested with the use of an extensometer, and both crosshead extension and gage-length extension were recorded. The procedure of

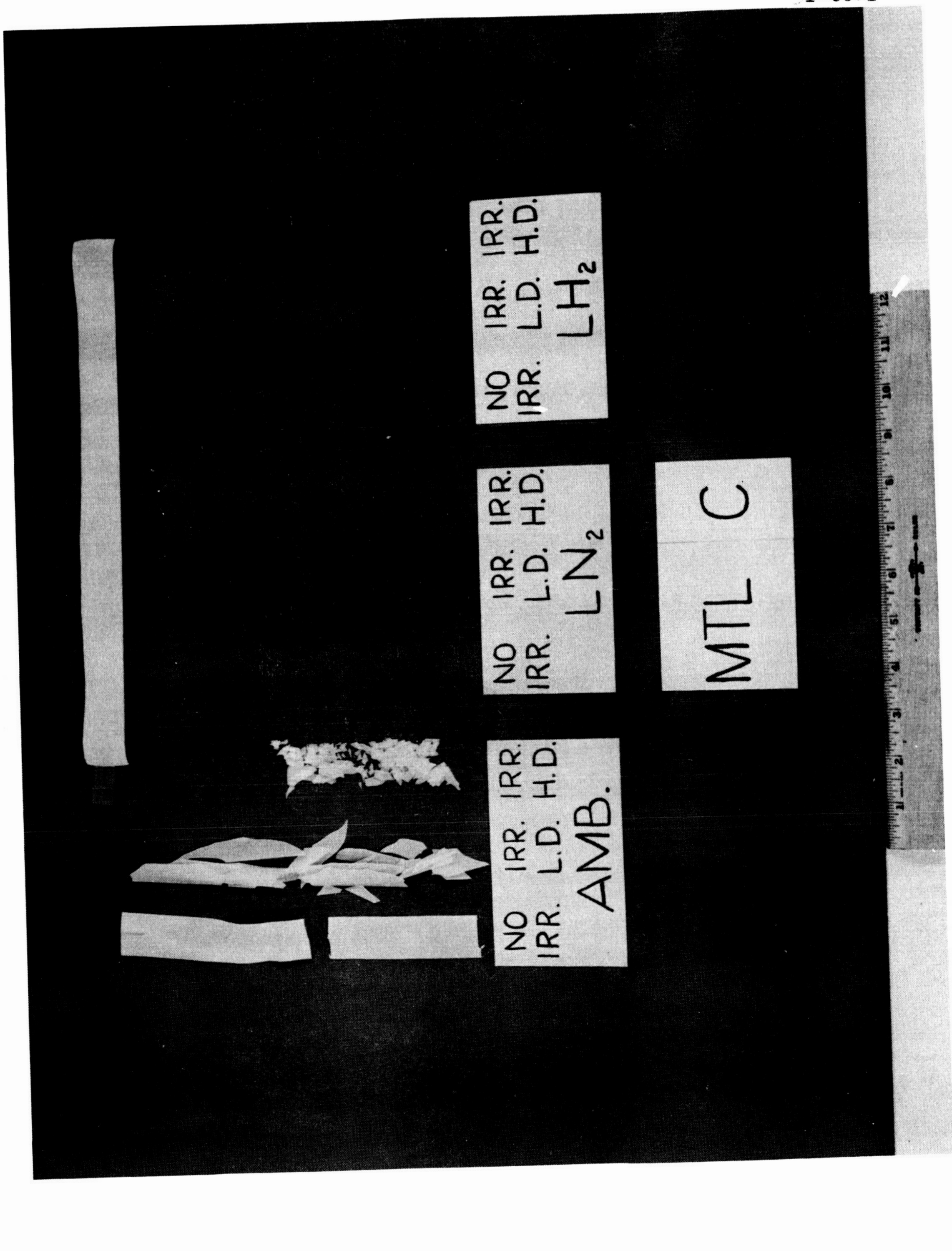

Figure 4.3 Material C Specimens

taking both extensometer and crosshead data on one group of specimens applied to all materials with dumbbell-type specimens, namely, Materials D, I, and J.

No tests were performed on Material D specimens that were irradiated to the high dose at ambient temperature. The environment had embrittled them to the point that they fractured as they were being removed from the mounting trays.

Material D was also machined into O-rings to test the sealing characteristics of the material under the combination environment of nuclear radiation and cryotemperature. Pressure chambers (Fig. 2.6) were fabricated to contain these O-rings as seals between the flanges. Both the O-ring and the O-ring groove in the flange were of standard dimensions. These chambers were pressurized with helium gas during the irradiations, and periodic checks of the leak rates were made. Postirradiation checks of the pressure-holding characteristics, as well as visual inspection of the rings, were made. In addition, tests were run to determine ultimate tensile strength, and the resulting values were checked against similar values for unirradiated O-rings.

As mentioned above, both extensometer deflection and crosshead deflection (or deflection between clamping jaws) were measured as a function of load for one group of specimens at ambient temperature. From these data, taken on three specimens for Material D, the average loads for unit crosshead (or pull-rod) deflection and unit extensometer deflection were determined (see Table A-5). With these average data, a constant equal to the ratio of extensometer deflection to pull-rod deflection was calculated. Each value of unit pull-rod deflection, corresponding to average loads of specimens pulled in the experimental assemblies under cryotemperature conditions, was then multiplied by this constant to obtain hypothetical extensometer strain values for these low-temperature specimens. These calculated values are included with the data taken for this material, as shown in Tables A-4 through A-11.

Figure 4.4 is a photograph of representative tensile specimens pulled during the experiment.

4.5 Material E: Stafoam AA-402

Tare loads resulting from drag on both the master-cylinder piston and the slave-cylinder piston existed with all tests that utilized this hydraulic servo system. These loads were a function of Instron crosshead speed, being larger for higher speeds, and varied from about 150 to 450 lb for crosshead speeds between 0.05 in./min and 0.50 in./min. These loads were discernible on the Instron chart during movement of both pistons just prior to contact with the specimens. In instances involving pull rods with dynamometers installed, the tare load of the slave piston itself was indicated on the dynamometer chart, with the total tare on the entire system being recorded on the Instron chart. In tabulating load data for all specimens, tare loads were of course subtracted to obtain the true loads on the specimens.

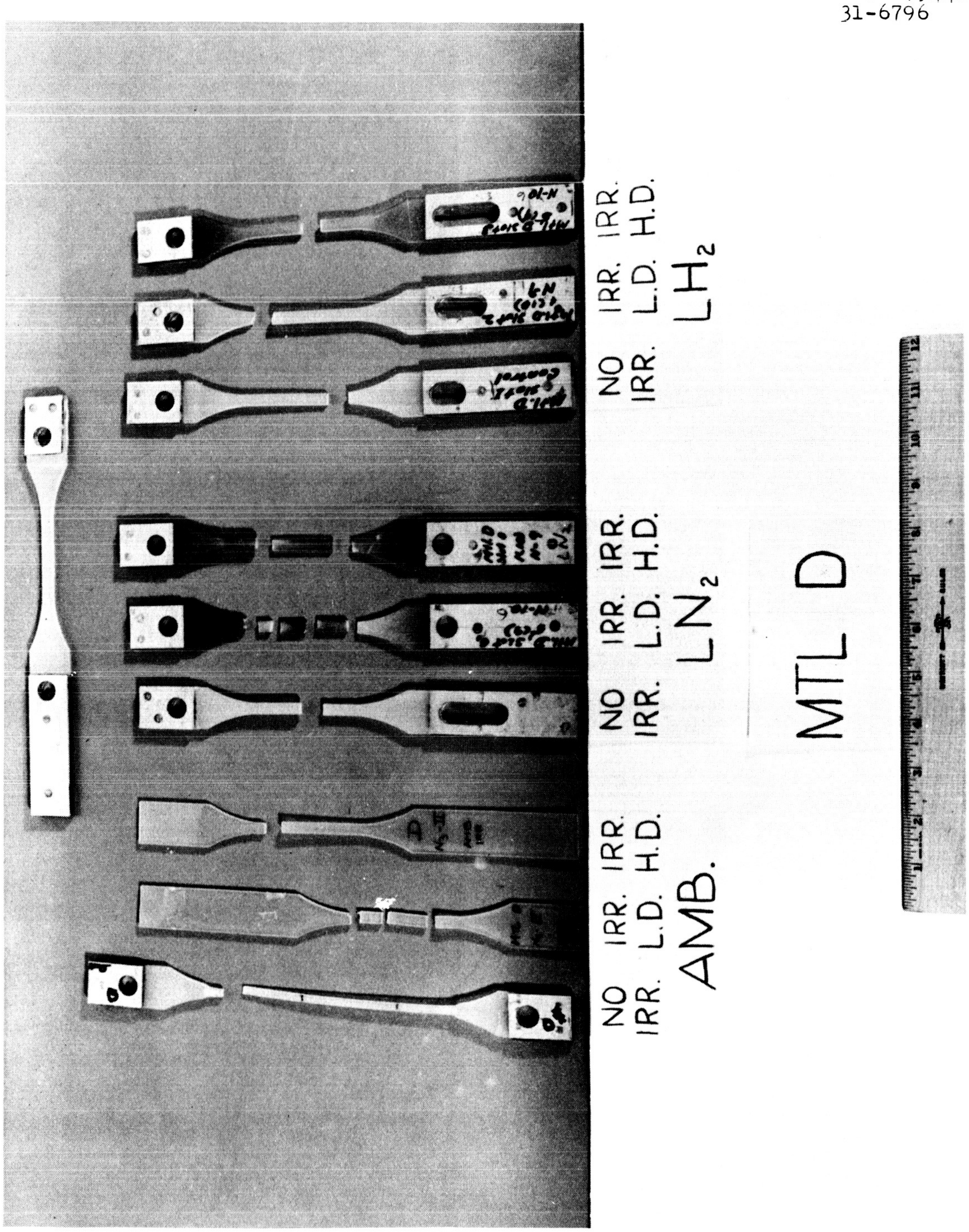

Figure 4.4 Material D Specimens

Materials E, F, G, and H all required net loads of from about 20 to 150 lb to complete the required test. A careful analysis of the charts was thus necessary to accurately subtract out the relatively high percentage of the total load which amounted to tare.

During the portions of these tests in which dynamometer data as well as Instron data were available, the pure tare load, which was recorded just prior to contact with a specimen, was lower on the dynamometer chart than on the Instron chart. This is to be expected, since the dynamometer was seeing tare load on the slave piston only. But when the specimen was picked up, the differential loads on the dynamometer chart were consistently higher than the differential (or specimen) loads recorded on the Instron chart. This was somewhat paradoxical, but it was finally concluded that when a specimen was picked up, the extra load on the pull rod served to slow down the pull-rod speed, thus lowering the total tare load by an amount equal to the difference between the specimen loads indicated on the two charts. Representative examples of Instron and dynamometer traces which illustrate this phenomenon are shown in Figure 4.5.

From this, it was decided that, for specimens requiring relatively lower loads during testing, dynamometer readings were more reliable and would be used in the data tabulation. In addition, it was decided that for low-load type specimens (Materials E, F, G, and H) tested on pull rods with no dynamometers installed, the specimen loads as indicated on the Instron chart should all be

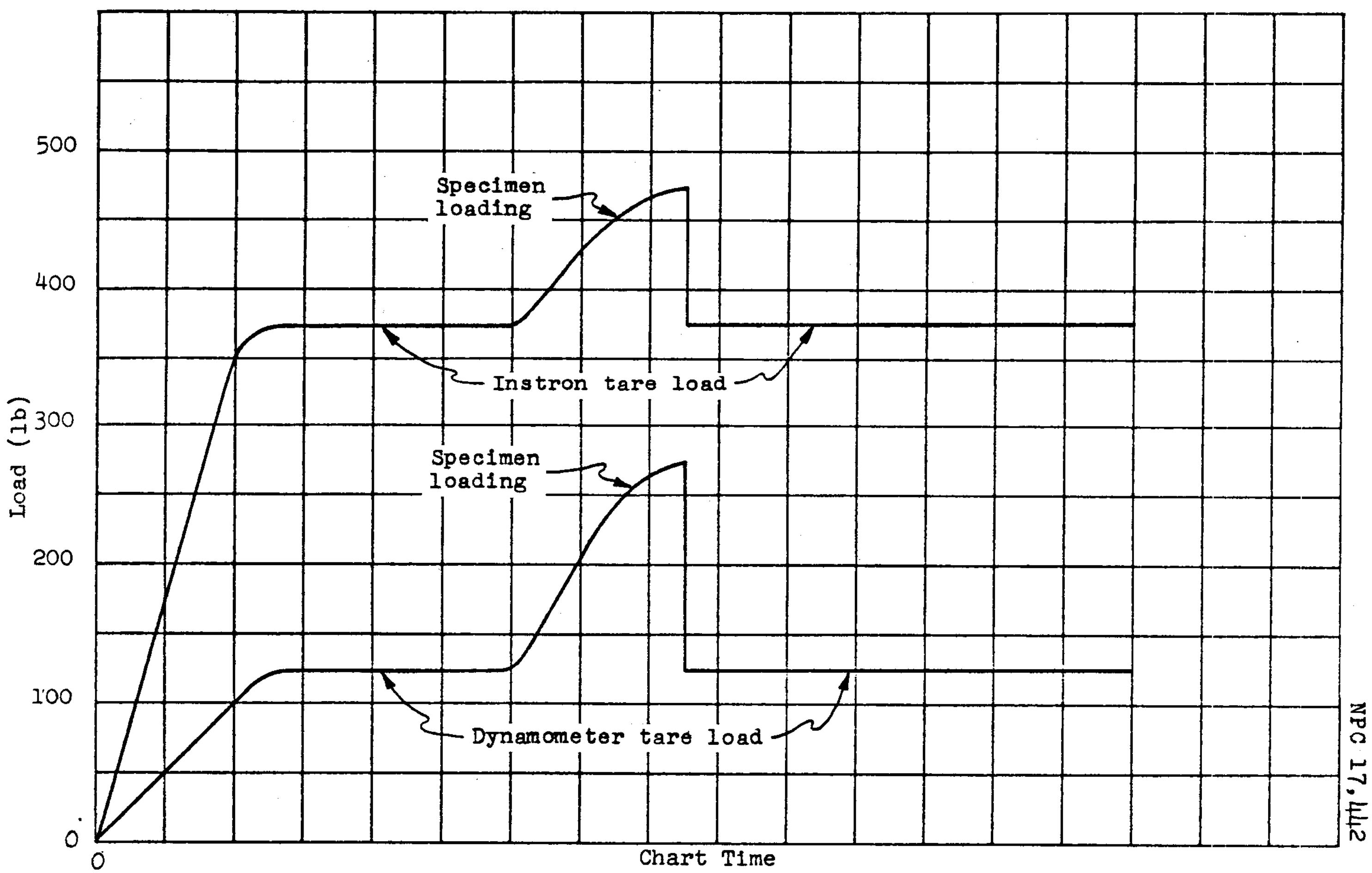

Figure 4.5 Representative Examples of Instron and Dynamometer Traces

multiplied by a factor which was determined as the average specimen load measured directly by a dynamometer divided by the corresponding specimen load taken from the Instron chart. This factor was 1.5.

Material E specimens were tested in compression, and stress-strain data were taken for deflections up to approximately 0.25 inch (50% of original specimen thickness). The above factor (1.5) was applied to specimens tested in the experimental assemblies on pull rods with no dynamometer installed.

As discussed under Section V , data were obtained from one specimen only for several data points. The material was tested under all nine conditions, however. The data are tabulated in Tables A-12 through A-17. Figure 4.6 is a photograph of representative specimens which have been tested under the various conditions.

4.6 Material F: Styrofoam 22

Specimen shape and size, tests, and test characteristics for this material were identical to those for Material E. The policies used for Material E in tabulating loads from dynamometer and Instron data were also followed for this material. The data are tabulated in Tables A-18 through A-23. A photograph of representative tested specimens is presented in Figure 4.7.

4.7 Material G: DuPont H-Film

This material was tested as a thin film and was pulled in tension to obtain stress-strain characteristics, ultimate tensile strength, and ultimate elongation. A 4-in. gage length was used. Total length of the original specimens was 12 inches, with each end

NPC 17,443
31-6794

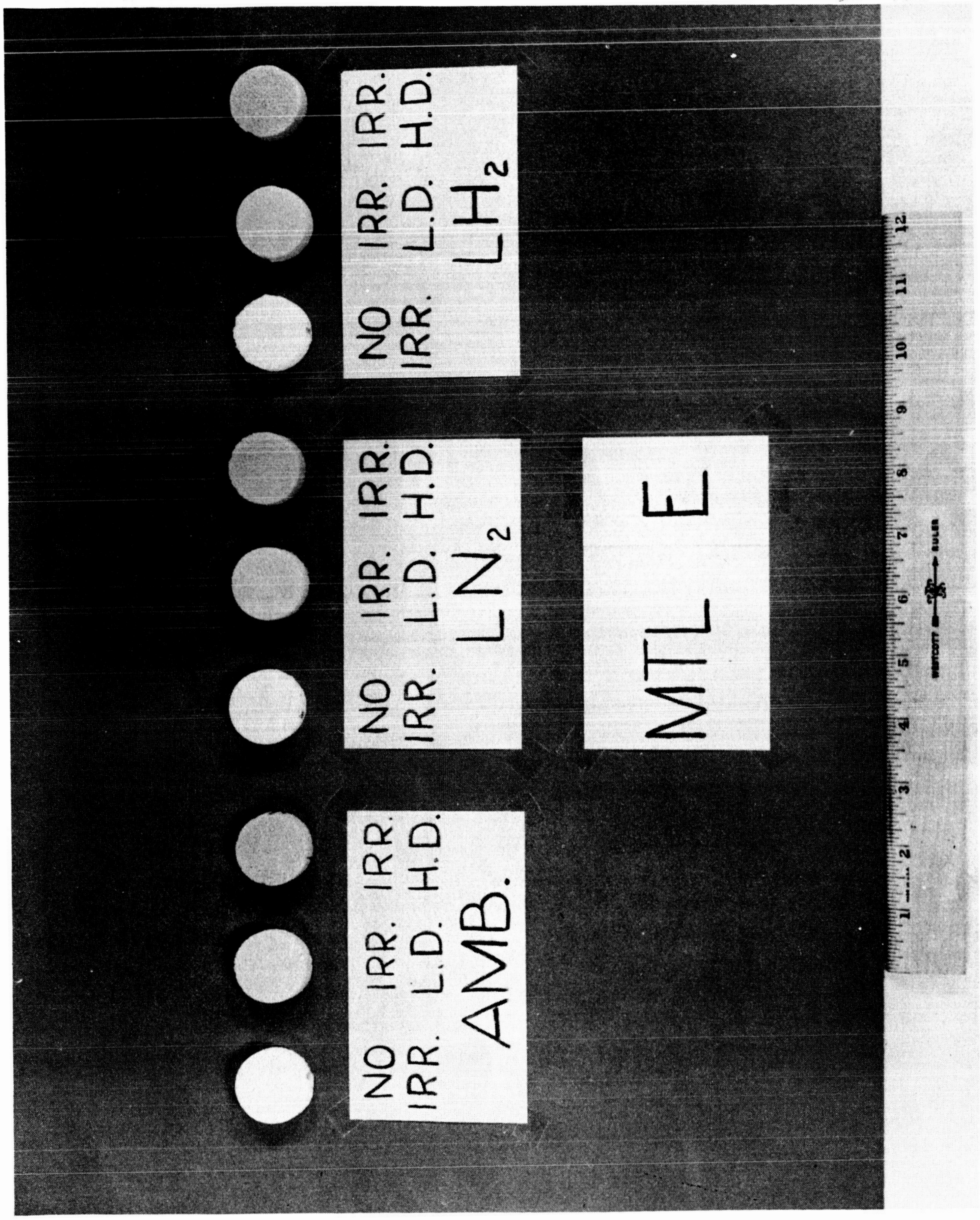

Figure 4.6 Material E Specimens

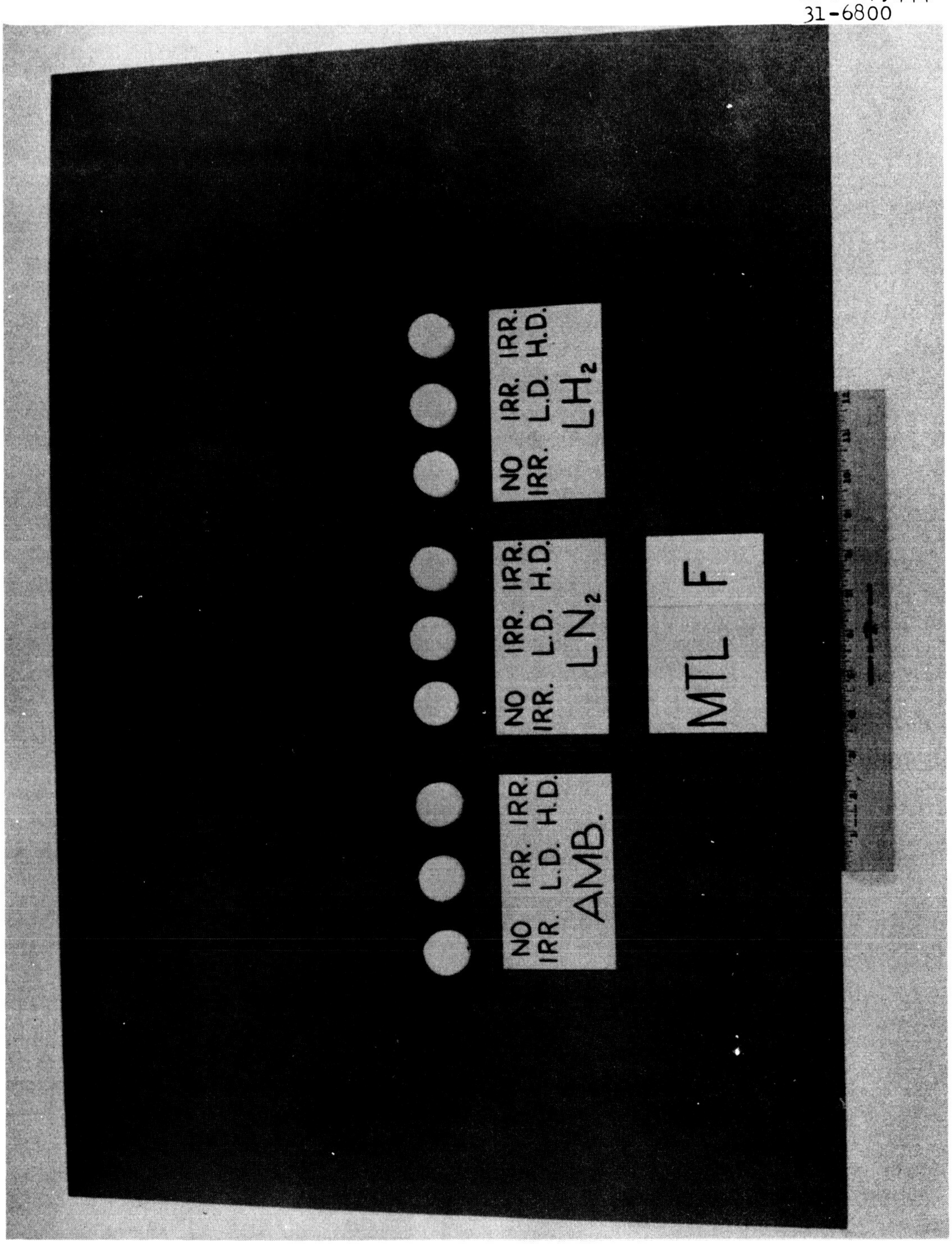

Figure 4.7 Material F Specimens

being glued and rolled up on a spool to the 4-in. gage-length spacing. Ambient-temperature tests were performed in the Instron machine. Cryotemperature tests were performed by use of the thin-film testers shown in Figure 2.5. Specimens were 1 inch wide and 2.5 mils thick.

Considerations involving load measurements (discussed in the above sections) are also applicable to tests on the H-film.

The data taken in the experiment for this material are shown in Tables A-24 through A-32. Figure 4.8 is a photograph of representative specimens, both tested and untested. No detectable difference existed between specimens tested under the various conditions.

4.8 Material H: DuPont Mylar-C

Specimens, tests, and test characteristics for this material were identical to those for Material G, except that thickness of the film tested was 1 mil. The data taken during tests are shown in Tables A-33 through A-40. Since the appearance of the material before and after testing was identical to that of Material G, no photographs were made. Photography would have been difficult anyway, since the material was perfectly clear both before and after irradiation. The H-film was amber colored, and its appearance did not change during irradiation.

4.9 Material I: Conolon 506

This material was milled into dumbbell-type specimens and tested in tension for stress-strain characteristics, ultimate tensile

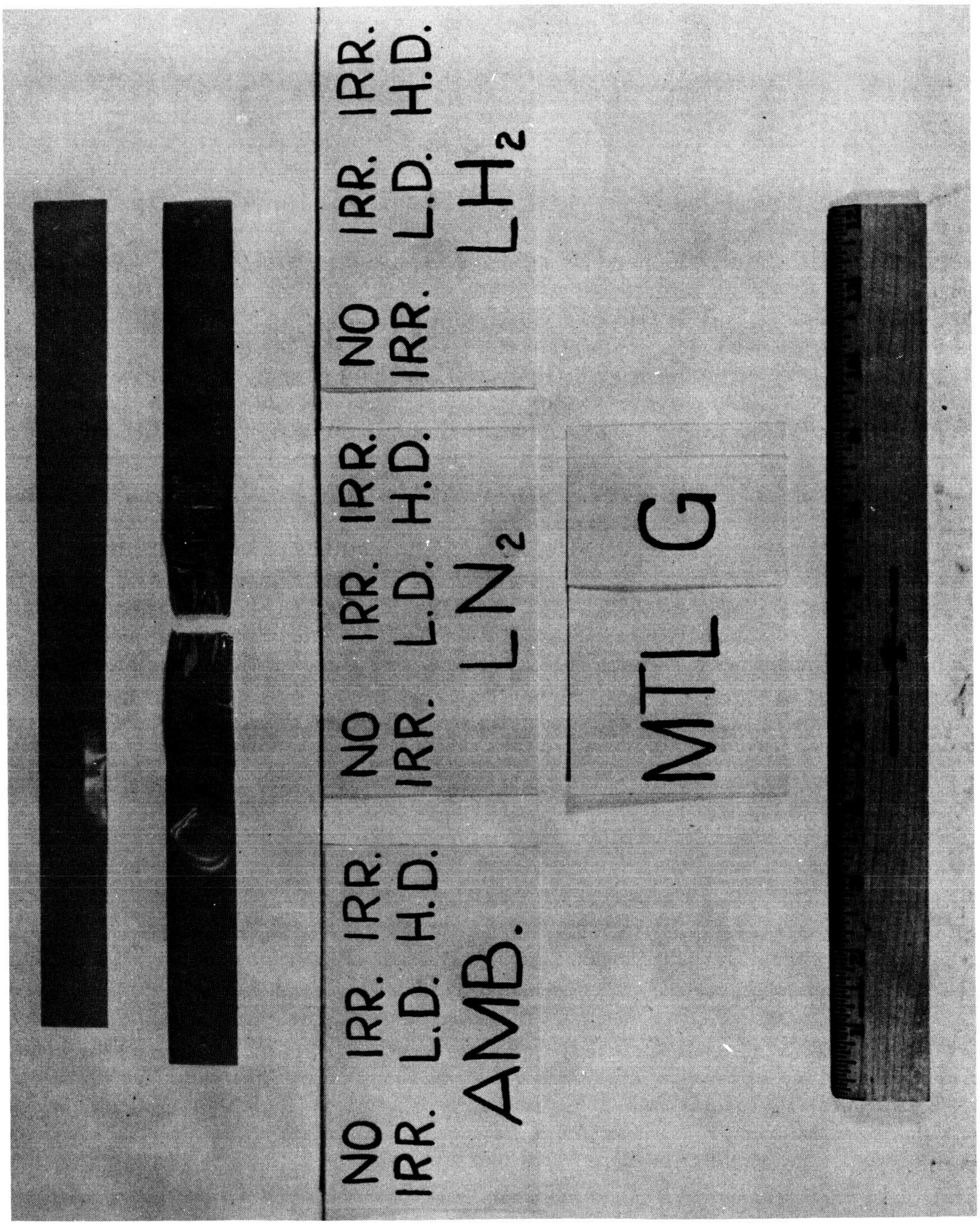

Figure 4.8 Material G Specimens

strength, and ultimate elongation. The specimens contained doublers made from the same material and glued into place.

As in the case of Material D, one group of ambient-temperature specimens was tested with the use of an extensometer. Strain values from both the extensometer extension and the crosshead movement were recorded, and unit deflections for average loads from two or three specimens were determined. With these data, a constant equal to the ratio of unit extensometer deflection to unit crosshead deflection was calculated and used to obtain the hypothetical extensions over a 2-in. gage length for specimens tested in the experimental assemblies at cryotemperatures.

Authenticity of these calculated (or hypothetical) extensions for specimens which have been irradiated and reduced in temperature to levels approaching absolute zero is dependent upon the reliability of the equation

$$\frac{x}{y} = \frac{x^1}{y^1} ,$$

where x = extensometer deflection at room temperature for an unirradiated specimen;

y = crosshead extension (or extension over the $5\frac{1}{4}$-in. portion of the specimen located between the top and bottom doublers) for an unirradiated specimen at room temperature;

x^1 = calculated (or hypothetical) extension of a 2-inch gage length of the irradiated, low-temperature specimen; and

y^1 = the crosshead (or pull-rod) extension of the irradiated, low-temperature specimen, as measured by the LVDT in the experimental assembly.

A theoretical discussion concerning the reliability of this relationship will not be attempted at this point. The calculated values, however, are included with the data taken for this material. These data are tabulated in Tables A-41 through A-48. Representative specimens tested are shown in Figure 4.9.

4.10 Material J: Paraplex P-43

Specimen shapes and sizes, tests, and test characteristics for this material were identical to those for Material I. The discussion under Section 4.9 concerning extensometer measurements is also applicable to Paraplex P-43 specimens. The tests for both materials I and J were performed satisfactorily and according to plan, except for the high-dose part of the LH_2 run. Data for Material J are shown in Tables A-49 through A-56. Figure 4.10 is a photograph of tested specimens.

4.11 Materials K and L: Coatings

Material K is a coating consisting of Skyspar A 423-SA9185, untinted epoxy white, with SA9184 epoxy primer; Material L consists of W49BC12 acrylic black lacquer, with P40GCL Kemacryl lacquer pretreatment primer. These coatings were prepared on 15/16-in.-diam aluminum wafers. Four coatings of the white were applied and two coatings of the black. Specimens were irradiated (1) at ambient temperature in air, (2) while submerged in LN_2, and (3) while submerged in LH_2. They were subsequently shipped, at room temperature, to General Dynamics/Astronautics, where optical measurements

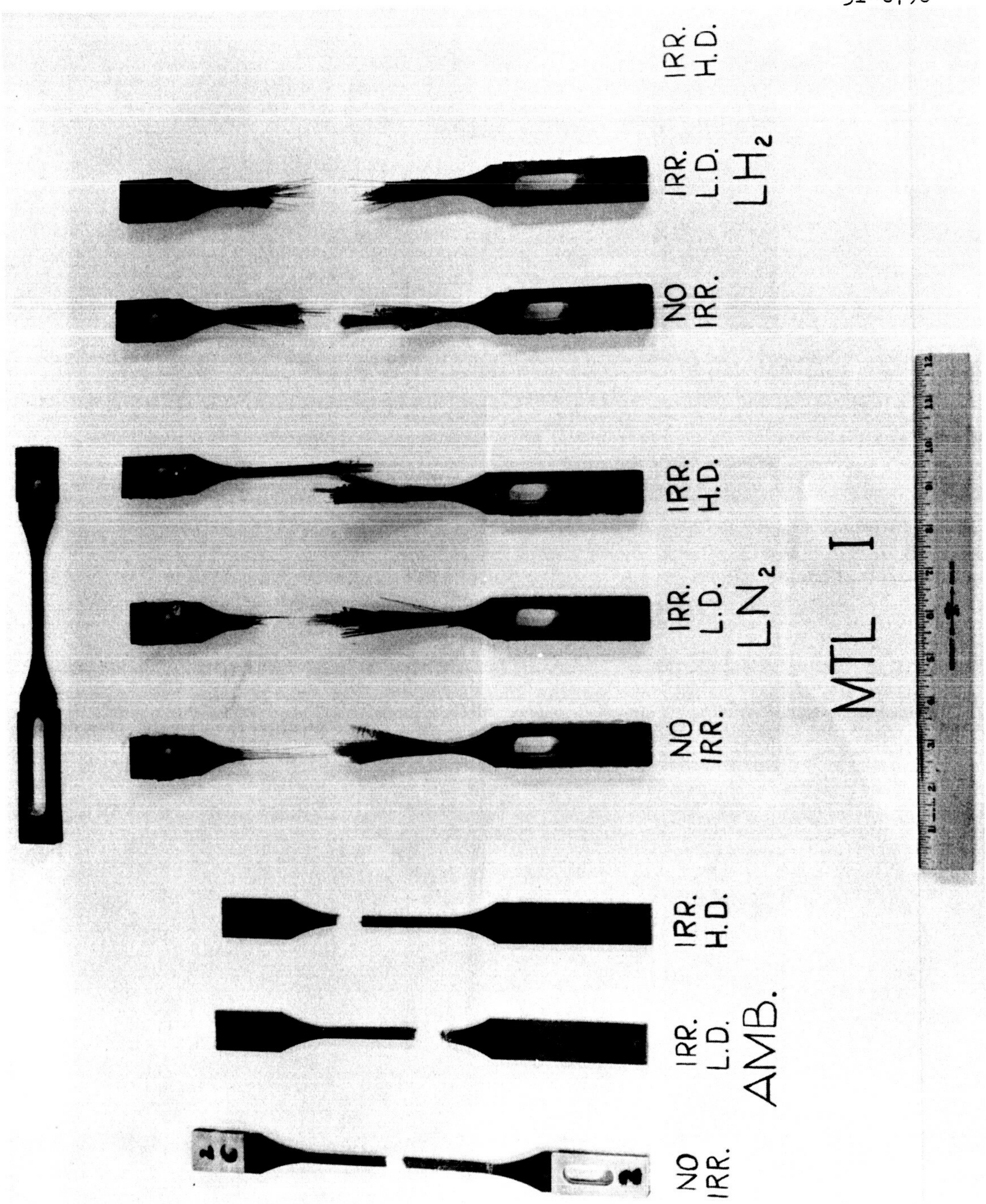

Figure 4.9 Material I Specimens

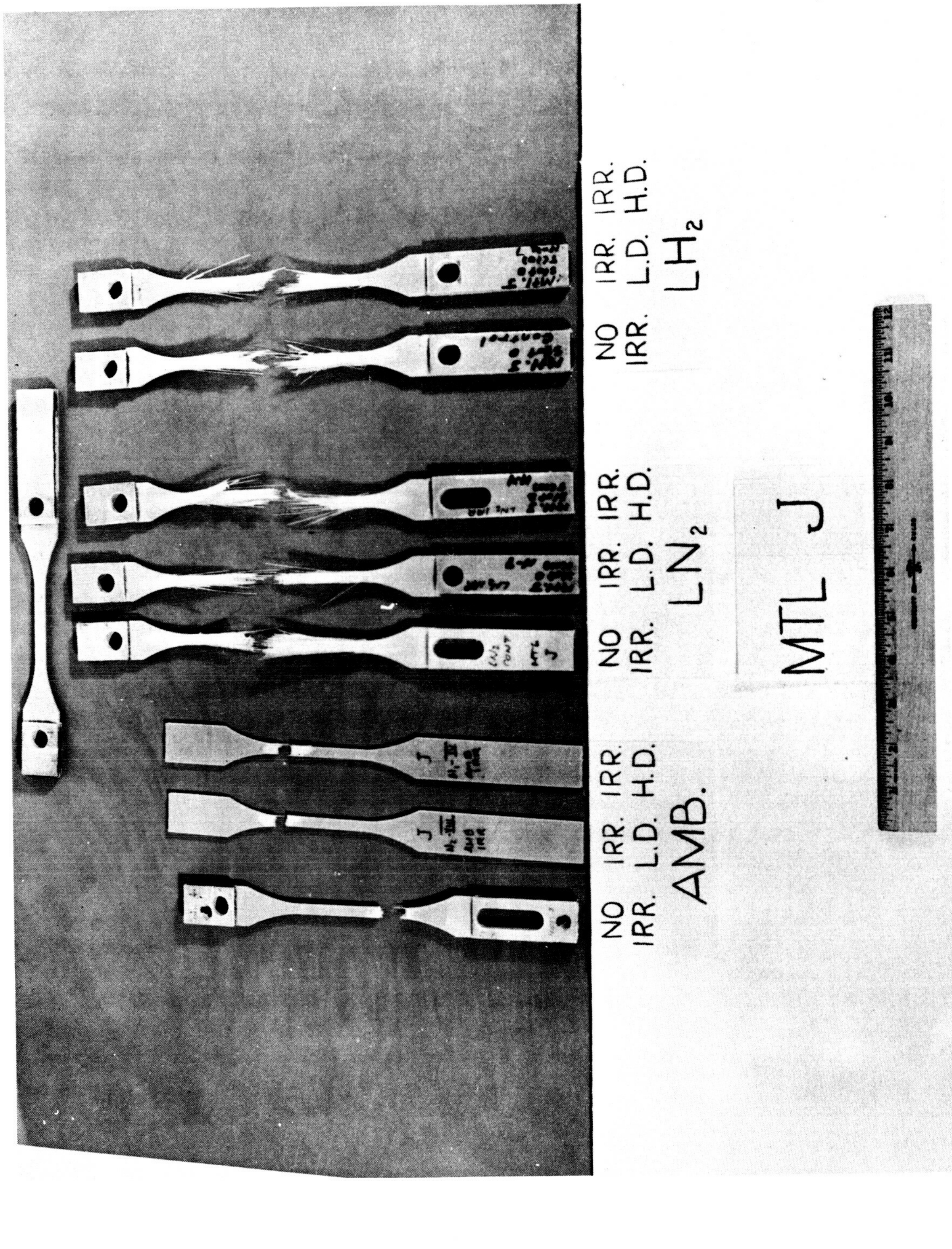

Figure 4.10 Material J Specimens

were made. With reference to these measurements, the following definitions apply:

<u>Normal monochromatic reflectance</u> is the ratio of the reflected radiant intensity from a body to that incident upon it at a particular wavelength when the incident radiation is directed normal to the surface.

<u>Monochromatic absorptance</u> is the ratio of the absorbed radiant intensity by a body to that incident upon it at a particular wavelength.

<u>Monochromatic emittance</u> is the ratio of the emitted radiant intensity to that of a blackbody at the same temperature at a particular wavelength.

<u>Total normal reflectance</u> is the ratio of the total (i.e., integrated over all wavelengths) reflected radiant intensity to the total intensity incident upon it in a normal direction.

<u>Total emittance</u> is the ratio of the emitted radiant intensity (integrated over all wavelengths) into a solid angle of 2π steradians to that of a blackbody at the same temperature.

<u>Total solar absorptivity</u> is the ratio of the absorbed radiant intensity by a body to that incident upon it from a blackbody at 6000°K.

The apparatus used was a Cary Model 14 spectrometer with an integrating sphere attachment, plus a Perkin-Elmer Model 13 double-beam photometer, which incorporates a hohlraum as a light source. The sample was placed inside the hohlraum, or the integrating sphere, where it was isotropically irradiated. The intensity of the normal, monochromatic component of the reflected radiation was compared to the monochromatic intensity of a blackbody. The ratio of these two intensities, which is equal to the monochromatic reflectance, was displayed on a recording instrument as a function of wavelength. The measurements were made over a wavelength region of from 0.30 to 33 microns.

From the measured monochromatic reflectance, ρ_λ, the monochromatic values of emittance, ϵ_λ, and absorptance, α_λ, were obtained as follows:

$$\epsilon_\lambda = \alpha_\lambda = 1 - \rho_\lambda$$

The total reflectance, ρ, solar absorptance, α, and total emittance, ϵ, at a given temperature were calculated by numerical integration from the following relationships:

$$\epsilon = \frac{\int_0^\infty e_{\lambda b}(T)\epsilon_\lambda d\lambda}{\int_0^\infty e_{\lambda b}(T)\, d\lambda} \quad ; \qquad \alpha = \frac{\int_0^\infty e_{\lambda b}(T)\alpha_\lambda d\lambda}{\int_0^\infty e_{\lambda b}(T)\, d\lambda} \quad ; \qquad \rho = 1 - \alpha$$

where $e_{\lambda b}$ = energy radiated per unit time per unit area by a blackbody at temperature T and wavelength λ. The numerical integration was done with an IBM 650 computer.

The reflectance of the sample was measured at one temperature (100°F) only. Assuming that the monochromatic emittance will show only second-order variations with temperatures, the total emittance was calculated for 100°, 300°, and 500°K.

Details of the equipment used in the experiment are shown in Table 4.2. Data are tabulated in Tables A-57 through A-60. Figure 4.11, a photograph of representative specimens, shows the aluminum framework used to mount them in the cryogen chamber during the cryotemperature irradiations. Reference 6 is the complete report on the thermal-control-coatings tests, as published by GD/Astronautics.

Table 4.2

Equipment for Spectral Reflectivity Tests

Source	Spectrograph Prism	Detector	Diagonal	Filter	Wavelength Coverage (microns)
Integrating Sphere Tungsten (1000°K)	Cary Model 14	Phototube	None	None	0.3 to 0.6
		Lead sulfide	None	None	0.6 to 2.0
Hohlraum (820°C)	Perkin-Elmer Model 13 Cs-Br	Thermocouple with Cs-Br window	Mirror	None	1.36 to 12.0
			Scatter-plate	None	12.0 to 19.1
			Scatter-plate	AgCℓ/AgS	19.1 to 24.4
			Reststrahlen Plate	None	24.4 to 33.0

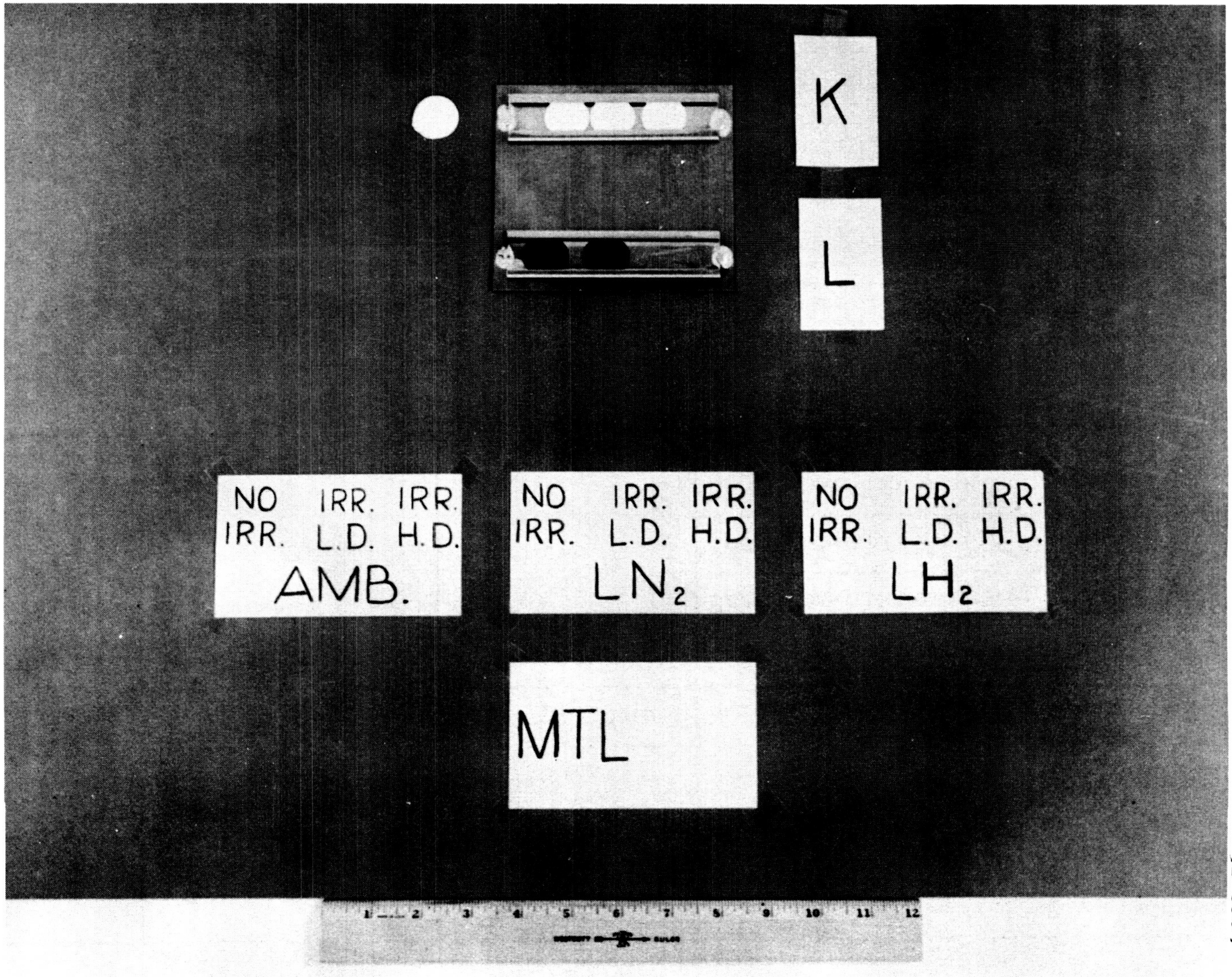

Figure 4.11 Material K and L Specimens

V. DISCUSSION OF RESULTS

The number of specimens tested for each data point varies from one to four, depending upon the number calculated to be sufficient for satisfactory data precision. The original schedule on these quantities had to be altered somewhat during actual tests because of equipment limitations which developed during the equipment design phase. For instance, the compression-button test apparatus was designed in such a manner that only one compression button could be tested on each pull rod. Thus, because of the limited number of pull rods and the large number of specimens required in the overall experiment, only one specimen per data point was tested for certain materials.

Another factor which lowered the quantity of specimens per data point was the rejection of occasional specimens because of improper breaks or loosening of the doublers during break. The actual number tested in each case is shown in the tabulated data.

Past work in radiation-effects testing has, for the most part, related radiation damage in organic materials to the gamma doses involved. Damage in all types of materials from incident neutrons is, of course, of utmost importance, but because of the above practice, the planned doses on each material in the experiment were based upon gamma-radiation levels. Two doses for each material at each temperature were scheduled. The doses chosen were such that the resulting change in engineering properties would fall between a threshold value and a critical value. The threshold value is defined as the radiation dose at which pertinent property changes just become apparent, whereas the critical value is defined as that dose at which a pertinent property changes by 40 to 60% of its initial value. The doses were selected by GD/FW personnel on the basis of results from prior radiation-effects tests.

Gamma doses which were actually recorded in the cryogen chambers of the experimental assemblies during both low-temperature runs deviated to some extent from values previously recorded in air at the same locations (see Figs. 3.9 and 3.12). For reasons that were given in Section III of this report, the gamma doses which were previously recorded in air will be regarded as being the actual doses at these locations. These values, along with measured neutron fluxes, are shown in Tables 5.1 and 5.2.

5.1 Material A: Hexcel 1252

Test data for Material A are plotted in Figure 5.1.* Tensile-shear strength (or force-to-break) in $lb/in.^2$ is plotted as a function of radiation dose for the three temperatures. As can be noted, the strength of the unirradiated specimens was more than doubled at reduced temperatures. Radiation, however, had an opposing effect. It served to reduce the strength of specimens at cryotemperatures and to increase significantly the strength of those at ambient temperature. All three curves appear to be asymptotic in character with increasing dose.

No value of tensile-shear strength for the high-dose, LH_2-temperature condition was obtained, but the nature of the LN_2 curve

*Figures 5.1 through 5.49 have been grouped at the end of this section to avoid interrupting text continuity.

Table 5.1

Average Low Radiation Exposures

Material Designation	Name of Material	Ambient Irradiation			LN_2 Irradiation			LH_2 Irradiation		
		Gamma [ergs/gm(C)]	Fast Neutron[a] (n/cm^2)	Thermal Neutron[b] (n/cm^2)	Gamma [ergs/gm(C)]	Fast Neutron[a] (n/cm^2)	Thermal Neutron[b] (n/cm^2)	Gamma [ergs/gm(C)]	Fast Neutron[a] (n/cm^2)	Thermal Neutron[b] (n/cm^2)
A	Hexcel 1252	1.0(10)	2.5(15)	3.4(14)	1.3(10)	2.3(15)	2.5(14)	1.3(10)	2.2(15)	5.5(15)
B	Metlbond 406	1.05(10)	2.5(15)	3.7(14)	1.3(10)	2.3(15)	2.5(14)	1.3(10)	2.2(15)	5.5(15)
C	Teflon TFE	4.9(9)	1.3(15)	1.5(14)	-	-	-	-	-	-
D	Kel-F-81	5.45(9)	1.08(15)	1.06(14)	4.7(9)	1.0(15)	9.5(13)	4.7(9)	1.0(15)	3.0(15)
E	Stafoam AA402	5.0(9)	1.2(15)	1.0(14)	5.3(9)	9.2(14)	9.8(13)	5.3(9)	9.0(14)	2.3(15)
F	Styrofoam 22	5.0(9)	1.2(15)	1.0(14)	5.2(9)	9.0(14)	9.5(13)	5.2(9)	8.5(14)	2.1(15)
G	H-Film	4.75(9)	1.3(15)	1.0(14)	5.2(9)	9.2(14)	9.8(13)	5.2(9)	9.0(14)	2.3(15)
H	Mylar-C	4.92(9)	1.3(15)	9.6(13)	5.3(9)	1.0(15)	9.5(13)	5.3(9)	1.0(15)	3.0(15)
I	Conolon 506	1.05(10)	2.5(15)	3.7(14)	1.3(10)	1.6(15)	1.7(14)	1.3(10)	1.6(15)	4.0(15)
J	Paraplex P-43	1.0(10)	2.5(15)	3.6(14)	1.3(10)	1.6(15)	1.7(14)	1.3(10)	1.4(15)	3.5(15)
K	Skyspar A423	4.92(9)	1.3(15)	9.6(13)	2.0(10)	4.0(14)	4.2(13)	5.6(9)	8.5(14)	2.1(15)
L	W-49-BC12	4.75(9)	1.3(15)	1.0(14)	2.0(10)	4.0(14)	4.2(13)	5.6(9)	8.5(14)	2.1(15)

a $E < 0.48$ ev
b $E > 2.9$ Mev

Table 5.2

Average High Radiation Exposures

Material Designation	Name of Material	Ambient Irradiation			LN_2 Irradiation			LH_2 Irradiation		
		Gamma ergs/gm(C)	Fast Neutron[a] (n/cm^2)	Thermal Neutron[b] (n/cm^2)	Gamma ergs/gm(C)	Fast Neutron[a] (n/cm^2)	Thermal Neutron[b] (n/cm^2)	Gamma ergs/gm(C)	Fast Neutron[a] (n/cm^2)	Thermal Neutron[b] (n/cm^2)
A	Hexcel 1252	6.0(10)	1.6(16)	2.4(14)	5.2(10)	1.3(16)	1.4(15)			
B	Metlbond 406	4.9(10)	1.6(16)	2.3(14)	5.2(10)	1.3(16)	1.4(15)			
C	Teflon TFE	1.16(10)	2.6(15)	3.5(14)						
D	Kel-F-81	1.0(10)	2.5(15)	3.6(14)	1.0(10)	1.9(15)	2.0(14)	1.0(10)	1.2(15)	3.0(15)
E	Stafoam AA402	8.0(9)	2.2(15)	3.2(14)	1.3(10)	2.2(15)	2.3(14)	1.3(10)	2.5(15)	6.6(15)
F	Styrofoam 22	1.0(10)	2.6(15)	3.5(14)	1.2(10)	2.2(15)	2.3(13)	1.2(10)	2.0(15)	5.0(15)
G	H-Film	8.0(9)	2.2(15)	3.2(14)	1.3(10)	5.0(15)	5.2(12)	1.3(10)	7.8(14)	2.0(15)
H	Mylar-C	8.0(9)	2.2(15)	3.2(14)	1.3(10)	1.5(15)	1.6(14)	1.3(10)	1.35(15)	3.4(16)
I	Conolon 506	6.7(10)	1.7(16)	4.7(14)	5.0(10)	4.8(16)	4.9(15)			
J	Paraplex P-43	6.0(10)	1.7(16)	2.13(14)	5.0(10)	4.8(16)	4.9(15)			
K	Skyspar A-423	1.05(10)	2.5(15)	3.7(14)	3.0(10)	4.0(15)	4.2(14)	2.0(10)	3.0(15)	7.0(15)
L	W-49-BC-12	8.0(9)	2.2(15)	3.2(14)	3.0(10)	4.0(15)	4.2(14)	2.0(10)	3.0(15)	7.0(15)

a $E < 0.48$ ev
b $E > 2.9$ Mev

suggests a possible leveling-off in strength reduction with successively higher radiation doses. The net effect of the two environmental components, both separately and in combination, was a definite increase in the tensile-shear strength of this adhesive.

One possible explanation for the opposing trend in strength between the ambient- and low-temperature specimens with incident radiation is proposed. The radiation-induced chain scission in the molecular structure serves to lower the shear strength of the adhesive, but the room-temperature annealing (or cross-linking) process in the ambient-temperature specimens ultimately results in a molecular configuration with higher shear-strength characteristics. In the low-temperature specimens, the chain scission occurs, but reduced molecular motion significantly inhibits the cross-linking process.

Visual analysis of the broken specimens revealed that about 75% of the failures were adhesive rather than cohesive.

5.2 Material B: Metlbond 406

The tensile-shear strength of this material is plotted in Figure 5.2 as a function of radiation dose for each of three temperatures. Tensile-shear strengths at low temperatures and no radiation are considerably lower than the ambient-temperature value for this material. This is contrary to Hexcel 1252. Another effect that was contrary to the Hexcel 1252 behavior was the sharp drop in tensile-shear strength at the higher dose at ambient temperature. No explanation for this is proposed, except to report that failure on these specimens was 100% adhesive, with 100% of the adhesive material remaining on one of the adherent strips.

The tensile-shear characteristics of the low-temperature specimens as a function of radiation dose were quite similar to those of Material A, as was the method of failure, except for the one condition discussed above.

5.3 Material C: Teflon TFE

Data taken in tests on this material are plotted in Figures 5.3 and 5.4. As discussed previously in this report, only ambient-temperature irradiations were made, and tests were performed on the ambient-temperature, no-irradiation condition only. Curves of breaking factor vs radiation dose and percent elongation vs radiation dose were both plotted, however, to show the zero values of breaking factor and elongation at the ambient-temperature, low-dose point. These zero values are representative of the crumbled specimens shown in Figure 4.3.

This material is notoriously poor in radiation resistance with air as the environment during irradiation. If irradiation and subsequent tensile tests could have been performed with the material submerged in cryogen, significantly different results could possibly have been obtained.

5.4 Material D: Kel-F-81

Data for this material are plotted in Figures 5.5 through 5.13. Figure 5.5 is a plot of ultimate tensile strength vs radiation dose at three temperatures. No data point is shown for the ambient-temperature, high-dose condition. As mentioned previously, the specimens for this condition broke in the process of removal from the static-irradiation mounting trays. This missing data-point should actually exist, therefore, on the zero-strength line somewhere between the low- and high-dose points.

The unirradiated specimens demonstrated a much higher tensile strength at lower temperatures, but still suffered degradation in strength after being irradiated.

At LN_2 temperatures, the ultimate tensile strength dropped only slightly with increased radiation, but at LH_2 temperatures the strength dropped sharply after receiving the two doses shown.

Two possible explanations for these observations are proposed. One is concerned with the competing reactions of scission (weakening) and cross-linking (strengthening) which occur during irradiation. If the rates of these reactions vary widely with temperature, then the cumulative effect of the two could be sufficiently different at different temperatures to cause varying values in the measured property. The other explanation is concerned with the possibility of hydrogen-fluoride formation in the Kel-F-81 when submerged in LH_2. The formation rate would be enhanced during irradiation because of ionization of the hydrogen, and the resultant hydrogen fluoride could react chemically with the Kel-F-81 to cause scission in the chains and consequent lowering of the tensile strength.

Figure 5.6 is a plot of percent total elongation vs radiation dose at three temperatures. These curves demonstrate the relatively high ductility of this material at room temperature compared to that at cryotemperatures. Again, the LN_2 and LH_2 environments imposed during irradiation and subsequent tests have contrasting effects on the measured property.

Figures 5.8, 5.10, and 5.12 are stress-strain diagrams for this material under zero-dose, low-dose, and high-dose conditions. They are all plotted to the breaking point for the specimens. Strain values are based upon pull-rod extensions.

The calculated (or hypothetical) extensometer extensions are plotted on stress-strain diagrams shown in Figures 5.9, 5.11, and 5.13.

The shapes of these latter curves follow closely those of the stress-strain diagrams for the measured (or pull-rod) strain. The percent elongation for calculated extensometer elongation are plotted as a function of radiation dose in Figure 5.7. The relative trends for these curves also follow closely those shown in Figure 5.6.

5.5 Material E: Stafoam AA 402

Data for this thermal-insulation material are plotted in Figures 5.14 through 5.17. Figure 5.14 is a plot of the force to compress 25% vs radiation dose for three temperatures. These forces are a function of (among other things) the bending strength of the cell walls, so that it is logical that unirradiated specimens would, at lower temperatures, require higher forces during compression. After irradiation to a gamma dose of approximately 0.5×10^{10} ergs/gm(C), however, opposing characteristics appear. The ambient-temperature specimens require less force to compress 25% and the low-temperature specimens require more. Then, at higher doses, the required compression forces for the low-temperature specimens drop off significantly.

The factors which enter into the distribution of forces during compression of rigid foams are quite numerous, and the added influence of radiation further complicates the picture. In view of this, a detailed analysis of reasons for the trends of these curves will not be attempted. Considerations of the plotted data in regard to end uses of the material, however, will be made.

Each of Figures 5.15, 5.16, and 5.17 are stress-strain plots for Material E over a deflection range of 0.25 inch (or 50% of specimen thickness) for three temperatures. The different figures are for zero-dose, low-dose, and high-dose conditions. The relative positions of the three curves in each figure are similar. It is obvious that the forces involved are significantly lower at the high dose, indicating an approximate threshold point for compressive resistance of this material at a dose of about 5×10^9 ergs/gm(C).

5.6 <u>Material F: Styrofoam 22</u>

Data for this material are plotted in Figures 5.18 through 5.21. These plots for the force-to-compress vs radiation dose at three temperatures and for stress-strain diagrams at three temperatures and three doses are identical in plan to those for Material E. The relative trends for curves on each plot are also similar to those for Material E. In addition, the material shows a radiation threshold for compressive strength. This varied from about 0.2×10^{10} to 0.5×10^{10} ergs/gm(C) of gamma dose, depending upon the specimen temperature (see Fig. 5.18). Other remarks in Section 5.5 pertaining to compression measurements are applicable to Material F.

5.7 Materials G (DuPont H-Film) and H (DuPont Mylar-C)

Data for Materials G and H are plotted in Figures 5.22 through 5.25. Figures 5.22 and 5.23 are plots of breaking factor vs radiation dose at three temperatures for the two materials. As suggested previously in this report, load data for these materials are regarded as possessing only borderline reliability because of the relatively high tare loads involved.

The plots of the data for the two materials are shown together to demonstrate the apparent similarity between the trends of comparable curves. The ultimate strength of both materials is significantly higher at lower temperatures, as was anticipated. The changes in breaking factor as a function of radiation at three temperatures seemed to follow the same pattern for both materials; that is, from zero dose up to a low-dose level, the strength of both materials increased at ambient and LH_2 temperatures and decreased at LN_2 temperature. At higher doses the strength of both materials at ambient and LH_2 temperatures decreased sharply, but those at the LN_2 temperature began to increase in strength. The percent elongation for both materials, as shown in Figures 5.24 and 5.25, followed the same trends at the three temperatures.

Observations on the characteristics of these materials are rather general, but in view of the circumstances surrounding the tests, as mentioned previously, no alternative was considered possible.

5.8 Material I: Conolon 506

Data from tests performed on Conolon 506 are plotted in

Figures 5.26 through 5.34. Figure 5.26 is a plot of ultimate tensile strength vs gamma radiation dose at three temperatures. It is interesting to note that at ambient and LN_2 temperatures, radiation doses up to $6x10^{10}$ ergs/gm(C) resulted in no significant change in this property of the material. At the LH_2 temperature, however, after a dose of $1.3x10^{10}$ ergs/gm(C), the ultimate tensile strength was up by a factor of 1.5. The difference in temperature between LN_2 and LH_2 is not regarded as the deciding factor in these contrasting tensile-strength curves; rather, it is felt that chemical reactions between ionized hydrogen and components of the adhesive served to strengthen the bond between the laminates.

Figures 5.27 and 5.28 are plots of percentage elongation vs radiation dose at three temperatures. The values of percentage elongation are based on pull-rod extension (or extension over the $5\frac{1}{4}$-in. portion of the specimen between the inside edges of the doublers) and upon a hypothetical (or calculated) extension of a 2-in. gage-length section in the narrowed portion of the specimen. Considering standard deviations of the data in the tables, no significant change, as a result of irradiation, is noted in this property.

Figures 5.29 through 5.34 are stress-strain diagrams for Conolon 506. In Figures 5.29 through 5.31, the strain is based on pull-rod extensions. As can be noted, the curves for unirradiated specimens at three temperatures all coincide within the elastic limit and deviate from each other only slightly beyond that point to the point of fracture. The curve for specimens which were irradiated and subsequently tested at ambient temperature was virtually a duplicate of the curve for unirradiated specimens, but diagrams for specimens which were irradiated and tested at cryotemperatures show decidedly higher slopes in the proportional range. This trend is contrary to all expectations, and a search of the literature has failed to uncover any previous work of a comparable nature on materials of this type and at these temperatures. No explanation for these data will be proffered at the present time.

Figures 5.32 through 5.34 are stress-strain diagrams based on the calculated extensions of a hypothetical 2-in. gage length in the narrowed section of the specimen. As can be seen, the relative trends of these curves are practically identical to those in Figures 5.29 through 5.31.

5.9 Material J: Paraplex P-43

Data from tests performed on this material are plotted in Figures 5.35 through 5.43. Figure 5.35 is a plot of ultimate tensile strength vs radiation dose for three different temperatures. As could be expected, the strength of unirradiated specimens is greater at lower temperatures. However, as in the case for Conolon 506, the effects of radiation at the different temperatures had little effect on this property of the material.

Figures 5.36 and 5.37 are plots of percent elongation vs radiation dose at three temperatures. Elongations in Figure 5.36 are based upon pull-rod extensions, and in Figure 5.37 on extensions of the hypothetical 2-in. gage length. The curves are similar for the two plots and, considering standard deviations for the data, the changes in elongation as a function of radiation are insignificant.

Figures 5.38 through 5.43 are stress-strain diagrams for this material. Figures 5.38 through 5.40 are based on pull-rod extensions. The curves for unirradiated specimens (shown in Figure 5.38) and for those which have been irradiated to a low dose (shown in Figure 5.39) fall fairly close to the same line, considering standard deviations. Under conditions of high dose (Fig. 5.40), the curve for specimens at the LN_2 temperature is displaced significantly from the ambient-temperature curve. Again, this is comparable to unexplained data received from tests on Material I.

Curves in Figures 5.41 through 5.43 are based on extensions of the hypothetical 2-in. gage length and are comparable to curves in Figures 5.38 through 5.40.

5.10 Materials K and L: Thermal-Control Coatings

Data received from tests on these thermal-control coatings are plotted in Figures 5.44 through 5.49. Figures 5.44 through 5.46 are for Material K. The radiation doses incident on the specimens irradiated at cryotemperatures were considerably different from those planned for the experiment and from those which were received by the ambient-temperature specimens. This resulted from an error in placement of the specimens in the experimental assemblies.

It is interesting to note the deviations in α/ϵ ratios as a function of radiation dose for the ambient-temperature specimens as compared to the absence of any change in this ratio (as a function of dose) for specimens which had been irradiated at cryotemperatures. The combined radiation and cryotemperature environment apparently serves to initially raise the value of the α/ϵ ratio, but increased radiation doses then have little further effect. These conditions were consistent at the three temperatures.

The curves for α/ϵ ratios as a function of radiation dose for Material L are rather inconclusive. There was little consistency between comparable curves at the three temperatures. These data are plotted in Figures 5.47 through 5.49.

The accuracy of the Cary Model 14 spectrometer, which works in the wavelength region of from 0.3 to 2 microns, is better than 2%. Since 95% of the solar energy is contained in this wavelength region, the error in the solar absorptance will not exceed 2%. The reproducibility of the Perkin-Elmer Model 13 spectrometer is approximately 3% of the full-scale pen deflection. This implies a relative error in the reflectance of 0.03 for the wavelength region between 2 and 33 microns. Since the blackbody energy peaks for 100°, 300°, and 500°K all fall within that wavelength interval, the emittances shown in Tables A-57 and A-59 may deviate within the limits of ± 0.015. The error in the ratio of solar absorptance to emittance is given by

$$\pm \frac{\alpha}{\epsilon}\left(\frac{\Delta\alpha}{\alpha} + \frac{\Delta\epsilon}{\epsilon}\right),$$

where $\Delta\alpha/\alpha = 0.01$, and $\Delta\epsilon = 0.015$.

In addition to these instrument errors, differences in surface roughness and contamination may result in a slight change of optical properties among apparently equal paint samples.

The influence of the nuclear radiation on the optical properties of the paints is most clearly observed on the monochromatic reflectivity curves (Ref. 6) (Figs. A-1 through A-13). There is no marked changed in the reflectivity of Material L specimens over the measured wavelength region, because the reflectivity is quite small in this region. Since the relative changes of reflectance, absorptance, and emittance are equal ($\Delta\rho = -\Delta\alpha = -\Delta\epsilon$), the changes in the solar absorptance and total normal emittance are also small. Tables A-57 and A-59 show that the changes in the optical properties of acrylic black paint are less than the instrumental errors shown above.

For Material K, the irradiation tends to lower the reflectivity in the visible and near-infrared region of the spectrum. The reflectivity of epoxy white paint is quite small for wavelengths longer than 3.6 microns. Since the emission of radiative energy from bodies at 100°, 300°, and 500°K occurs primarily at wavelengths greater than 3.6 microns, an appreciable change in the emissivity does not occur. However, the solar absorptance changes considerably, as can be observed from the data in Tables A-57 and A-59.

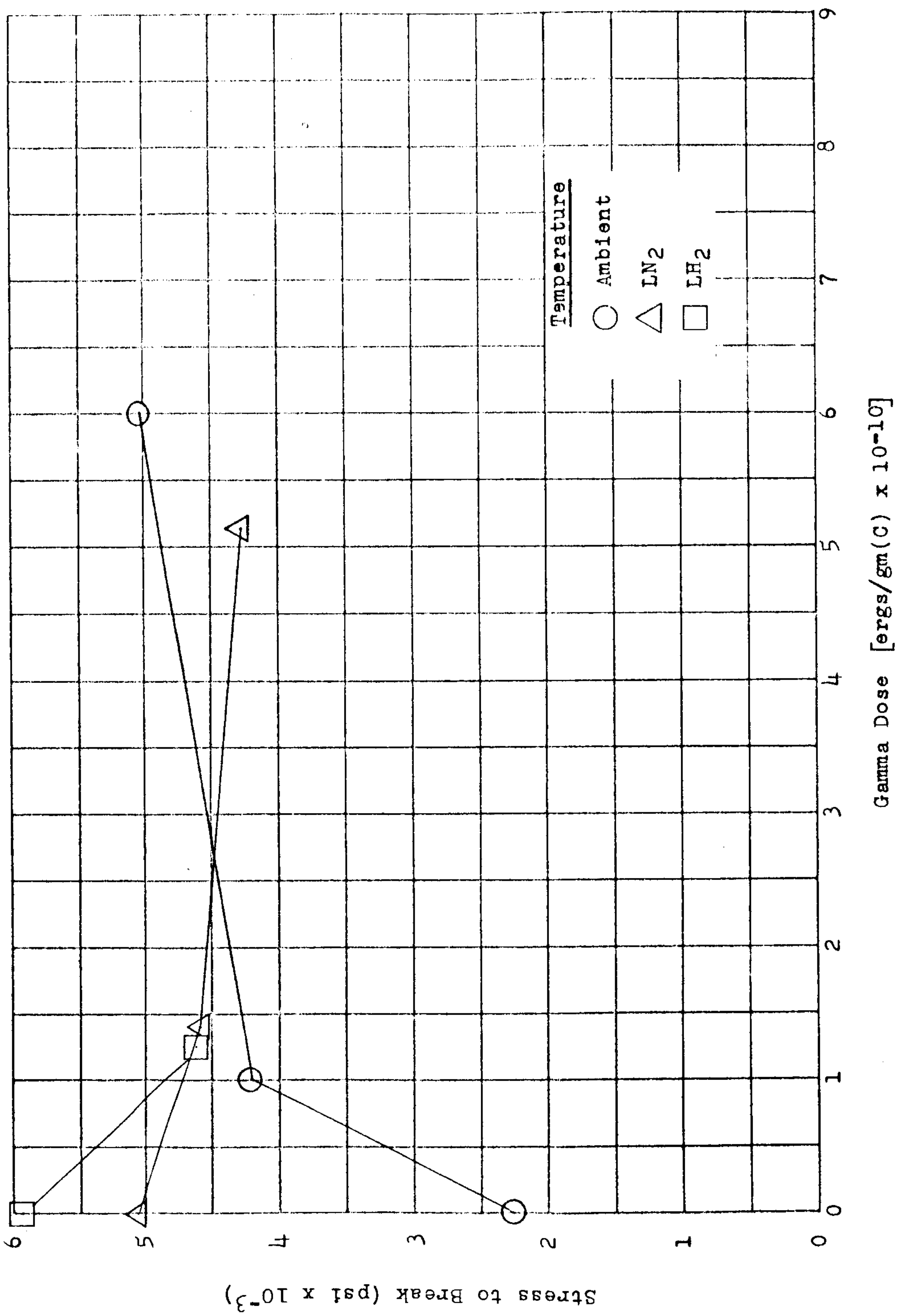

Figure 5.1 Stress to Break vs Gamma Dose for Three Different Temperatures: Material A (Hexcel 1252)

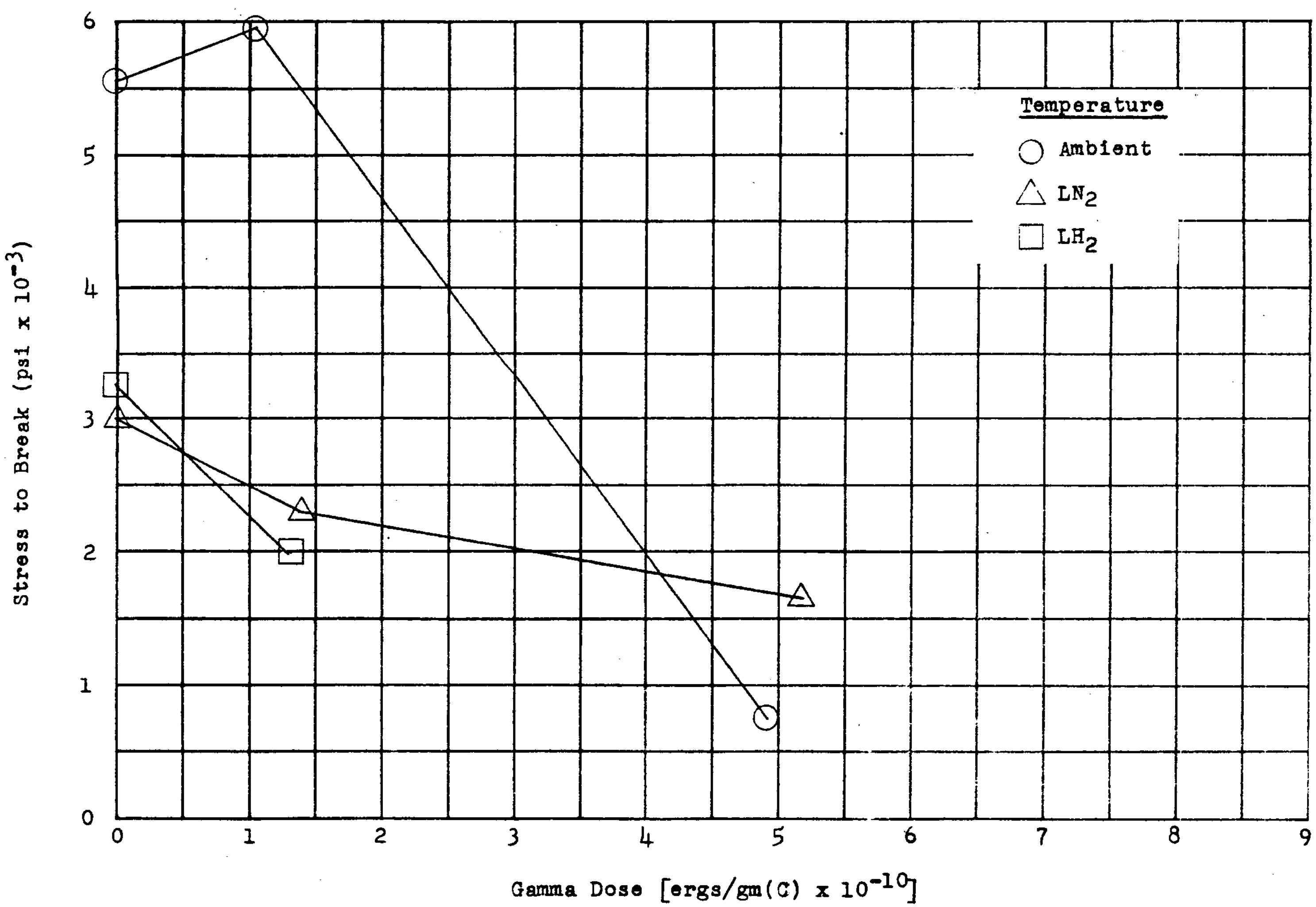

Figure 5.2 Stress to Break vs Gamma Dose for Three Different Temperatures: Material B (Metlbond 406)

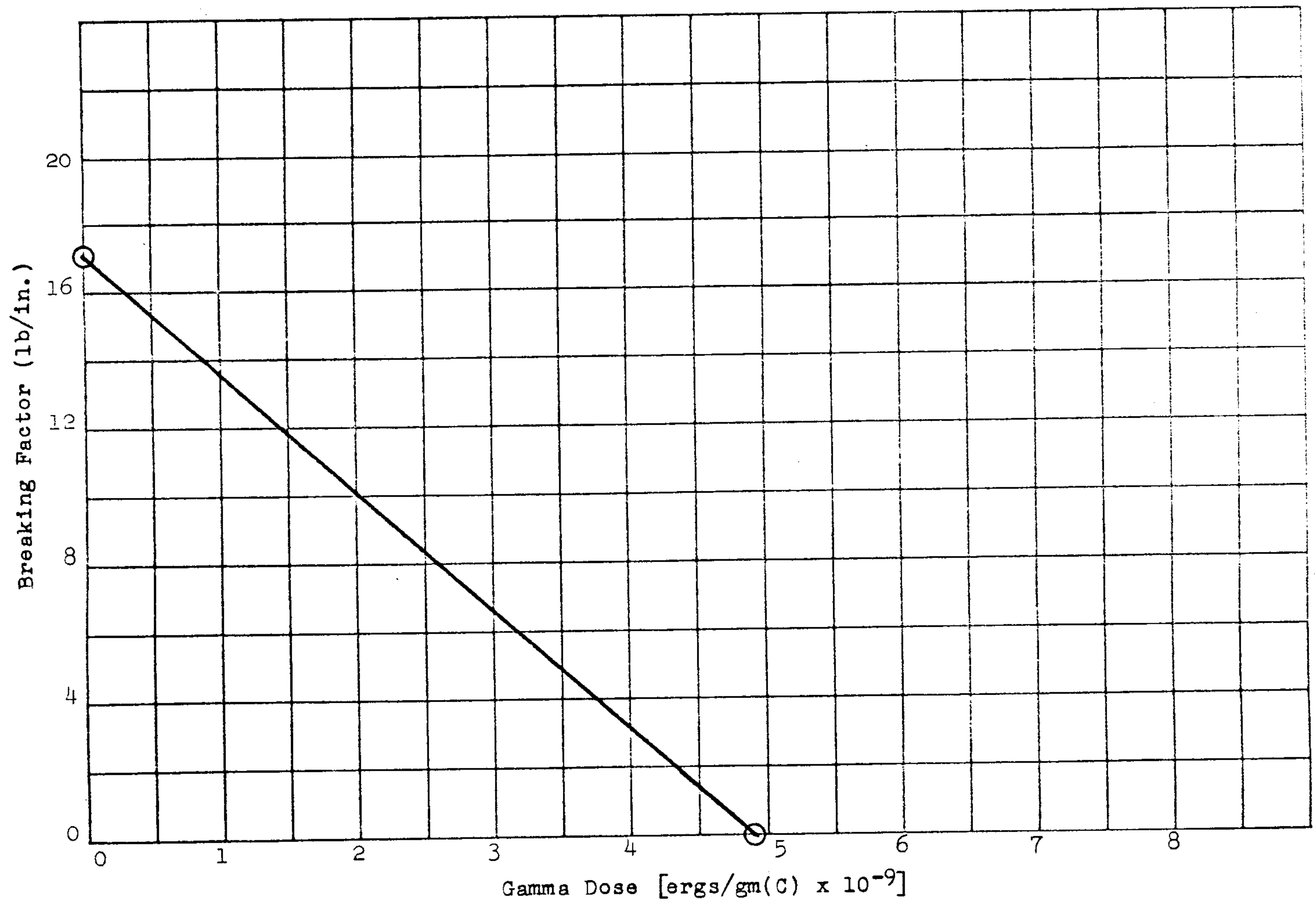

Figure 5.3 Breaking Factor vs Gamma Dose for Ambient Temperature: Material C (Teflon TFE)

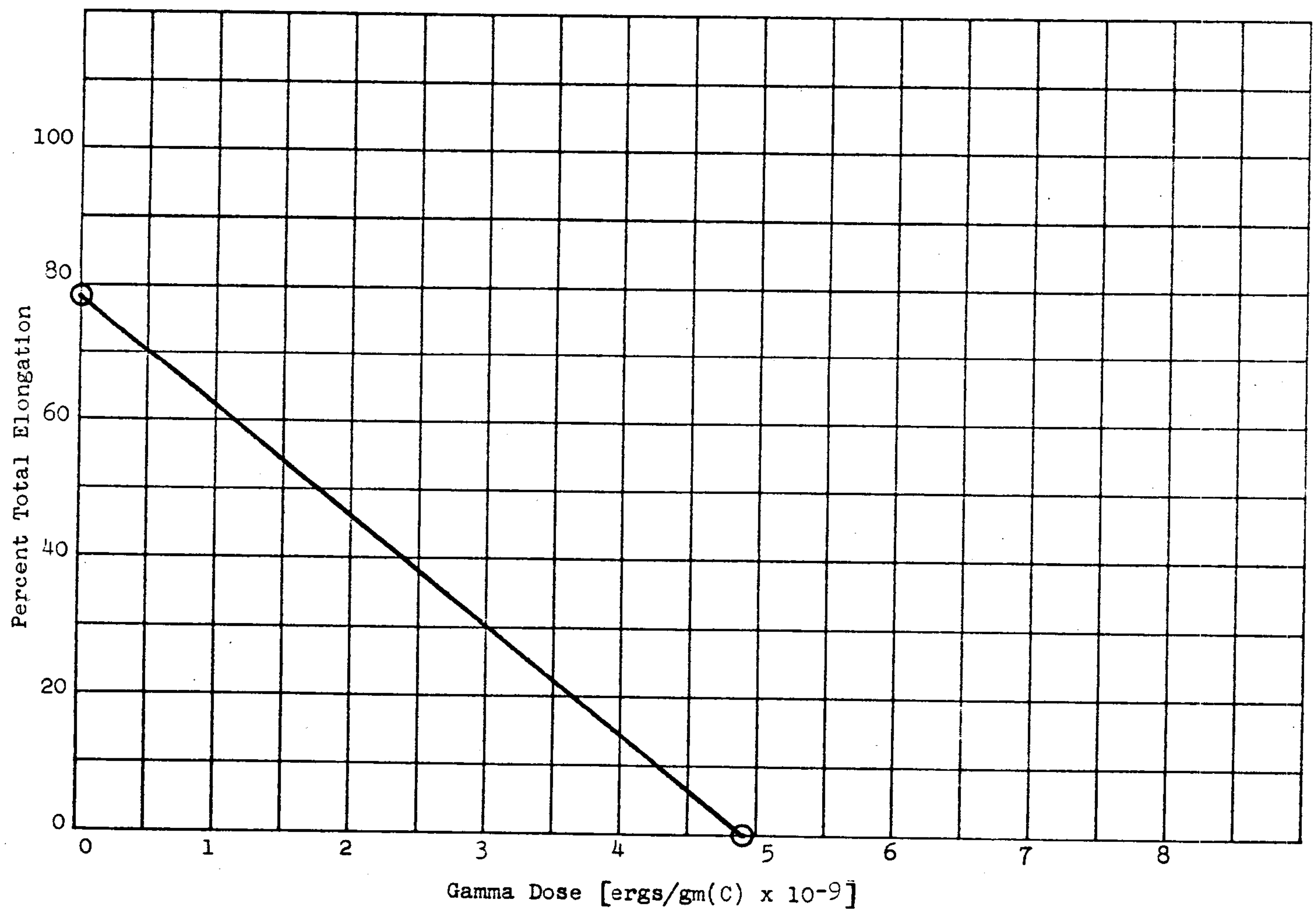

Figure 5.4 Percent Total Elongation vs Gamma Dose for Ambient Temperature: Material C (Teflon TFE)

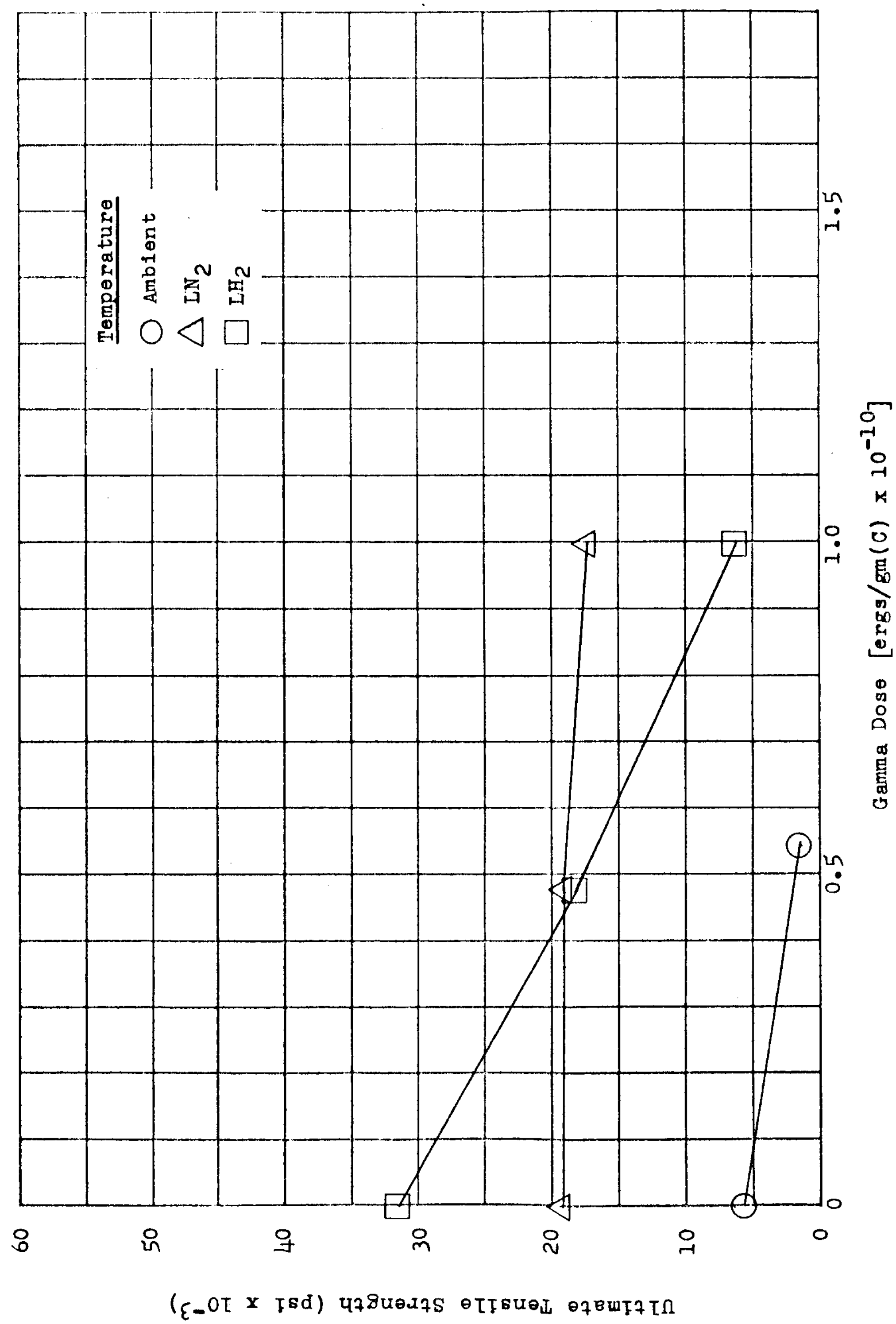

Figure 5.5 Ultimate Tensile Strength vs Gamma Dose for Three Different Temperatures: Material D (Kel-F-81)

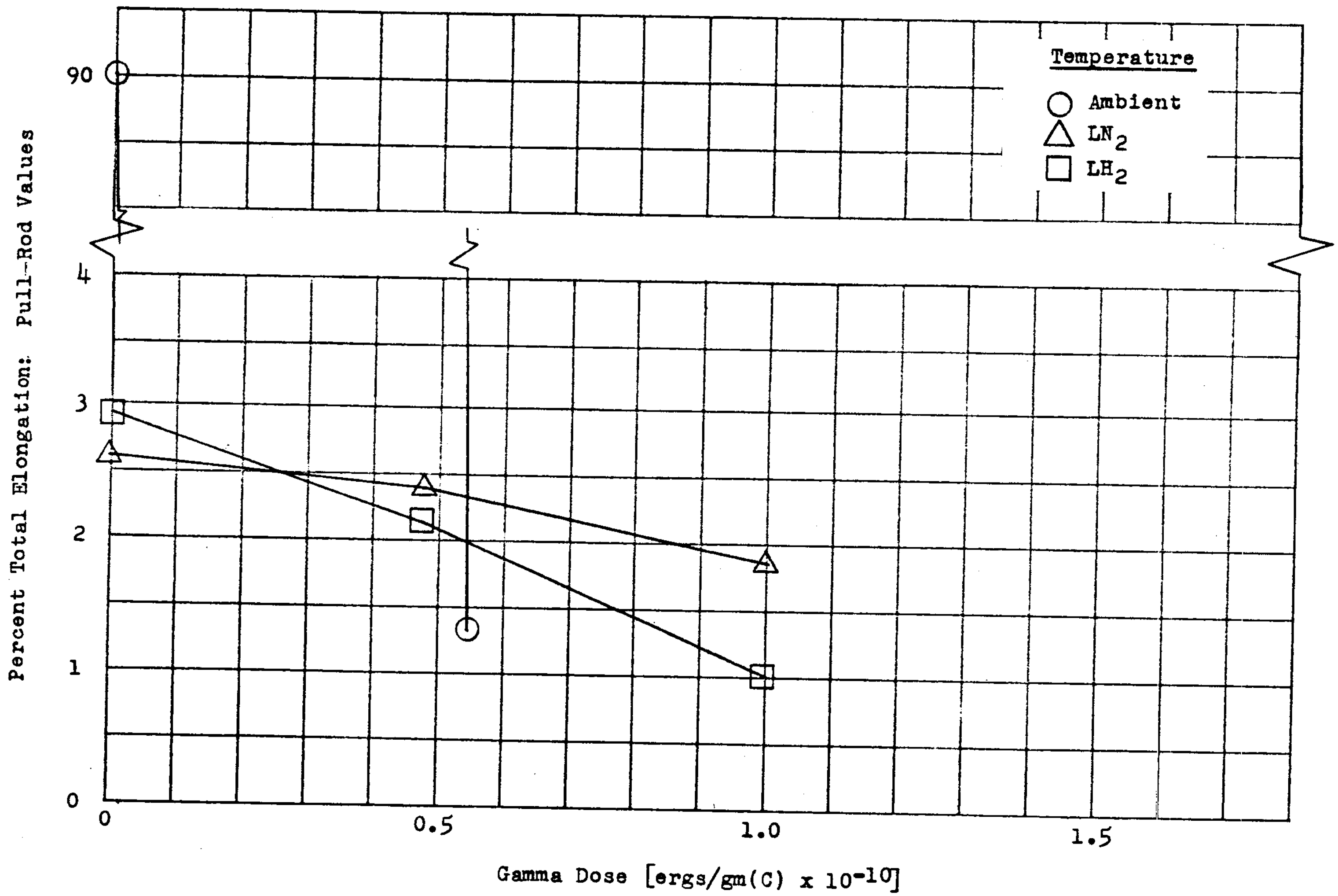

Figure 5.6 Percent Total Elongation (Pull-Rod Values) vs Gamma Dose for Three Different Temperatures: Material D (Kel-F-81)

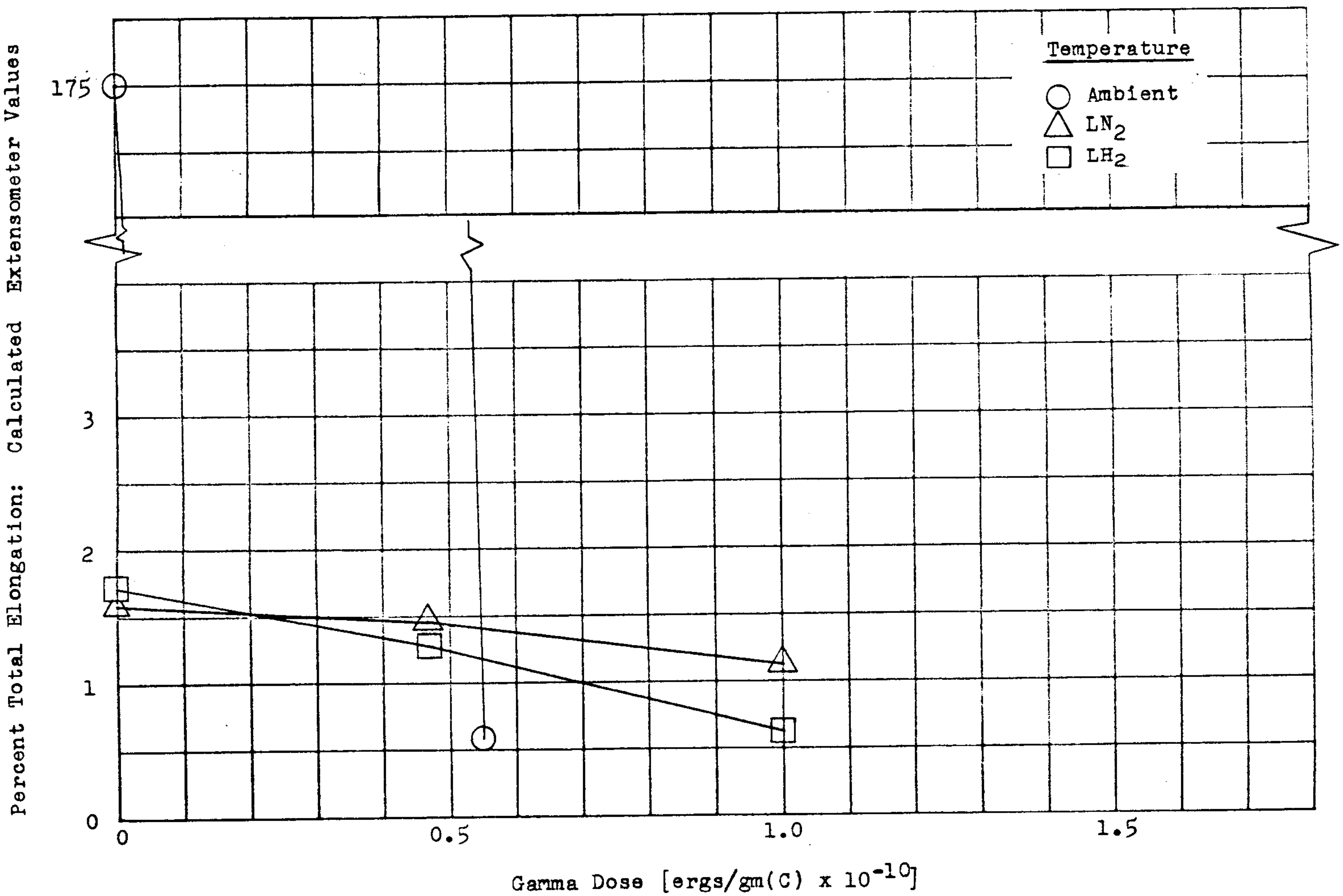

Figure 5.7 **Percent Total Elongation (Calculated Extensometer Values) vs Gamma Dose for Three Different Temperatures: Material D (Kel-F-81)**

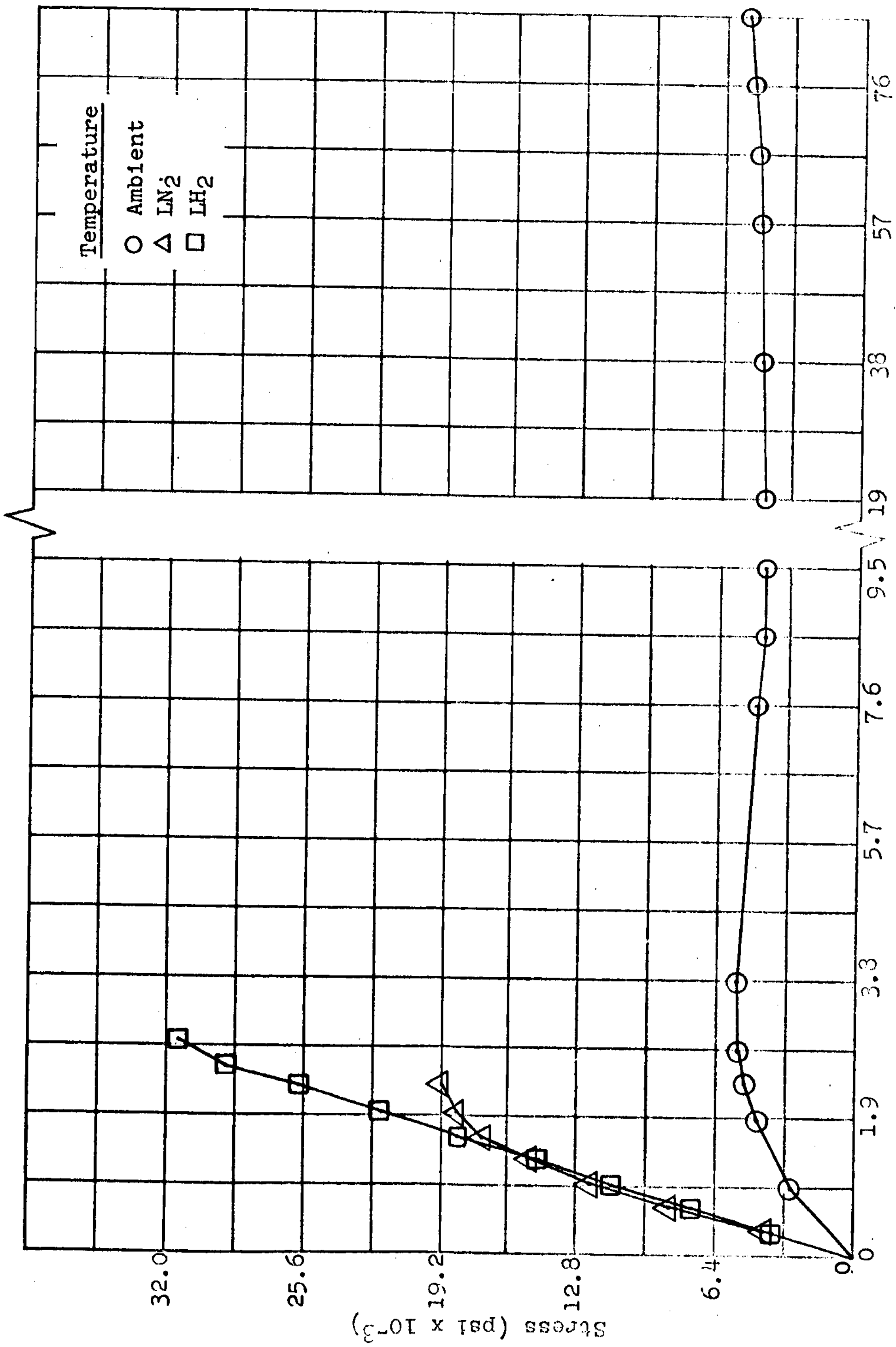

Figure 5.8 Stress vs Strain (Pull-Rod Values) for Three Different Temperatures: Material D (Kel-F-81); Unirradiated (Control)

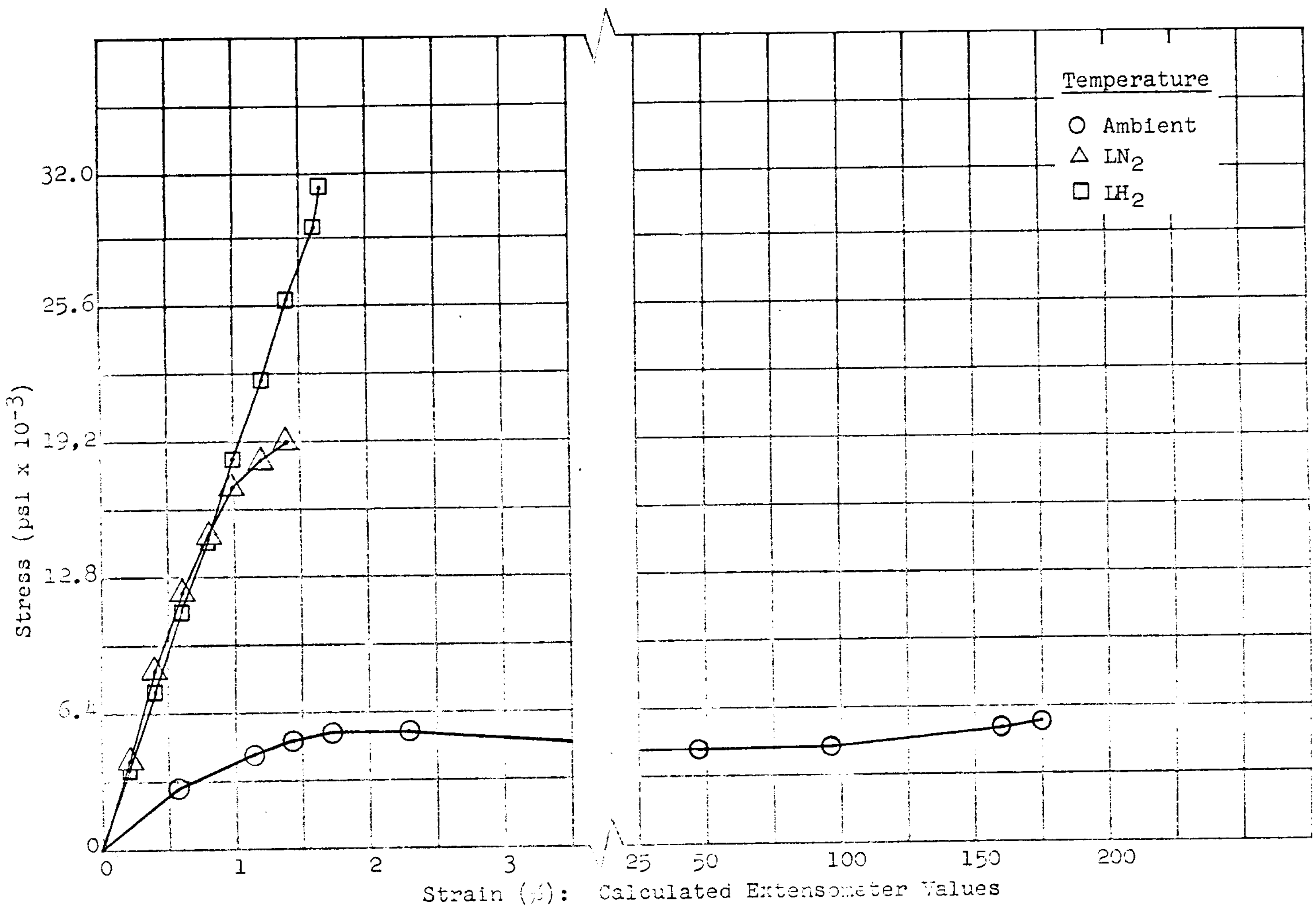

Figure 5.9 **Stress vs Strain (Calculated Extensometer Values) for Three Different Temperatures: Material D (Kel-F-81); Unirradiated (Control)**

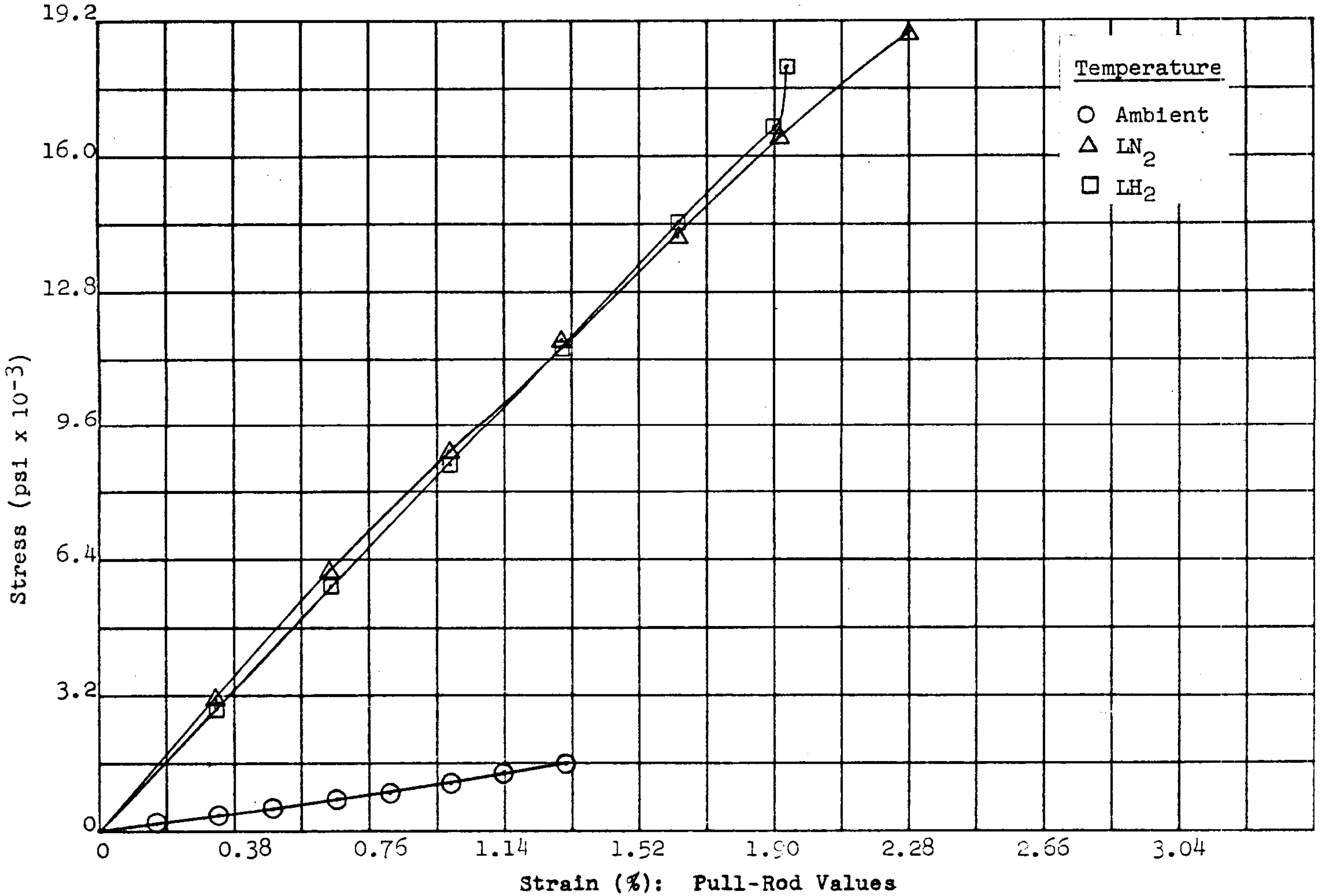

Figure 5.10 **Stress vs Strain (Pull-Rod Values) for Three Different Temperatures: Material D (Kel-F-81); Low-Dose Exposure**

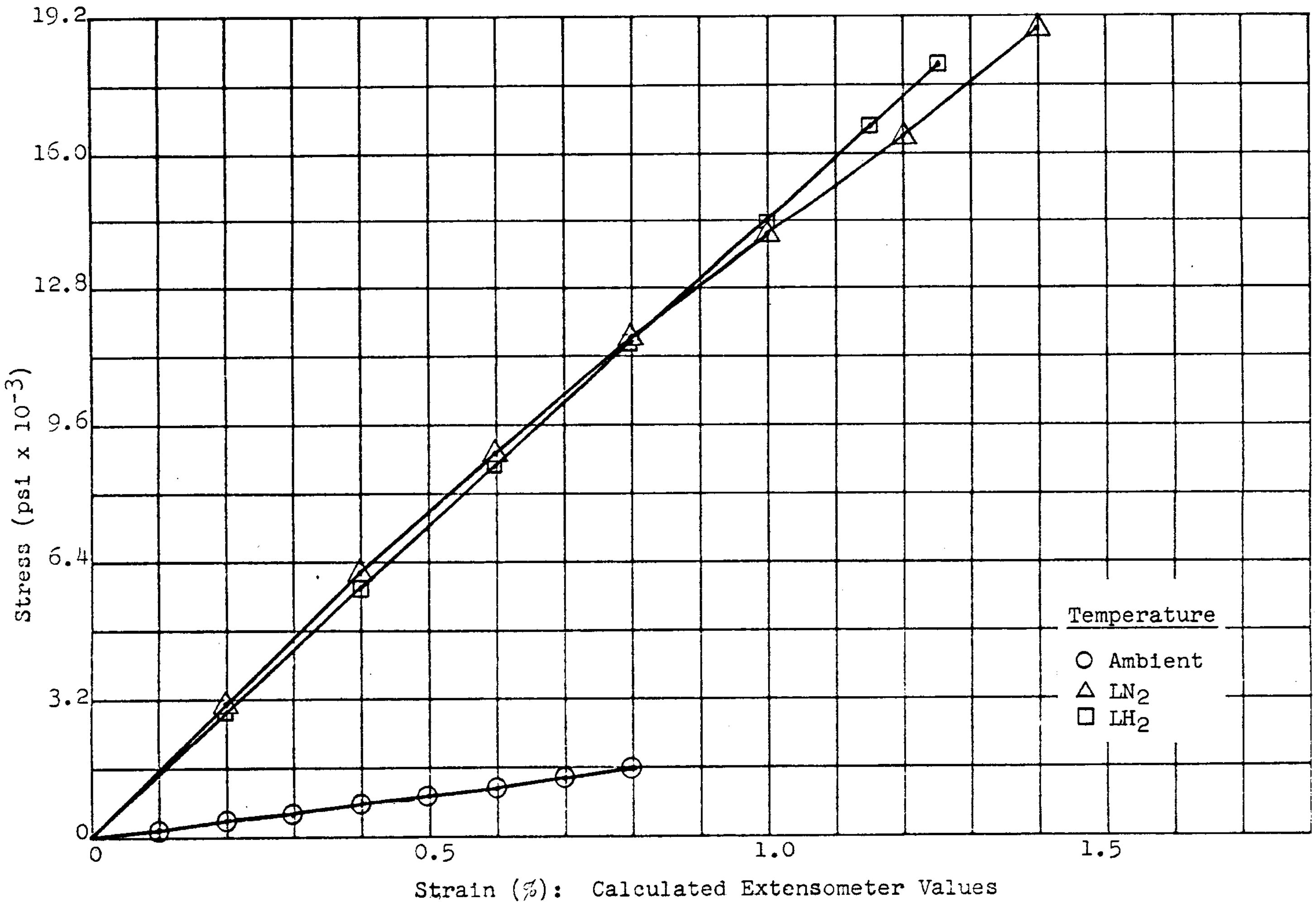

Figure 5.11 **Stress vs Strain (Calculated Extensometer Values) for Three Different Temperatures: Material D (Kel-F-81); Low-Dose Exposure**

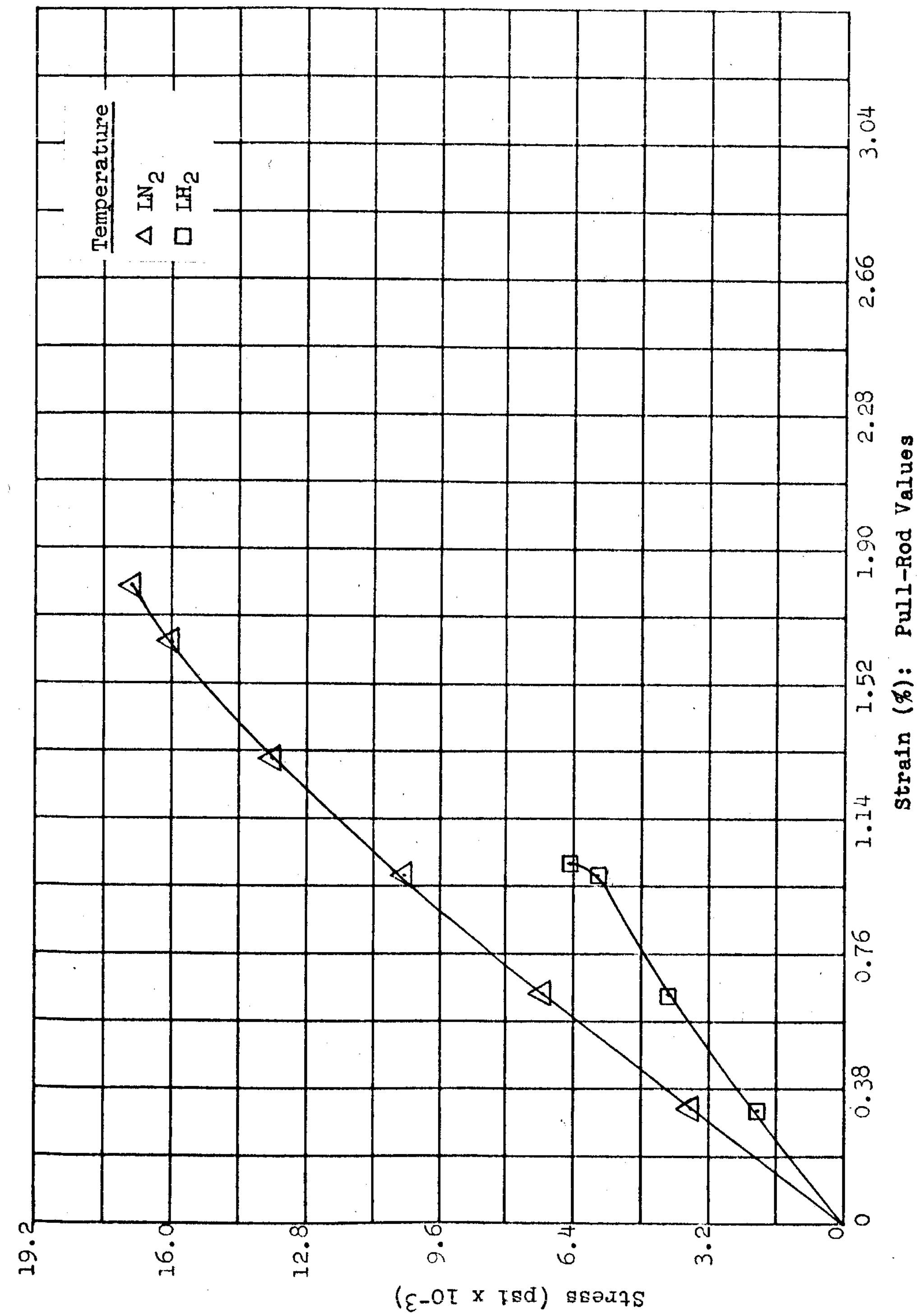

Figure 5.12 Stress vs Strain (Pull-Rod Values) for Two Different Temperatures: Material D (Kel-F-81); High-Dose Exposure

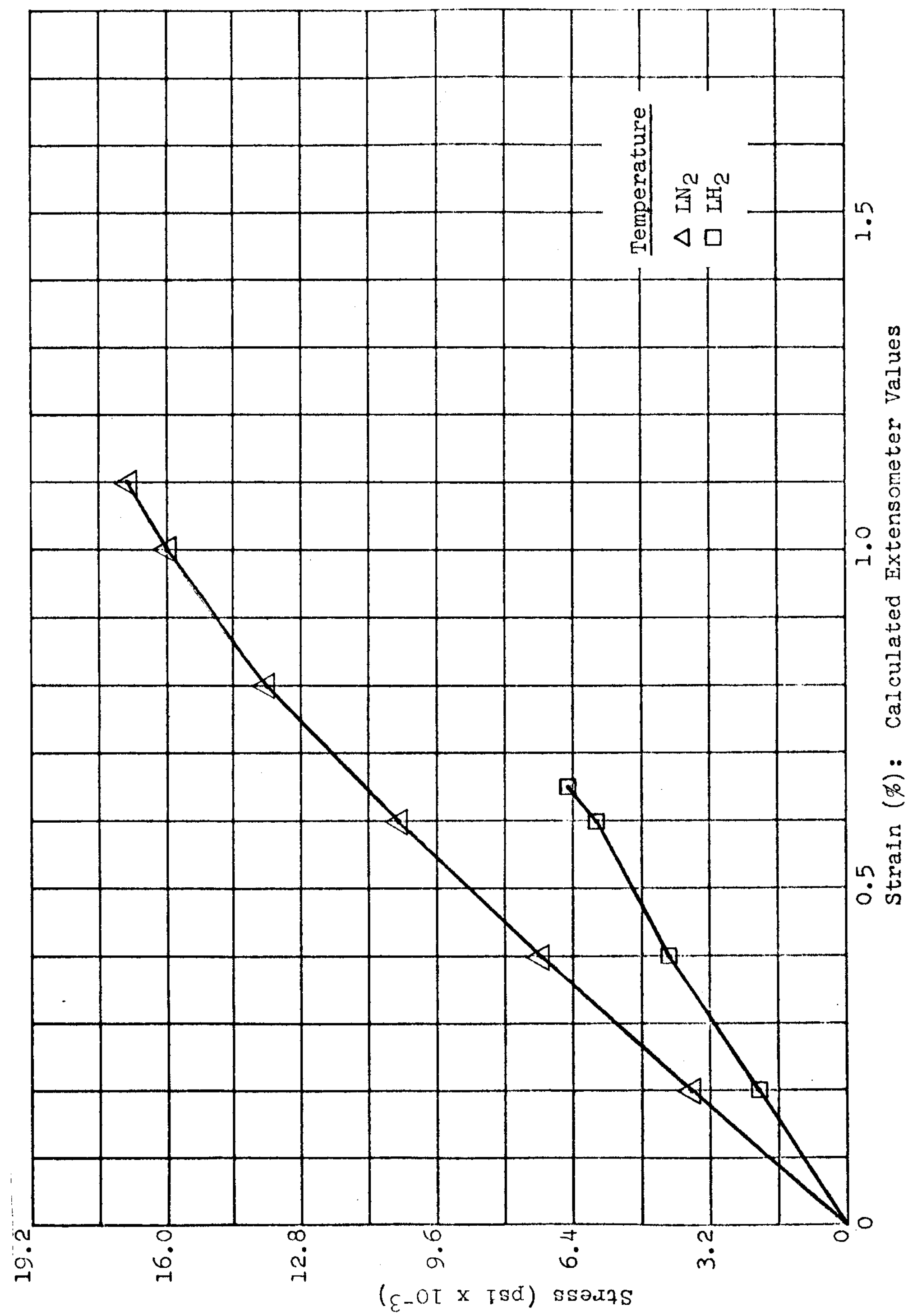

Figure 5.13 Stress vs Strain (Calculated Extensometer Values) for Three Different Temperatures: Material D (Kel-F-81); High-Dose Exposure

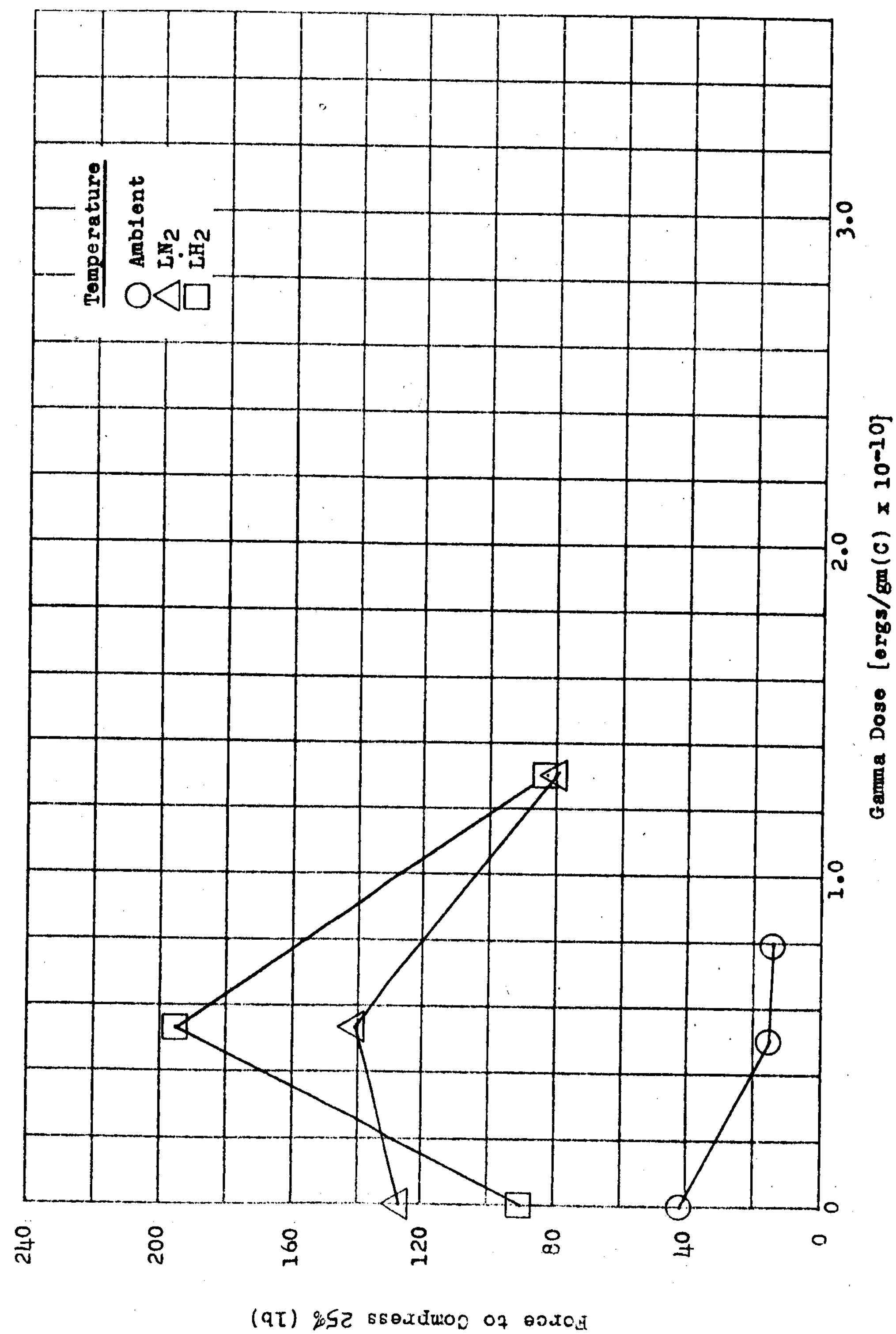

Figure 5.14 Force to Compress 25% vs Gamma Dose for Three Different Temperatures: *Material E* (Stafoam AA402)

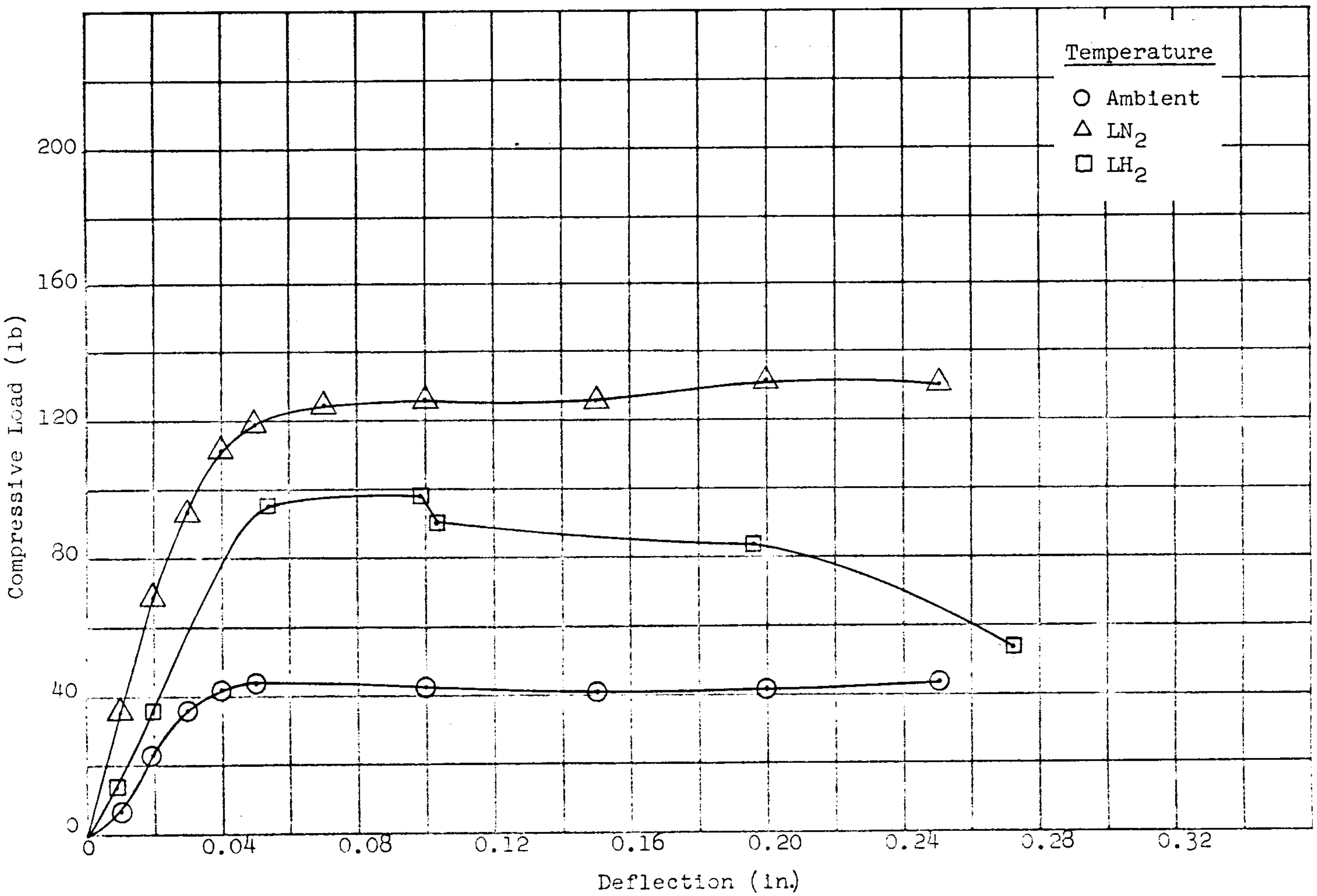

Figure 5.15 Compressive Load vs Deflection for Three Different Temperatures: Material E (Stafoam AA402); Unirradiated (Control)

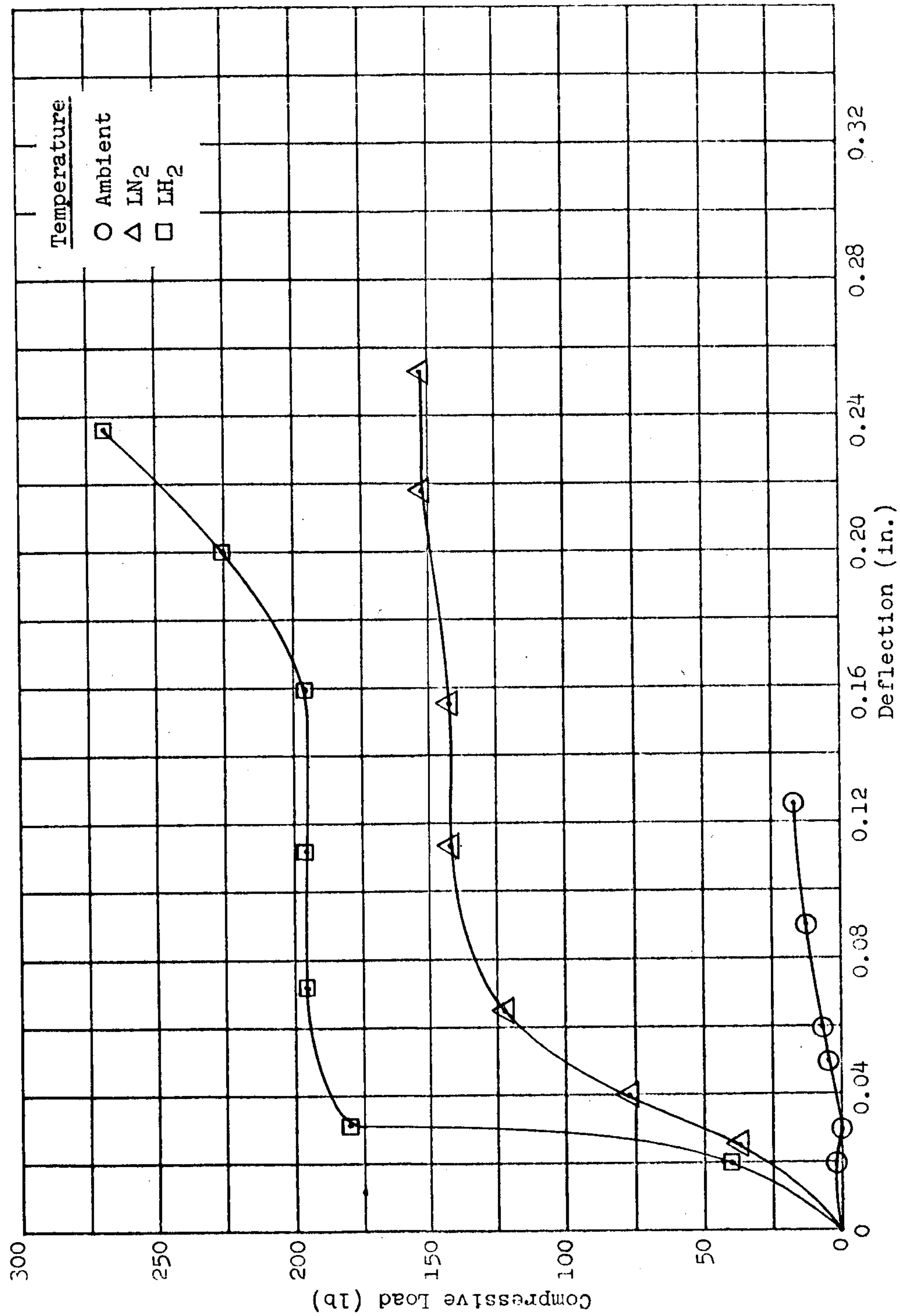

Figure 5.16 Compressive Load vs Deflection for Three Different Temperatures: Material E (Stafoam AA402); Low-Dose Exposure

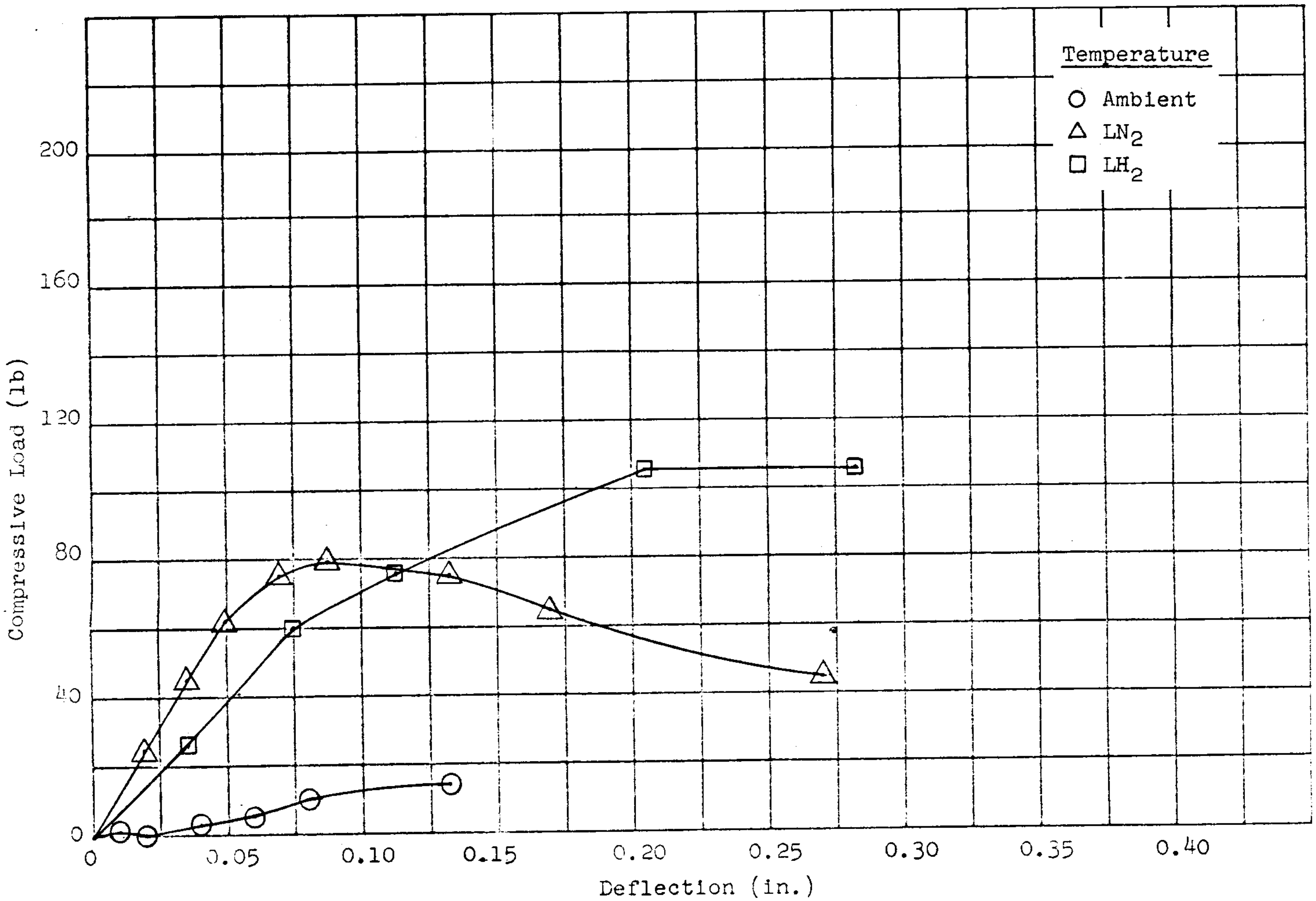

Figure 5.17 Compressive Load vs Deflection for Three Different Temperatures: Material E (Stafoam AA402); High-Dose Exposure

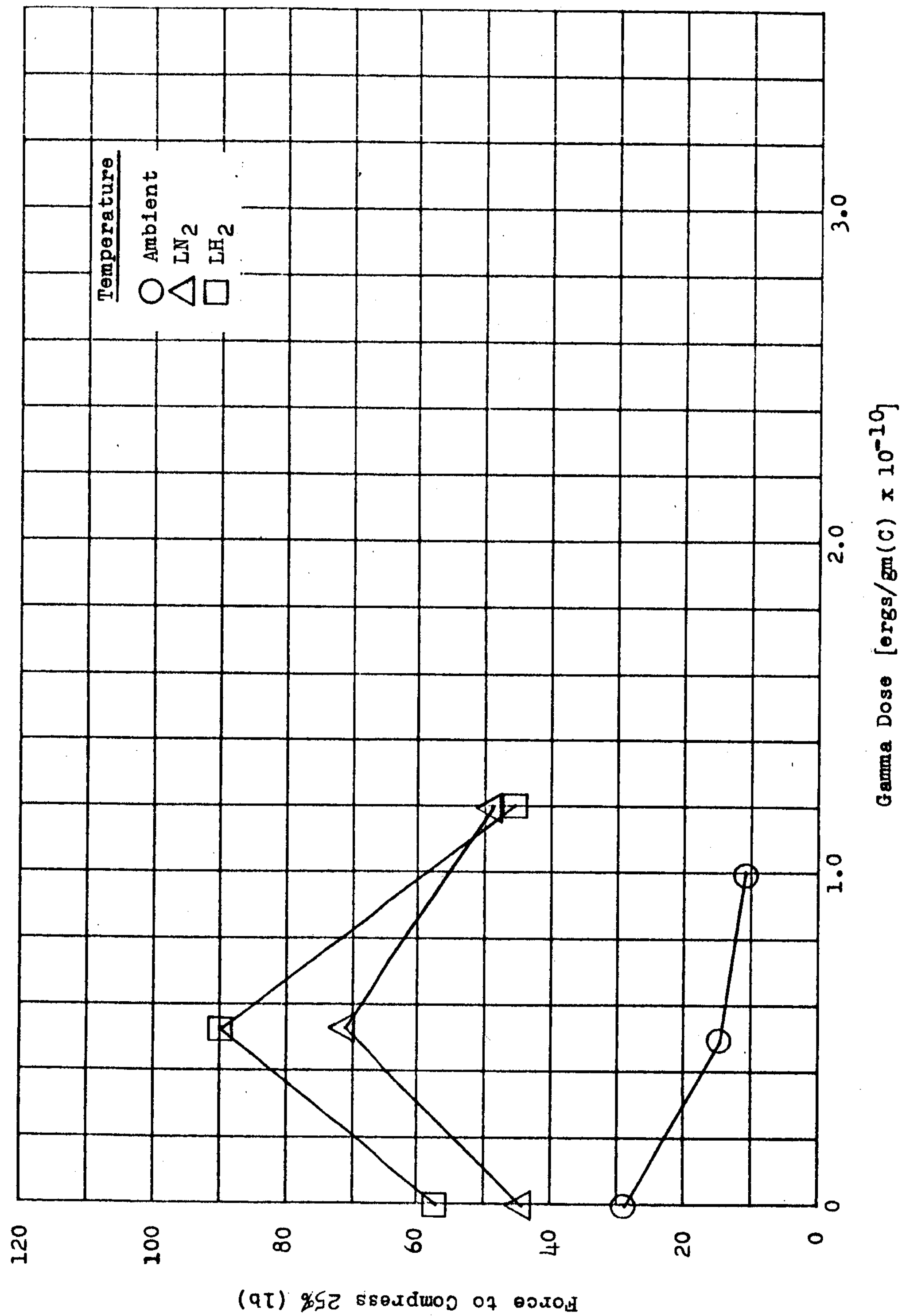

Figure 5.18 Force to Compress 25% vs Gamma Dose for Three Different Temperatures: Material F (Styrofoam 22)

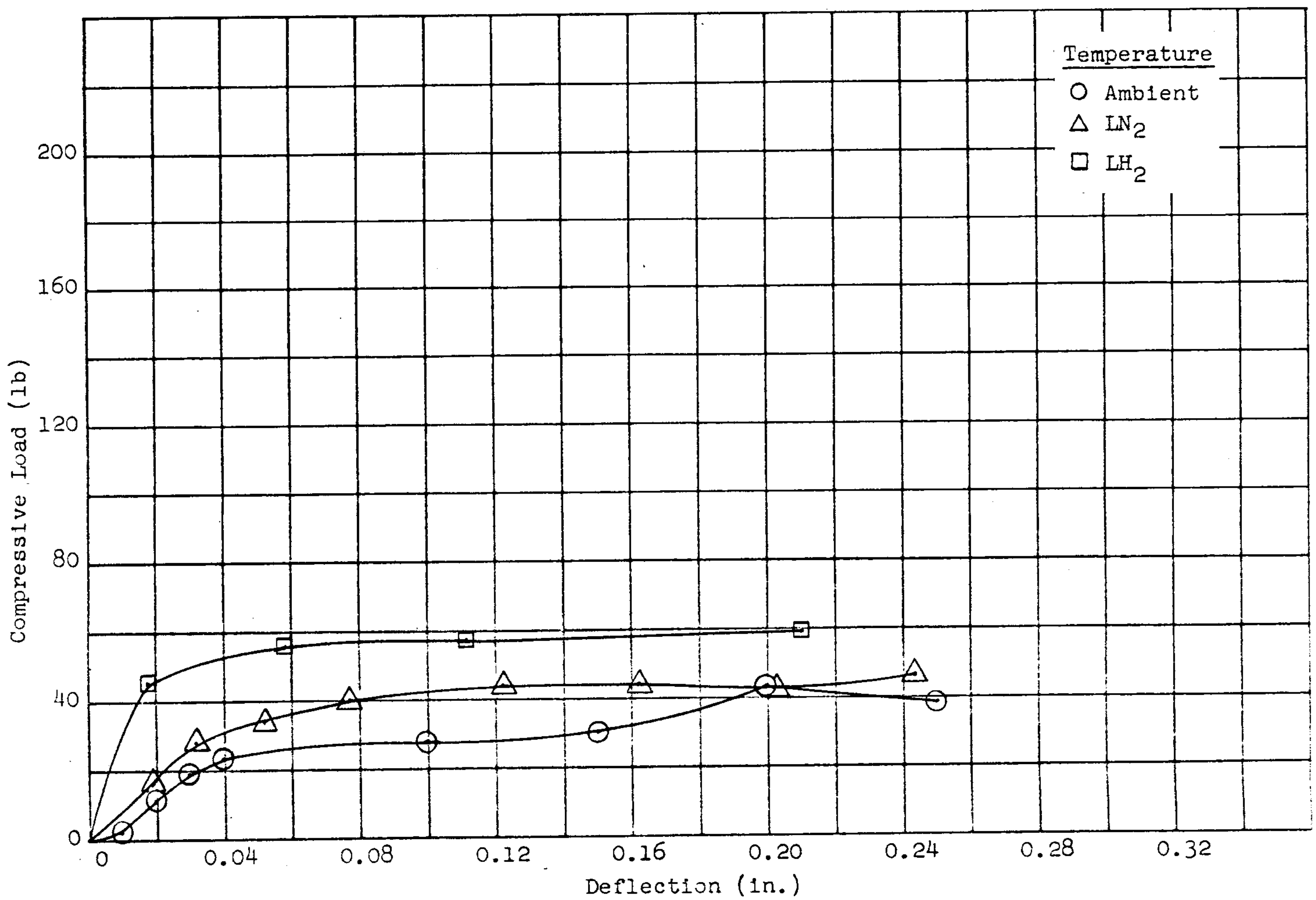

Figure 5.19 Compressive Load vs Deflection for Three Different Temperatures: Material F (Styrofoam 22); Unirradiated (Control)

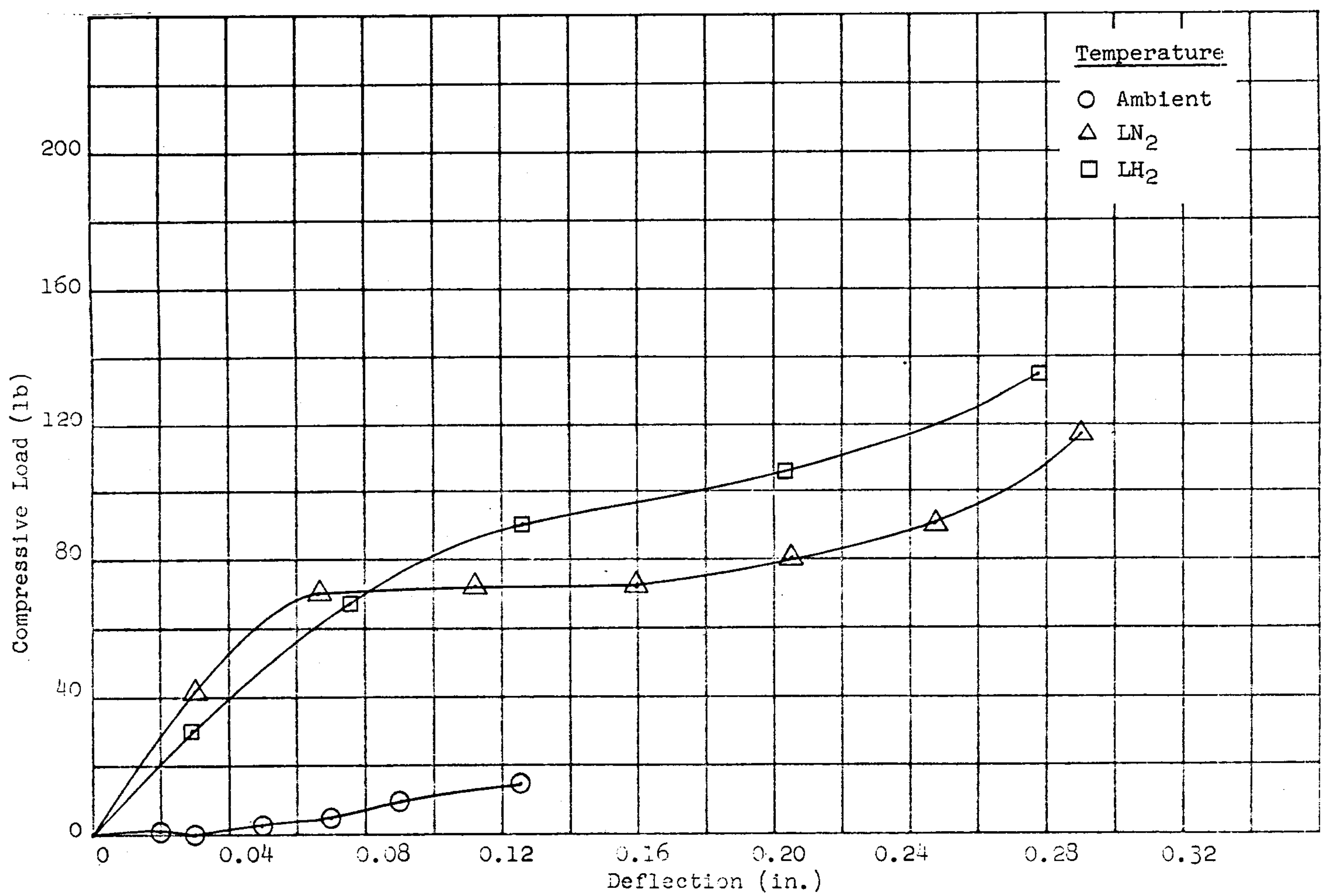

Figure 5.20 Compressive Load vs Deflection for Three Different Temperatures: Material F (Styrofoam 22); Low-Dose Exposure

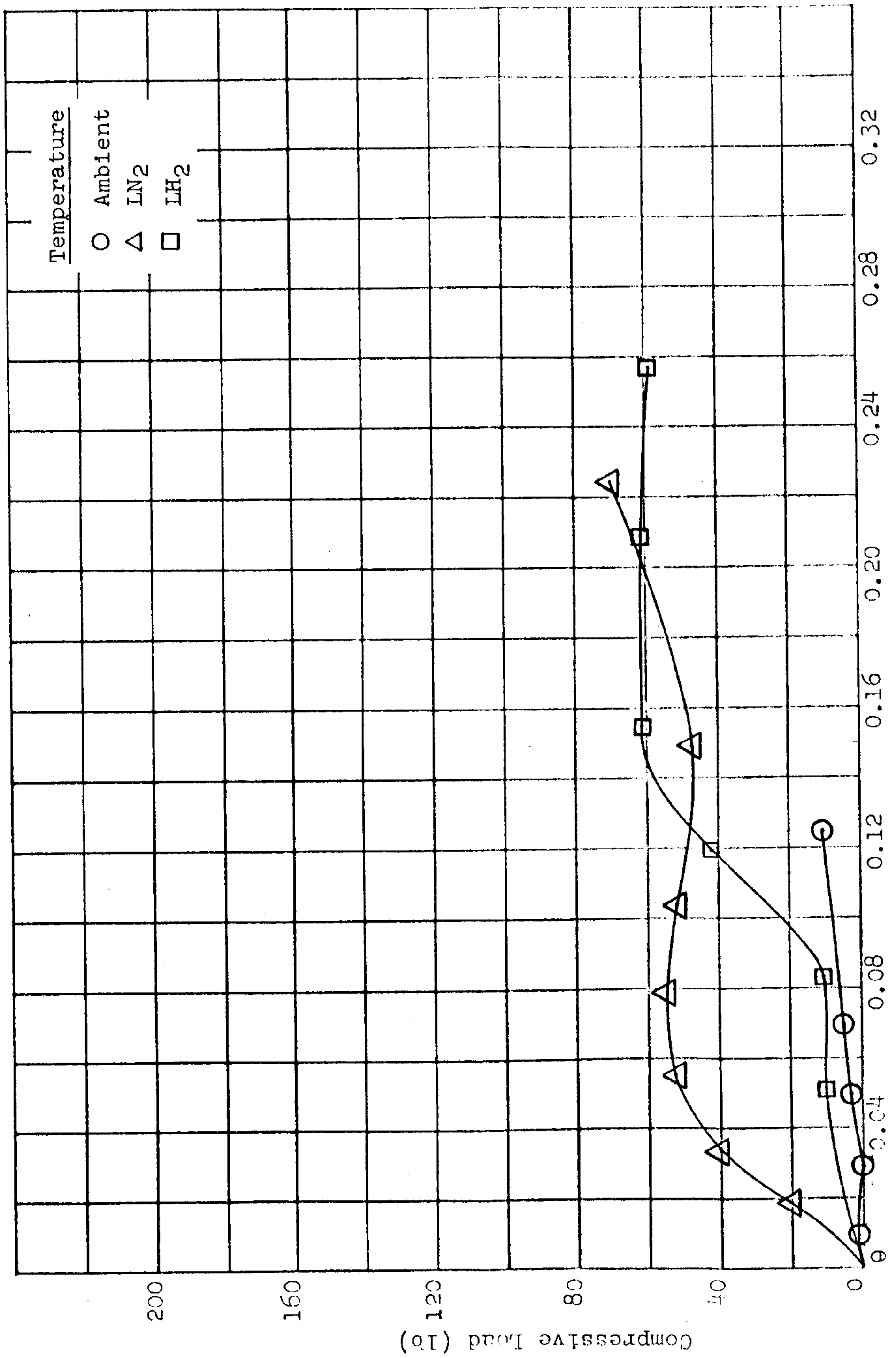

Figure 5.21 Compressive Load vs Deflection for Three Different Temperatures: Material F (Styrofoam 22); High-Dose Exposure

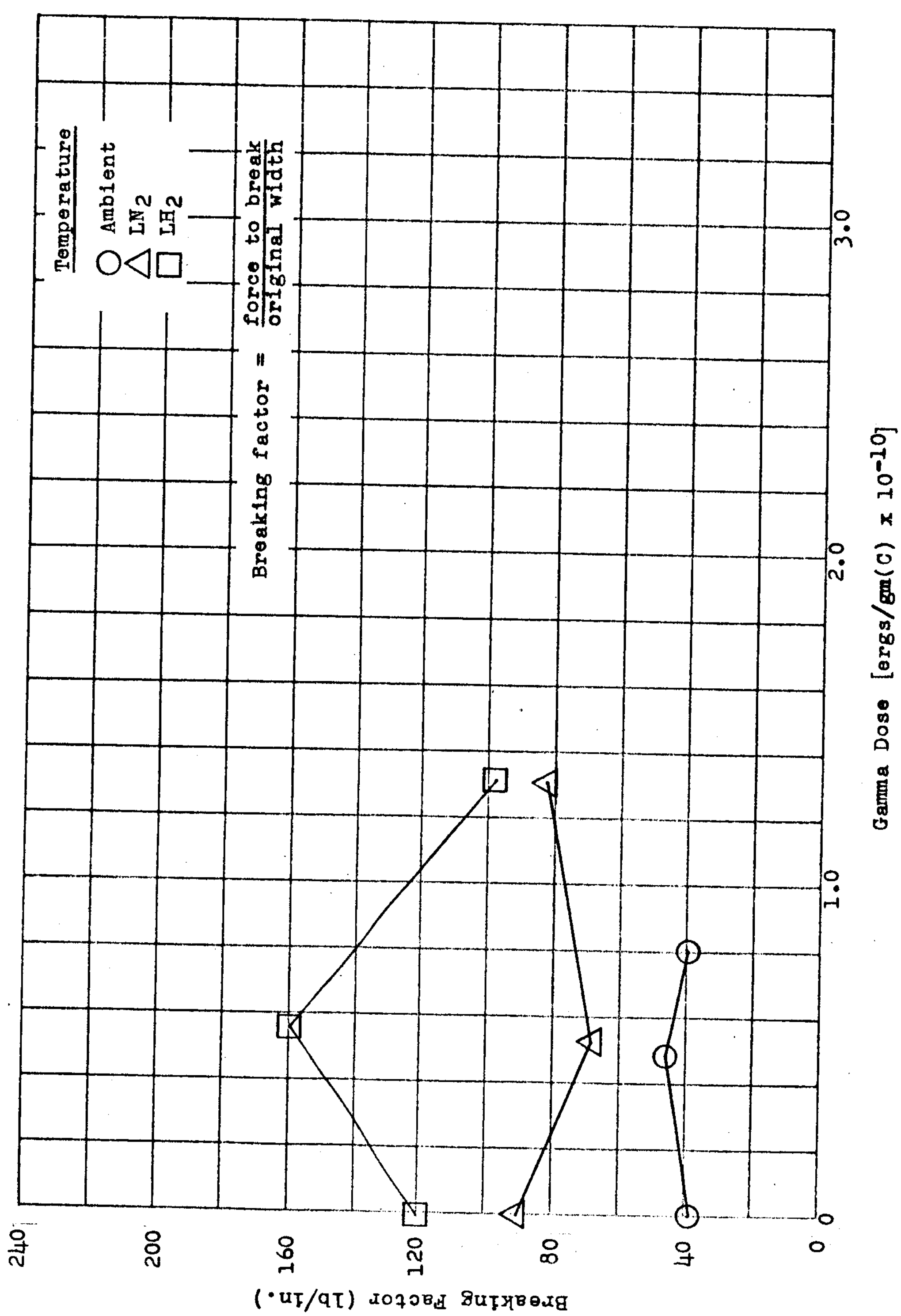

Figure 5.22 Breaking Factor vs Gamma Dose for Three Different Temperatures: Material G (H-Film)

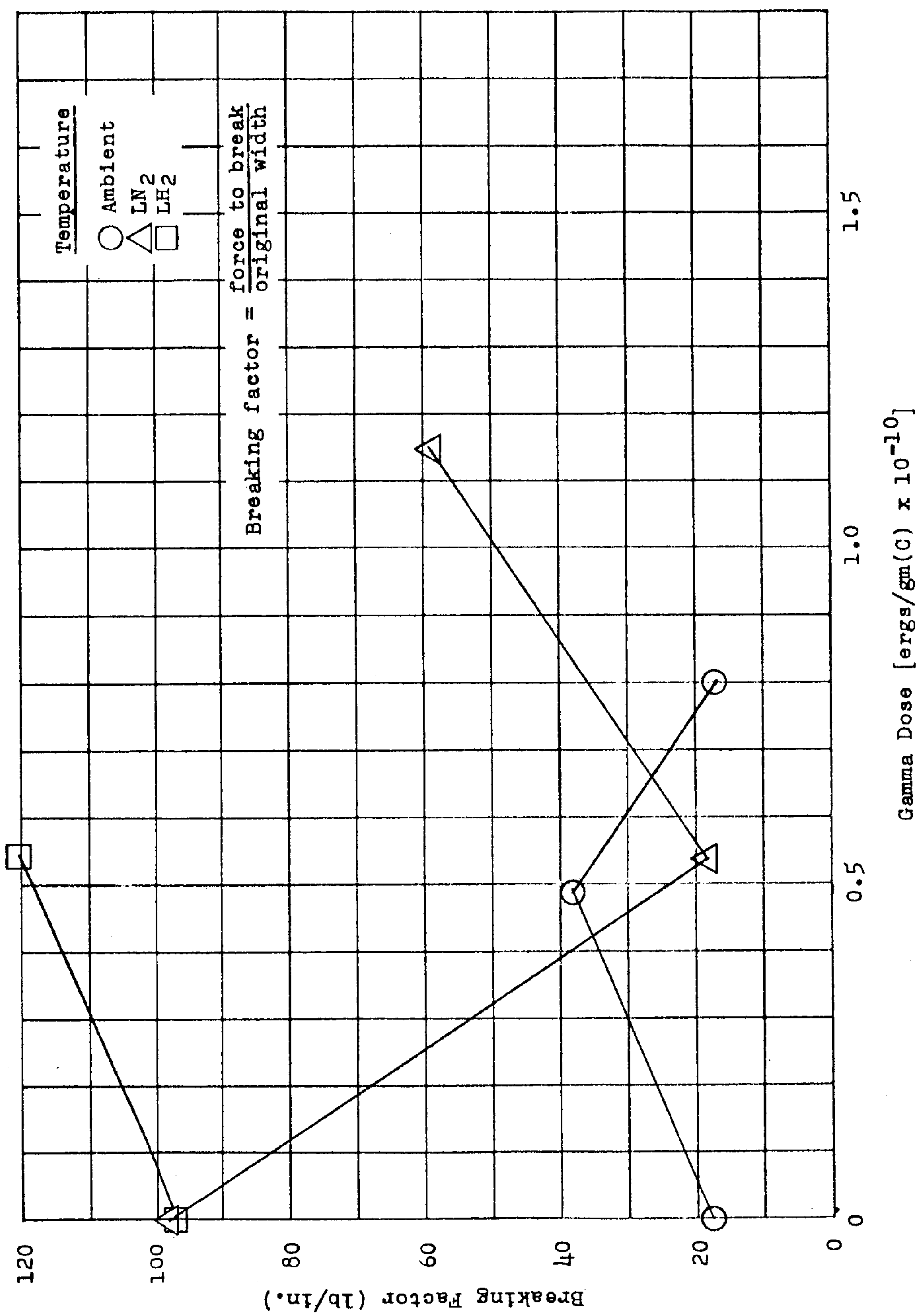

Figure 5.23 Breaking Factor vs Gamma Dose for Three Different Temperatures: Material H (Mylar-C)

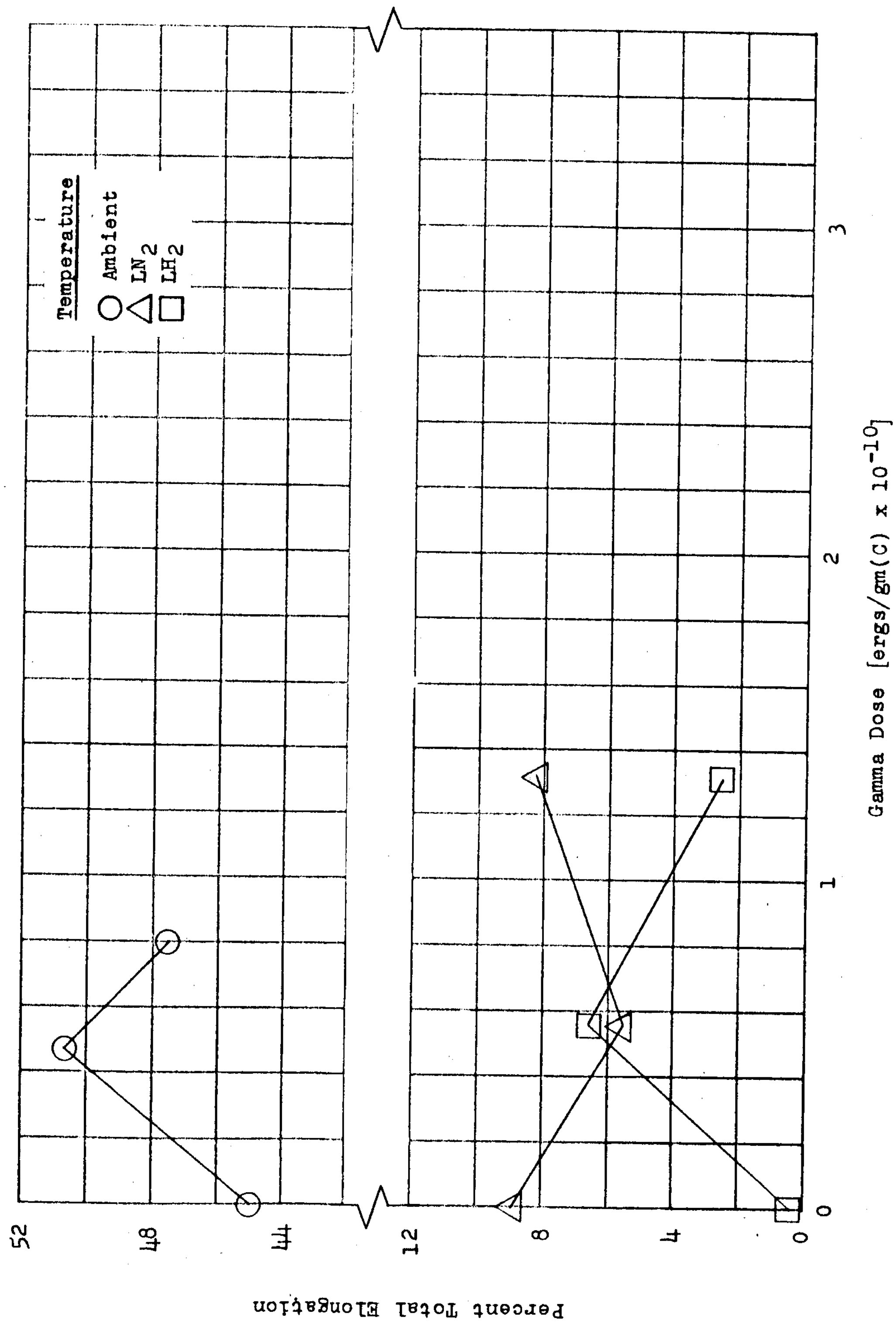

Figure 5.24 Percent Total Elongation vs Gamma Dose for Three Different Temperatures: Material G (H-Film)

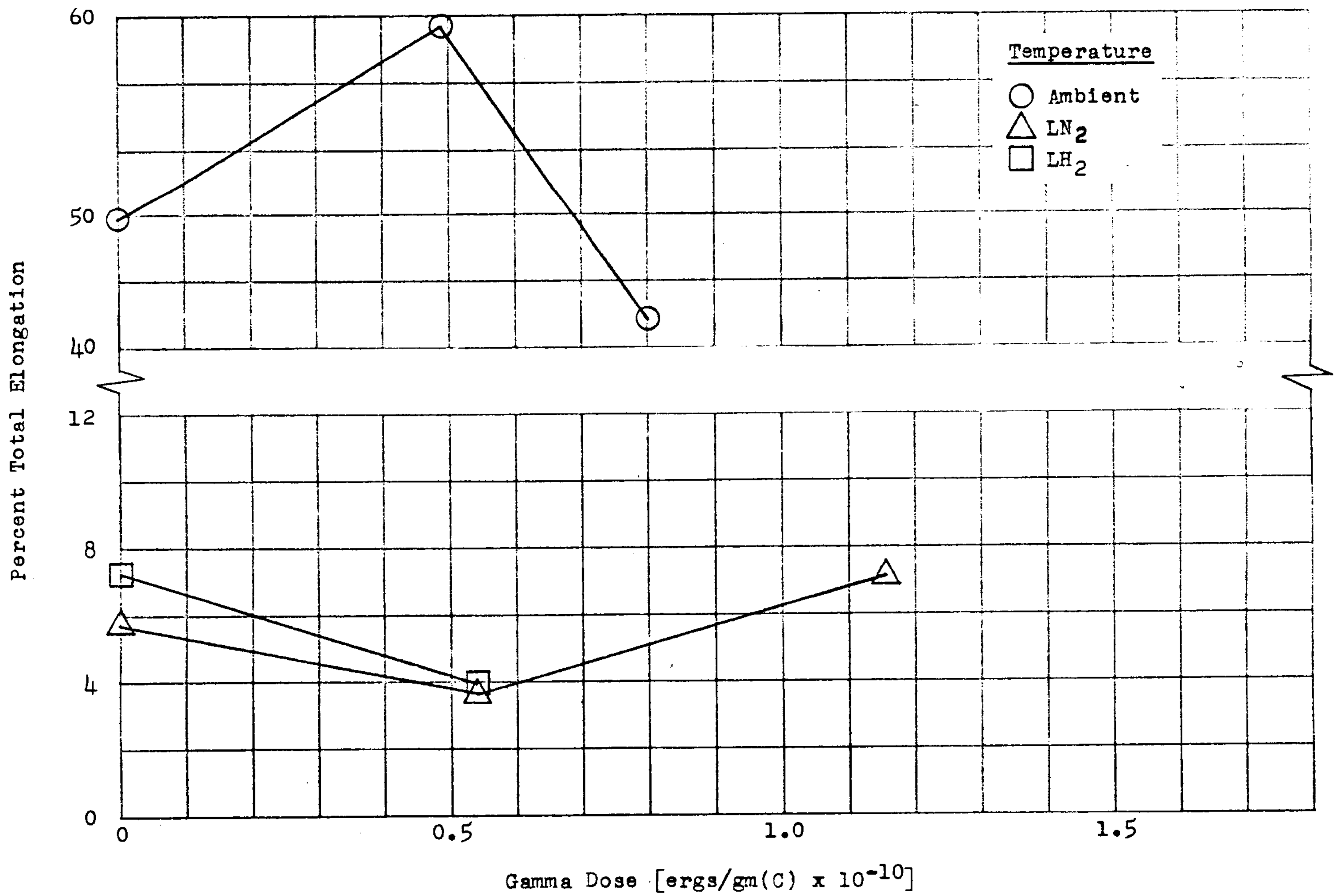

Figure 5.25 Percent Total Elongation vs Gamma Dose for Three Different Temperatures: Material H (Mylar-C)

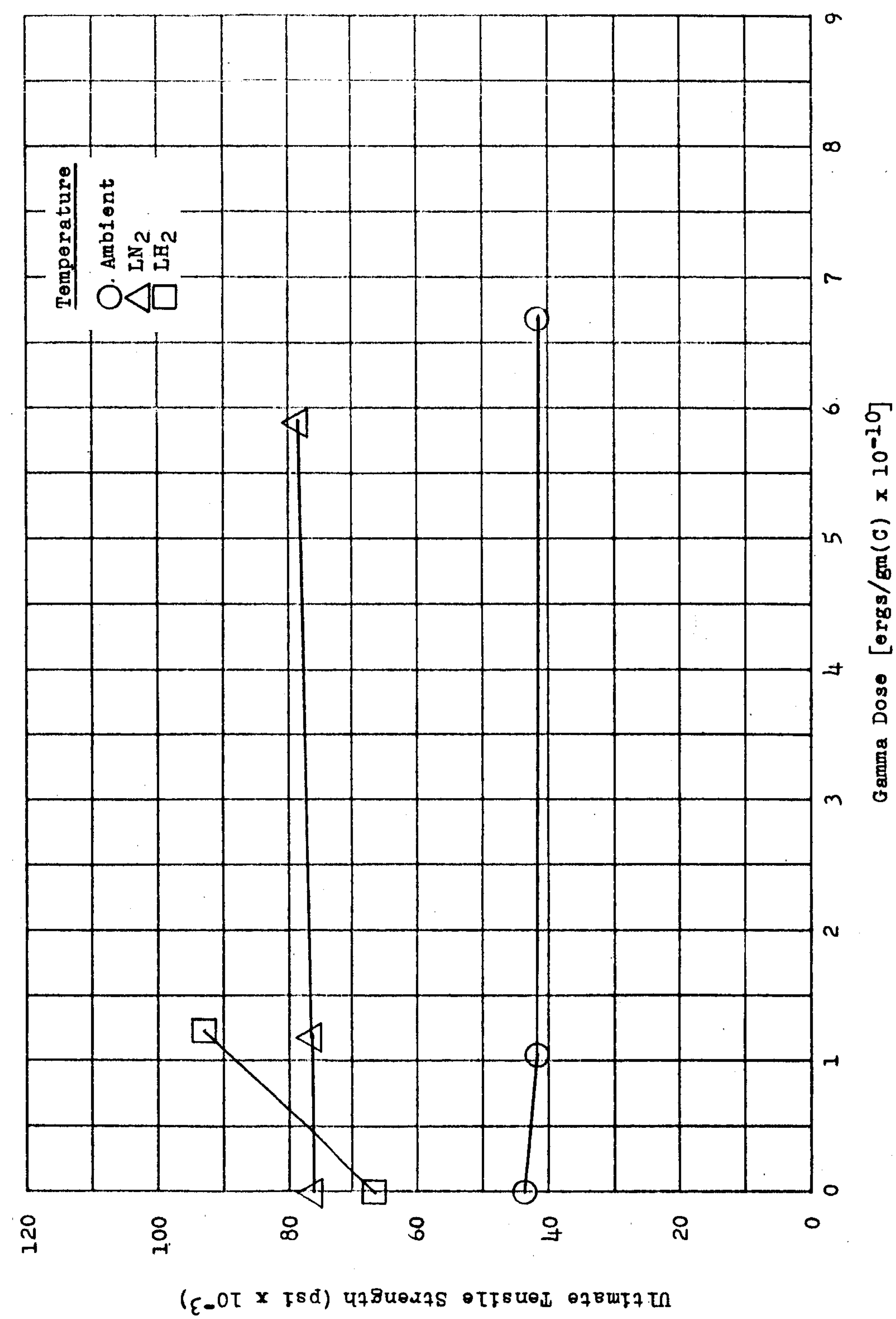

Figure 5.26 Ultimate Tensile Strength vs Gamma Dose for Three Different Temperatures: Material I (Conolon 506)

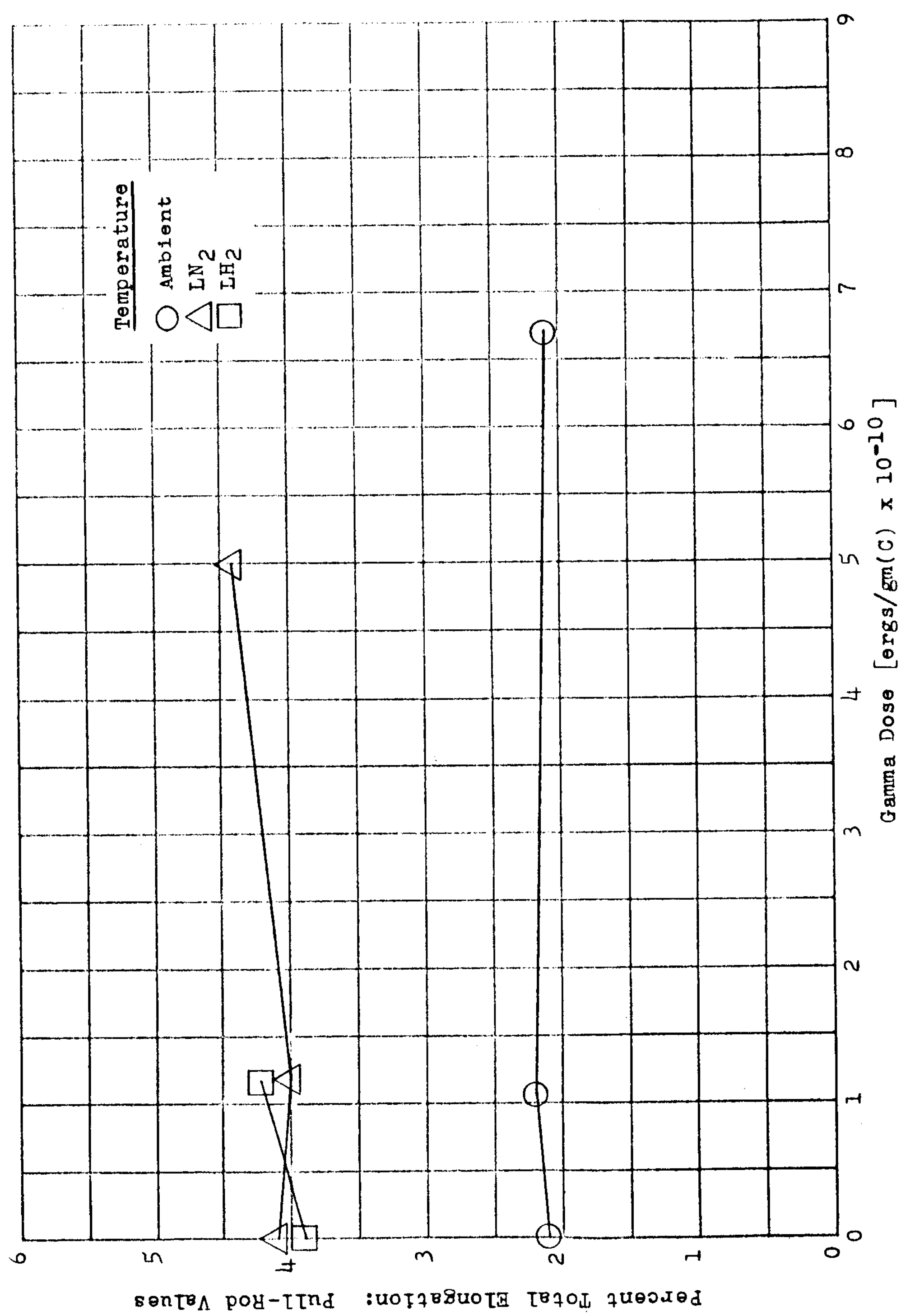

Figure 5.27 Percent Total Elongation (Pull-Rod Valves) vs Gamma Dose for Three Different Temperatures: Material I (Conolon 506)

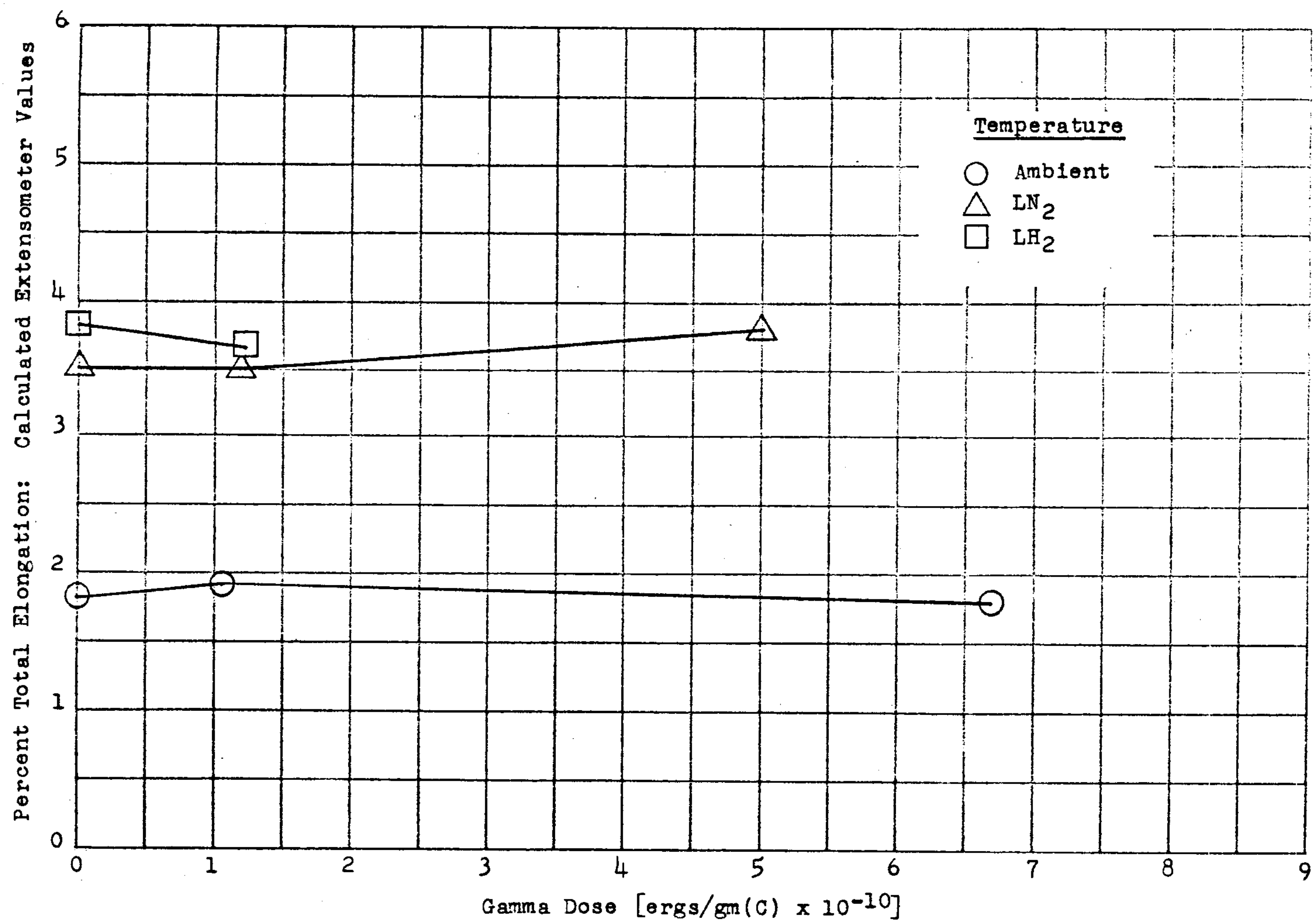

Figure 5.28 Percent Total Elongation (Calculated Extensometer Values) vs Gamma Dose for Three Different Temperatures: Material I (Conolon 506)

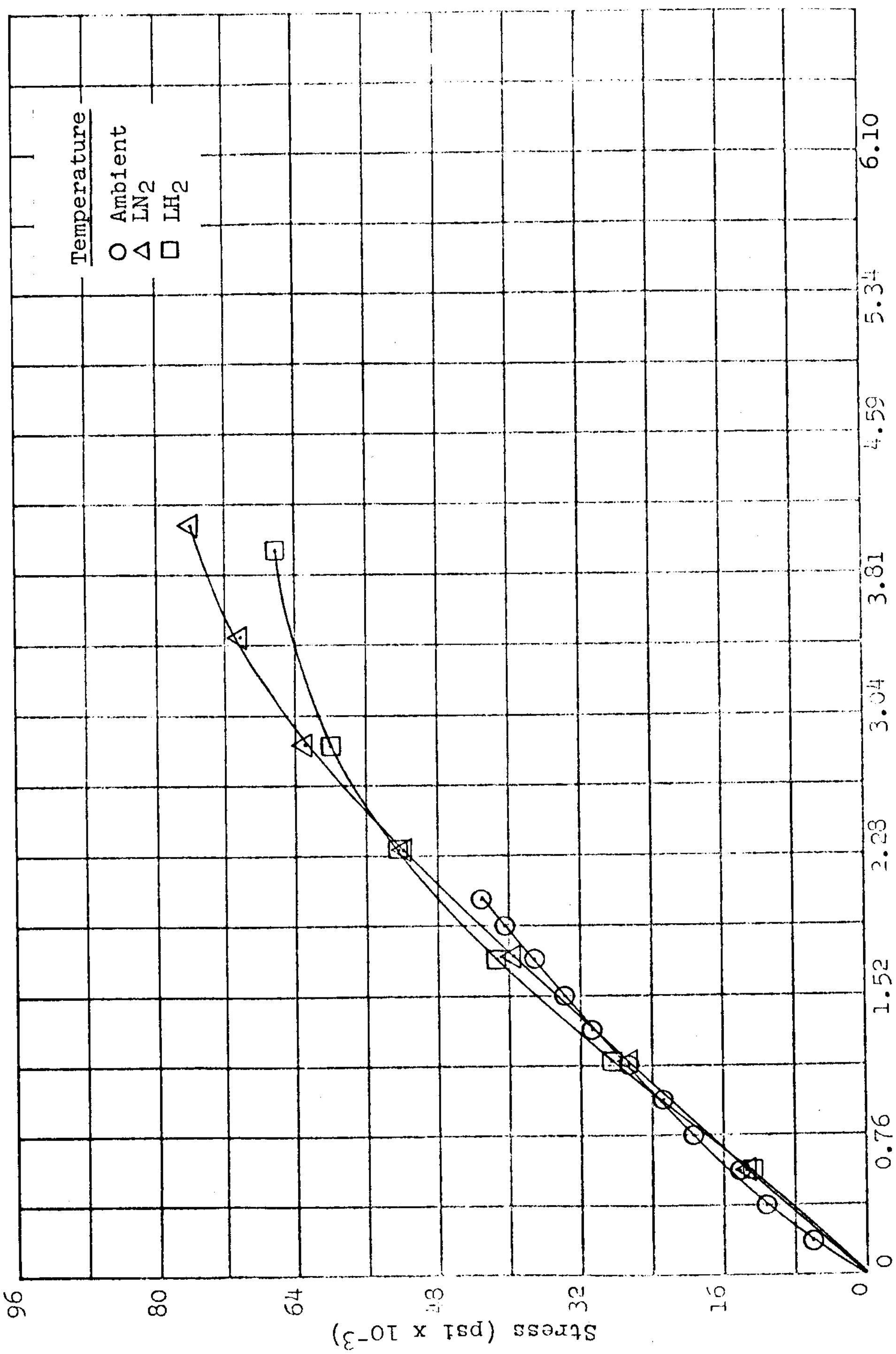

Figure 5.29 Stress vs Strain (Pull-Rod Values) for Three Different Temperatures: Material I (Conolon 506); Unirradiated (Control)

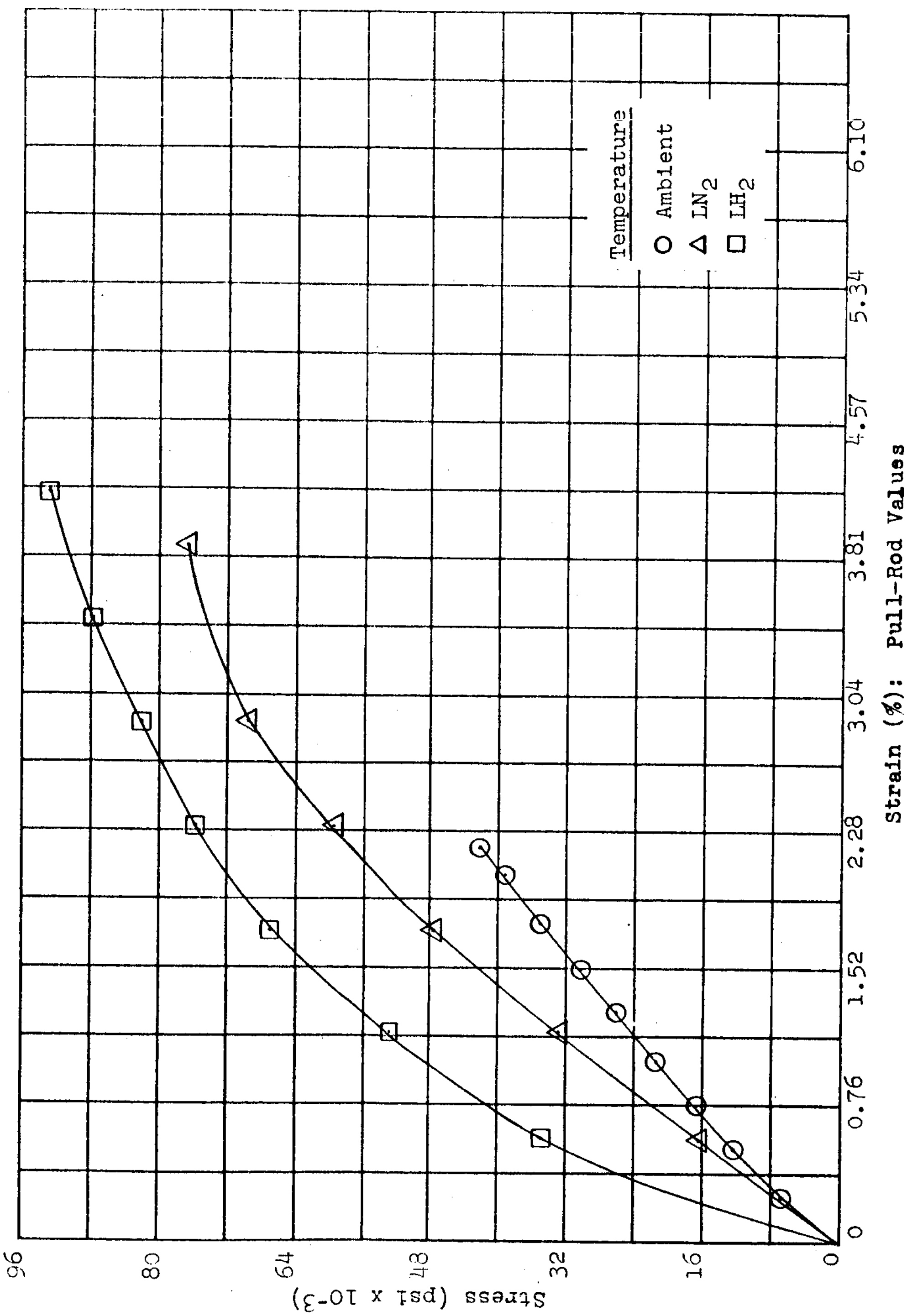

Figure 5.30 Stress vs Strain (Pull-Rod Values) for Three Different Temperatures: Material I (Conolon 506); Low-Dose Exposure

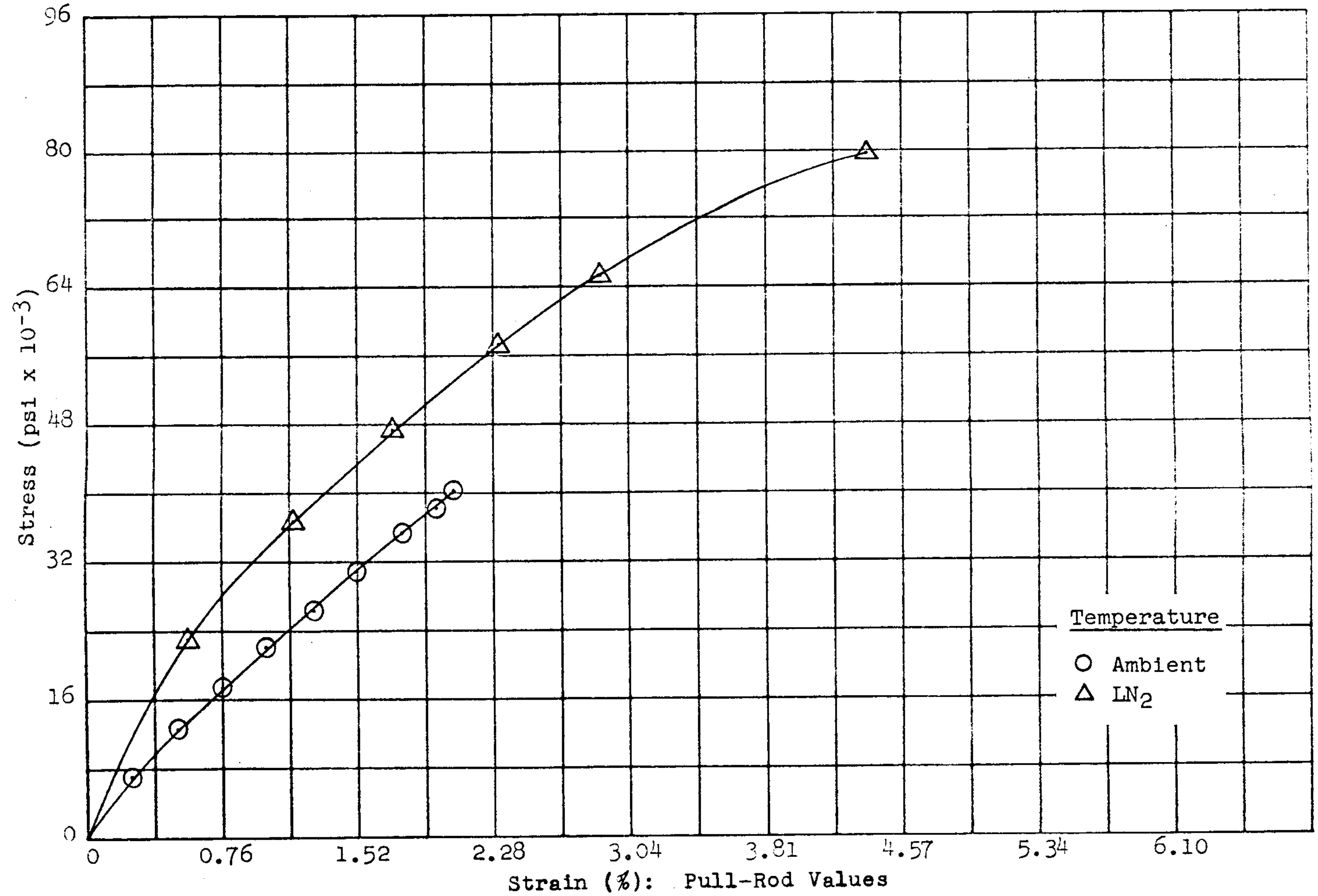

Figure 5.31 Stress vs Strain (Pull-Rod Values) for Two Different Temperatures: Material I (Conolon 506); High-Dose Exposure

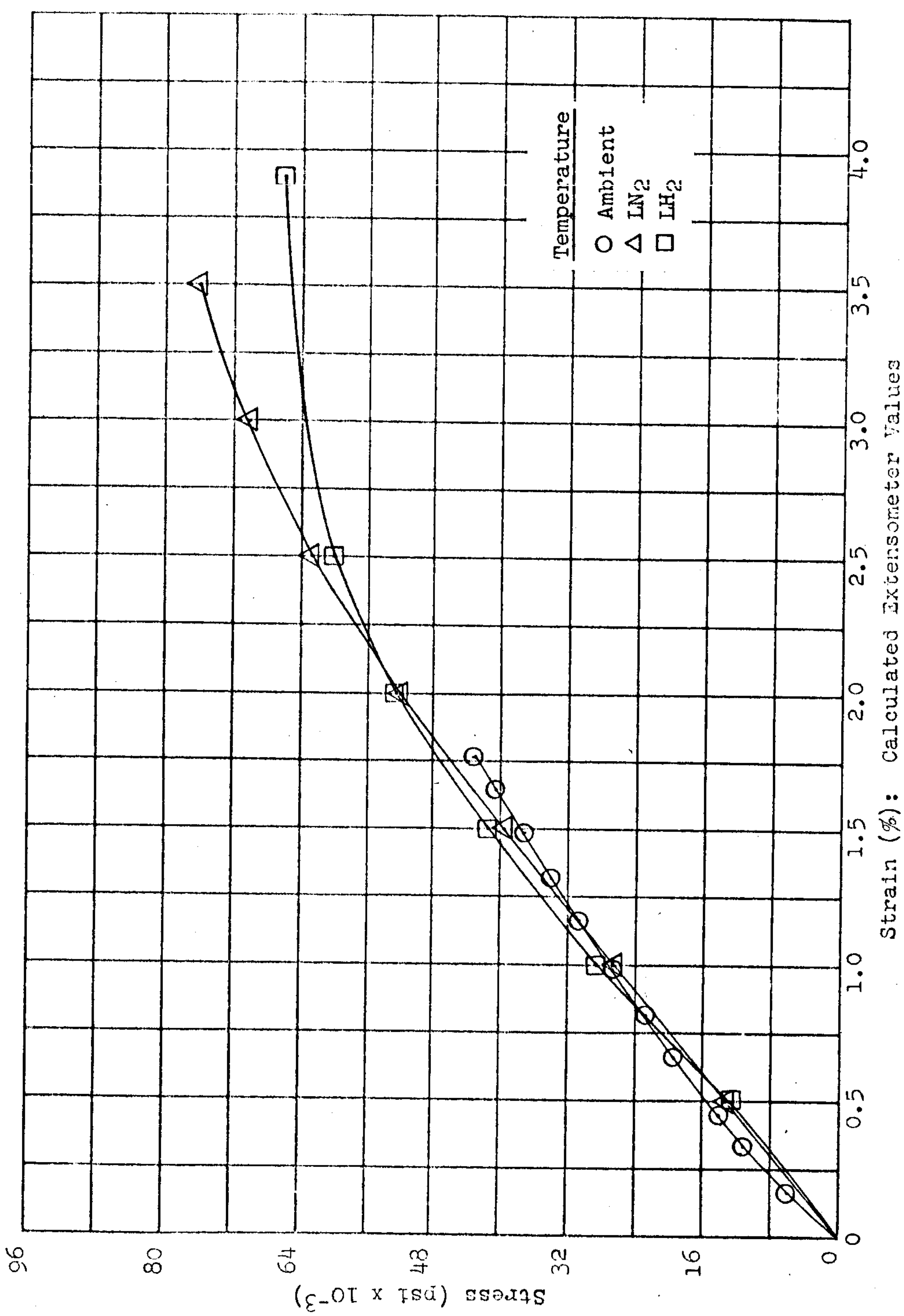

Figure 5.32 Stress vs Strain (Calculated Extensometer Values) for Three Different Temperatures: Material I (Conolon 506); Unirradiated (Control)

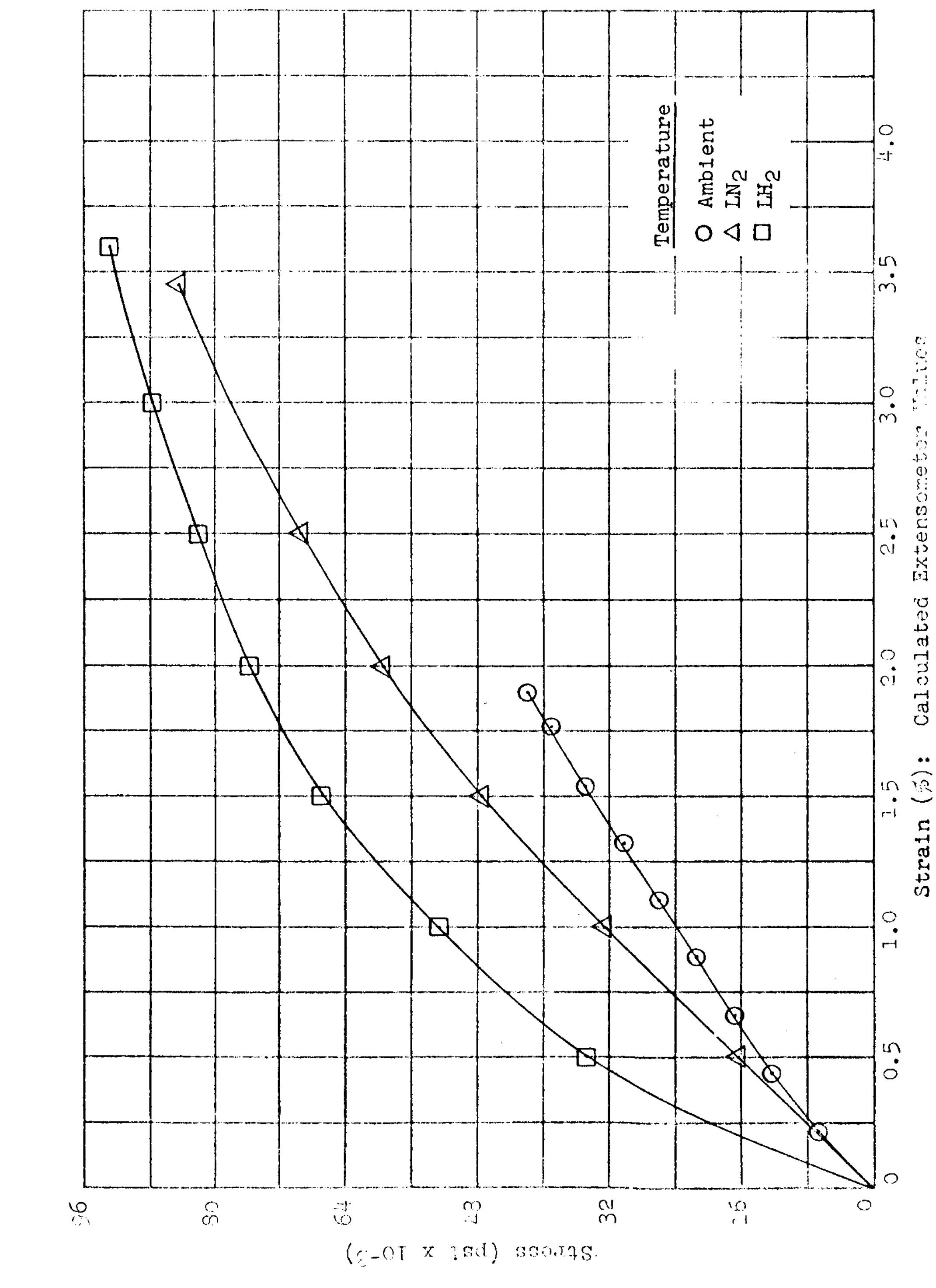

Figure 5.33 Stress vs Strain (Calculated Extensometer Values) for Three Different Temperatures: Material I (Conolon 506); Low-Dose Exposure

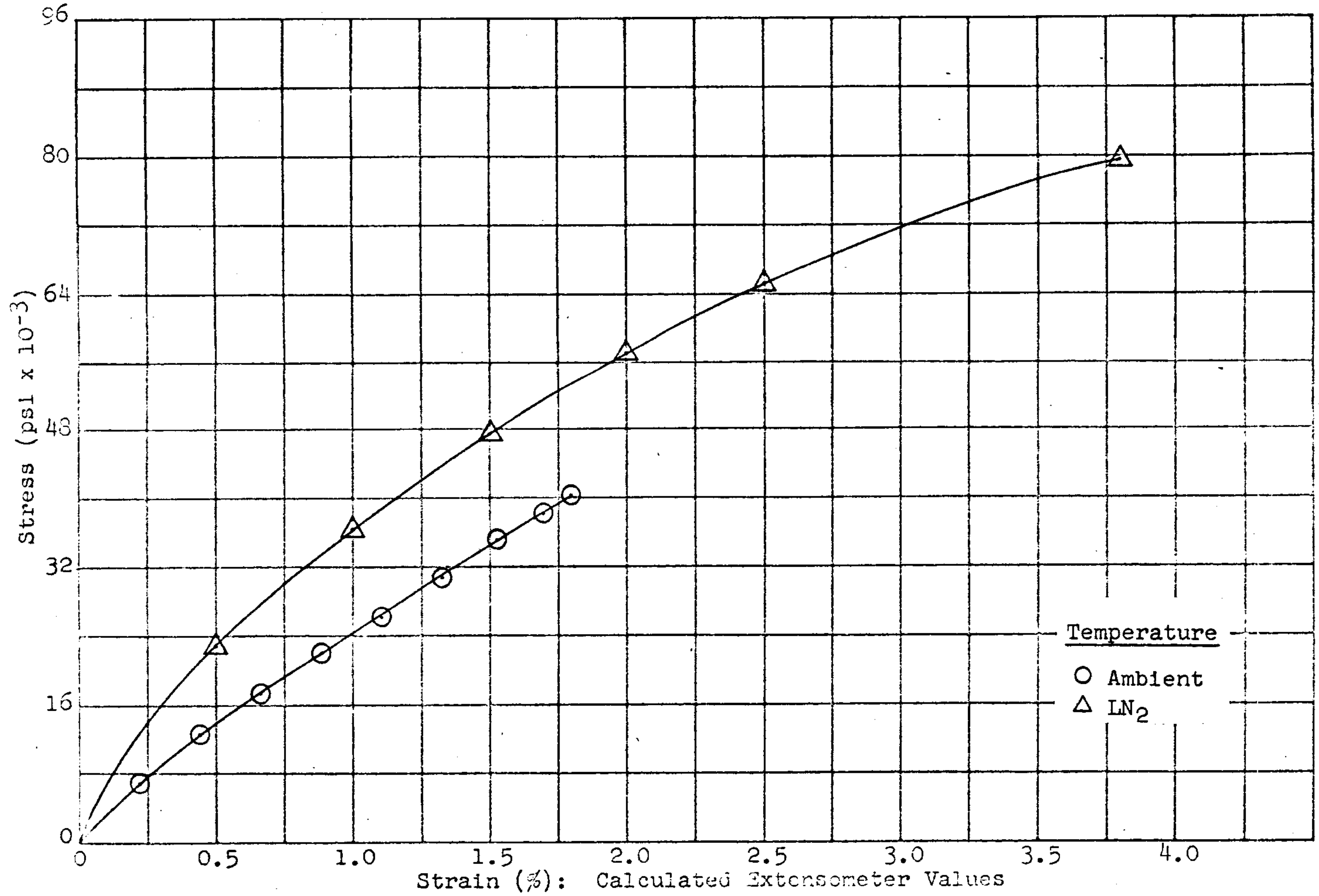

Figure 5.34 Stress vs Strain (Calculated Extensometer Values) for Two Different Temperatures: Material I (Conolon 506); High-Dose Exposure

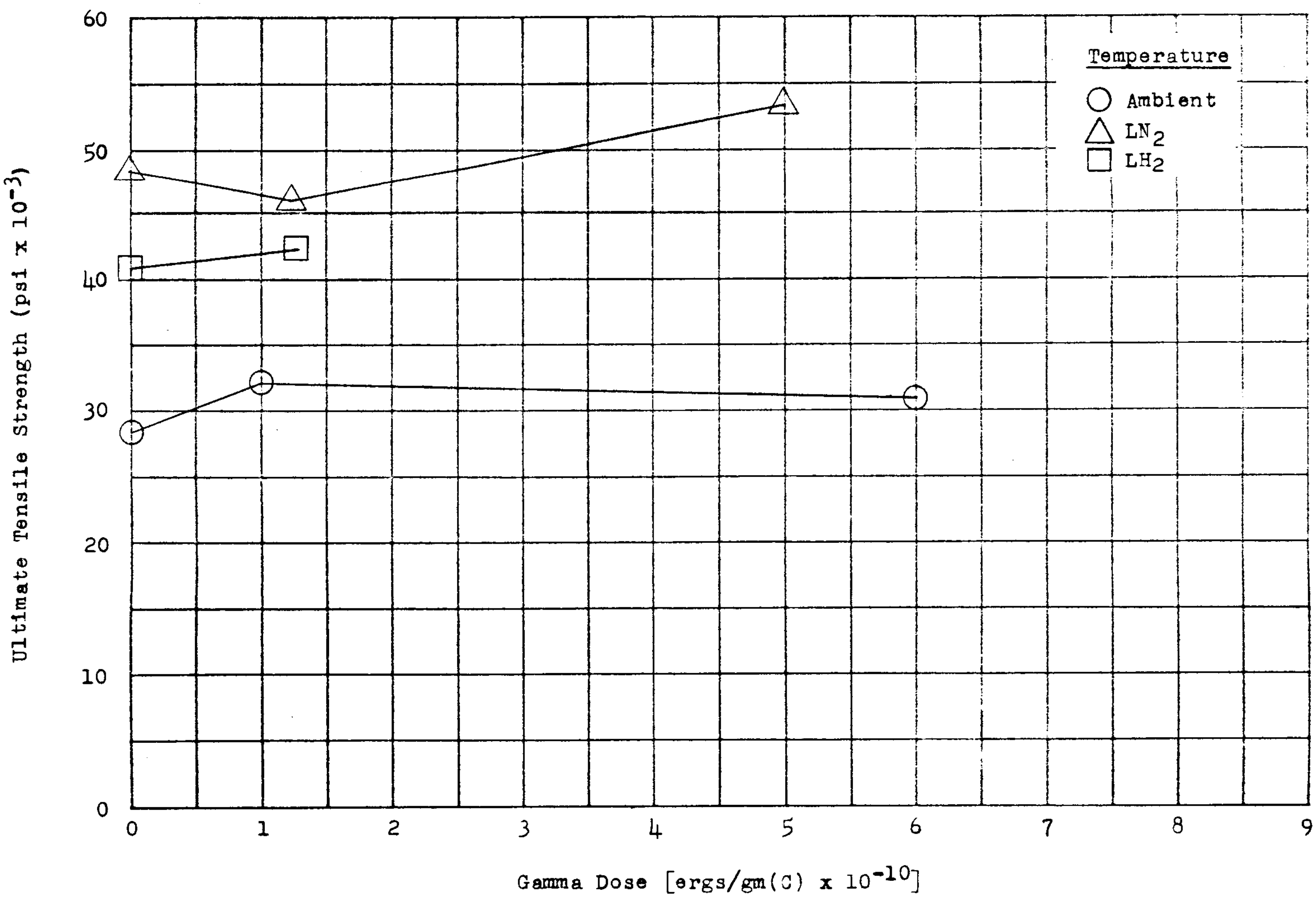

Figure 5.35 Ultimate Tensile Strength vs Gamma Dose for Three Different Temperatures: Material J (Paraplex P-43)

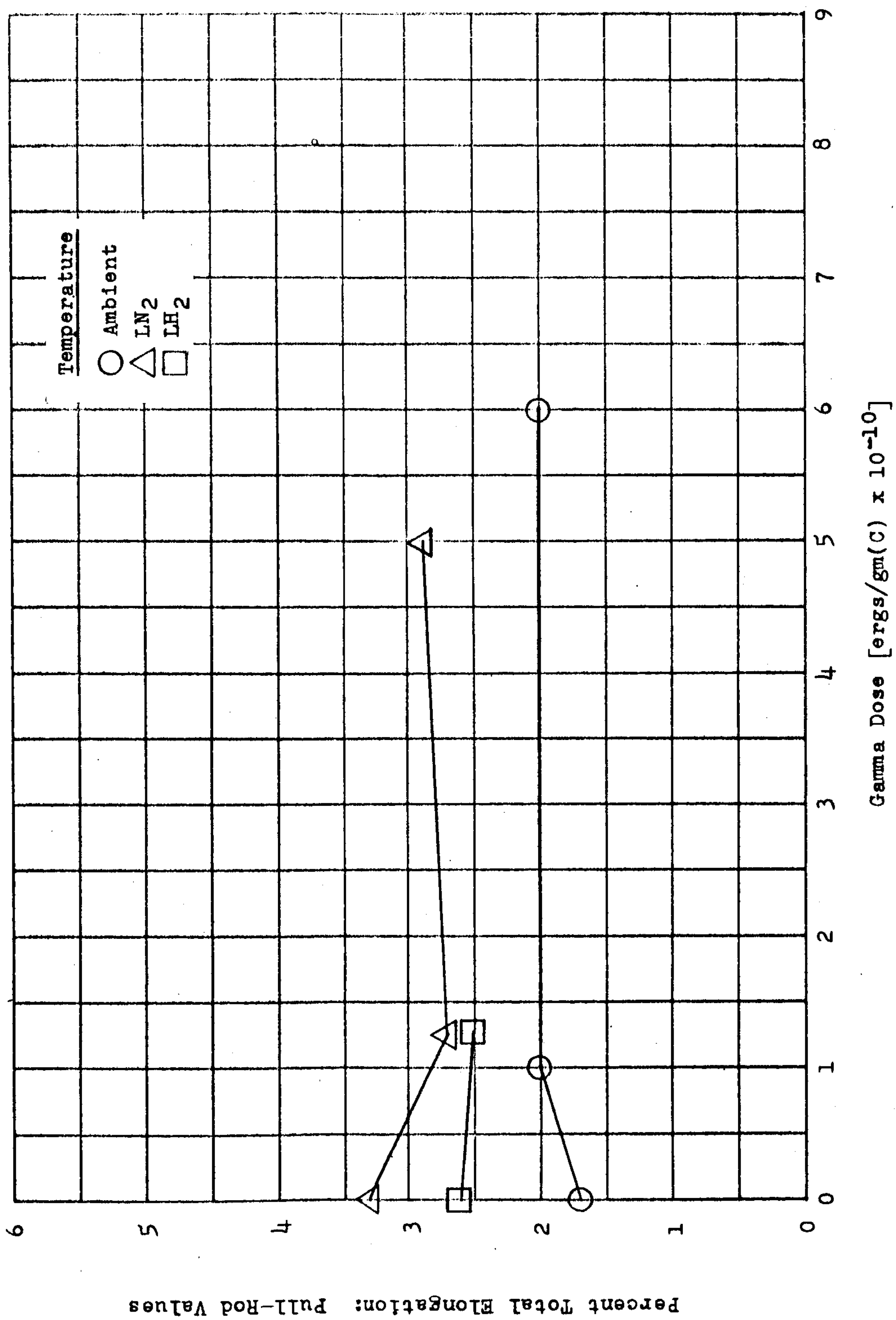

Figure 5.36 Percent Total Elongation (Pull-Rod Values) vs Gamma Dose for Three Different Temperatures: Material J (Paraplex P-43)

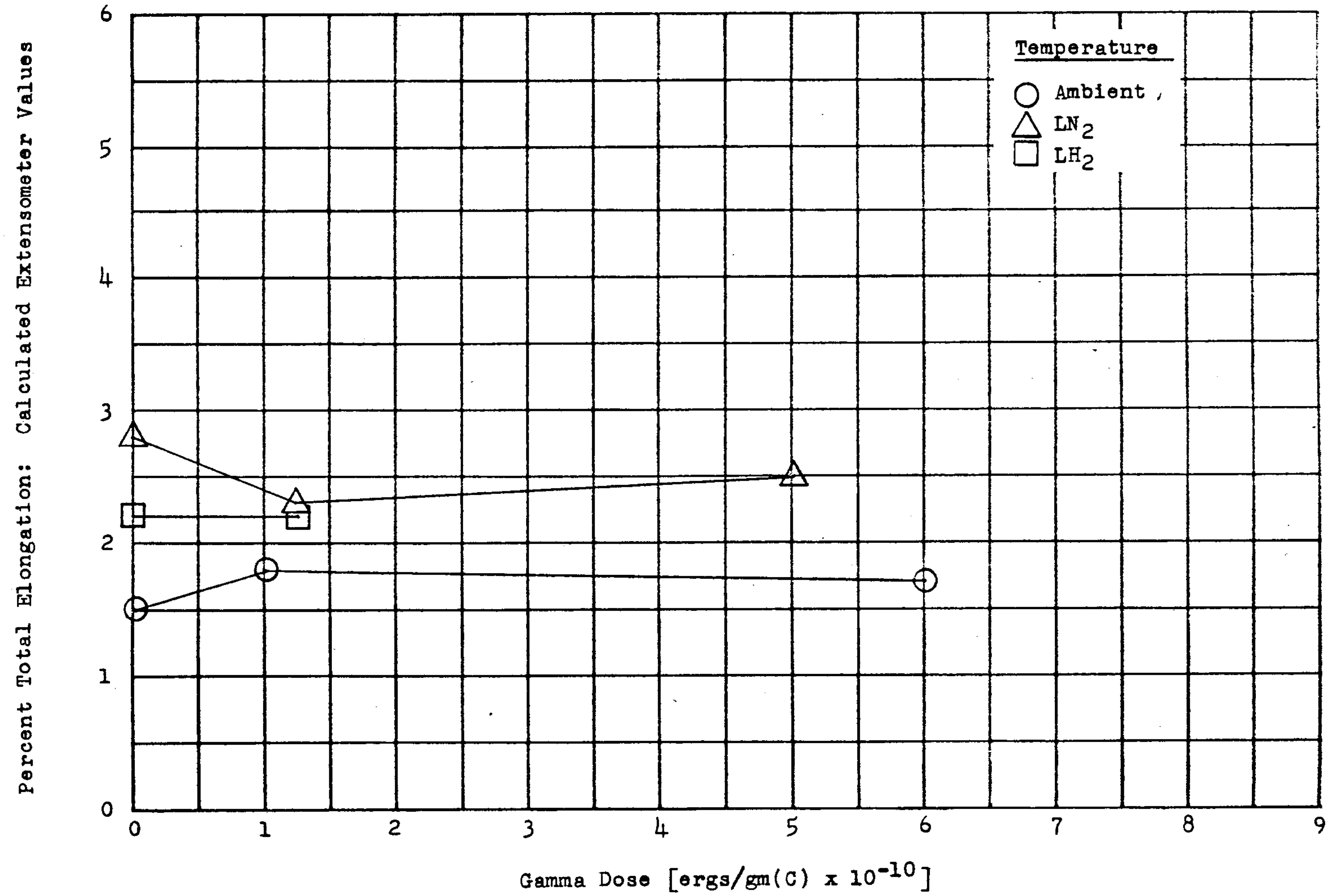

Figure 5.37 Percent Total Elongation (Calculated Extensometer Values) vs Gamma Dose for Three Different Temperatures: Material J (Paraplex P-43)

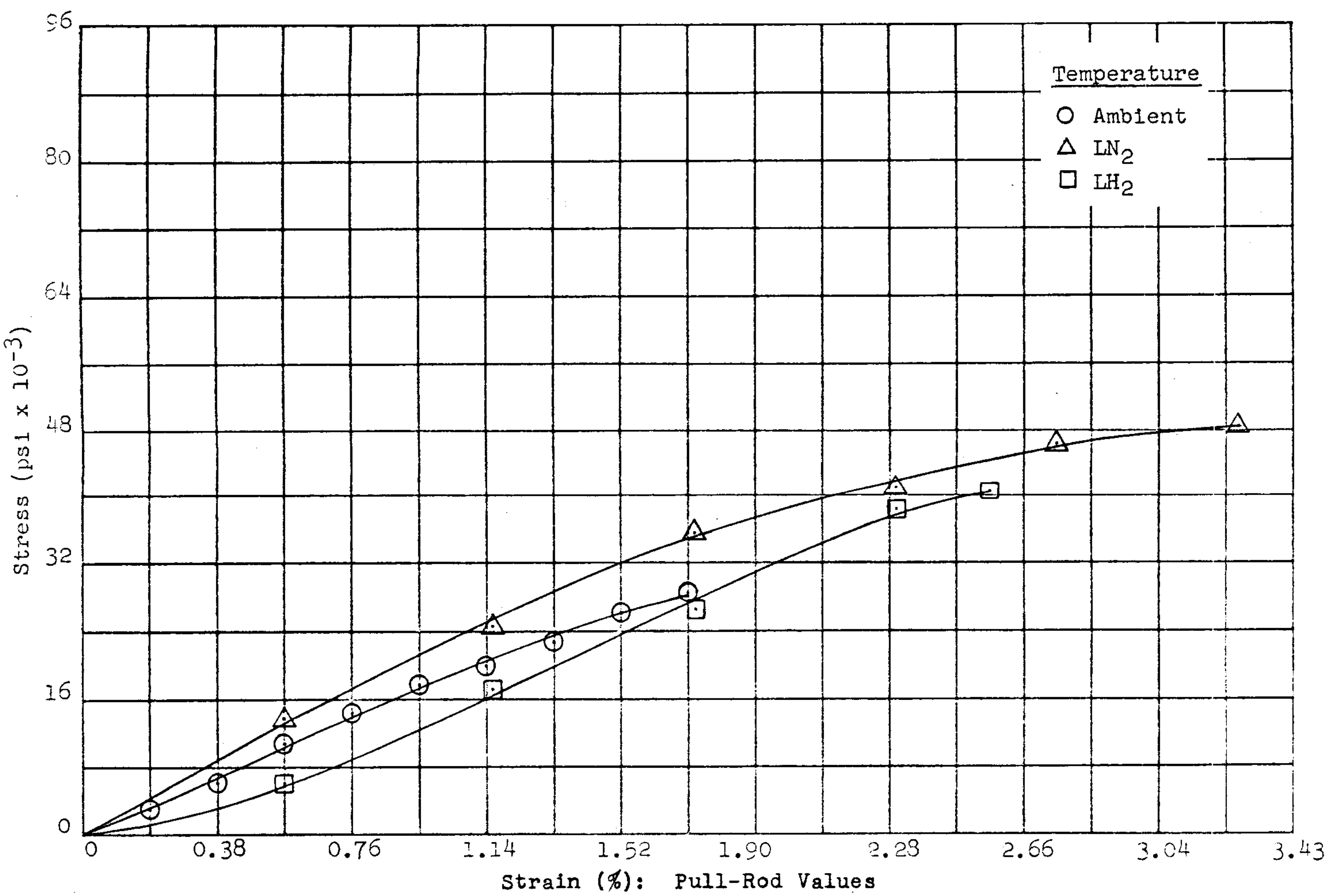

Figure 5.38 Stress vs Strain (Pull-Rod Valus) for Three Different Temperatures: Material J (Paraplex P-43); Unirradiated (Control)

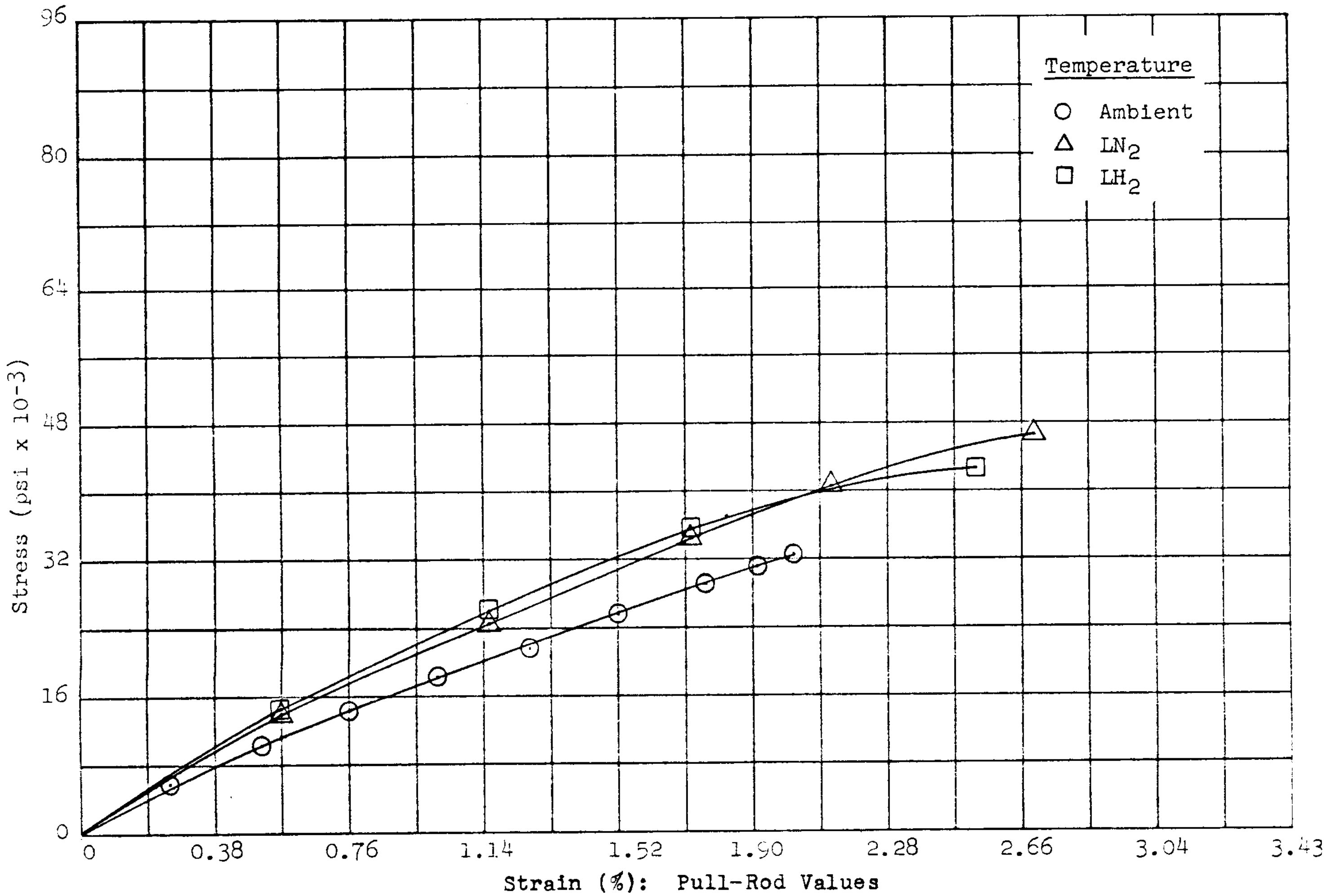

Figure 5.39 Stress vs Strain (Pull-Rod Values) for Three Different Temperatures: Material J (Paraplex P-43); Low-Dose Exposure

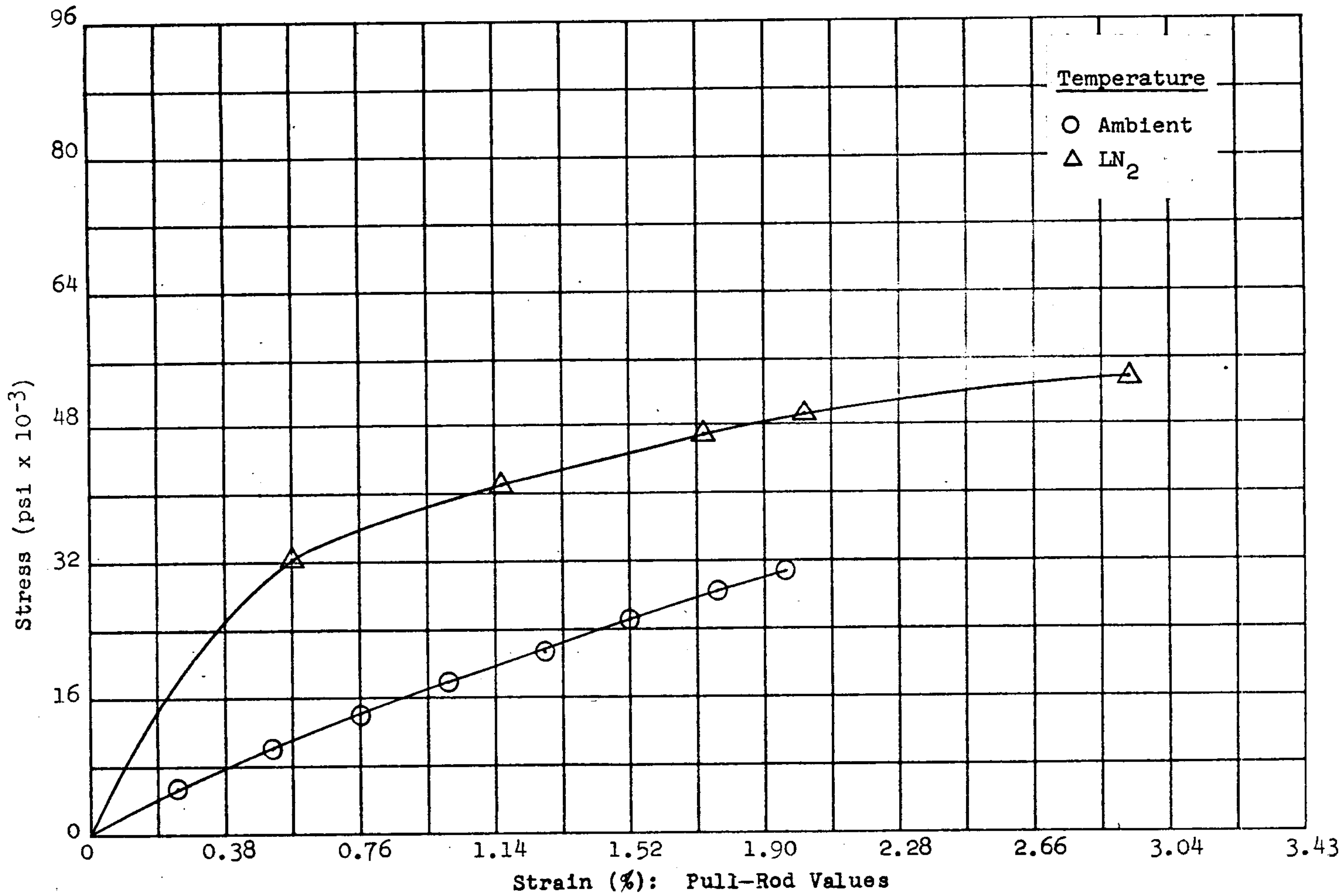

Figure 5.40 **Stress vs Strain (Pull-Rod Values) for Two Different Temperatures: Material J (Paraplex P-43); High-Dose Exposure**

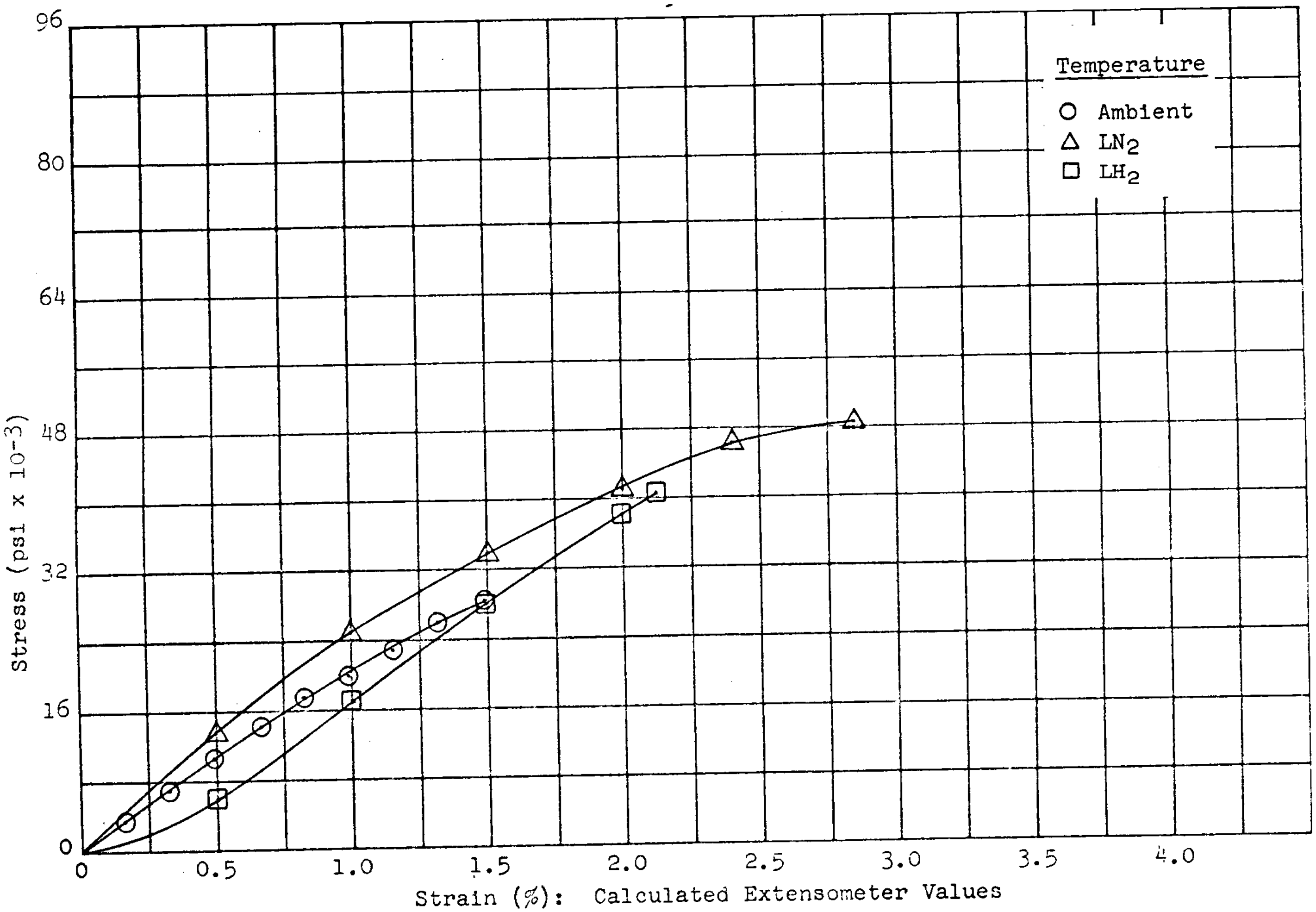

Figure 5.41 **Stress vs Strain (Calculated Extensometer Values) for Three Different Temperatures: Material J (Paraplex P-43); Unirradiated (Control)**

ated

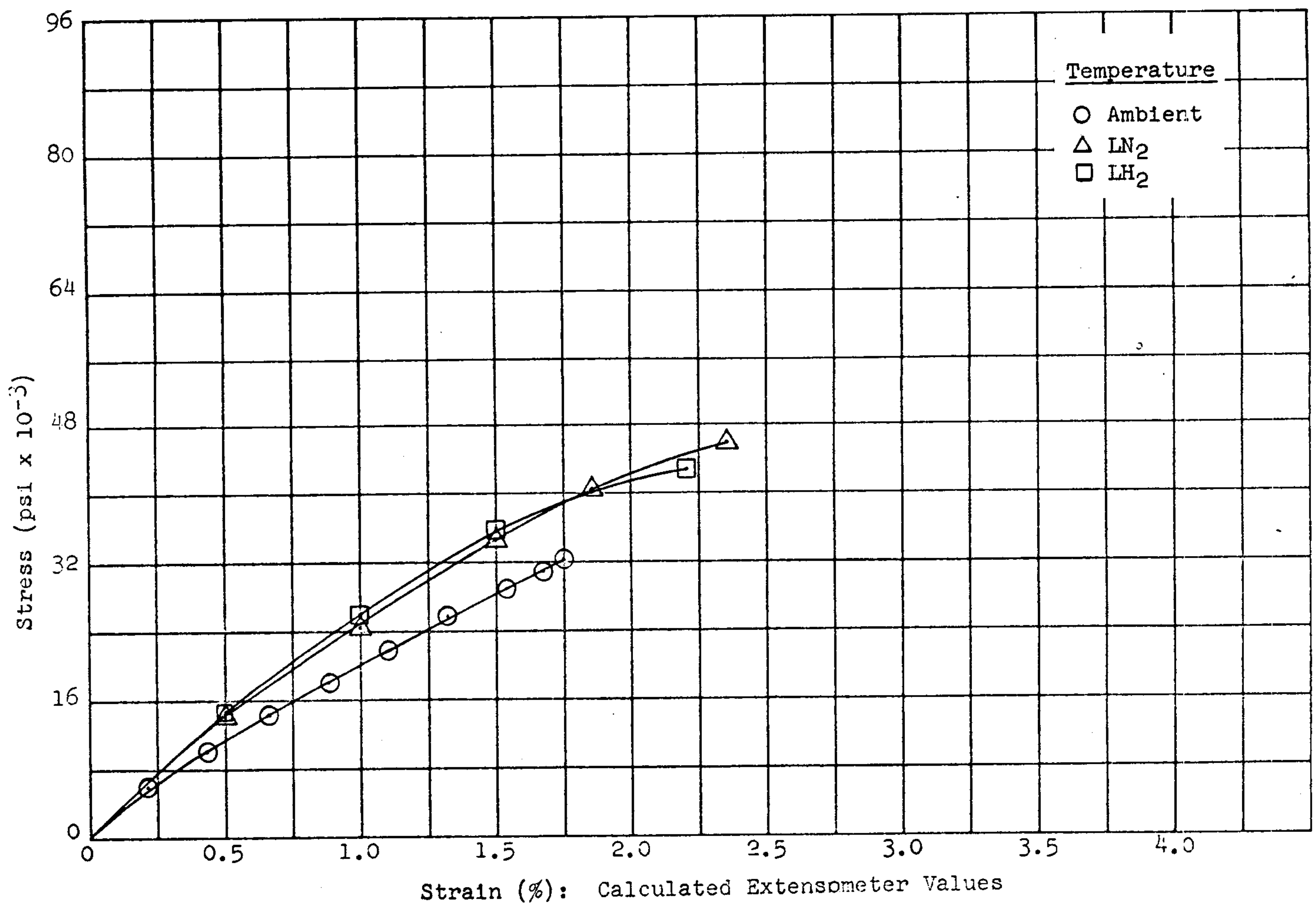

Figure 5.42 Stress vs Strain (Calculated Extensometer Values) for Three Different Temperatures: Material J (Paraplex P-43); Low-Dose Exposure

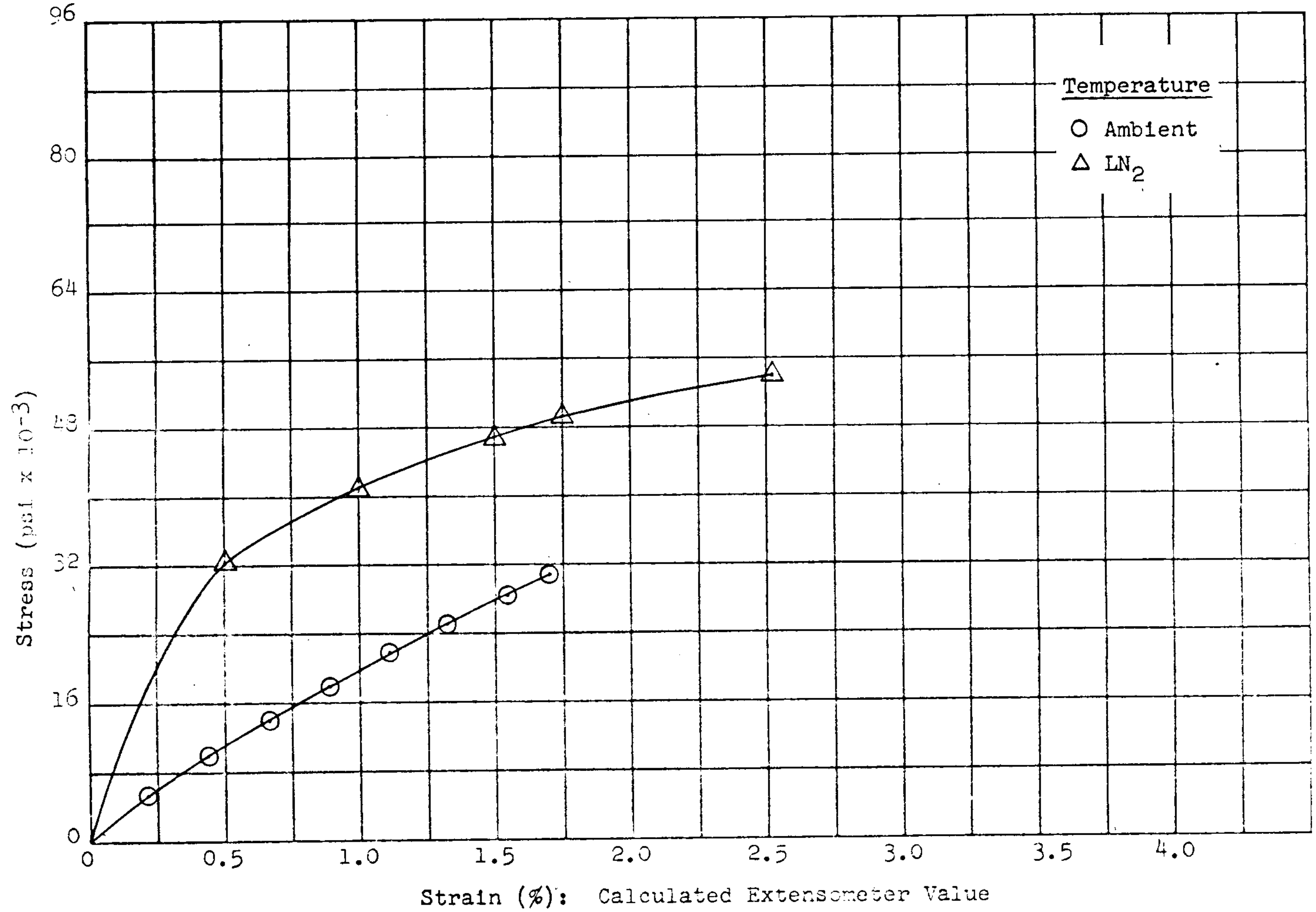

Figure 5.43 Stress vs Strain (Calculated Extensometer Values) for Two Different Temperatures: Material J (Paraplex P-43); High-Dose Exposure

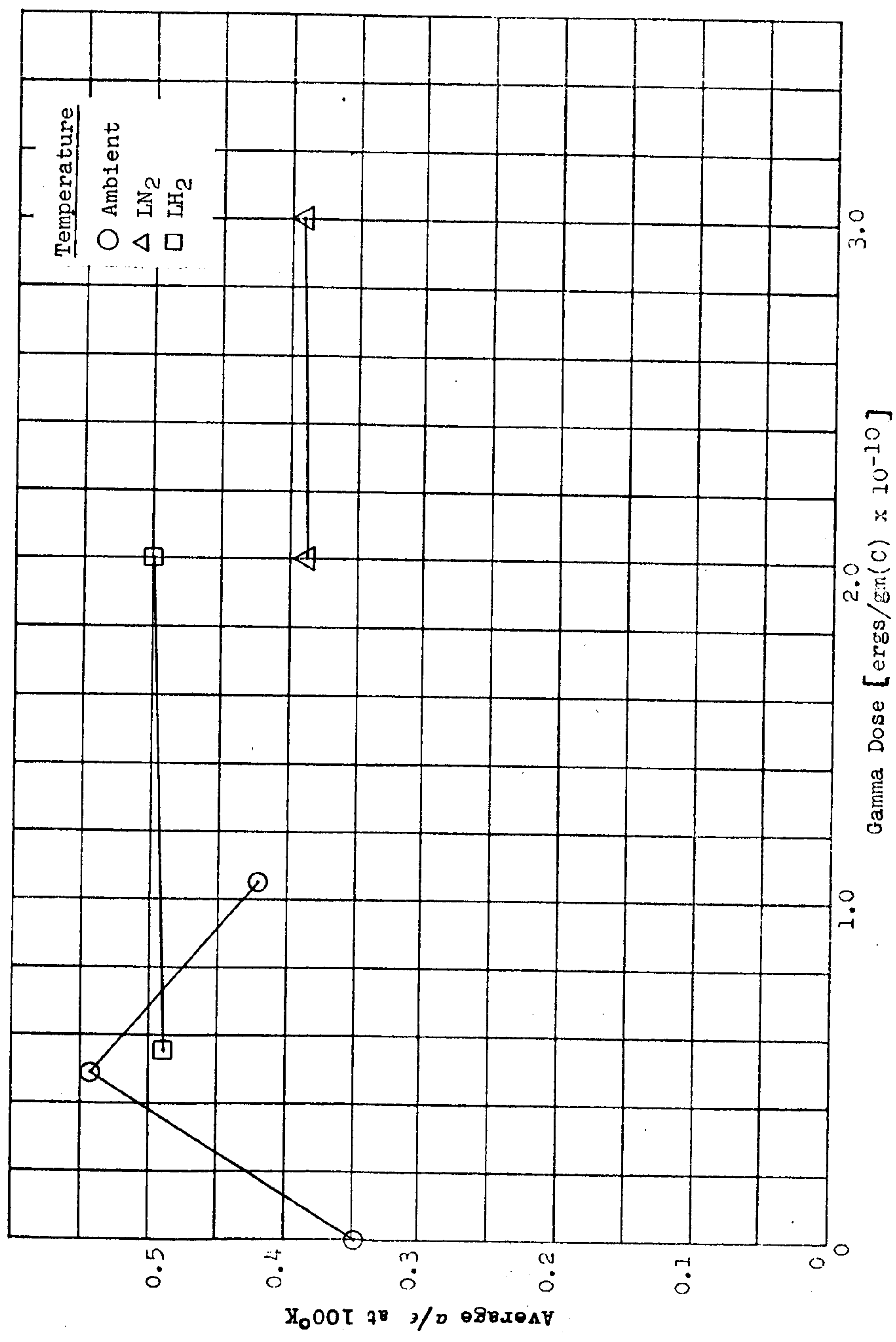

Figure 5.44 Average α/ϵ at 100°K vs Gamma Dose for Three Different Temperatures: Material K (Skyspar A423-SA9185)

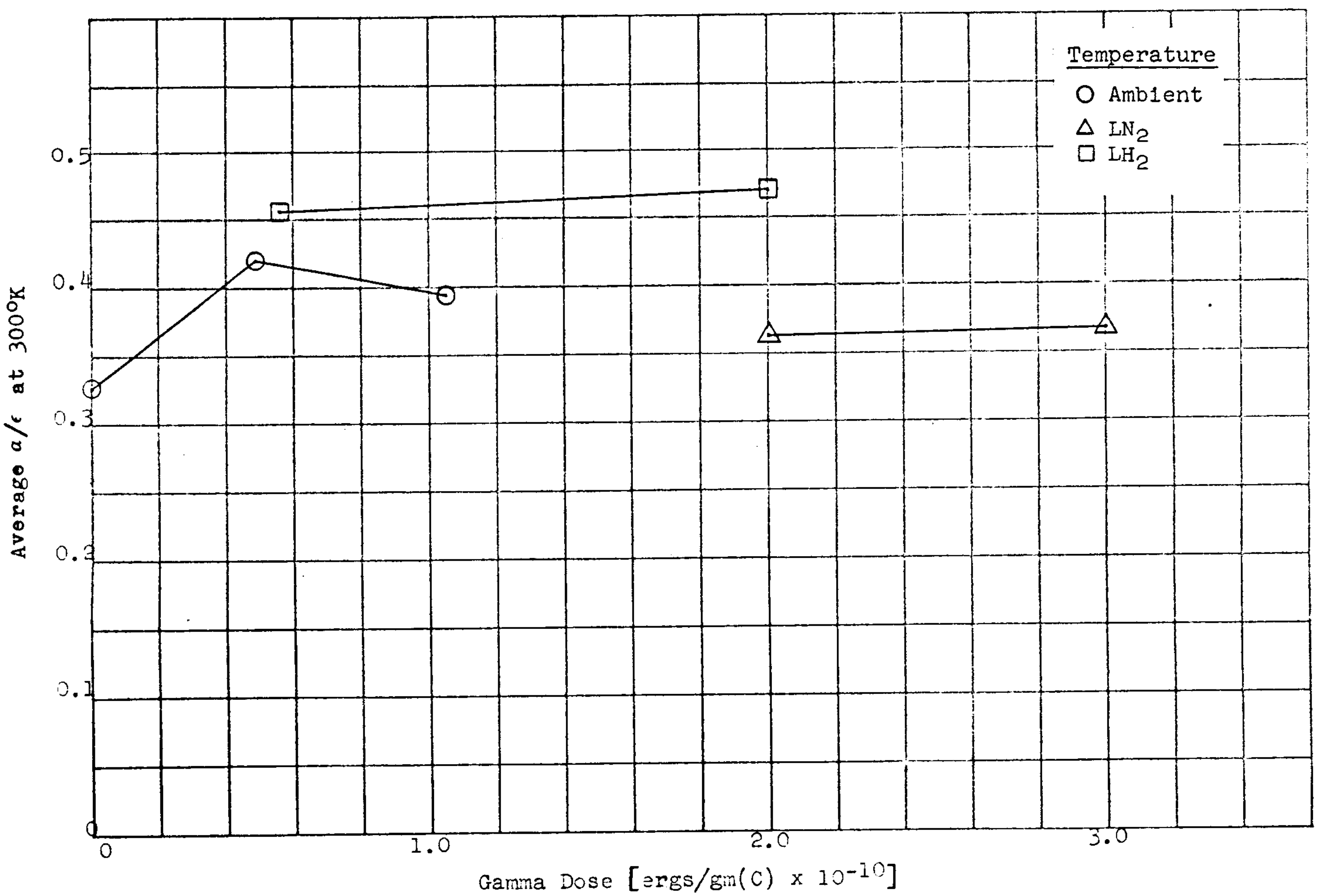

Figure 5.45 **Average α/ϵ at 300°K vs Gamma Dose for Three Different Temperatures: Material K (Skyspar A423-SA9185)**

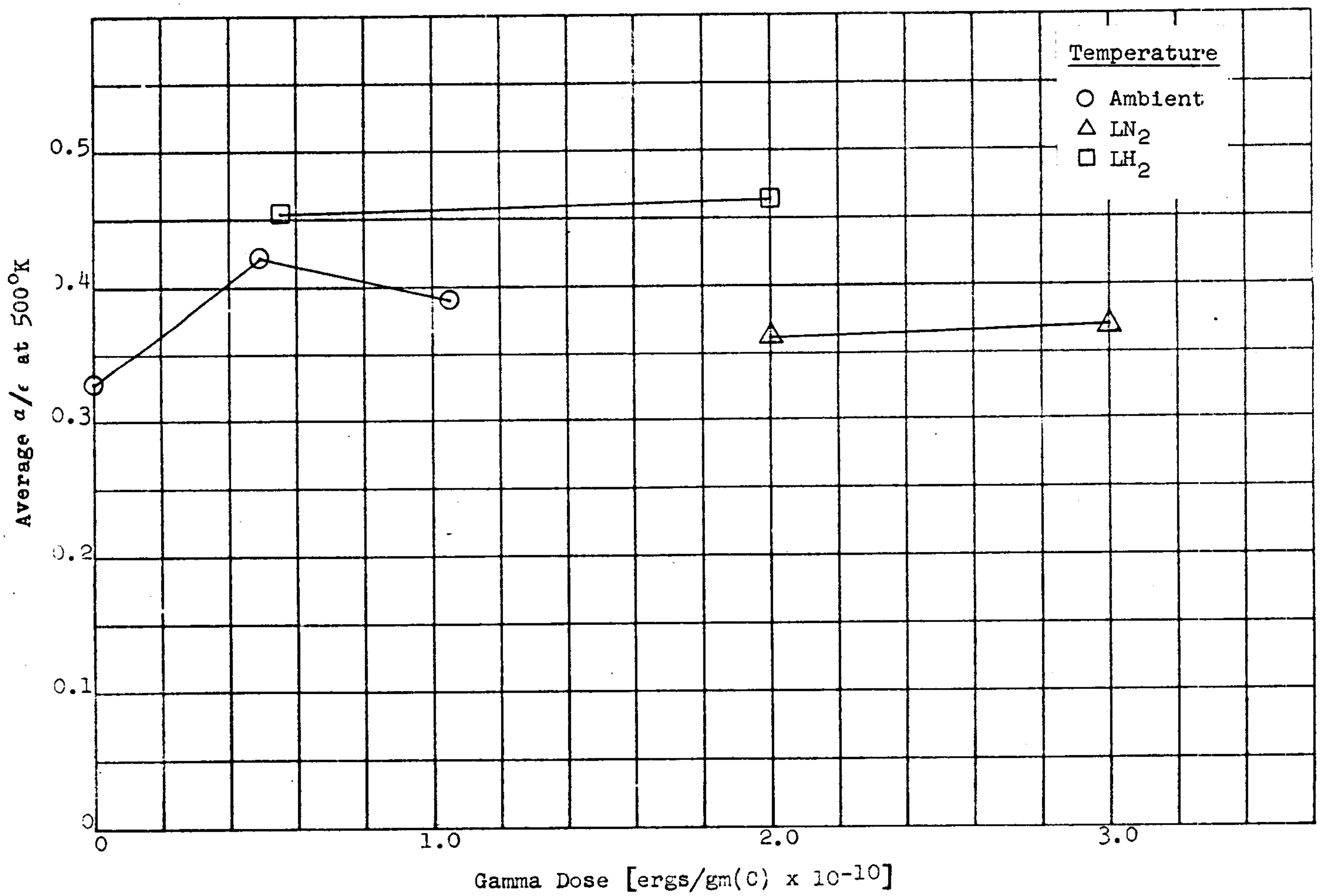

Figure 5.46 Average α/ϵ at 500°K vs Gamma Dose for Three Different Temperatures: Material K (Skyspar A423-SA9185)

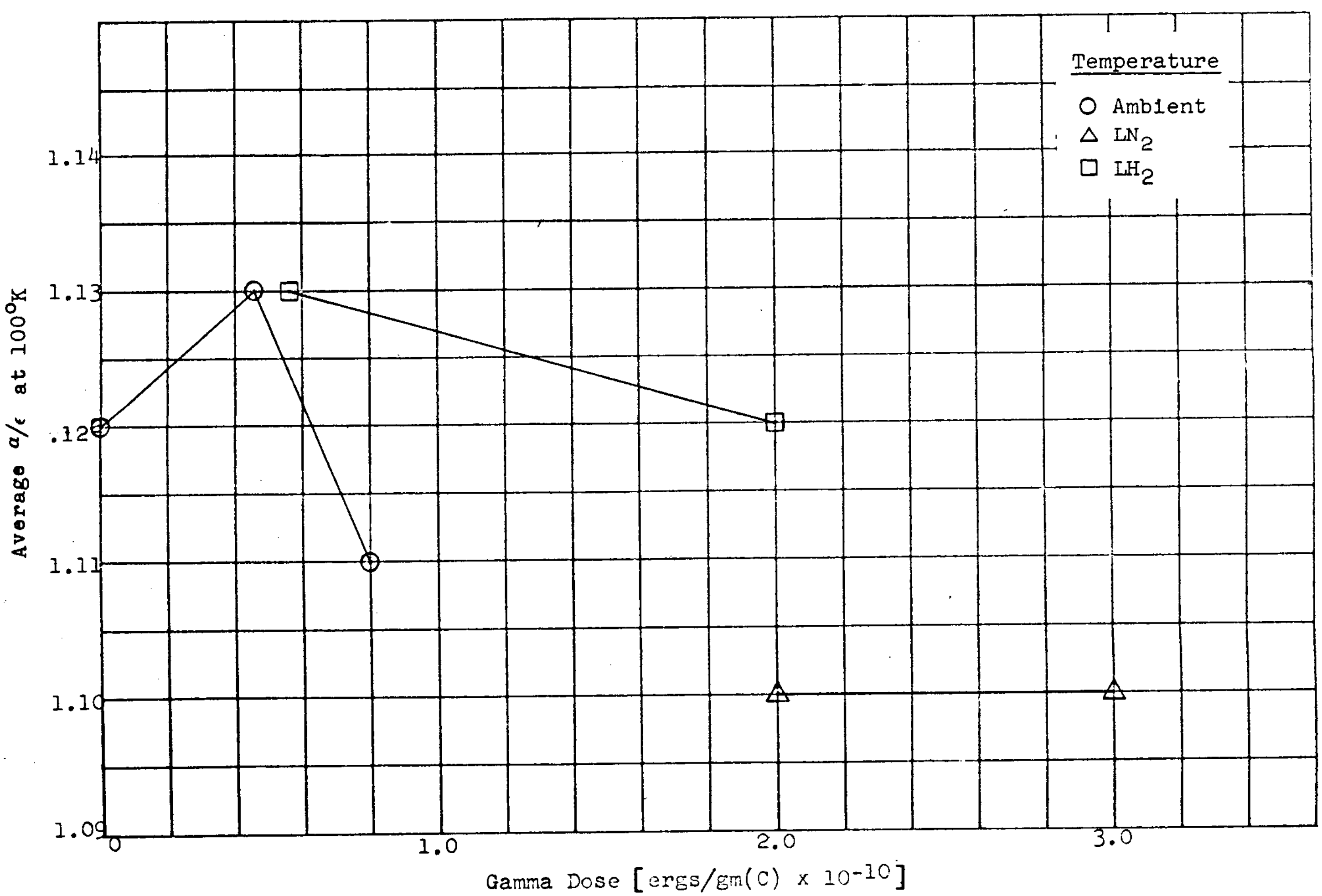

Figure 5.47 Average α/ϵ at 100°K vs Gamma Dose for Three Different Temperatures: Material L (W-49-BC-12)

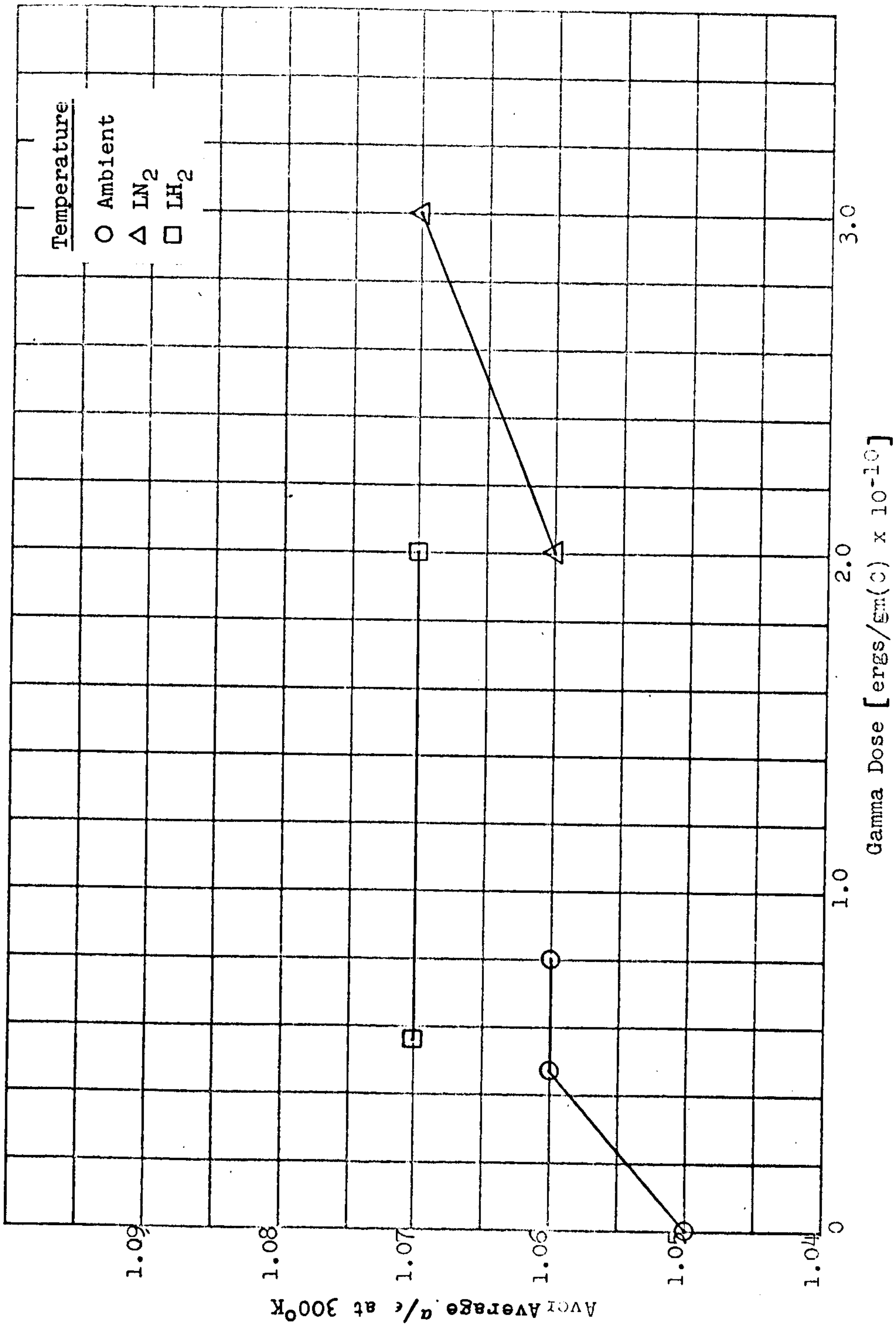

Figure 5.48 Average α/ε at 300°K vs Gamma Dose for Three Different Temperatures: Material L (W-49-BC-12)

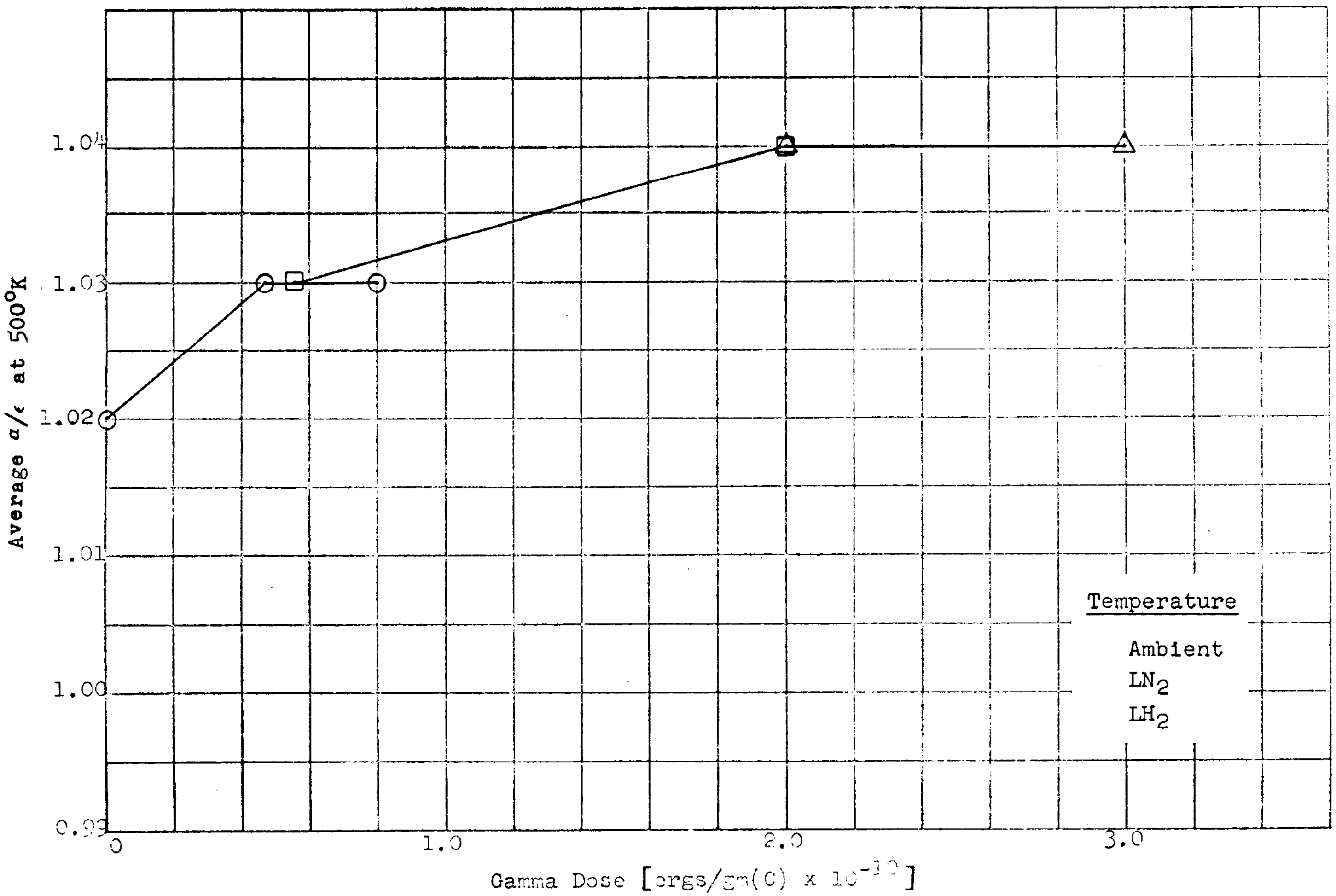

Figure 5.49 Average α/ϵ at 500°K vs Gamma Dose for Three Different Temperatures: Material L (W-49-BC-12)

VI. CONCLUSIONS AND RECOMMENDATIONS

Completion of this experiment marks the first known attempt to measure engineering properties of nonmetallic materials under the combination environment of nuclear radiation and cryotemperatures, i.e., to irradiate test specimens which are submerged in cryogen fluids and then to perform tensile and compressive tests on the irradiated specimens before removal from the cryogen. Practically every phase of the experiment, from designing and constructing test equipment to conducting the tests and analyzing the resulting data, was unique from the standpoint of the absence of any previously generated information in the field. The procedures and methods that were observed during these phases of the experimental program are documented in three quarterly progress reports (Refs. 7, 8, and 9).

As a result of the first year's operation, several conclusions can be drawn concerning the test techniques, test equipment, dosimetry measurements, and test data. In addition, recommendations can be made for modifications in the techniques and equipment as well as for future use or rejection of the test materials.

6.1 Test Techniques and Experimental Equipment

Because of the particular configurations of the irradiation facility and the necessity for remote-control operation in the experiment, all of the test methods and test equipment were unique and, in some cases, radical in design. Even so, the most applicable ASTM specification for each material was adhered to as closely as possible during the tests.

All of the test equipment operated satisfactorily and according to the original plan. An overall review of the tests, however, reveals that improvements in operation would result with certain changes in the equipment and instrumentation. Modifications which are recommended for incorporation into the experimental assemblies include (1) installation of additional dynamometers to several pull rods and (2) redesign of the support frameworks, shield components, liquid-level probe, and some of the specimen-mounting apparatus. These changes are expected to provide better operation of the assemblies and more reliable data from low-load specimens. A rework of the hydraulic servo system is also recommended to eliminate small leaks through valves and fittings and thus to raise the pressures in the slave cylinders.

As was pointed out in Section IV, the glued area of the adhesive material Hexcel 1252 was reduced to allow the specimens to be broken at the lower slave-cylinder pressures attainable at the relatively low crosshead speeds involved. It is now felt that raising the crosshead speeds for these specimens, as was done in the case of other high-strength materials, would have been a more satisfactory solution to the problem. Raising the crosshead speed actually results in a speed for the slave cylinder which more closely approximates that called for in the test plan. There will probably always be some small leaks in the hydraulic servo system which will cause slower slave-cylinder speeds with higher loads for a given crosshead speed. Plotting calibration curves of slave-cylinder speed vs load for a given servo system installation would be impractical, but occasional spot-checks of slave-cylinder speeds with the LVDT instrumentation is both possible and advisable.

During the tests, deviations in pull-rod speeds from those called out in the test plan were invariably on the low side. This, according to some additional checks made with Material A adhesive specimens, had only a slight effect on the data.

In the case of rigid cellular foams, such as the thermal insulation Materials E and F, a 1.129-in.-diam by $\frac{1}{2}$-in.-thick specimen was used in the experiment so that recorded data would be compatible with that produced in the vacuum section of the experiment. It is now felt that future tests on this type of material would provide better data if specimen sizes conformed to those called out in ASTM Designation D 1621-59T. This is because of the relatively high tare loads that exist on the pull rods.

High tare loads are also a problem when testing thin plastic films. It would be desirable, in the case of both films and cellular foams, to use a dynamometer in all pull rods that test these materials.

6.2 Dosimetry Measurements

A review of the nuclear radiation measurements which were made during the first year's operations leads to several conclusions and recommendations. First, the data obtained are satisfactory for predicting radiation-damage levels in the materials tested, although they may be lacking somewhat in desired accuracy and completeness.

One reason for these short-comings is the fact that the test equipment is radically different in design and, consequently, techniques for making nuclear measurements within this equipment are in the first experimental stages. In addition, previously measured values of gamma doses around the reactor, which were made in air, were insufficient for predicting ideal locations for placement of foils throughout the metallic structure of the experimental assemblies. Other contributing factors were the unexpectedly high activation of the equipment, which hampered the manual retrieval of foils; problems involving the lead shield, which resulted in the loss of several foils; and lack of nuclear-measurement technology at cryotemperatures.

It is felt that unexpected factors are normal when new approaches to nuclear testing techniques are being explored, and that the experience gained in this first year of operation will result in improved data in successive tests.

Recommendations for improvement in the quality and quantity of future data include the following: (1) tests should be conducted to determine the response of several types of gamma and neutron dosimeters at cryotemperatures; (2) methods for mounting measurement devices should be improved to facilitate their manual removal from a highly radioactive experimental assembly; and (3) nuclear measurement data received from the first irradiation tests using these expanded experimental assemblies should be analyzed from the standpoint of establishing future radiation levels at various points in the cryogen chambers.

6.3 Test Results and Recommendations for Materials

As outlined previously in the text, the procedure for the cryotemperature tests was to position the test specimens in the cryogen chamber of the experimental assemblies and locate the assemblies next to the reactor face. The irradiation run was carried out with the specimens submerged in cryogen fluid. Operation of the reactor was terminated after the required radiation dose was achieved, and the specimens were then pulled in tension and compression without intervening warmup. Nine data points were recorded during each test on each material. These included those from all combinations of three radiation doses (zero, low, and high) and three temperatures (ambient, -320°F, and -423°F). Ambient-temperature irradiations were conducted in an air environment with specimen temperatures ranging from 110°F to 143°F. Subsequent tensile and compression tests were carried out with an Instron test machine in the Irradiated Materials Laboratory of GD/FW.

A resume of the results of the tests on each material, along with recommendations for its use, is given below.

Adhesives

Hexcel 1252. This material demonstrated increased tensile-shear strength after irradiation at room temperature. At cryotemperatures, the strength before irradiation was considerably higher than the room-temperature value. Radiation then served to reduce this strength somewhat, but the value still remained higher than the room-temperature/no-irradiation level. The material is therefore highly recommended for use in this combination environment, up to the tested dose level of 5×10^{10} ergs/gm(C) of gamma radiation.

Metlbond 406. This adhesive suffered severe degradation in tensile-shear strength at all temperatures after irradiation to a dose level of about 3×10^{10} ergs/gm(C). It is not recommended for use under these environmental conditions.

Seals

Teflon TFE. This material was tested at ambient temperature in air only. After a relatively low dose of radiation under these conditions the test specimens crumbled to powder. Further testing is needed before recommendations can be made.

Kel-F-81. This fluorocarbon plastic was tested under all conditions. Its properties were excellent under no-irradiation conditions, but relatively small doses of gamma and neutron radiation were sufficient to cause significant degradation in tensile strength and severe embrittlement. It is not recommended for use in a radiation environment at any temperature.

Thermal Insulations

Stafoam AA402 and Styrofoam 22. Results of tests were similar for both of these materials. Their compressive strength at cryotemperatures increased with incident radiation up to a gamma dose of about 5×10^9 ergs/gm(C). Beyond this dose level, the strength dropped off severely. Irradiation at ambient temperature ($\sim 120^\circ F$) served to reduce the compressive strength significantly. Both materials are recommended for use under relatively low radiation environments at cryotemperatures.

Electrical Insulations

DuPont H-Film and Mylar-C. These materials were tested in tension in thin-film form. Contrasting values in tensile strength for different radiation doses and different temperatures were noted. Further testing is needed, and specific recommendations are not considered possible at this time.

Structural Laminates

Conolon 506 and Paraplex P-43. Tensile properties of these two laminates were measured and found to be similar. The ultimate tensile strength of both materials was higher at cryotemperatures than at room temperature, as could be expected, and remained high after doses of 5 to 10^{10} ergs/gm(C). Both materials are recommended for use under a radiation-cryotemperature environment to the above-mentioned dose level.

Thermal-Control Coatings

Skyspar A-423-SA9185 and Sherwin Williams W-49-BC12. After irradiation at room temperature, the subsequently measured optical properties of these two coatings showed variations as a function of radiation dose. After irradiation at cryotemperatures, the properties remained fairly constant as a function of radiation dose. No recommendations are attempted with the data available from these tests, but the data shown in the text are suitable for possible correlation with results from other related tests.

The test results are given in this report as plotted and tabluated data (Section V and Appendix A). Thus, further analyses can be made when more detailed information is required concerning specific properties of the various test materials.

Overall, the tests conducted in the combined environment of nuclear radiation and cryotemperature were successful, particularly in view of the radically different testing techniques that were used. Refinement of these techniques will be accomplished with future use of the experimental assemblies.

Since the information learned from tests of this nature is required in the development of nuclear-powered spacecraft, and since the potential for future tests that utilize the assemblies in conjunction with the GTR at NARF is regarded as being almost unlimited, it is recommended that the testing of engineering materials in radiation fields at cryotemperatures be continued.

APPENDIX A

TABULATED TEST DATA ON ALL MATERIALS AND PLOTS OF MONOCHROMATIC REFLECTIVITY AND ABSORPTIVITY OF THERMAL-CONTROL COATINGS

Preceding page blank

TABLE A-1

Radiation-Cryotemperature Test Data: Material A
Hexcel 1252

Material Type Structural Adhesive

Test Temperature	Average Radiation Exposure			Pull Rod Speed (in/min)	Tensile Shear Strength (lb/in.^{2})					
					Specimen					Average Strength (lb/in.^{2})
	Type	Gamma [ergs/gm(C)]	Fast ** Neutron (n/cm^2)		1	2	3	4	5	
Ambient	No	0	0	0.05	2436	2532	2028	2300	1912	2240
	Low	1.0(10)*	2.5(15)	0.05	3840	3280	4560	4840	4560	4212
	High	6.0(10)	1.6(16)	0.05	4600	5440	5640	4800	4680	5028
Liquid Nitrogen	No	0	0	0.010	5120	4880	5120	--	--	5040
	Low	1.30(10)	2.3(15)	0.003	4640	5200	3760	4760	--	4592
	High	5.2(10)	1.3(16)	0.003	3520	4320	4920	--	--	4248
Liquid Hydrogen	No	0	0	~0.010	6000	6000	5800	5920	--	5928
	Low	1.3(10)	2.2(15)	~0.010	4400	4600	4560	4600	--	4536
	High	0	0	--	--	--	--	--	--	--

*Read 1.0(10) as 1.0 x 10^{10}

**E > 2.9 Mev

Preceding page blank

TABLE A-2

Radiation-Cryotemperature Test Data: Material B

Metlbond 406

Material Type Adhesive

Test Temperature	Average Radiation Exposure			Pull Rod Speed (in/min)	Tensile Shear Strength ($lb/in.^2$)					
					Specimen					Average Strength ($lb/in.^2$)
	Type	Gamma [ergs/gm(C)]	Fast** Neutron (n/cm^2)		1	2	3	4	5	
Ambient	No	-- --	--	0.05	5000	5800	5950	5350	5724	5560
	Low	1.05(10)*	2.5(15)	0.05	5500	6080	5520	6160	5950	5940
	High	4.9(10)	1.6(16)	0.05	1000	500	690	800	770	752
Liquid Nitrogen	No	--	--	0.007	3340	2920	2740	2960	--	2990
	Low	1.30(10)	2.3(15)	~0.005	2320	2400	2160	--	--	2292
	High	5.2(10)	1.3(16)	0.003	1600	1760	1440	--	--	1600
Liquid Hydrogen	No	--	--	~0.010	3120	3080	3560	--	--	3250
	Low	1.3(10)	2.2(15)	~0.005	1550	1660	2490	2210	--	1978
	High	--	--	--	--	--	--	--	--	--

*Read 1.05(10) as 1.05×10^{10}

**E $>$ 2.9 Mev

TABLE A-3

Radiation-Cryotemperature Test Data: Material C

Teflon TFE

Test Temperature Ambient
Pull-Rod Speed 0.50" in./min
% Total Elongation 78
(4.00-in. Gage)

Material Type Seal
Exposure
Gamma Unirradiated ergs/gm(C)
Neutron " n/cm^2
(Control)

Specimen No. 1 Load (lb)	Specimen No. 1 Defl. (in.)	Specimen No. 2 Load (lb)	Specimen No. 2 Defl. (in.)	Specimen No. 3 Load (lb)	Specimen No. 3 Defl. (in.)	Average Load for Given Deflection Load (lb)	Average Load for Given Deflection Defl. (in.)
0	0	0	0			0	0
6.0	0.05	5.4	0.05			5.7	0.05
9.6	0.10	10.4	0.10			10.0	0.10
10.8	0.15	12.0	0.15			11.4	0.15
13	0.35	13.3	0.25			13.2	0.35
13.6	0.50	14.25	0.50			13.9	0.50
14.3	0.75	15.1	0.75			14.7	0.75
14.8	1.00	15.7	1.00			15.3	1.00
15.6	1.50	16.7	1.50			16.2	1.50
16.3	2.00	17.4	2.0			16.9	2.00
17.0	2.50	17.95	2.5			17.5	2.50
17.25	2.75	18.1	2.82			17.7	2.75
17.2	3.0					17.2	3.0
17.1	3.12					17.1	3.12

Note: No data were obtained from specimens irradiated at ambient temperature. The specimens crumbled before tests could be performed. The LN_2 & LH_2 tests were cancelled because of inability to successfully glue specimens to the film tester spools.

TABLE A-4

Radiation-Cryotemperature Test Data: **Material** D

Kel-F-81

Pull-Rod Speed (Avg) 0.50 in/min **in./min**
Ultimate Tensile Strength (Avg) 5600 lb/in^2 **psi**
% Total Elongation
Pull-Rod (5.25-in. Gage) 90 **%**
Extensometer (2-in. Gage) 175 **%**

Matl Type Seal
Test Temp Ambient
Exposure
Gamma Unirradiated **ergs/gm(C)**
Neutron " **n/cm^2**

Specimen												Average Load for Given Deflection			
No. 1			No. 2			No. 3			No. 4						
Load (lb)	Defl. (Rod) (in.)	Defl. (Exts.) (in.)	Load (lb)	Defl. (Rod) (in.)	Defl. (Exts.) (in.)	Load (lb)	Defl. (Rod) (in.)	Defl. (Exts.) (in.)	Load (lb)	Defl. (Rod) (in.)	Defl. (Exts.) (in.)	Load (lb)	Load lb/in.^{2}	Defl. (Rod) (in.)	Defl. (Exts.) (in.)
0	0		0	0								0	0	0	0
80	.05		100	.05								90	2800	0.05	.0115
130	.10		150	.10								140	4480	.10	.0230
150	.125		168	.125								159	5088	.125	.0288
167	.150		174	.150								171	5472	.150	.0345
173	.20		173	.20								173	5536	.20	.0460
143	.40		147	.40								145	4640	.40	
134	.45		134	.45								134	4288	.45	.43
135	.50		133	.50								134	4288	.50	
138	1.0		136	1.0								137	4384	1.0	0.95
144	2.0		142	2.0								143	4576	2.0	1.90
146	3.0		148	3.0								147	4704	3.0	
148	3.5		151	3.5								150	4800	3.5	
158	4.0		162	4.0								160	5120	4.0	
180	4.75	3.80	170	4.18	3.20							166	5312	4.18	3.20
												175	5600	4.46	3.50

TABLE A-5

Radiation-Cryotemperature Test Data: **Material** D

Kel - F - 81

Pull-Rod Speed (Avg) 0.2 **in./min**
Ultimate Tensile Strength (Avg) 1568 **psi**
% Total Elongation
Pull-Rod (5.25-in. Gage) 1.31 **%**
Extensometer (2-in. Gage) 0.58 **%**

Matl Type Seal
Test Temp Ambient
Exposure
Gamma 5.45×10^9 **ergs/gm(C)**
Neutron 1.08×10^{15} **n/cm^2**

Specimen No. 1 Load (lb)	No. 1 Defl. (Rod) (in.)	No. 1 Defl. (Exts.) (in.)	No. 2 Load (lb)	No. 2 Defl. (Rod) (in.)	No. 2 Defl. (Exts.) (in.)	No. 3 Load (lb)	No. 3 Defl. (Rod) (in.)	No. 3 Defl. (Exts.) (in.)	No. 4 Load (lb)	No. 4 Defl. (Rod) (in.)	No. 4 Defl. (Exts.) (in.)	Average Load for Given Deflection Load (lb)	Load lb/in^2	Defl. (Rod) (in.)	Defl. (Exts.) (in.)
0	0	0	0	0	0	0	0	0				0	0	0	0
14	.0185	.0048	17	.024	.0051	11	.0167	.0038				6	192	.0086	.002
27	.036	.0093	32	.045	.0096	24	.037	.0084				12	384	.0174	.004
40	.053	.0137	45	.063	.0135	36	.055	.0125				18	576	.0258	.006
49	.065	.0168	52	.073	.0156	46	.070	.016				24	768	.0344	.008
												30	960	.0429	.010
												36	1152	.0515	.012
												43	1376	.0601	.014
												49	1568	.0693	.016

TABLE A-6

Radiation-Cryotemperature Test Data: Kel - F - 81

Material D

Pull-Rod Speed (Avg) 0.18 **in./min**
Ultimate Tensile Strength (Avg) 19,200 **psi**
% Total Elongation
Pull-Rod (5.25-in. Gage) 2.59 **%**
Extensometer (2-in. Gage) 1.60 **%**

Matl Type Seal
Test Temp Liquid Nitrogen
Exposure
Gamma Unirradiated ergs/gm(C)
Neutron " n/cm^2
(Control)

Specimen												Average Load for Given Deflection			
No. 1			No. 2			No. 3			No. 4						
Load (lb)	Defl. (Rod) (in.)	Defl. (Exts.) (in.)	Load (lb)	Defl. (Rod) (in.)	Defl. (Exts.) (in.)	Load (lb)	Defl. (Rod) (in.)	Defl. (Exts.) (in.)	Load (lb)	Defl. (Rod) (in.)	Defl. (Exts.) (in.)	Load (lb)	Load lb/in^2	Defl. (Rod) (in.)	Defl. (Exts.) (in.)
0	0		0	0								0	0	0	0
80	.015		180	.020								133	4256	.0172	.004
220	.035		300	.031								265	8480	.0342	.008
500	.087		450	.053								378	12096	.0514	.012
600	.137	.0319	600	.107	.0249							466	14902	.0686	.016
												535	17120	.0858	.020
												575	18400	.1030	.024
												600	19200	.122	.028

TABLE A-7

Radiation-Cryotemperature Test Data: Kel - F - 81

Material D

Pull-Rod Speed (Avg) 0.30 **in./min**
Ultimate Tensile Strength (Avg) 18880 **psi**
% Total Elongation
Pull-Rod (5.25-in. Gage) 2.30 **%**
Extensometer (2-in. Gage) 1.41 **%**

Matl Type Seal
Test Temp Liquid Nitrogen
Exposure
Gamma 4.7 x 10^9 **ergs/gm(C)**
Neutron 1.0 x 10^{15} **n/cm^2**

Specimen												Average Load for Given Deflection			
No. 1			No. 2			No. 3			No. 4						
Load (lb)	Defl. (Rod) (in.)	Defl. (Exts.) (in.)	Load (lb)	Defl. (Rod) (in.)	Defl. (Exts.) (in.)	Load (lb)	Defl. (Rod) (in.)	Defl. (Exts.) (in.)	Load (lb)	Defl. (Rod) (in.)	Defl. (Exts.) (in.)	Load (lb)	Load lb/in^2	Defl. (Rod) (in.)	Defl. (Exts.) (in.)
0	0	0	0	0								0	0	0	0
40	.003		130	.016								98	3136	.0172	.004
250	.067		280	.042								193	7176	.0342	.008
600	.137	.0319	450	.070								281	8992	.0514	.012
			580	.105	.0245							365	11680	.0686	.016
												441	14112	.0858	.020
												512	16384	.1030	.024
												590	18880	.121	.028

TABLE A-8

Radiation-Cryotemperature Test Data: Kel - F - 81   **Material** D

Pull-Rod Speed (Avg) 0.30 **in./min**
Ultimate Tensile Strength (Avg) 16,900 **psi**
% Total Elongation
Pull-Rod (5.25-in. Gage) 1.81 **%**
Extensometer (2-in. Gage) 1.10 **%**

Matl Type Seal
Test Temp Liquid Nitrogen
Exposure
Gamma 1.00×10^{10} ergs/gm(C)
Neutron 1.9×10^{15} n/cm^2

Specimen												Average Load for Given Deflection			
No. 1			No. 2			No. 3			No. 4						
Load (lb)	Defl. (Rod) (in.)	Defl. (Exts.) (in.)	Load (lb)	Defl. (Rod) (in.)	Defl. (Exts.) (in.)	Load (lb)	Defl. (Rod) (in.)	Defl. (Exts.) (in.)	Load (lb)	Defl. (Rod) (in.)	Defl. (Exts.) (in.)	Load (lb)	Load lb/in^2	Defl. (Rod) (in.)	Defl. (Exts.) (in.)
0	0		0	0								0	0	0	0
100	.011		100	.015								112	3584	.0172	.004
215	.033		250	.038								223	7136	.0342	.008
365	.058		400	.064								327	10464	.0514	.012
515	.090	.0209	540	.099	.0231							426	13632	.0686	.016
												501	16032	.0858	.020
												528	16900	.0945	.022

TABLE A-9

Radiation-Cryotemperature Test Data: **Material** D
Kel - F - 81

Pull-Rod Speed (Avg) 0.24 **in./min**
Ultimate Tensile Strength (Avg) 31360 **psi**
% Total Elongation
Pull-Rod (5.25-in. Gage) 2.92 **%**
Extensometer (2-in. Gage) 1.66 **%**

Matl Type Seal
Test Temp Liquid Hydrogen
Exposure
Gamma Unirradiated **ergs/gm(C)**
Neutron " **n/cm²**
(Control)

Specimen												Average Load for Given Deflection			
No. 1			No. 2			No. 3			No. 4						
Load (lb)	Defl. (Rod) (in.)	Defl. (Exts.) (in.)	Load (lb)	Defl. (Rod) (in.)	Defl. (Exts.) (in.)	Load (lb)	Defl. (Rod) (in.)	Defl. (Exts.) (in.)	Load (lb)	Defl. (Rod) (in.)	Defl. (Exts.) (in.)	Load (lb)	Load lb/in.²	Defl. (Rod) (in.)	Defl. (Exts.) (in.)
0	0		0	0								0	0	0	0
285	.023		280	.040								118	3776	.0172	.004
370	.059		500	.068								232	7424	.0342	.008
620	.093		740	.102								348	11136	.0514	.012
820	.129		960	.140	.0326							462	14784	.0686	.016
1000	.167	.0337										575	18400	.0858	.020
												691	22112	.1030	.024
												807	25824	.1202	.028
												915	29280	.1362	.032
												980	31360	.1535	.033

TABLE A-10

Radiation-Cryotemperature Test Data: Kel - F - 81 **Material** D

Pull-Rod Speed (Avg) 0.24 **in./min**
Ultimate Tensile Strength (Avg) 18080 **psi**
% Total Elongation
Pull-Rod (5.25-in. Gage) 2.06 **%**
Extensometer (2-in. Gage) 1.26 **%**

Matl Type Seal
Test Temp Liquid Hydrogen
Exposure
Gamma 4.7×10^9 ergs/gm(C)
Neutron 1.0×10^{15} n/cm^2

Specimen												Average Load for Given Deflection			
No. 1			No. 2			No. 3			No. 4						
Load (lb)	Defl. (Rod) (in.)	Defl. (Exts.) (in.)	Load (lb)	Defl. (Rod) (in.)	Defl. (Exts.) (in.)	Load (lb)	Defl. (Rod) (in.)	Defl. (Exts.) (in.)	Load (lb)	Defl. (Rod) (in.)	Defl. (Exts.) (in.)	Load (lb)	Load lb/in.^{2}	Defl. (Rod) (in.)	Defl. (Exts.) (in.)
0	0		0	0								0	0	0	0
60	.015		110	.023								90	2880	.0172	.004
130	.029		190	.043								180	5760	.0342	.008
230	.043		270	.056								270	8640	.0514	.012
320	.058		360	.075								360	11520	.0686	.016
420	.071		440	.093								451	14432	.0858	.020
530	.085		520	.110	.0256							520	16640	.099	.023
610	.106	.0247										565	18080	.108	.025

TABLE A-11

Radiation-Cryotemperature Test Data: Kel - F - 81

Material D

Pull-Rod Speed (Avg) 0.39 **in./min**
Ultimate Tensile Strength (Avg) 6490 **psi**
% Total Elongation
Pull-Rod (5.25-in. Gage) 1.01 **%**
Extensometer (2-in. Gage) 0.625 **%**

Matl Type Seal
Test Temp Liquid Hydrogen
Exposure
Gamma 1.0×10^{10} **ergs/gm(C)**
Neutron 1.2×10^{15} **n/cm²**

Specimen												Average Load for Given Deflection			
No. 1			No. 2			No. 3			No. 4						
Load (lb)	Defl. (Rod) (in.)	Defl. (Exts.) (in.)	Load (lb)	Defl. (Rod) (in.)	Defl. (Exts.) (in.)	Load (lb)	Defl. (Rod) (in.)	Defl. (Exts.) (in.)	Load (lb)	Defl. (Rod) (in.)	Defl. (Exts.) (in.)	Load (lb)	Load lb/in²	Defl. (Rod) (in.)	Defl. (Exts.) (in.)
0	0		0	0								0	0	0	0
70	.019		75	.029								64	2048	.0172	.004
180	.040	.0093	145	.051								130	4160	.0342	.008
			225	.067	.0156							182	5824	.0514	.012
												203	6490	.0535	.013

TABLE A-12

Radiation-Cryotemperature Test Data: **Material** E
Stafoam AA 402

Test Temperature Ambient
Pull-Rod Speed (Avg) 0.05 in./min
Force to Compress 25% (Avg.) 42.3 lb

Matl Type Thermal Insulation
Exposure
Gamma Unirrad.(Control) ergs/gm(C)
Neutron " n/cm^2

Specimen 1		Specimen 2		Specimen 3		Avg Load for Given Deflection	
Load (Instron) (lb)	Deflection (in.)	Load (Instron) (lb)	Deflection (in.)	Load (Instron) (lb)	Deflection (in.)	Load (lb)	Deflection (in.)
0	0	0	0	0	0	0	0
10	.01	5	.01	5	.01	6.7	.01
27.5	.02	22	.02	20.2	.02	23.2	.02
37.5	.03	35	.03	34	.03	35.5	.03
42.5	.04	41.3	.04	41	.04	41.6	.04
44	.05	43.8	.05	44	.05	43.9	.05
45	.10	41.8	.10	43.5	.10	43.4	.10
42	.15	41.9	.15	41	.15	41.3	.15
42	.20	43.2	.20	41.5	.20	42.2	.20
42.5	.25	47.2	.25	43	.25	44.2	.25
49	.30	52.5	.30	49	.30	50.2	.30

TABLE A-13

Radiation-Cryotemperature Test Data: Material E
Stafoam AA402

Test Temperature Ambient

Matl Type Thermal Insulation

Low Exposure

Gamma 5.0×10^9 ergs/gm(C)
Neutrons 1.2×10^{15} n/cm^2
Pull-Rod Speed 0.05 in./min
Force to Compress 25% 15.0 lb

Low-Exposure Specimen		
Load (Instron) (lb)	Load (Dynamometer) (lb)	Deflection (in.)
1.0		.02
0.0		.03
2.5		.05
5.0		.06
10.0		.09
15.0		.125

High Exposure

Gamma 8.0×10^9 ergs/gm(C)
Neutron 2.2×10^{15} n/cm^2
Pull-Rod Speed 0.05 in./min
Force to Compress 25% 14.0 lb

High-Exposure Specimen		
Load (Instron) (lb)	Load (Dynamometer) (lb)	Deflection (in.)
1.0		.01
0.0		.02
2.5		.04
5.0		.06
10.0		.08
14.0		.125

TABLE A-14

Radiation-Cryotemperature Test Data: **Material** E
Stafoam AA402

Test Temperature Liquid Nitrogen
Pull-Rod Speed (Avg) 0.05 in./min
Force to Compress 25% (Avg) 126 lb

Matl Type Thermal Insulation
Exposure
Gamma Unirradiated ergs/gm(C)
Neutron " n/cm^2
(Control)

Specimen						Avg Load for given Deflection	
No. 1			No. 2				
Load (Instron) (lb)	Load (Dyn.)* (lb)	Defl. (in.)	Load (Instron) (lb)	Load (Dyn.)* (lb)	Defl. (in.)	Load (Dyn.)* (lb)	Defl. (in.)
0	0	0	0	0	0	0	0
27	60	.0156	16	32	.012	36	0.01
65	110	.0400	40	77	.020	69	0.02
88	120	.077	60	98	.033	94	0.03
95	120	.123	77	121	.048	112	0.04
97	128	.167	90	131	.091	119	0.05
100	128	.216	93	126	.139	125	0.07
100	120	.264	94	131	.187	126	0.10
95	115	.311	95	136	.234	126	0.15
92	110	.328	93	126	.285	131	0.20
143	200	.352	85	117	.338	130	0.25
			125	172	.365	120	0.30
						113	0.333
						184	0.36

* Dynamometer

TABLE A-15

Radiation-Cryotemperature Test Data: **Material** E
Stafoam AA402

Test Temperature Liquid Nitrogen

Matl Type Thermal Insulation

Low Exposure
Gamma 5.3×10^9 ergs/gm(C)
Neutrons 9.2×10^{14} n/cm^2
Pull-Rod Speed 0.045 in./min
Force to Compress 25% 140 lb

High Exposure
Gamma 1.3×10^{10} ergs/gm(C)
Neutron 2.2×10^{15} n/cm^2
Pull-Rod Speed 0.046 in./min
Force to Compress 25% 77 lb

Low-Exposure Specimen		
Load (Instron) (lb)	Load (Dynamometer) (lb)	Deflection (in.)
0	0	0
23	35	0.025
51	77	0.040
81	122	0.065
93	140	0.114
93	140	0.155
102	153	0.218
102	153	0.253
95	142	0.293
175	262	0.328

High-Exposure Specimen		
Load (Instron) (lb)	Load (Dynamometer) (lb)	Deflection (in.)
0	0	0
10	25	0.018
20	45	0.036
33	62	0.051
43	75	0.068
47	79	0.088
45	75	0.133
43	65	0.170
30	45	0.271
23	52	0.323
70	125	0.345

TABLE A-16

Radiation-Cryotemperature Test Data: **Material** E

Stafoam AA402

Test Temperature Liquid Hydrogen
Pull-Rod Speed (Avg) 0.047 in./min
Force to Compress 25% (Avg) 89 lb

Matl Type Thermal Insulation
Exposure
Gamma Unirradiated ergs/gm(C)
Neutron " n/cm^2
(Control)

Specimen No. 1 Load (Instron) (lb)	Specimen No. 1 Load (Dyn.)* (lb)	Specimen No. 1 Defl. (in.)	Specimen No. 2 Load (Instron) (lb)	Specimen No. 2 Load (Dyn.)* (lb)	Specimen No. 2 Defl. (in.)	Avg Load for given Deflection Load (Dyn.)* (lb)	Avg Load for given Deflection Defl. (in.)
0	0	0				0	0
9	14	0.009				14	0.009
24	36	0.020				36	0.020
63	95	0.054				95	0.054
65	98	0.099				98	0.099
60	90	0.103				90	0.103
55	83	0.196				83	0.196
35	53	0.272				53	0.272
70	105	0.282				105	0.282

* Dynamometer

TABLE A-17

Radiation-Cryotemperature Test Data: **Material** E
Stafoam AA402

Test Temperature Liquid Hydrogen

Matl Type Thermal Insulation

Low Exposure
- Gamma 5.3×10^9 ergs/gm(C)
- Neutrons 9.0×10^{14} n/cm^2
- Pull-Rod Speed 0.034 in./min
- Force to Compress 25% 195 lb

High Exposure
- Gamma 1.3×10^{10} ergs/gm(C)
- Neutron 2.5×10^{15} n/cm^2
- Pull-Rod Speed 0.036 in./min
- Force to Compress 25% 80 lb

Low-Exposure Specimen		
Load (Instron) (lb)	Load (Dynamometer) (lb)	Deflection (in.)
0	0	0
25	39	0.020
120	180	0.031
130	195	0.072
130	195	0.112
130	195	0.160
150	225	0.200
190	285	0.236
190	285	0.330

High-Exposure Specimen		
Load (Instron) (lb)	Load (Dynamometer) (lb)	Deflection (in.)
0	0	0
10	26	0.037
20	60	0.075
28	75	0.112
43	105	0.206
43	105	0.283
42	85	0.370
77	175	0.425

TABLE A-18

Radiation-Cryotemperature Test Data: **Material** F
Styrofoam 22

Test Temperature Ambient
Pull-Rod Speed (Avg) 0.05 **in./min**
Force to Compress 25% (Avg) 28.5 **lb**

Matl Type Thermal Insulation
Exposure
Gamma Unirrad.(Control) ergs/gm(C)
Neutron " " n/cm^2

Specimen 1		Specimen 2		Specimen 3		Avg Load for Given Deflection	
Load (Instron) (lb)	Deflection (in.)	Load (Instron) (lb)	Deflection (in.)	Load (Instron) (lb)	Deflection (in.)	Load (lb)	Deflection (in.)
0	0	0	0	0	0	0	0
1.5	0.01	2	0.01	2.5	0.01	2.0	0.01
10	0.02	11	0.02	12	0.02	11.0	0.02
17	0.03	20	0.03	20	0.03	19.0	0.03
20.5	0.04	24	0.04	24	0.04	22.8	0.04
22	0.05	26	0.05	25.3	0.05	24.4	0.05
26	0.10	29.3	0.10	27.3	0.10	27.5	0.10
28	0.15	31	0.15	29.8	0.15	29.6	0.15
31.6	0.20	35	0.20	33.5	0.20	43.4	0.20
35.7	0.25	40	0.25	39.	0.25	38.2	0.25
41.5	0.30	47.8	0.30	46.3	0.30	45.2	0.30

TABLE A-19

Radiation-Cryotemperature Test Data: **Material** F
Styrofoam 22

Test Temperature Ambient

Matl Type Thermal Insulation

Low Exposure
- Gamma 5.0×10^{9} ergs/gm(C)
- Neutrons 1.2×10^{15} n/cm^2
- Pull-Rod Speed 0.05 in./min
- Force to Compress 25% 14.5 lb

High Exposure
- Gamma 1.0×10^{10} ergs/gm(C)
- Neutron 2.6×10^{15} n/cm^2
- Pull-Rod Speed 0.05 in./min
- Force to Compress 25% 10.5 lb

Low-Exposure Specimen		
Load (Instron) (lb)	Load (Dynamometer) (lb)	Deflection (in.)
0		0
1		0.02
0		0.03
2.5		0.05
5		0.07
10		0.09
14.5		0.125

High-Exposure Specimen		
Load (Instron) (lb)	Load (Dynamometer) (lb)	Deflection (in.)
0		0
1		0.01
0		0.03
2.5		0.05
5.0		0.07
10.5		0.125

TABLE A-20

Radiation-Cryotemperature Test Data: **Material** F

Styrofoam 22

Test Temperature Liquid Nitrogen
Pull-Rod Speed (Avg) 0.046 in./min
Force to Compress 25% (Avg) 44 lb.

Matl Type Thermal Insulation
Exposure
Gamma Unirradiated ergs/gm(C)
Neutron " n/cm^2
(Control)

Specimen						Avg Load for given Deflection	
No. 1			No. 2				
Load (Instron) (lb)	Load (Dyn.)* (lb)	Defl. (in.)	Load (Instron) (lb)	Load (Dyn.)* (lb)	Defl. (in.)	Load (Dyn.)* (lb)	Defl. (in.)
0	0	0				0	0
10	16	0.019				16	0.019
20	28	0.032				28	0.032
25	34	0.052				34	0.052
27	40	0.077				40	0.077
28	44	0.122				44	0.122
29	44	0.162				44	0.162
30	42	0.202				42	0.202
32	46	0.243				46	0.243
40	52	0.282				52	0.282
58	85	0.318				85	0.318
85	130	0.350				130	0.350

* Dynamometer

TABLE A-21

Radiation-Cryotemperature Test Data: **Material** F
Styrofoam 22

Test Temperature Liquid Nitrogen

Matl Type Thermal Insulation

Low Exposure
Gamma 5.2×10^9 ergs/gm(C)
Neutrons 9.0×10^{14} n/cm^2
Pull-Rod Speed 0.048 in./min
Force to Compress 25% 72 lb

High Exposure
Gamma 1.2×10^{10} ergs/gm(C)
Neutron 2.2×10^{15} n/cm^2
Pull-Rod Speed 0.041 in./min
Force to Compress 25% 49.3 lb

Low-Exposure Specimen		
Load (Instron) (lb)	Load (Dynamometer) (lb)	Deflection (in.)
0	0	0
18	42	0.030
40	70	0.066
45	72	0.112
47	72	0.160
52	80	0.205
57	90	0.247
67	117	0.290

High-Exposure Specimen		
Load (Instron) (lb)	Load (Dynamometer) (lb)	Deflection (in.)
0	0	0
9	20	0.019
20	40	0.034
32	52	0.055
35	55	0.079
32	52	0.104
30	47	0.149
45	70	0.224
57	90	0.287

TABLE A-22

Radiation-Cryotemperature Test Data: Material F
Styrofoam 22

Test Temperature Liquid Hydrogen
Pull-Rod Speed (Avg) 0.05 in./min
Force to Compress 25% (Avg) 57.3 lb

Matl Type Thermal Insulation
Exposure
Gamma Unirradiated ergs/gm(C)
Neutron " n/cm^2
(Control)

Specimen No. 1 Load (Instron) (lb)	Specimen No. 1 Load (Dyn.)* (lb)	Specimen No. 1 Defl. (in.)	Specimen No. 2 Load (Instron) (lb)	Specimen No. 2 Load (Dyn.)* (lb)	Specimen No. 2 Defl. (in.)	Avg Load for given Deflection Load (Dyn.)* (lb)	Avg Load for given Deflection Defl. (in.)
0	0	0				0	0
30	45	0.017				45	0.017
37	56	0.058				56	0.058
38	57	0.111				57	0.111
39	59	0.210				59	0.210
50	75	0.308				75	0.308

* Dynamometer

TABLE A-23

Radiation-Cryotemperature Test Data: Material F
Styrofoam 22

Test Temperature Liquid Hydrogen

Matl Type Thermal Insulation

Low Exposure

Gamma 5.2×10^9 ergs/gm(C)
Neutrons 8.5×10^{14} n/cm^2
Pull-Rod Speed 0.044 in./min
Force to Compress 25% 90 lb

High Exposure

Gamma 1.2×10^{10} ergs/gm(C)
Neutron 2.0×10^{15} n/cm^2
Pull-Rod Speed 0.030 in./min
Force to Compress 25% 45 lb

Low-Exposure Specimen		
Load (Instron) (lb)	Load (Dynamometer) (lb)	Deflection (in.)
0	0	0
20	30	0.029
45	67	0.076
60	90	0.126
70	105	0.203
90	135	0.278
105	158	0.319

High-Exposure Specimen		
Load (Instron) (lb)	Load (Dynamometer) (lb)	Deflection (in.)
0	0	0
10	10	0.051
30	20	0.083
43	42	0.120
48	61	0.155
48	61	0.209
50	59	0.257
55	59	0.302
78	90	0.338
108	133	0.369

TABLE A-24

Radiation-Cryotemperature Test Data: Material G

H-Film

Test Temperature Ambient
Pull-Rod Speed 0.50 in./min
Breaking Factor (Avg) 38.5 lb/in.
% Total Elongation (Avg) 45 %
(4.00-in. Gage)

Mat'l Type Electrical Insulation
Exposure
Gamma Unirradiated ergs/gm(C)
Neutron " n/cm²
(Control)

Specimen									Avg Load for Given Deflection	
No. 1			No. 2			No. 3				
Load (Instron) (lb)	Load (Dyn.)* (lb)	Defl. (in.)	Load (Instron) (lb)	Load (Dyn.)* (lb)	Defl. (in.)	Load (Instron) (lb)	Load (Dyn.)* (lb)	Defl. (in.)	Load (Instron) (lb)	Defl. (in.)
0		0	0		0				0	0
12		0.10	15		0.10				13.5	0.10
17.5		0.15	20		0.17				21.0	0.20
22.5		0.25	25		0.33				24.5	0.30
29.0		0.50	30		0.55				27.0	0.40
32.5		0.75	34.5		1.00				29.0	0.50
34.5		1.00	37		1.50				32.5	0.75
36		1.25	40		2.20				34.5	1.00
37		1.45							37.0	1.50
									38.5	1.80

* Dynamometer

TABLE A-25

Radiation-Cryotemperature Test Data: H-Film **Material** G

Test Temperature Ambient
Pull-Rod Speed 0.50 in./min
Breaking Factor (Avg) 46.0 lb/in.
% Total Elongation (Avg) 50.7 %
(4.00-in. Gage)

Matl Type Electrical Insulation
Exposure
Gamma 4.75×10^9 ergs/gm(C)
Neutron 1.3×10^{15} n/cm^2

Specimen									Avg Load for Given Deflection	
No. 1			No. 2			No. 3				
Load (Instron) (lb)	Load (Dyn.)* (lb)	Defl. (in.)	Load (Instron) (lb)	Load (Dyn.)* (lb)	Defl. (in.)	Load (Instron) (lb)	Load (Dyn.)* (lb)	Defl. (in.)	Load (Instron) (lb)	Defl. (in.)
0		0	0		0	0		0	0	0
10		0	10		0	10		0.02	10	0.007
20		0.06	20		0.04	20		0.12	20	0.07
30		0.24	30		0.26	30		0.40	30	0.27
40		0.70	40		0.52	41		1.98	40	1.05
46		1.96	52		2.16				46	2.03

* Dynamometer

TABLE A-26

Radiation-Cryotemperature Test Data: **Material** G

H-Film

Test Temperature Ambient
Pull-Rod Speed 0.50 in./min
Breaking Factor (Avg) 39.2 lb/in.
% Total Elongation (Avg) 47.5 %
(4.00-in. Gage)

Matl Type Electrical Insulation
Exposure
Gamma 8.0 x 10^9 ergs/gm(C)
Neutron 2.2 x 10^{15} n/cm^2

Specimen									Avg Load for Given Deflection	
No. 1			No. 2			No. 3				
Load (Instron) (lb)	Load (Dyn.)* (lb)	Defl. (in.)	Load (Instron) (lb)	Load (Dyn.)* (lb)	Defl. (in.)	Load (Instron) (lb)	Load (Dyn.)* (lb)	Defl. (in.)	Load (Instron) (lb)	Defl. (in.)
0		0	0		0				0	0
10		0.08	10		0.02				10	0.05
20		0.24	20		0.14				20	0.19
30		0.55	30		0.40				30	0.48
39		2.081	39.5		1.694				39.2	1.90

* Dynamometer

TABLE A-27

Radiation-Cryotemperature Test Data: **Material** G
H-Film

Test Temperature Liquid Nitrogen
Pull-Rod Speed 0.476 in./min
Breaking Factor (Avg) 90 lb/in.
% Total Elongation (Avg) 8.9 %
(4.00-in. Gage)

Matl Type Electrical Insulation
Exposure
Gamma Unirradiated ergs/gm(C)
Neutron " n/cm²
(Control)

Specimen									Avg Load for Given Deflection	
No. 1			No. 2			No. 3				
Load (Instron) (lb)	Load (Dyn.)* (lb)	Defl. (in.)	Load (Instron) (lb)	Load (Dyn.)* (lb)	Defl. (in.)	Load (Instron) (lb)	Load (Dyn.)* (lb)	Defl. (in.)	Load (Dyn.*) (lb)	Defl. (in.)
0	0	0	0	0	0				0	0
10	22	0.092		10	0.092				19.5	0.092
20	40	0.178	18	40	0.181				40	0.180
27	52	0.265		68	0.278				60	0.271
43	80	0.345	43	100	0.370				90	0.358

* Dynamometer

TABLE A-28

Radiation-Cryotemperature Test Data: **Material** G
H-Film

Test Temperature Liquid Nitrogen
Pull-Rod Speed 0.450 in./min
Breaking Factor (Avg) 66.5 lb/in.
% Total Elongation (Avg) 5.1 %
(4.00-in. Gage)

Matl Type Electrical Insulation
Exposure
Gamma 5.2×10^{9} ergs/gm(C)
Neutron 9.2×10^{14} n/cm^2

Specimen									Avg Load for Given Deflection	
No. 1			No. 2			No. 3				
Load (Instron) (lb)	Load (Dyn.)* (lb)	Defl. (in.)	Load (Instron) (lb)	Load (Dyn.)* (lb)	Defl. (in.)	Load (Instron) (lb)	Load (Dyn.)* (lb)	Defl. (in.)	Load (Dyn.)* (lb)	Defl. (in.)
0	0	0	0	0	0				0	0
20	30	0.053	13	20	0.092				25	0.07
25	38	0.089	27	40	0.161				40	0.12
33	50	0.126	43	65	0.220				50	0.14
42	63	0.166							66.5	0.215
45	68	0.209								

* Dynamometer

TABLE A-29

Radiation-Cryotemperature Test Data: **Material** G
H-Film

Test Temperature Liquid Nitrogen
Pull-Rod Speed 0.360 in./min
Breaking Factor (Avg) 82 lb/in.
% Total Elongation (Avg) 8.1 %
(4.00-in. Gage)

Matl Type Electrical Insulation
Exposure
Gamma 1.3×10^{10} ergs/gm(C)
Neutron 5.0×10^{15} n/cm^2

Specimen									Avg Load for Given Deflection	
No. 1			No. 2			No. 3				
Load (Instron) (lb)	Load (Dyn.)* (lb)	Defl. (in.)	Load (Instron) (lb)	Load (Dyn.)* (lb)	Defl. (in.)	Load (Instron) (lb)	Load (Dyn.)* (lb)	Defl. (in.)	Load (Dyn.*) (lb)	Defl. (in.)
0	0	0	0	0	0	0	0	0	0	0
33	50	0.162	35	52	0.208	20	30	0.200	50	0.210
60	90	0.302	57	85	0.352	47	70	0.320	82	0.325

* Dynamometer

TABLE A-30

Radiation-Cryotemperature Test Data: **Material** G
H-Film

Test Temperature Liquid Hydrogen
Pull-Rod Speed 0.130 in./min
Breaking Factor (Avg) 120 lb/in.
% Total Elongation (Avg) 0.45 %
(4.00-in. Gage)

Matl Type Electrical Insulation
Exposure
Gamma Unirradiated ergs/gm(C)
Neutron " n/cm^2
(Control)

Specimen									Avg Load for Given Deflection	
No. 1			No. 2			No. 3				
Load (Instron) (lb)	Load (Dyn.)* (lb)	Defl. (in.)	Load (Instron) (lb)	Load (Dyn.)* (lb)	Defl. (in.)	Load (Instron) (lb)	Load (Dyn.)* (lb)	Defl. (in.)	Load (Dyn.)* (lb)	Defl. (in.)
0	0	0	0	0	0				0	0
20	30	0.003	20	30	0.007				30	0.005
44	66	0.005	55	83	0.015				85	0.0106
80	120	0.008	80	120	0.028				120	0.018

* Dynamometer

TABLE A-31

Radiation-Cryotemperature Test Data: **Material** G

H-Film

Test Temperature Liquid Hydrogen
Pull-Rod Speed 0.455 in./min
Breaking Factor (Avg) 160 lb/in.
% Total Elongation (Avg) 6.6 %
(4.00-in. Gage)

Matl Type Electrical Insulation
Exposure
Gamma 5.2×10^9 ergs/gm(C)
Neutron 9.0×10^{14} n/cm^2

Specimen									Avg Load for Given Deflection	
No. 1			No. 2			No. 3				
Load (Instron) (lb)	Load (Dyn.)* (lb)	Defl. (in.)	Load (Instron) (lb)	Load (Dyn.)* (lb)	Defl. (in.)	Load (Instron) (lb)	Load (Dyn.)* (lb)	Defl. (in.)	Load (Dyn.)* (lb)	Defl. (in.)
0	0	0	0	0	0	0	0	0	0	0
15	23	0.081	70	105	0.045	20	30	0.045	49	0.045
27	40	0.133	90	135	0.088	40	60	0.091	79	0.100
40	60	0.171	100	150	0.130	60	90	0.138	101	0.150
53	80	0.218	110	165	0.170	80	120	0.187	125	0.200
68	102	0.259	120	180	0.215	100	150	0.236	160	0.265
80	120	0.293				120	180	0.288		

* Dynamometer

TABLE A-32

Radiation-Cryotemperature Test Data: **Material** G
H-Film

Test Temperature Liquid Hydrogen
Pull-Rod Speed 0.480 in./min
Breaking Factor (Avg) 98 lb/in.
% Total Elongation (Avg) 2.6 %
(4.00-in. Gage)

Matl Type Electrical Insulation
Exposure
Gamma 1.3×10^{10} ergs/gm(C)
Neutron 7.8×10^{14} n/cm^2

Specimen									Avg Load for Given Deflection	
No. 1			No. 2			No. 3				
Load (Instron) (lb)	Load (Dyn.)* (lb)	Defl. (in.)	Load (Instron) (lb)	Load (Dyn.)* (lb)	Defl. (in.)	Load (Instron) (lb)	Load (Dyn.)* (lb)	Defl. (in.)	Load (Dyn.*) (lb)	Defl. (in.)
0	0	0							0	0
20	30	0.056							30	0.056
35	53	0.110							53	0.110
50	75	0.160							75	0.160
65	98	0.206							98	0.206

* Dynamometer

TABLE A-33

Radiation-Cryotemperature Test Data: **Material** H

Mylar - C

Test Temperature Ambient
Full-Rod Speed 0.50 in./min
Breaking Factor (Avg) 17.6 lb/in.
% Total Elongation (Avg) 49.7 %
(4.00-in. Gage)

Matl Type Electrical Insulation
Exposure
Gamma Unirradiated ergs/gm(C)
Neutron " n/cm^2
(Control)

Specimen									Avg Load for Given Deflection	
No. 1			No. 2			No. 3				
Load (Instron) (lb)	Load (Dyn.)* (lb)	Defl. (in.)	Load (Instron) (lb)	Load (Dyn.)* (lb)	Defl. (in.)	Load (Instron) (lb)	Load (Dyn.)* (lb)	Defl. (in.)	Load (Instron) (lb)	Defl. (in.)
0		0	0		0				0	0
4.0		0.05	7.0		0.05				5.5	0.05
9.4		0.10	11.6		0.10				10.5	0.10
13.0		0.15	13.5		0.15				13.2	0.15
14.0		0.20	14.2		0.25				14.3	0.25
14.4		0.25	14.3		0.40				14.4	0.42
14.5		0.45	15.1		0.75				15.2	0.75
15.3		0.75	15.7		1.00				15.8	1.00
15.9		1.00	16.9		1.50				16.9	1.50
16.9		1.50	17.7		2.00				17.6	1.99
17.4		1.89	17.7		2.10					

* Dynamometer

TABLE A-34

Radiation-Cryotemperature Test Data: **Material** H
Mylar - C

Test Temperature Ambient
Pull-Rod Speed 0.50 in./min
Breaking Factor (Avg) 38 lb/in.
% Total Elongation (Avg) 64 %
(4.00-in. Gage)

Matl Type Electrical Insulation
Exposure
Gamma 4.92×10^9 ergs/gm(C)
Neutron 1.3×10^{15} n/cm^2

Specimen									Avg Load for Given Deflection	
No. 1			No. 2			No. 3				
Load (Instron) (lb)	Load (Dyn.)* (lb)	Defl. (in.)	Load (Instron) (lb)	Load (Dyn.)* (lb)	Defl. (in.)	Load (Instron) (lb)	Load (Dyn.)* (lb)	Defl. (in.)	Load (Instron) (lb)	Defl. (in.)
0		0	0		0	0		0	0	0
10		0.02	10		0.02	10		0.02	10	0.02
20		0.06	20		0.06	20		0.06	20	0.06
28		0.16	28		0.16	28		0.16	28	0.16
28		0.26	28		0.26	28		0.26	28	0.26
30		0.60	30		0.60	30		0.60	30	0.60
35		1.60	35		1.60	35		1.60	35	1.60
38		2.56	38		2.56	38		2.56	38	2.56

* Dynamometer

TABLE A-35

Radiation-Cryotemperature Test Data: **Material** H
Mylar-C

Test Temperature: Ambient
Full-Rod Speed: 0.50 in./min
Breaking Factor (Avg): 16.8 lb/in.
% Total Elongation (Avg): 42 %
(4.00-in. Gage)

Matl Type: Electrical Insulation
Exposure
Gamma: 8.0×10^9 ergs/gm(C)
Neutron: 2.2×10^{15} n/cm^2

Specimen									Avg Load for Given Deflection	
No. 1			No. 2			No. 3				
Load (Instron) (lb)	Load (Dyn.)* (lb)	Defl. (in.)	Load (Instron) (lb)	Load (Dyn.)* (lb)	Defl. (in.)	Load (Instron) (lb)	Load (Dyn.)* (lb)	Defl. (in.)	Load (Instron) (lb)	Defl. (in.)
0		0	0		0	0		0	0	0
5		0.10	5		0.03	5		0.03	5	0.053
10		0.16	10		0.10	10		0.10	10	0.12
13.5		0.20	13.5		0.30	13.5		0.25	13.5	0.25
13.5		0.40	13.5		0.50	13.5		0.45	13.5	0.45
15		0.80	15		0.80	15		0.70	15	0.77
16.5		1.54	15.5		0.90	17		1.60	16.8	1.73
						18.5		2.75		

* Dynamometer

TABLE A-36

Radiation-Cryotemperature Test Data: **Material** H
Mylar-C

Test Temperature Liquid Nitrogen
Pull-Rod Speed 0.448 in./min
Breaking Factor (Avg) 98 lb/in.
% Total Elongation (Avg) 5.7 %
(4.00-in. Gage)

Matl Type Electrical Insulation
Exposure
Gamma Unirradiated ergs/gm(C)
Neutron " n/cm²
(Control)

Specimen No. 1			Specimen No. 2			Specimen No. 3			Avg Load for Given Deflection	
Load (Instron) (lb)	Load (Dyn.)* (lb)	Defl. (in.)	Load (Instron) (lb)	Load (Dyn.)* (lb)	Defl. (in.)	Load (Instron) (lb)	Load (Dyn.)* (lb)	Defl. (in.)	Load (Dyn.)* (lb)	Defl. (in.)
0	0	0							0	0
35	56	0.138							56	0.138
70	98	0.227							98	0.227

*** Dynamometer**

TABLE A-37

Radiation-Cryotemperature Test Data: **Material** H
Mylar-C

Test Temperature Liquid Nitrogen
Pull-Rod Speed 0.480 in./min
Breaking Factor (Avg) 18 lb/in.
% Total Elongation (Avg) 3.6 %
(4.00-in. Gage)

Matl Type Electrical Insulation
Exposure
Gamma 5.3×10^{9} ergs/gm(C)
Neutron 1.0×10^{15} n/cm^2

Specimen									Avg Load for Given Deflection	
No. 1			No. 2			No. 3				
Load (Instron) (lb)	Load (Dyn.)* (lb)	Defl. (in.)	Load (Instron) (lb)	Load (Dyn.)* (lb)	Defl. (in.)	Load (Instron) (lb)	Load (Dyn.)* (lb)	Defl. (in.)	Load (Dyn.*) (lb)	Defl. (in.)
0	0	0							0	0
5	7.5	0.73							7.5	0.073
12	18	0.143							18	0.143

* Dynamometer

TABLE A-38

Radiation-Cryotemperature Test Data: **Material** H
Mylar-C

Test Temperature Liquid Nitrogen
Pull-Rod Speed 0.450 in./min
Breaking Factor (Avg) 58.5 lb/in.
% Total Elongation (Avg) 6.95 %
(4.00-in. Gage)

Matl Type Electrical Insulation
Exposure
Gamma 1.3×10^{10} ergs/gm(C)
Neutron 1.5×10^{15} n/cm^2

Specimen									Avg Load for Given Deflection	
No. 1			No. 2			No. 3				
Load (Instron) (lb)	Load (Dyn.)* (lb)	Defl. (in.)	Load (Instron) (lb)	Load (Dyn.)* (lb)	Defl. (in.)	Load (Instron) (lb)	Load (Dyn.)* (lb)	Defl. (in.)	Load (Dyn.)* (lb)	Defl. (in.)
0	0	0	0	0	0				0	0
10	15	0.097	20	30	0.037				17.7	0.037
22	33	0.193	25	38	0.081				28.0	0.100
32	48	0.282	30	45	0.140				34.0	0.140
38	57	0.352	40	60	0.205				47.0	0.205
									58.5	0.278

* Dynamometer

TABLE A-39

Radiation-Cryotemperature Test Data: **Material** H
Mylar-C

Test Temperature Liquid Hydrogen
Full-Rod Speed 0.50 in./min
Breaking Factor (Avg) 97.7 lb/in.
% Total Elongation (Avg) 7.2 %
(4.00-in. Gage)

Matl Type Electrical Insulation
Exposure
Gamma Unirradiated ergs/gm(C)
Neutron " n/cm^2
(Control)

Specimen									Avg Load for Given Deflection	
No. 1			No. 2			No. 3				
Load (Instron) (lb)	Load (Dyn.)* (lb)	Defl. (in.)	Load (Instron) (lb)	Load (Dyn.)* (lb)	Defl. (in.)	Load (Instron) (lb)	Load (Dyn.)* (lb)	Defl. (in.)	Load (Dyn.*) (lb)	Defl. (in.)
0	0	0	0	0	0	0	0	0	0	0
30	45	0.099	12	18	0.095	8	12	0.096	26.7	0.100
45	68	0.173	30	45	0.170	20	30	0.200	55.3	0.200
60	90	0.224	65	98	0.315	70	105	0.326	64.3	0.224
									97.7	0.288

* Dynamometer

TABLE A-40

Radiation-Cryotemperature Test Data: **Material** H
Mylar

Test Temperature Liquid Hydrogen
Pull-Rod Speed 0.435 in./min
Breaking Factor (Avg) 120 lb/in.
% Total Elongation (Avg) 3.9 %
(4.00-in. Gage)

Matl Type Electrical Insulation
Exposure
Gamma 5.3×10^9 ergs/gm(C)
Neutron 1.0×10^{15} n/cm^2

Specimen No. 1 Load (Instron) (lb)	No. 1 Load (Dyn.)* (lb)	No. 1 Defl. (in.)	No. 2 Load (Instron) (lb)	No. 2 Load (Dyn.)* (lb)	No. 2 Defl. (in.)	No. 3 Load (Instron) (lb)	No. 3 Load (Dyn.)* (lb)	No. 3 Defl. (in.)	Avg Load for Given Deflection: Load (Dyn.)* (lb)	Avg Load for Given Deflection: Defl. (in.)
0	0	0							0	0
20	30	0.028							30	0.028
40	60	0.052							60	0.052
50	75	0.079							75	0.079
60	90	0.100							90	0.100
70	105	0.128							105	0.128
80	120	0.154							120	0.154

* Dynamometer

TABLE A-41

Radiation-Cryotemperature Test Data: **Material** I
Conolon 506

Pull-Rod Speed (Avg) 0.05 **in./min**
Ultimate Tensile Strength (Avg) 43,200 **psi**
% Total Elongation
Pull-Rod (5.25-in. Gage) 2.1 **%**
Extensometer (2-in. Gage) 1.8 **%**

Matl Type Structural Laminate
Test Temp Ambient
Exposure
Gamma Unirradiated ergs/gm(C)
Neutron " n/cm^2
(Control)

Specimen												Average Load for Given Deflection			
No. 1			No. 2			No. 3			No. 4						
Load (lb)	Defl. (Rod) (in.)	Defl. (Exts.) (in.)	Load (lb)	Defl. (Rod) (in.)	Defl. (Exts.) (in.)	Load (lb)	Defl. (Rod) (in.)	Defl. (Exts.) (in.)	Load (lb)	Defl. (Rod) (in.)	Defl. (Exts.) (in.)	Load (lb)	Load lb/in^2	Defl. (Rod) (in.)	Defl. (Exts.) (in.)
0	0	0	0	0	0	0	0	0	0	0	0	0	0	0	0
80	.004	.0014	180	.005	.0016	70	.004	.0012	130	.008	.0026	190	6080	.010	.0032
180	.010	.0032	320	.014	.0044	190	.010	.0034	270	.016	.0053	350	11200	.020	.0066
300	.019	.0062	450	.024	.0073	330	.020	.0064	400	.026	.0086	440	14080	.030	.0090
440	.028	.0092	580	.035	.0116	460	.030	.0100	530	.036	.0120	605	19360	.040	.0132
570	.039	.0129	710	.046	.0152	600	.040	.0138	650	.047	.0156	710	22720	.050	.0164
690	.050	.0164	840	.056	.0186	710	.053	.0174	780	.058	.0190	830	26560	.060	.0198
810	.060	.0198	970	.067	.0220	850	.064	.0210	900	.069	.0228	960	30710	.070	.0232
940	.070	.0232	1100	.077	.0256	980	.075	.0248	1030	.079	.0262	1060	33900	.080	.0263
1050	.080	.0264	1210	.088	.0290	1090	.085	.0280	1140	.090	.0297	1160	37100	.090	.0295
1150	.089	.0295	1300	.102	.0336	1210	.096	.0316	1260	.101	.0334	1265	40500	.100	.0328
1250	.098	.0323	1370	.108	.0358	1310	.105	.0348	1360	.110	.0362	1350	43200	.108	.0355
1360	.107	.0354													

TABLE A-42

Radiation-Cryotemperature Test Data: Conolon 506 **Material** I

Pull-Rod Speed (Avg) 0.05 **in./min**
Ultimate Tensile Strength (Avg) 41850 **psi**
% Total Elongation
Pull-Rod (5.25-in. Gage) 2.2 **%**
Extensometer (2-in. Gage) 1.9 **%**

Matl Type Structural Laminate
Test Temp Ambient
Exposure
Gamma 1.05×10^{10} **ergs/gm(C)**
Neutron 2.5×10^{15} **n/cm²**

Specimen												Average Load for Given Deflection			
No. 1			No. 2			No. 3			No. 4						
Load (lb)	Defl. (Rod) (in.)	Defl. (Exts.) (in.)	Load (lb)	Defl (Rod) (in.)	Defl (Exts.) (in.)	Load (lb)	Defl. (Rod) (in.)	Defl. (Exts.) (in.)	Load (lb)	Defl. (Rod) (in.)	Defl (Exts. (in.	Load (lb)	Load lb/in²	Defl. (Rod) (in.)	Defl. (Exts.) (in.)
0		0	0		0	0		0				0	0	0	0
200		.0044	220		.0044	205		.0044				208	6655	.013	.0044
380		.0088	395		.0088	370		.0088				382	12230	.027	.0088
515		.0132	540		.0132	510		.0132				522	16700	.040	.0132
670		.0176	685		.0176	645		.0176				667	21350	.053	.0176
810		.0220	830		.0220	775		.0220				805	25770	.067	.0220
950		.0264	975		.0264	910		.0264				945	30240	.080	.0264
1095		.0308	1120		.0308	1045		.0308				1087	34770	.093	.0308
1230		.0352	1255		.0352	1170		.0352				1218	38950	.107	.0352
1265	.109	.0360	1350	.115	.0380	1295		.0396				1308	41850	.115	.0380
						1310	.121	.0400							

TABLE A-43

Radiation-Cryotemperature Test Data: **Material** I
Conolon 506

Pull-Rod Speed (Avg) 0.05 **in./min**
Ultimate Tensile Strength (Avg) 40160 **psi**
% Total Elongation
Pull-Rod (5.25-in. Gage) 2.1 **%**
Extensometer (2-in. Gage) 1.8 **%**

Matl Type Structural Laminate
Test Temp Ambient
Exposure
Gamma 6.7 x 10^{10} **ergs/gm(C)**
Neutron 1.7 x 10^{16} **n/cm²**

Specimen												Average Load for Given Deflection			
No. 1			No. 2			No. 3			No. 4						
Load (lb)	Defl. (Rod) (in.)	Defl. (Exts.) (in.)	Load (lb)	Defl. (Rod) (in.)	Defl. (Exts.) (in.)	Load (lb)	Defl. (Rod) (in.)	Defl. (Exts.) (in.)	Load (lb)	Defl. (Rod) (in.)	Defl. (Exts.) (in.)	Load (lb)	Load lb/in²	Defl. (Rod) (in.)	Defl. (Exts.) (in.)
0		0	0		0	0		0				0	0	0	0
225		.0044	200		.0044	240		.0044				222	7110	.013	.0044
410		.0088	380		.0088	400		.0088				397	12700	.027	.0088
560		.0132	530		.0132	550		.0132				547	17500	.040	.0132
690		.0176	675		.0176	690		.0176				685	21920	.053	.0176
835		.0220	810		.0220	825		.0220				823	26350	.067	.0220
975		.0264	950		.0264	960		.0264				962	30780	.080	.0264
1110		.0308	1090		.0308	1100		.0308				1100	35200	.093	.0308
1255		.0350	1225		.0352	1140	.097	.0320				1195	38220	.103	.0340
1270	.108	.0357	1350		.0393							1255	40160	.108	.0358
			1355	.120	.0396										

TABLE A-44

Radiation-Cryotemperature Test Data: **Material** I

Conolon 506

Pull-Rod Speed (Avg) .014 in./min
Ultimate Tensile Strength (Avg) 76000 psi
% Total Elongation
Pull-Rod (5.25-in. Gage) 4.1 %
Extensometer (2-in. Gage) 3.5 %

Matl Type Structural Laminate
Test Temp Liquid Nitrogen
Exposure
Gamma Unirradiated ergs/gm(C)
Neutron " n/cm^2
(Control)

Specimen												Average Load for Given Deflection			
No. 1			No. 2			No. 3			No. 4						
Load (lb)	Defl. (Rod) (in.)	Defl. (Exts.) (in.)	Load (lb)	Defl. (Rod) (in.)	Defl. (Exts.) (in.)	Load (lb)	Defl. (Rod) (in.)	Defl. (Exts.) (in.)	Load (lb)	Defl. (Rod) (in.)	Defl. (Exts.) (in.)	Load (lb)	Load lb/in^2	Defl. (Rod) (in.)	Defl. (Exts.) (in.)
0	0		0	0		0	0					0	0	0	0
60	.012		190	.010		260	.028					423	13540	.030	.010
195	.018		820	.049		850	.073					833	26640	.061	.020
610	.042		1400	.094		1450	.118					1237	39580	.091	.030
1160	.083		1850	.130		1780	.150					1623	51900	.121	.040
1640	.123		2050	.153		1950	.172					1967	62950	.152	.050
1800	.131		2250	.172		2000	.200					2198	70300	.182	.060
2020	.155		2300	.192	.063	2150	.219					2377	76000	.214	.070
2120	.163					2200	.225								
2370	.185					2250	.232								
2570	.213	.070				2260	.237	.078							

TABLE A-45

Radiation-Cryotemperature Test Data: Conolon 506 **Material** I

Pull-Rod Speed (Avg) 0.011 **in./min**
Ultimate Tensile Strength (Avg) 76500 **psi**
% Total Elongation
Pull-Rod (5.25-in. Gage) 4.0 **%**
Extensometer (2-in. Gage) 3.5 **%**

Matl Type Structural Laminate
Test Temp Liquid Nitrogen
Exposure
Gamma 1.3×10^{10} **ergs/gm(C)**
Neutron 1.6×10^{15} **n/cm^2**

Specimen												Average Load for Given Deflection			
No. 1			No. 2			No. 3			No. 4						
Load (lb)	Defl. (Rod) (in.)	Defl. (Exts.) (in.)	Load (lb)	Defl. (Rod) (in.)	Defl. (Exts.) (in.)	Load (lb)	Defl. (Rod) (in.)	Defl. (Exts.) (in.)	Load (lb)	Defl. (Rod) (in.)	Defl. (Exts.) (in.)	Load (lb)	Load lb/in^2	Defl. (Rod) (in.)	Defl. (Exts.) (in.)
0	0		0	0		0	0					0	0	0	0
115	.007		160	.018		300	.019					507	16220	.030	.010
410	.024		500	.040		920	.041					1023	32760	.061	.020
900	.057		1200	.076		1550	.085					1483	47490	.091	.030
1410	.097		1780	.112		1950	.114					1850	59160	.121	.040
1800	.129		1950	.141		2250	.145					2170	69460	.152	.050
2000	.143		2300	.180		2350	.165					2392	76500	.209	.069
2150	.158		2450	.188		2475	.211								
2050	.187	.062	2550	.205	.068	2500	.232								
						2575	.236	.078							

TABLE A-46

Radiation-Cryotemperature Test Data: Conolon 506 **Material** I

Pull-Rod Speed (Avg)	.014	in./min	
Ultimate Tensile Strength (Avg)	78670	psi	
% Total Elongation			
Pull-Rod (5.25-in. Gage)	4.4	%	
Extensometer (2-in. Gage)	3.8	%	
Matl Type	Structural Laminate		
Test Temp	Liquid Nitrogen		
Exposure			
Gamma	5.0×10^{10}	ergs/gm(C)	
Neutron	4.8×10^{16}	n/cm^2	

Specimen												Average Load for Given Deflection			
No. 1			No. 2			No. 3			No. 4						
Load (lb)	Defl. (Rod) (in.)	Defl. (Exts.) (in.)	Load (lb)	Defl (Rod) (in.)	Defl (Exts.) (in.)	Load (lb)	Defl. (Rod) (in.)	Defl. (Exts.) (in.)	Load (lb)	Defl. (Rod) (in.)	Defl (Exts.) (in.)	Load (lb)	Load lb/in^2	Defl. (Rod) (in.)	Defl. (Exts.) (in.)
0	0		0	0								0	0	0	0
440	.025		840	.025								715	23870	.030	.010
1040	.065		1290	.061								1140	36450	.061	.020
1640	.112		1590	.094								1480	47400	.091	.030
1990	.147		1990	.138								1785	57100	.121	.040
2190	.165		2190	.214	.071							2037	65140	.152	.050
2390	.182											2490	78670	.230	.076
2470	.193														
2490	.204														
2660	.222														
2790	.246	.081													

TABLE A-47

Radiation-Cryotemperature Test Data: **Material** I

Conolon 506

Pull-Rod Speed (Avg) .033 **in./min**
Ultimate Tensile Strength (Avg) 66240 **psi**
% Total Elongation
Pull-Rod (5.25-in. Gage) 3.9 **%**
Extensometer (2-in. Gage) 3.4 **%**

Matl Type Structural Laminate
Test Temp Liquid Hydrogen
Exposure
Gamma Unirradiated **ergs/gm(C)**
Neutron " **n/cm^2**
(Control)

Specimen												Average Load for Given Deflection			
No. 1			No. 2			No. 3			No. 4						
Load (lb)	Defl. (Rod) (in.)	Defl. (Exts.) (in.)	Load (lb)	Defl. (Rod) (in.)	Defl. (Exts.) (in.)	Load (lb)	Defl. (Rod) (in.)	Defl. (Exts.) (in.)	Load (lb)	Defl. (Rod) (in.)	Defl. (Exts.) (in.)	Load (lb)	Load lb/in^2	Defl. (Rod) (in.)	Defl. (Exts.) (in.)
0	0		0	0								0	0	0	0
300	.022		370	.030								402	12870	.030	.010
940	.064		1020	.067								895	28630	.061	.020
1540	.117		1600	.113								1295	41450	.091	.030
1820	.152		1740	.132								1630	52150	.121	.040
1940	.185	.061	1940	.155								1875	60000	.152	.050
			2110	.182								2070	66240	.207	.078
			2240	.200											
			2200	.228	.075										

TABLE A-48

Radiation-Cryotemperature Test Data: **Material** I

Conolon 506

Pull-Rod Speed (Avg) .054 **in./min**
Ultimate Tensile Strength (Avg) 92750 **psi**
% Total Elongation
Pull-Rod (5.25-in. Gage) 4.2 **%**
Extensometer (2-in. Gage) 3.6 **%**

Matl Type Structural Laminate
Test Temp Liquid Hydrogen
Exposure
Gamma 3.0×10^{10} ergs/gm(C)
Neutron 1.6×10^{12} n/cm^2

Specimen												Average Load for Given Deflection			
No. 1			No. 2			No. 3			No. 4						
Load (lb)	Defl. (Rod) (in.)	Defl. (Exts.) (in.)	Load (lb)	Defl. (Rod) (in.)	Defl. (Exts.) (in.)	Load (lb)	Defl. (Rod) (in.)	Defl. (Exts.) (in.)	Load (lb)	Defl. (Rod) (in.)	Defl. (Exts.) (in.)	Load (lb)	Load lb/in^2	Defl. (Rod) (in.)	Defl. (Exts.) (in.)
0	0		0	0								0	0	0	0
1560	.064		1100	.028								1080	34570	.030	.010
2170	.099		1775	.075								1645	52600	.061	.020
2550	.143		2250	.112								2085	66770	.091	.030
2750	.170		2500	.147								2360	75500	.121	.040
2850	.195		2600	.173								2565	82100	.152	.050
2950	.222	.073	2750	.196								2745	87900	.182	.060
			2850	.215	.071							2900	92750	.219	.072

TABLE A-49

Radiation-Cryotemperature Test Data: Paraplex P-43

Material J

Pull-Rod Speed (Avg) .05 **in./min**
Ultimate Tensile Strength (Avg) 28480 **psi**
% Total Elongation
Pull-Rod (5.25-in. Gage) 1.7 **%**
Extensometer (2-in. Gage) 1.5 **%**

Matl Type Structural Laminate
Test Temp Ambient
Exposure
Gamma Unirradiated **ergs/gm(C)**
Neutron " **n/cm²**
(Control)

Specimen												Average Load for Given Deflection			
No. 1			No. 2			No. 3			No. 4						
Load (lb)	Defl. (Rod) (in.)	Defl. (Exts.) (in.)	Load (lb)	Defl. (Rod) (in.)	Defl. (Exts.) (in.)	Load (lb)	Defl. (Rod) (in.)	Defl. (Exts.) (in.)	Load (lb)	Defl. (Rod) (in.)	Defl. (Exts.) (in.)	Load (lb)	Load lb/in²	Defl. (Rod) (in.)	Defl. (Exts.) (in.)
0	0	0	0	0	0	0	0	0				0	0	0	0
138	.011	.0038	120	.011	.0028	95	.008	.0027				110	3520	.010	.0033
252	.021	.0070	212	.021	.0068	190	.017	.0054				220	7040	.020	.0065
375	.031	.0104	315	.030	.0100	300	.026	.0084				335	10710	.030	.0099
490	.041	.0136	430	.042	.0138	420	.036	.0118				450	14400	.040	.0132
610	.051	.0170	530	.053	.0176	530	.046	.0152				550	17600	.050	.0165
719	.062	.0204	625	.065	.0216	640	.057	.0187				625	20000	.060	.0198
810	.071	.0236	720	.078	.0258	750	.067	.0223				715	22870	.070	.0231
874	.082	.0270	800	.091	.0300	850	.078	.0258				820	26230	.080	.0264
920	.091	.0300				950	.089	.0295				890	28480	.090	.0298

TABLE A-50

Radiation-Cryotemperature Test Data: **Material** J

Paraplex P-43

Pull-Rod Speed (Avg) .05 **in./min**
Ultimate Tensile Strength (Avg) 32180 **psi**
% Total Elongation
Pull-Rod (5.25-in. Gage) 2.0 **%**
Extensometer (2-in. Gage) 1.8 **%**

Matl Type Structural Laminate
Test Temp Ambient
Exposure
Gamma 1.0×10^{10} **ergs/gm(C)**
Neutron 2.5×10^{15} **n/cm^2**

Specimen No. 1 Load (lb)	No. 1 Defl. (Rod) (in.)	No. 1 Defl. (Exts.) (in.)	No. 2 Load (lb)	No. 2 Defl. (Rod) (in.)	No. 2 Defl. (Exts.) (in.)	No. 3 Load (lb)	No. 3 Defl. (Rod) (in.)	No. 3 Defl. (Exts.) (in.)	No. 4 Load (lb)	No. 4 Defl. (Rod) (in.)	No. 4 Defl. (Exts.) (in.)	Average Load for Given Deflection Load (lb)	Load lb/in^2	Defl. (Rod) (in.)	Defl. (Exts.) (in.)
0		0	0		0	0		0	0		0	0	0	0	0
170		.0044	195		.0044	170		.0044	190		.0044	181	5790	.013	.0044
310		.0088	340		.0088	310		.0088	335		.0088	324	10370	.027	.0088
430		.0132	470		.0132	440		.0132	460		.0132	450	14400	.040	.0132
550		.0176	590		.0176	560		.0176	580		.0176	570	18230	.053	.0176
670		.0220	710		.0220	675		.0220	690		.0220	686	21970	.067	.0220
780		.0264	825		.0264	790		.0264	810		.0264	801	25920	.080	.0264
890		.0308	935		.0308	900		.0308	915		.0308	910	29110	.093	.0308
990		.0352	1015	.103	.0340	970	.103	.0340	1020		.0352	970	31020	.101	.0335
1010	.109	.0360							1030	.109	.0360	1006	32180	.106	.0350

TABLE A-51

Radiation-Cryotemperature Test Data: **Material** J
Paraplex P-43

Pull-Rod Speed (Avg) 0.05 **in./min**
Ultimate Tensile Strength (Avg) 30830 **psi**
% Total Elongation
Pull-Rod (5.25-in. Gage) 2.0 **%**
Extensometer (2-in. Gage) 1.7 **%**

Matl Type Structural Laminate
Test Temp Ambient
Exposure
Gamma 6.0×10^{10} **ergs/gm(C)**
Neutron 1.7×10^{16} **n/cm²**

Specimen												Average Load for Given Deflection			
No. 1			No. 2			No. 3			No. 4						
Load (lb)	Defl. (Rod) (in.)	Defl. (Exts.) (in.)	Load (lb)	Defl. (Rod) (in.)	Defl. (Exts.) (in.)	Load (lb)	Defl. (Rod) (in.)	Defl. (Exts.) (in.)	Load (lb)	Defl. (Rod) (in.)	Defl. (Exts.) (in.)	Load (lb)	Load lb/in²	Defl. (Rod) (in.)	Defl. (Exts.) (in.)
0		0	0		0	0		0	0		0	0	0	0	0
160		.0044	175		.0044	180		.0044	165		.0044	170	5440	.013	.0044
295		.0088	315		.0088	320		.0088	300		.0088	308	9860	.027	.0088
420		.0132	445		.0132	445		.0132	420		.0132	433	13850	.040	.0132
540		.0176	565		.0176	565		.0176	540		.0176	553	17700	.053	.0176
650		.0220	680		.0220	685		.0220	655		.0220	668	21380	.067	.0220
765		.0264	795		.0264	800		.0264	770		.0264	783	25040	.080	.0264
870		.0308	910		.0308	910		.0308	880		.0308	893	28560	.093	.0308
920	.100	.0330	975	.103	.0340	975	.103	.0340	985	.106	.0350	964	30830	.103	.0340

TABLE A-52

Radiation-Cryotemperature Test Data: Paraplex P-43

Material J

Pull-Rod Speed (Avg) .012 **in./min**
Ultimate Tensile Strength (Avg) 48480 **psi**
% Total Elongation
Pull-Rod (5.25-in. Gage) 3.3 **%**
Extensometer (2-in. Gage) 2.8 **%**

Matl Type Structural Laminate
Test Temp Liquid Nitrogen
Exposure
Gamma Unirradiated **ergs/gm(C)**
Neutron " **n/cm^2**
(Control)

Specimen												Average Load for Given Deflection			
No. 1			No. 2			No. 3			No. 4						
Load (lb)	Defl. (Rod) (in.)	Defl. (Exts.) (in.)	Load (lb)	Defl. (Rod) (in.)	Defl. (Exts.) (in.)	Load (lb)	Defl. (Rod) (in.)	Defl. (Exts.) (in.)	Load (lb)	Defl. (Rod) (in.)	Defl. (Exts.) (in.)	Load (lb)	Load lb/in^2	Defl. (Rod) (in.)	Defl. (Exts.) (in.)
0	0		0	0		0	0					0	0	0	0
150	.008		140	.006		250	.015					427	13670	.030	.010
360	.026		400	.031		645	.043					777	24840	.061	.020
615	.050		820	.067		1085	.086					1062	34000	.091	.030
900	.077		1180	.106		1385	.138					1287	41160	.121	.040
1150	.105		1460	.148	.049	1535	.162	.053				1450	46400	.145	.048
1380	.134											1515	48480	.172	.057
1420	.150														
1500	.165														
1550	.180														
1490	.195														
1550	.207	.068													

TABLE A-53

Radiation-Cryotemperature Test Data: Paraplex P-43 **Material** J

Pull-Rod Speed (Avg) .046 **in./min**
Ultimate Tensile Strength (Avg) 46000 **psi**
% Total Elongation
Pull-Rod (5.25-in. Gage) 2.7 **%**
Extensometer (2-in. Gage) 2.3 **%**

Matl Type Structural Laminate
Test Temp Liquid Nitrogen
Exposure
Gamma 1.3×10^{10} **ergs/gm(C)**
Neutron 1.6×10^{15} **n/cm^2**

Specimen No. 1 Load (lb)	No. 1 Defl. (Rod) (in.)	No. 1 Defl. (Exts.) (in.)	No. 2 Load (lb)	No. 2 Defl. (Rod) (in.)	No. 2 Defl. (Exts.) (in.)	No. 3 Load (lb)	No. 3 Defl. (Rod) (in.)	No. 3 Defl. (Exts.) (in.)	No. 4 Load (lb)	No. 4 Defl. (Rod) (in.)	No. 4 Defl. (Exts.) (in.)	Average Load for Given Deflection: Load (lb)	Load lb/in^2	Defl. (Rod) (in.)	Defl. (Exts.) (in.)
0	0		0	0		0	0		0	0		0	0	0	0
260	.012		160	.010		85	.005		300	.020		449	1437	.030	.010
700	.047		340	.025		400	.028		520	.039		765	24480	.061	.020
1150	.095		560	.043		920	.070		750	.062		1085	34720	.091	.030
1490	.138	.046	810	.064		1400	.120		1000	.086		1270	40600	.112	.037
			1060	.089		1700	.157		1220	.114	.038	1436	46000	.142	.047
			1260	.111	.037	1775	.206	.068							

TABLE A-54

Radiation-Cryotemperature Test Data: Paraplex P-43 **Material** J

Pull-Rod Speed (Avg) .096 **in./min**
Ultimate Tensile Strength (Avg) 53650 **psi**
% Total Elongation
Pull-Rod (5.25-in. Gage) 2.9 **%**
Extensometer (2-in. Gage) 2.5 **%**

Matl Type Structural Laminate
Test Temp Liquid Nitrogen
Exposure
Gamma 5.0×10^{10} **ergs/gm(C)**
Neutron 4.8×10^{16} **n/cm^2**

Specimen												Average Load for Given Deflection			
No. 1			No. 2			No. 3			No. 4						
Load (lb)	Defl. (Rod) (in.)	Defl. (Exts.) (in.)	Load (lb)	Defl. (Rod) (in.)	Defl. (Exts.) (in.)	Load (lb)	Defl. (Rod) (in.)	Defl. (Exts.) (in.)	Load (lb)	Defl. (Rod) (in.)	Defl. (Exts.) (in.)	Load (lb)	Load lb/in^2	Defl. (Rod) (in.)	Defl. (Exts.) (in.)
0	0		0	0		0	0		0	0		0	0	0	0
910	.029		1100	.023		1170	.031		550	.011		1010	32300	.030	.010
1440	.072		1440	.070		1470	.081		910	.045		1283	41060	.061	.020
1900	.121		1670	.156	.052	1530	.170	.056	1150	.075		1468	46950	.091	.030
2145	.184	.061							1370	.105	.035	1540	49270	.106	.035
												1679	53650	.154	.051

TABLE A-55

Radiation-Cryotemperature Test Data: Paraplex P-43 **Material** J

Pull-Rod Speed (Avg) .057 **in./min**
Ultimate Tensile Strength (Avg) 40760 **psi**
% Total Elongation
Pull-Rod (5.25-in. Gage) 2.6 **%**
Extensometer (2-in. Gage) 2.2 **%**

Matl Type Structural Laminate
Test Temp Liquid Hydrogen
Exposure
Gamma Unirradiated **ergs/gm(C)**
Neutron " **n/cm²**
(Control)

Specimen												Average Load for Given Deflection			
No. 1			No. 2			No. 3			No. 4						
Load (lb)	Defl. (Rod) (in.)	Defl. (Exts.) (in.)	Load (lb)	Defl. (Rod) (in.)	Defl. (Exts.) (in.)	Load (lb)	Defl. (Rod) (in.)	Defl. (Exts.) (in.)	Load (lb)	Defl. (Rod) (in.)	Defl. (Exts.) (in.)	Load (lb)	Load lb/in²	Defl. (Rod) (in.)	Defl. (Exts.) (in.)
0	0		0	0		0	0					0	0	0	0
220	.036		130	.026		200	.030					192	6146	.030	.010
810	.085		430	.054		470	.050					538	17200	.061	.020
1290	.142	.047	620	.069		780	.075					883	28240	.091	.030
			920	.100		1060	.106					1200	38400	.121	.040
			1210	.129	.043	1320	.133	.044				1273	40760	.135	.045

TABLE A-56

Radiation-Cryotemperature Test Data: Paraplex P-43

Material J

Pull-Rod Speed (Avg) .042 **in./min**
Ultimate Tensile Strength (Avg) 42540 **psi**
% Total Elongation
Pull-Rod (5.25-in. Gage) 2.5 **%**
Extensometer (2-in. Gage) 2.2 **%**

Matl Type Structural Laminate
Test Temp Liquid Hydrogen
Exposure
Gamma 1.3×10^{10} **ergs/gm(C)**
Neutron 1.4×10^{15} **n/cm^2**

Specimen No. 1 Load (lb)	No. 1 Defl. (Rod) (in.)	No. 1 Defl. (Exts.) (in.)	No. 2 Load (lb)	No. 2 Defl. (Rod) (in.)	No. 2 Defl. (Exts.) (in.)	No. 3 Load (lb)	No. 3 Defl. (Rod) (in.)	No. 3 Defl. (Exts.) (in.)	No. 4 Load (lb)	No. 4 Defl. (Rod) (in.)	No. 4 Defl. (Exts.) (in.)	Average Load for Given Deflection: Load (lb)	Load lb/in^2	Defl. (Rod) (in.)	Defl. (Exts.) (in.)
0	0		0	0		0	0		0	0		0	0	0	0
410	.023		800	.036		600	.050		50	.015		453	14500	.030	.010
660	.051		1280	.077		850	.070		300	.042		818	26180	.061	.020
900	.075		1600	.108		1000	.087		600	.066		1115	35650	.091	.030
1080	.096	.032	1700	.122		1150	.105	.035	800	.086		1333	42540	.133	.044
			1750	.151					950	.103					
			1850	.168					1100	.120					
			1900	.181					1150	.129	.043				
			1950	.203	.067										

TABLE A-57

Radiation-Cryotemperature Test Data: Material K

Skyspar A423-SA9185

α/ϵ Measurements (Raw Data) Material Type Thermal Control Coating

Specimen No.	Irradiation Temp. (°F)	Average Radiation Exposure: Gamma [ergs/gm (C)]	Neutrons/cm²: E > 2.9 Mev	Neutrons/cm²: E < 0.048 ev	Solar Absorptance α	100°K ϵ	100°K α/ϵ	300°K ϵ	300°K α/ϵ	500°K ϵ	500°K α/ϵ
Average*		0	0	0	.288	.826	.349	.882	.327	.883	.326
EW 14	125	4.92(9)**	1.3(15)	9.6(13)	.374	.830	.451	.890	.420	.888	.421
EW 26					.374	.830	.451	.890	.420	.888	.421
EW 37					.374	.830	.451	.890	.420	.888	.421
EW 16		1.05(10)	2.5(15)	3.7(14)	.351	.835	.420	.890	.394	.903	.389
EW 17					.351	.835	.420	.888	.395	.895	.392
EW 22					.351	.835	.420	.890	.394	.903	.389
EW 21	-320	2.0(10)	4.0(14)	4.2(13)	.324	.835	.388	.895	.362	.898	.361
EW 25					.324	.835	.388	.895	.362	.895	.362
EW 29					.324	.835	.388	.895	.362	.895	.362
EW 7		3.0(10)	4.0(15)	4.2(14)	.325	.838	.388	.890	.365	.891	.365
EW 8					.325	.840	.387	.894	.364	.890	.365
EW 9					.334	.838	.399	.889	.376	.882	.379
EW 40	-423	5.0(9)	8.5(14)	2.1(15)	.405	.828	.489	.891	.455	.901	.450
EW 41					.405	.828	.489	.890	.455	.889	.456
EW 42					.405	.828	.489	.891	.455	.895	.453
EW 10		1.0(10)	3.0(15)	7.0(15)	.422	.837	.504	.892	.473	.903	.467
EW 11					.422	.837	.504	.892	.473	.903	.467
EW 12					.412	.837	.492	.892	.462	.903	.456

*Average - refers to an average value for all unirradiated specimens.

**4.92(9) read as 4.92×10^9

TABLE A-58

Radiation-Cryotemperature Test Data: Material K

Skyspar A423-SA9185

α/ϵ Measurements (Avg.)

Material Type Thermal Control Coating

Irradiation Temp. (°F)	Average Radiation Exposure			Average α/ϵ Measurements		
	Gamma [ergs/gm (C)]	Neutrons/cm²		Specimen Temperature		
		E > 2.9 Mev	E < 0.048 ev	100°K	300°K	500°K
125	0	0	0	0.349	0.327	0.326
	4.92(9)*	1.3(15)	9.6(13)	0.541	0.420	0.421
	1.05(10)	2.5(15)	3.7(14)	0.420	0.394	0.390
-320	0	0	0	--	--	--
	2.0(10)	4.0(14)	4.2(13)	0.388	0.362	0.362
	3.0(10)	4.0(15)	4.2(14)	0.391	0.368	0.370
-423	0	0	0	--	--	--
	5.6(9)	8.5(14)	2.1(15)	0.489	0.455	0.453
	2.0(10)	3.0(15)	7.0(15)	0.500	0.470	0.463

*Read 4.92(9) as 4.92×10^9

TABLE A-59

Radiation-Cryotemperature Test Data: Material L

W-49-BC-12

α/ϵ Measurements (Raw Data) Material Type Thermal Control Coating

Specimen No.	Irradiation Temp. (°F)	Average Radiation Exposure: Gamma [ergs/gm (C)]	Neutrons/cm²: E > 2.9 Mev	Neutrons/cm²: E < 0.048 ev	Solar Absorptance α	Calculated Total Normal Emittance, Specimen Measurement Temperatures: 100°K ϵ	100°K α/ϵ	300°K ϵ	300°K α/ϵ	500°K ϵ	500°K α/ϵ
Average*		0	0	0	.947	.849	1.12	.901	1.05	.925	1.02
AC 30					.948	.840	1.13	.893	1.06	.923	1.03
AC 31	125	4.75(9)**	1.3(15)	1.0(14)	.948	.840	1.13	.893	1.06	.923	1.03
AC 33					.948	.840	1.13	.893	1.06	.923	1.03
AC 7					.951	.856	1.11	.895	1.06	.925	1.03
AC 8		8.0(9)	2.2(15)	3.2(14)	.951	.856	1.11	.895	1.06	.925	1.03
AC 32					.951	.856	1.11	.895	1.06	.925	1.03
AC 16					.945	.857	1.10	.890	1.06	.910	1.04
AC 17		2.0(10)	4.0(14)	1.0(13)	.945	.857	1.10	.890	1.06	.910	1.04
AC 38	-320				.945	.856	1.10	.890	1.06	.910	1.04
AC 21					.945	.856	1.10	.882	1.07	.907	1.04
AC 36		3.0(10)	4.0(15)	2.0(14)	.945	.857	1.10	.882	1.07	.907	1.04
AC 42					.945	.857	1.10	.890	1.06	.910	1.04
AC 23					.948	.836	1.13	.889	1.07	.918	1.03
AC 24		5.0(9)	8.5(14)	3.0(15)	.948	.836	1.13	.889	1.07	.918	1.03
AC 25	-423				.948	.836	1.13	.889	1.07	.918	1.03
AC 13					.948	.847	1.12	.883	1.07	.912	1.04
AC 14		1.0(10)	3.0(15)	7.0(15)	.948	.847	1.12	.883	1.07	.912	1.04
AC 15					.948	.847	1.12	.883	1.07	.912	1.04

*Average - refers to an average value for all unirradiated specimens.

**Read 4.75(9) as 4.75×10^9

TABLE A-60

Radiation-Cryotemperature Test Data: Material L

W-49-BC-12

α/ϵ Measurements (Avg.) Material Type Thermal Control Coating

Irradiation Temp. (°F)	Average Radiation Exposure			Average α/ϵ Measurements		
	Gamma [ergs/gm (C)]	Neutrons/cm²		Specimen Temperature		
		E > 2.9 Mev	E < 0.048 ev	100°K	300°K	500°K
125	0	0	0	1.12	1.05	1.02
	4.75(9)*	1.3(15)	1.0(14)	1.13	1.06	1.03
	8.0(9)	2.2(15)	3.2(14)	1.11	1.06	1.03
-320	0	0	0	--	--	--
	2.0(10)	4.0(14)	1.0(13)	1.10	1.06	1.04
	3.0(10)	4.0(15)	2.0(14)	1.10	1.07	1.04
-423	0	0	0	--	--	--
	5.6(9)	8.5(14)	3.0(15)	1.13	1.07	1.03
	2.0(10)	3.0(15)	7.0(15)	1.12	1.07	1.04

*Read 4.75(9) as 4.75×10^9

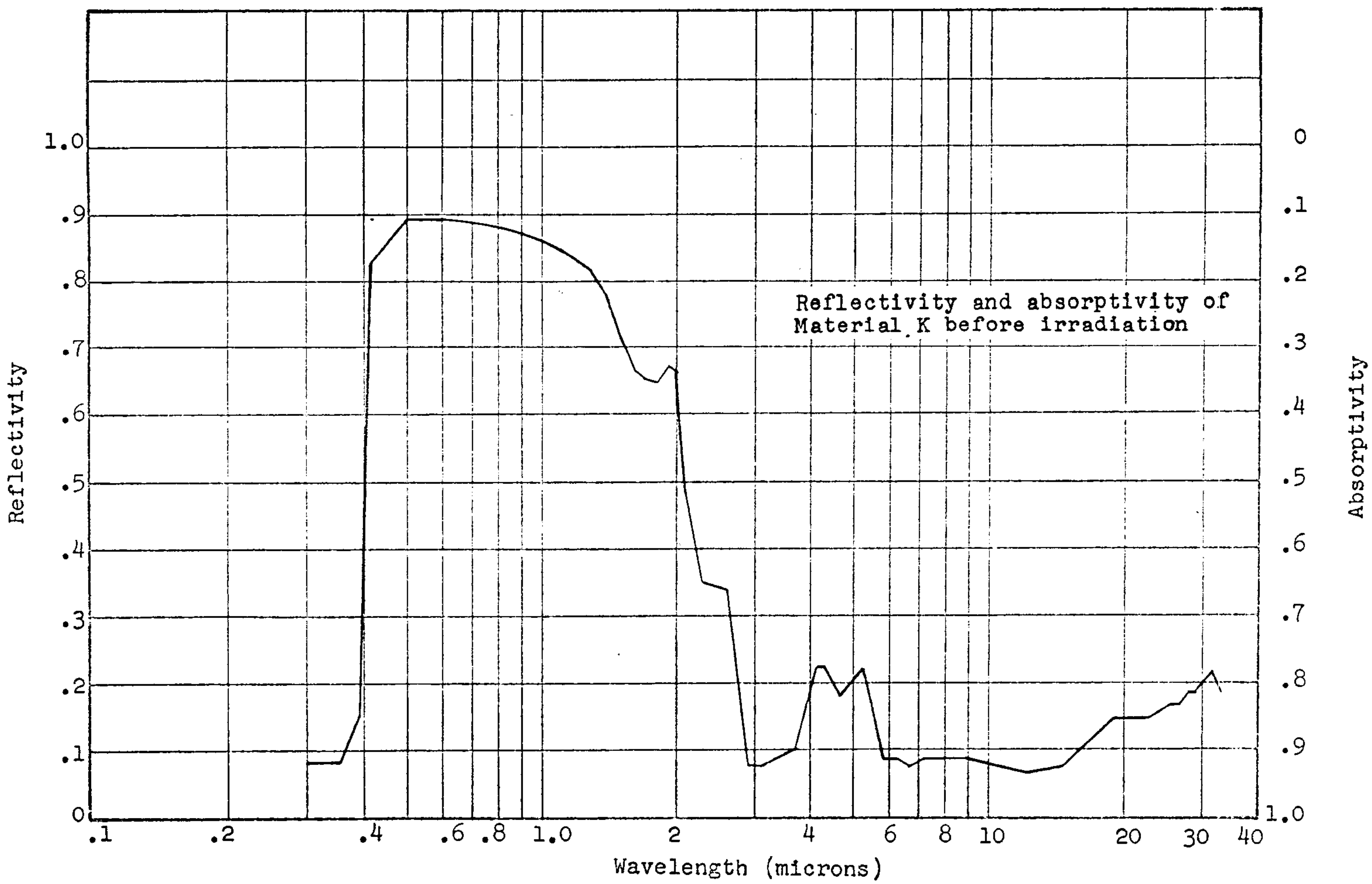

Figure A-1 Monochromatic Reflectivity and Absorptivity: Material K (Skyspar A423-SA9184); Unirradiated; Ambient Temperature

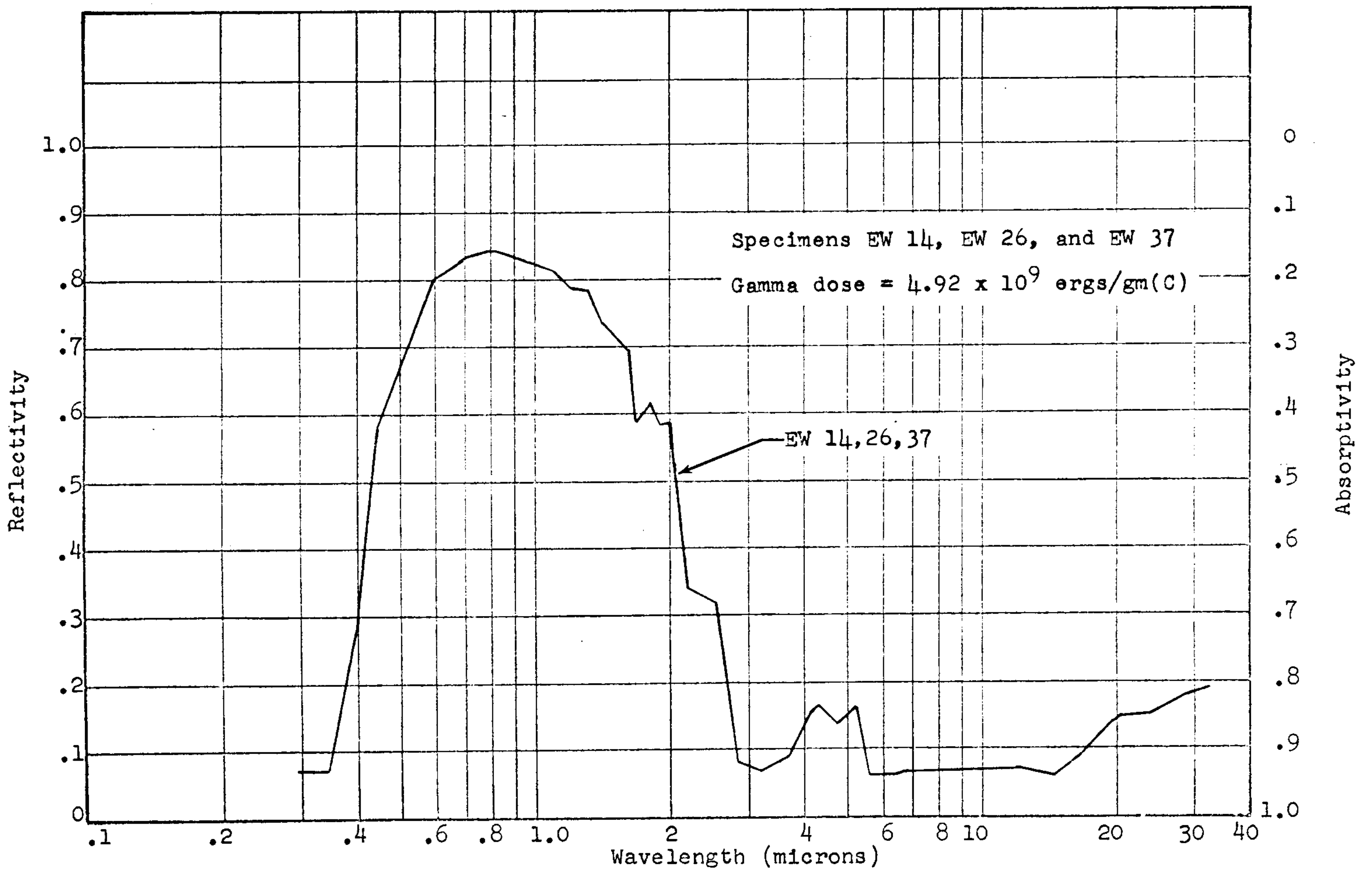

Figure A-2 Monochromatic Reflectivity and Absorptivity: Material K (Skyspar A423-SA9184); Low Dose; Ambient Temperature

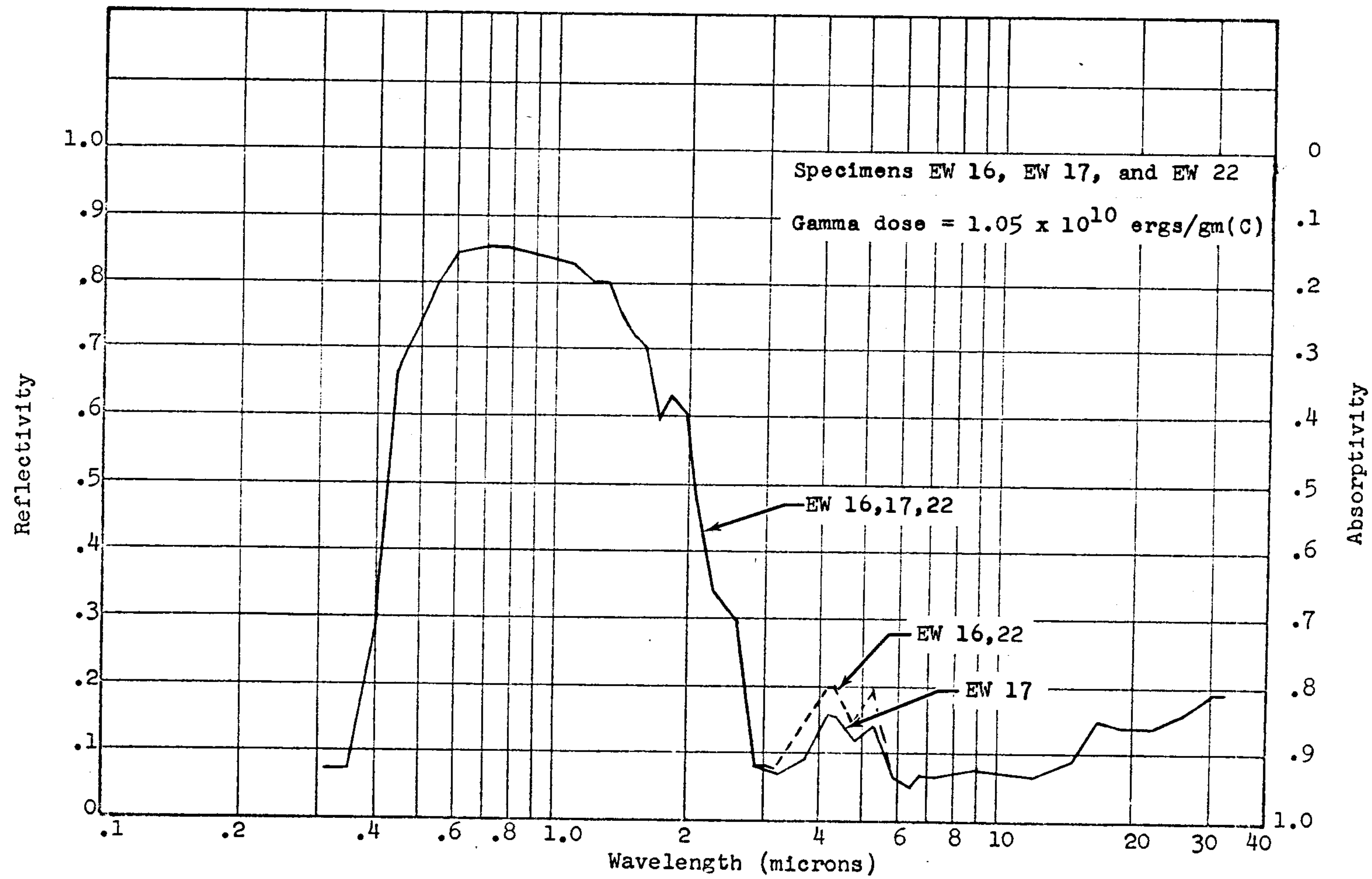

Figure A-3 Monochromatic Reflectivity and Absorptivity: Material K (Skyspar A423-SA9184); High Dose; Ambient Temperature

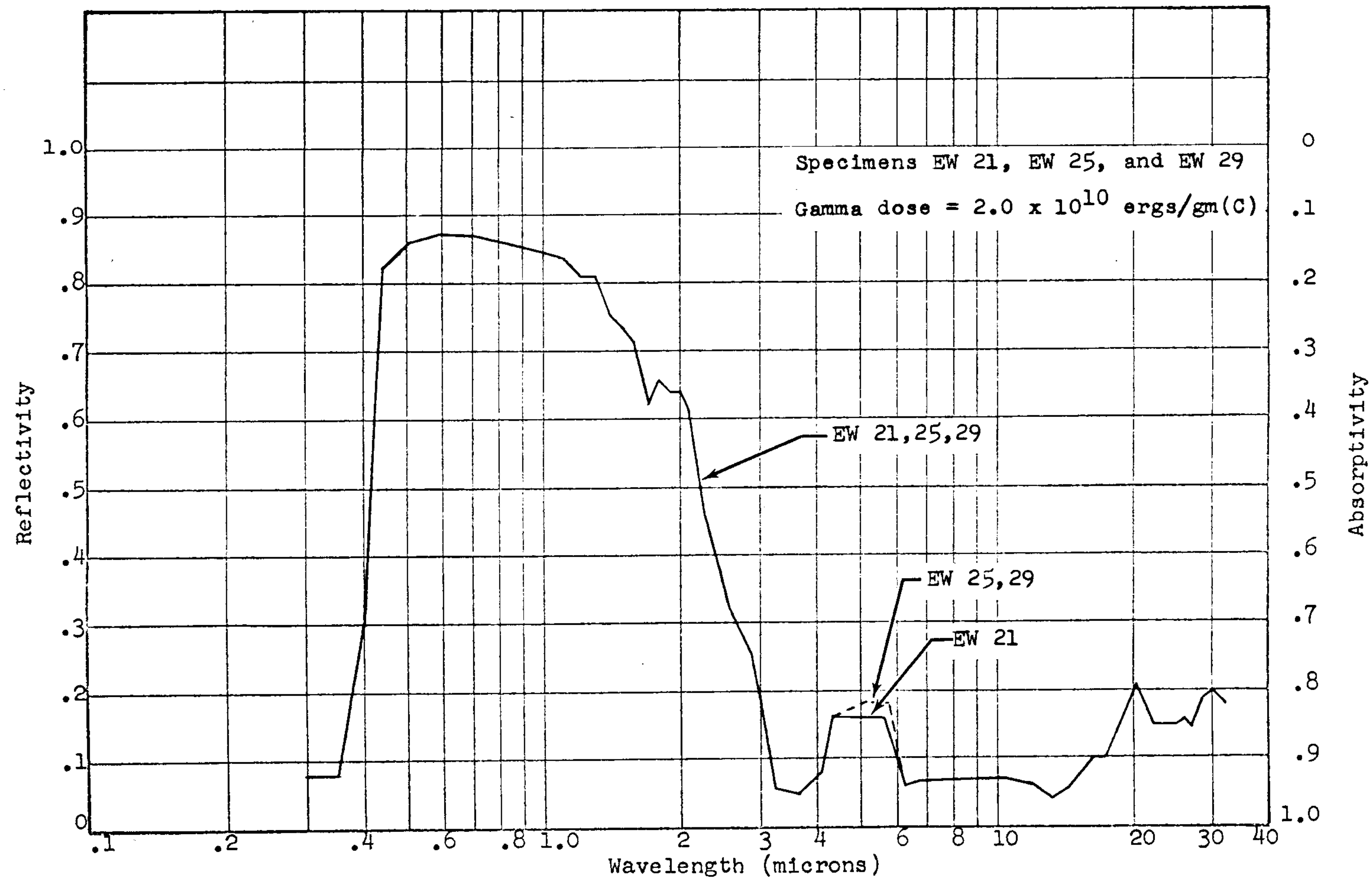

Figure A-4 Monochromatic Reflectivity and Absorptivity: Material K (Skyspar A423-SA9184); Low Dose; LN_2 Temperature

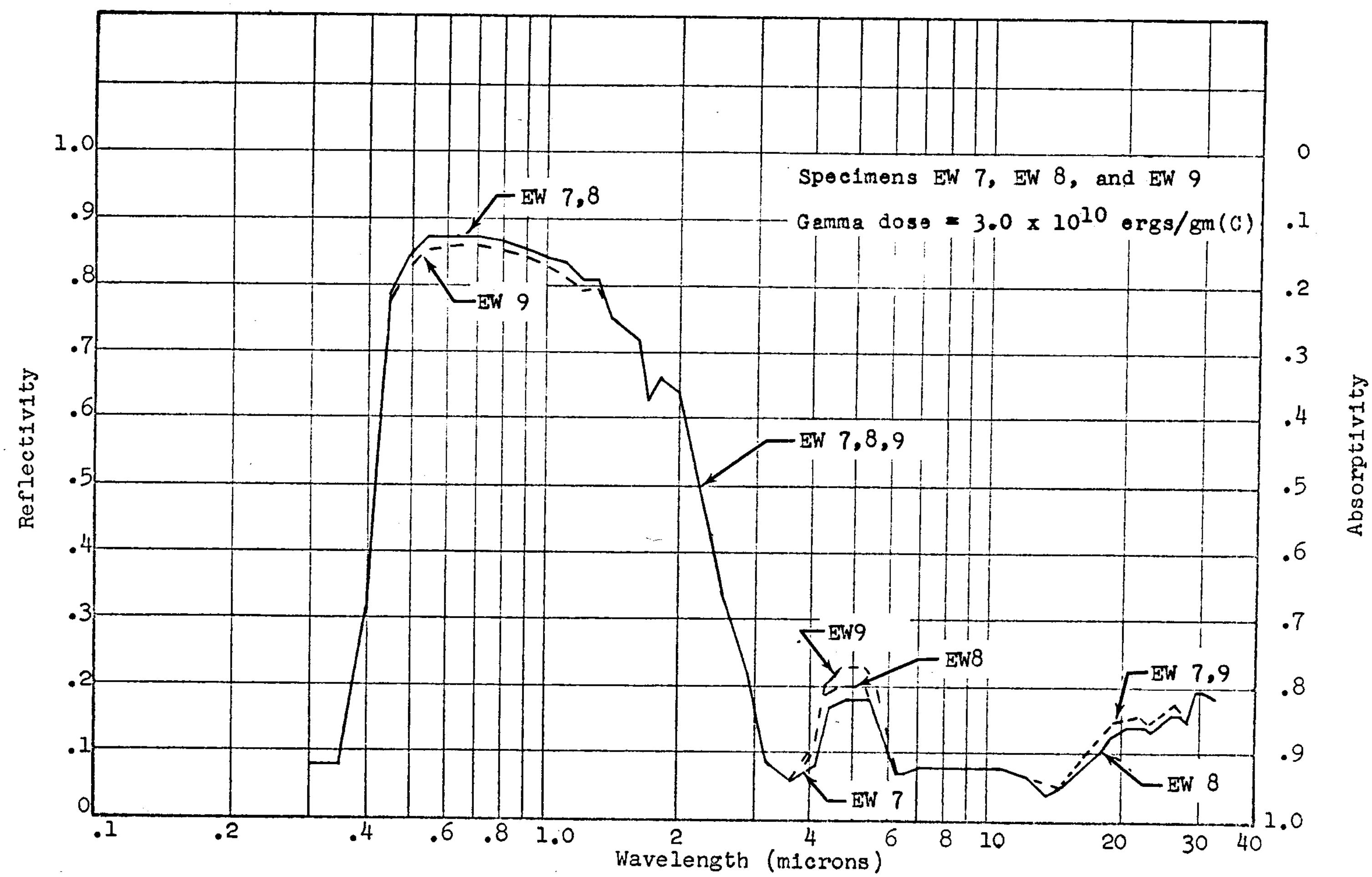

Figure A-5 Monochromatic Reflectivity and Absorptivity: Material K (Skyspar A423-SA9184); High Dose; LN_2 Temperature

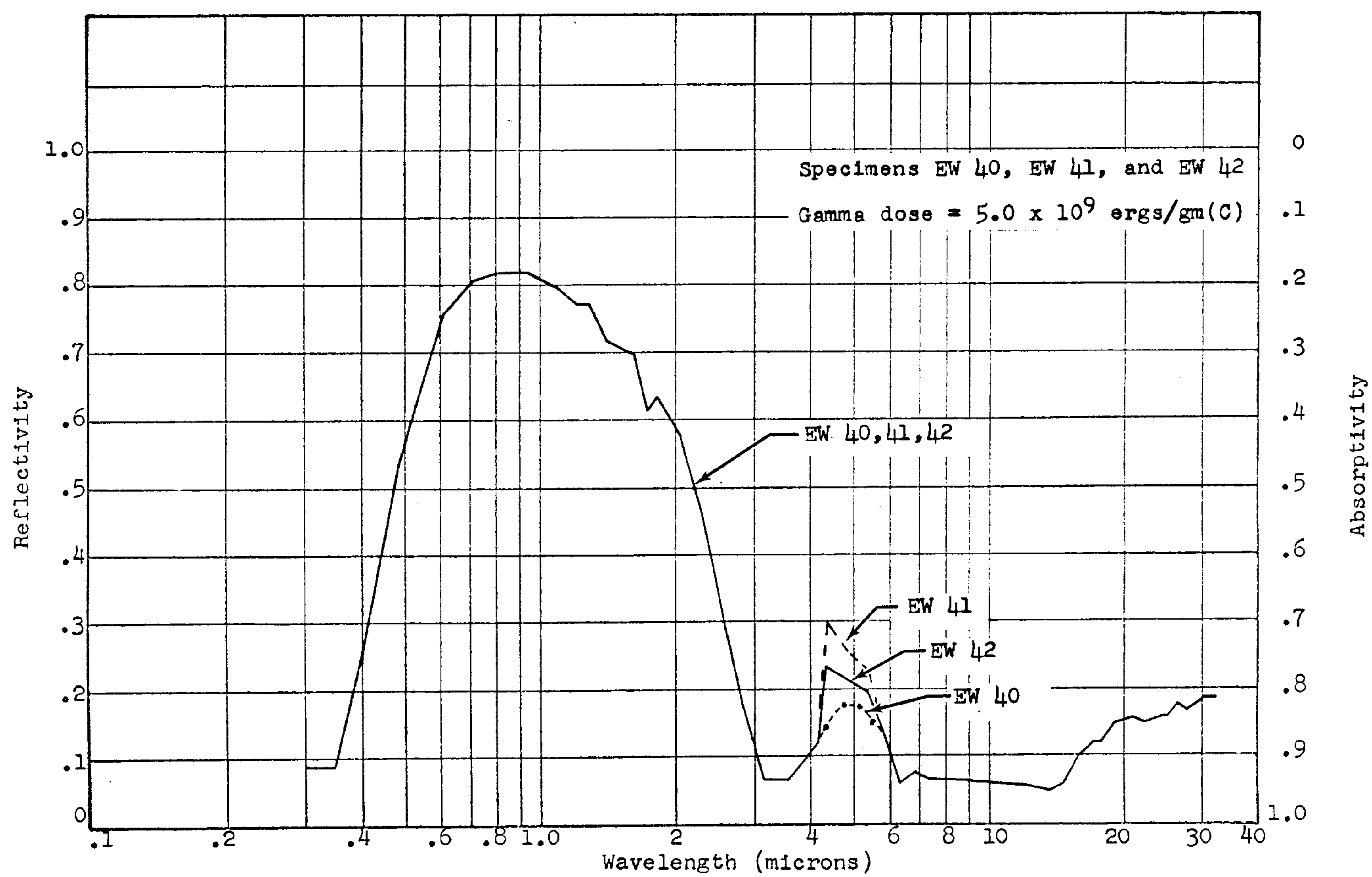

Figure A-6 Monochromatic Reflectivity and Absorptivity: Material K (Skyspar A423-SA9184); Low Dose; LH_2 Temperature

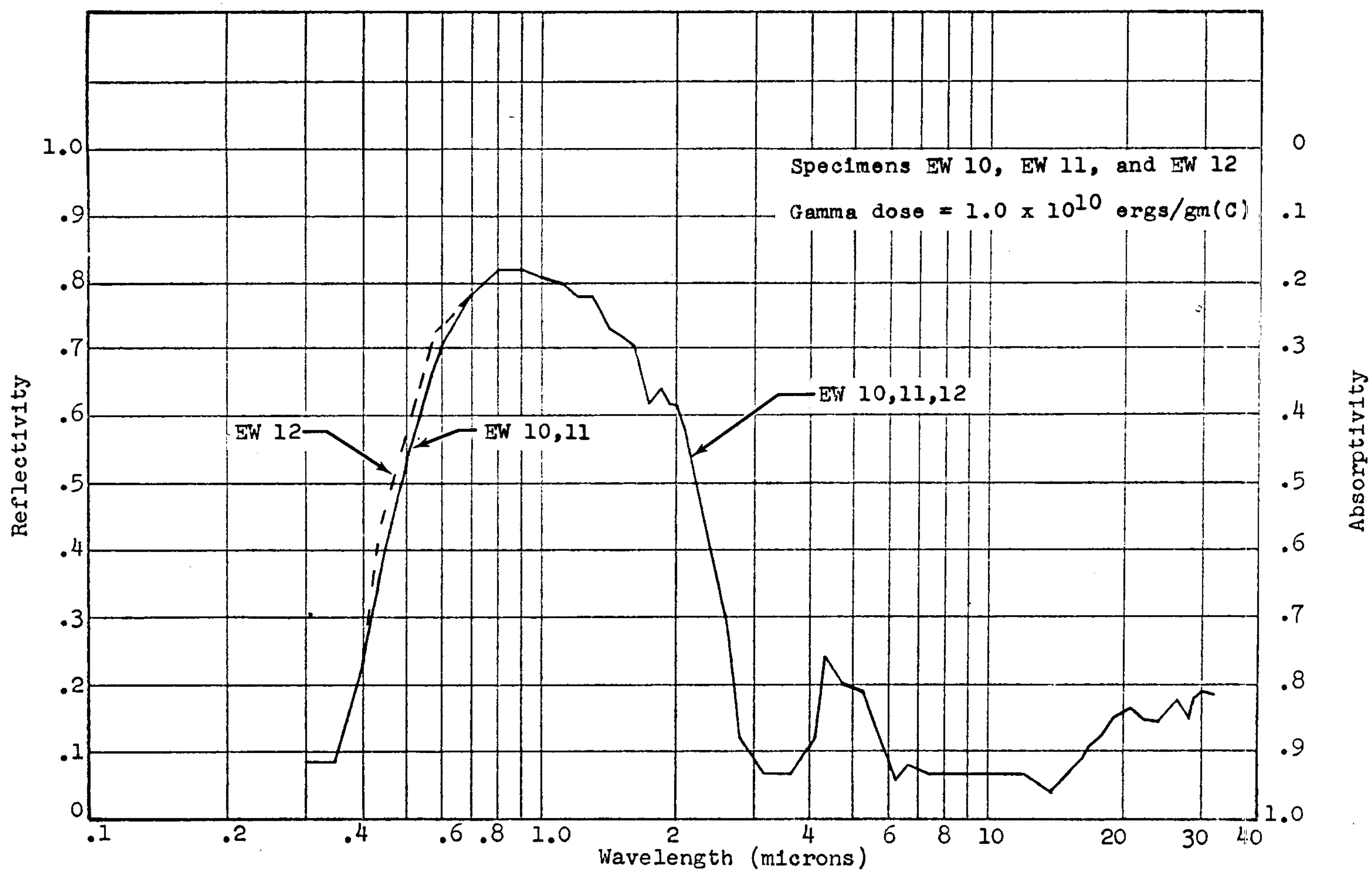

Figure A-7 Monochromatic Reflectivity and Absorptivity: Material K (Skyspar A423-SA9184); High Dose; LH_2 Temperature

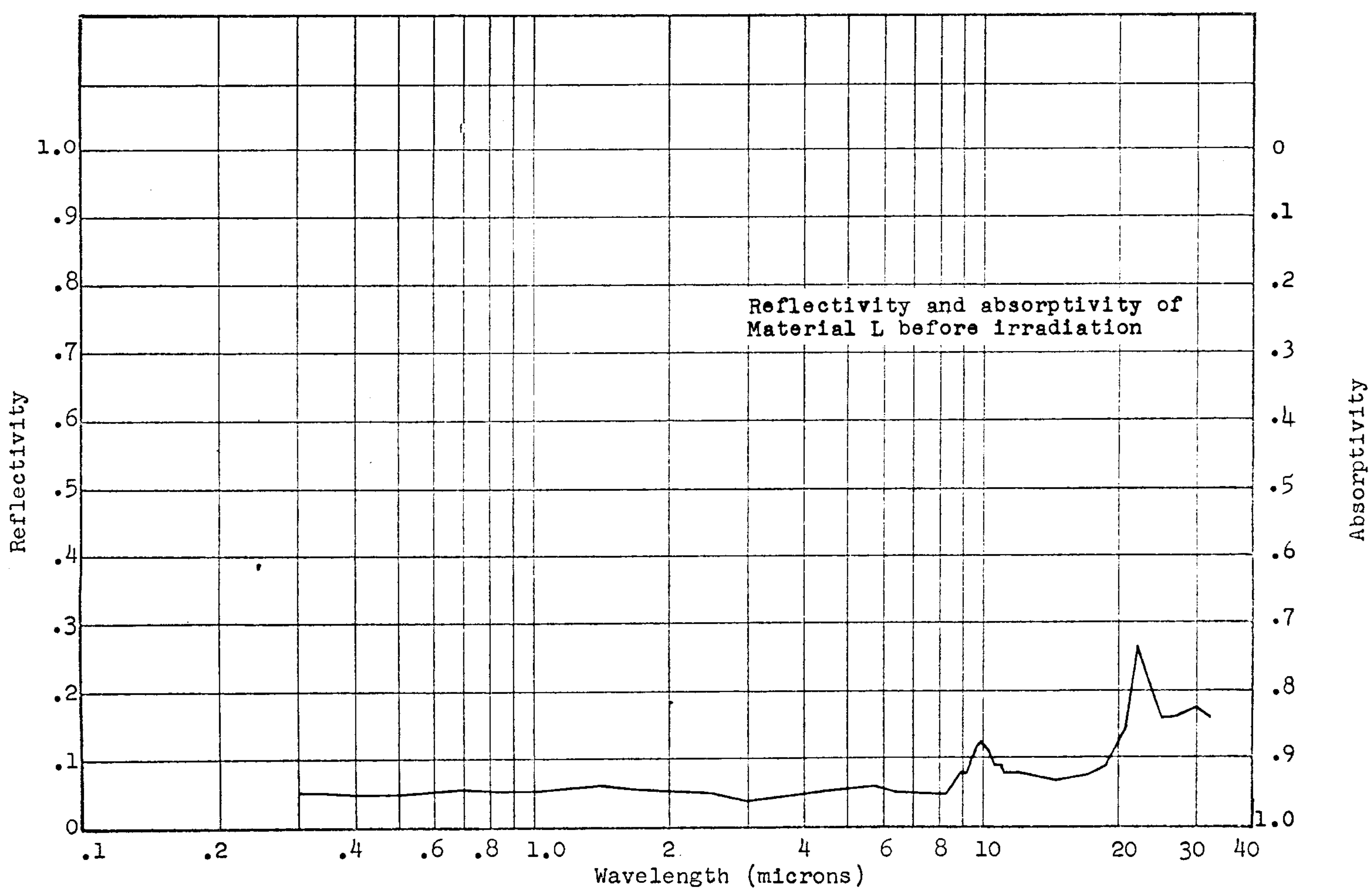

Figure A-8 Monochromatic Reflectivity and Absorptivity: Material L (W49-BC-12); Unirradiated; Ambient Temperature

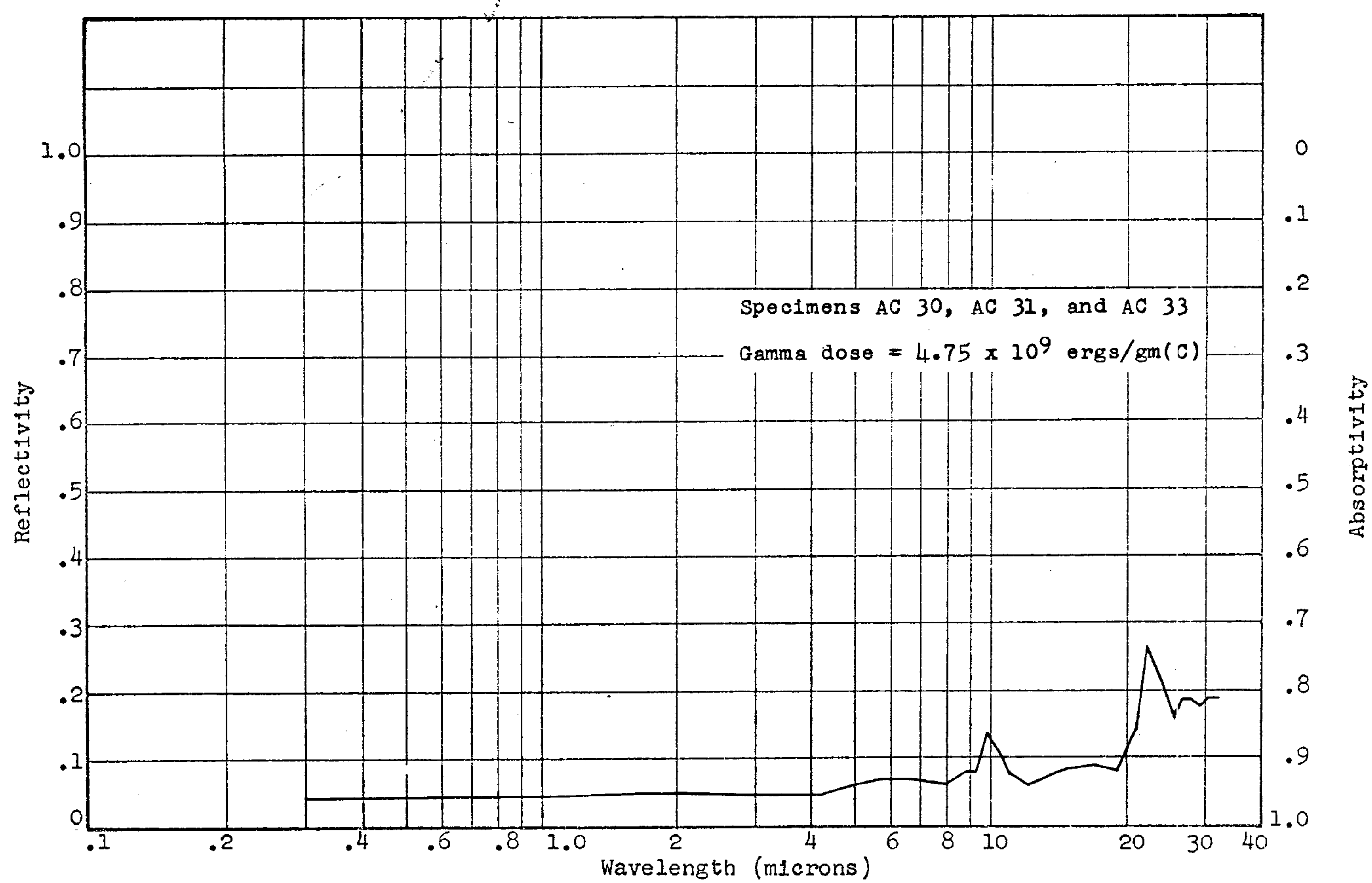

Figure A-9 Monochromatic Reflectivity and Absorptivity: Material L (W49-BC-12); Low Dose; Ambient Temperature

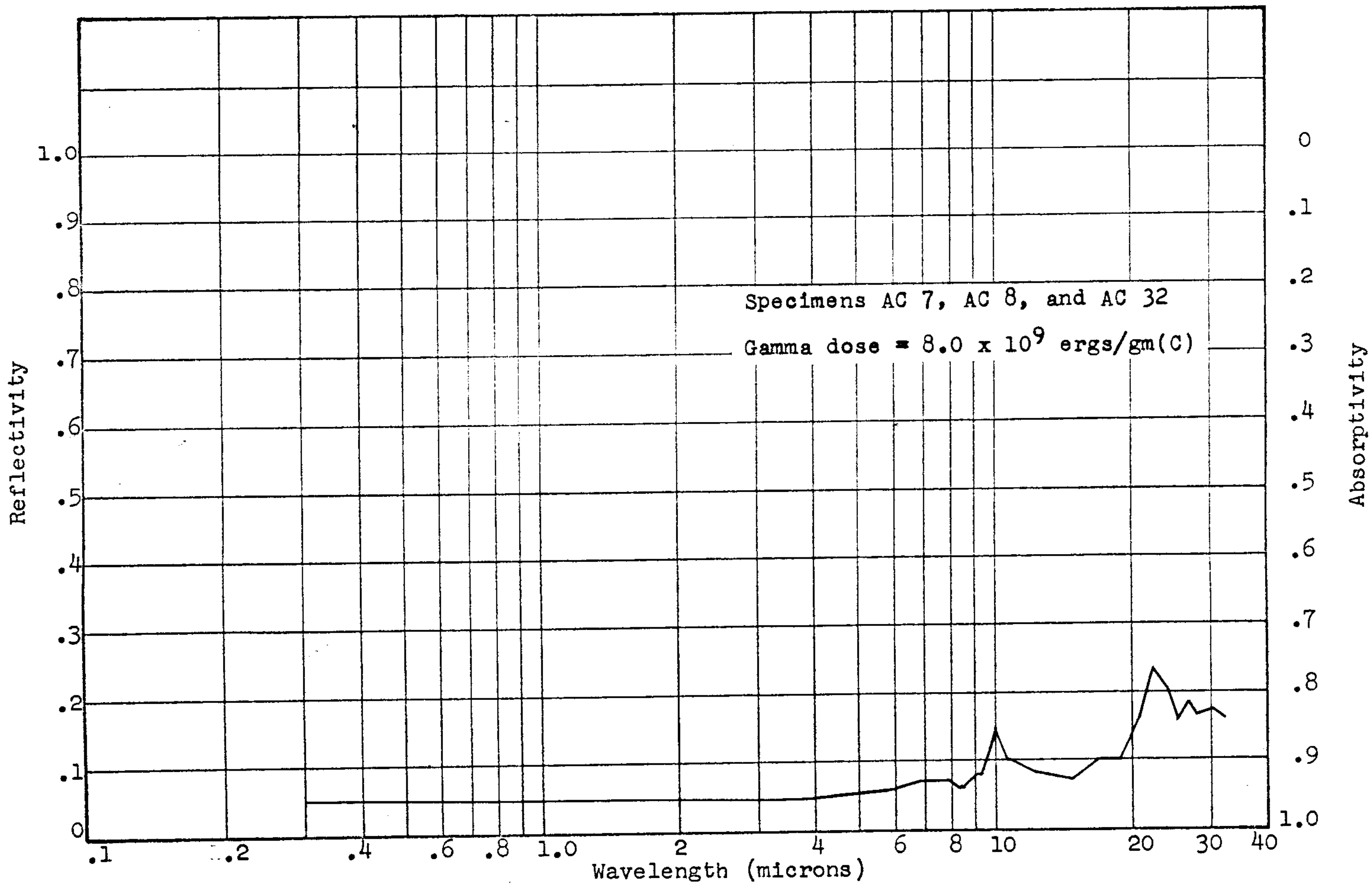

Figure A-10 Monochromatic Reflectivity and Absorptivity: Material L (W49-BC-12); High Dose; Ambient Temperature

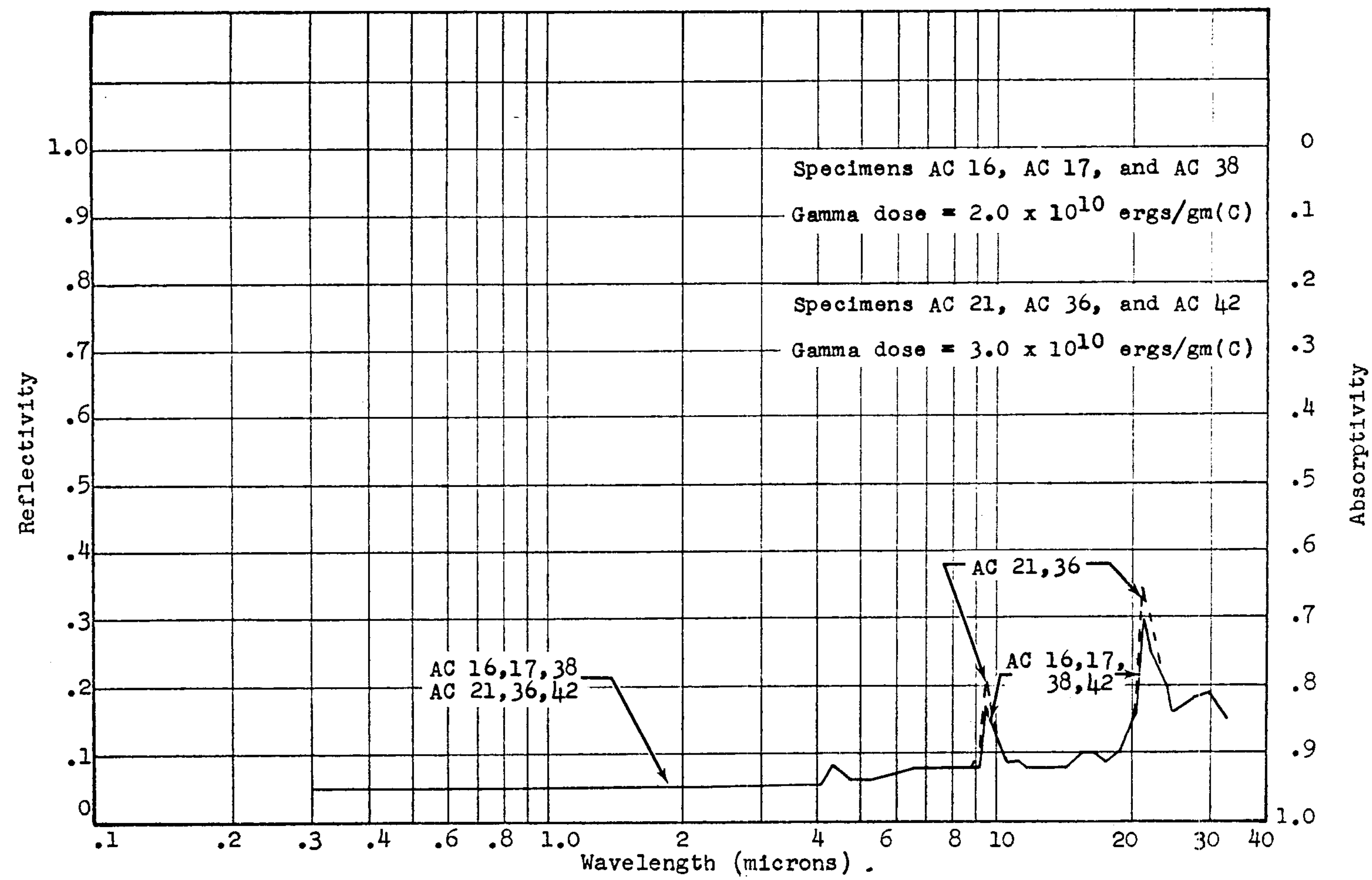

Figure A-11 Monochromatic Reflectivity and Absorptivity: Material L (W49-BC-12); Low and High Doses; LN_2 Temperature

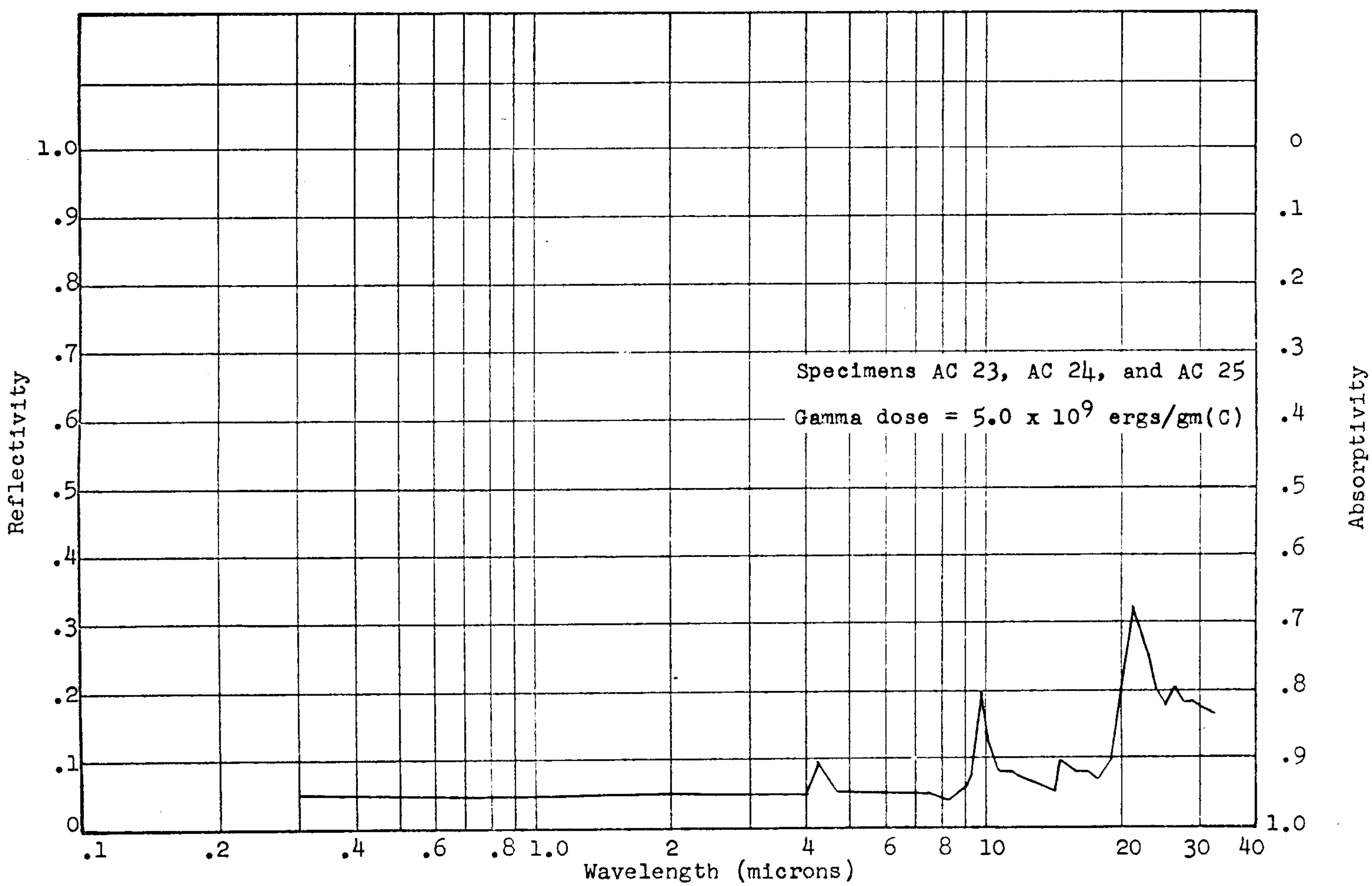

Figure A-12 **Monochromatic Reflectivity and Absorptivity: Material L (W49-BC-12); Low Dose; LH_2 Temperature**

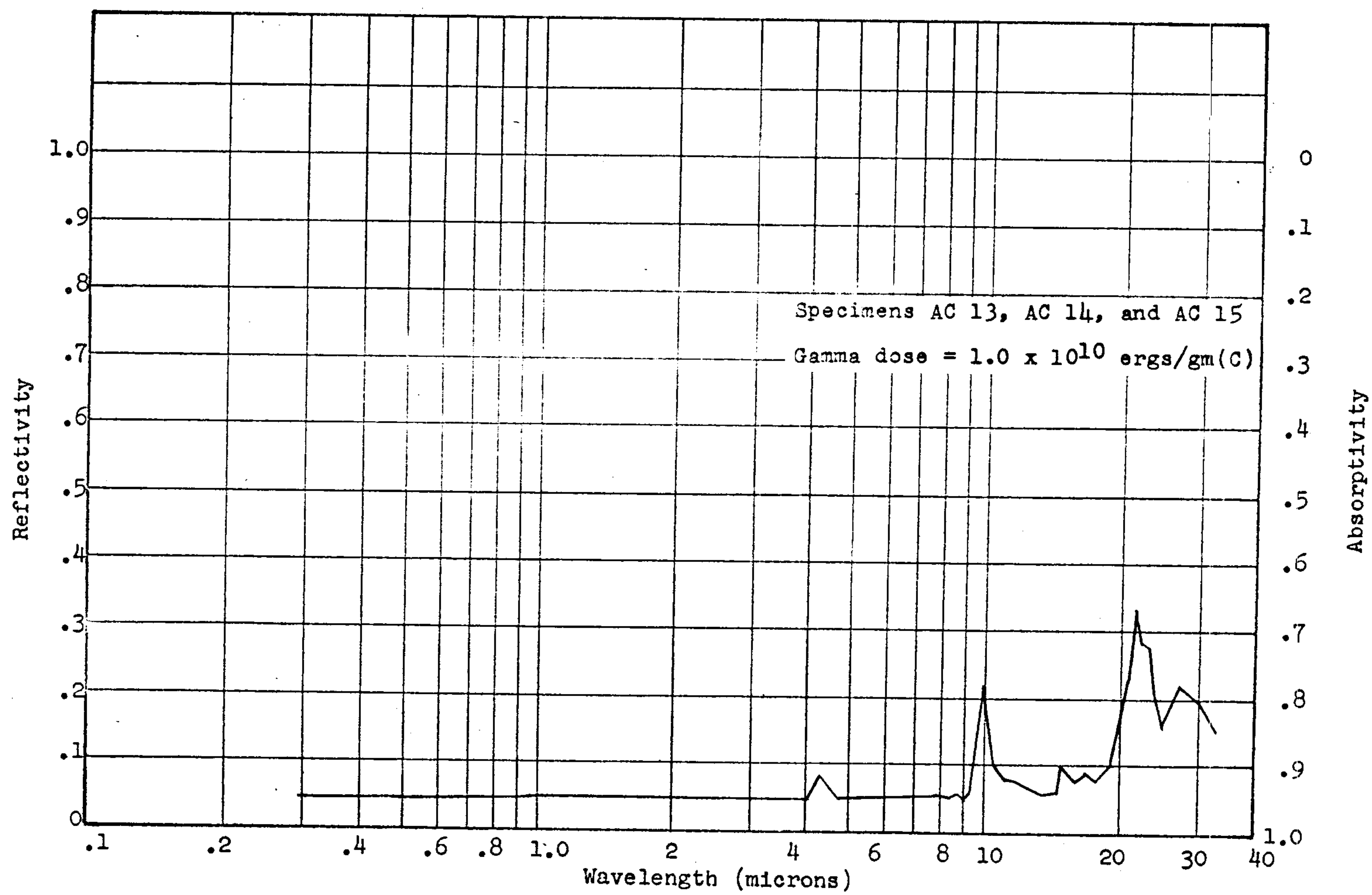

Figure A-13 Monochromatic Reflectivity and Absorptivity: Material L (W49-BC-12); High Dose; LH_2 Temperature

REFERENCES

1. Park, W., Test Analysis of the 3-Mw Ground Test Reactor. Convair-Fort Worth Report MR-N-254 (NARF-61-15T, 31 May 1961). U

2. Romanko, J., and Dungan, W. E., The Neutron Flux Spectrum of the Ground Test Reactor. Convair-Fort Worth Report FZM-929 (June 1957). U

3. Sandia-Convair Irradiation Test No. 1, Addendum 1. Convair-Fort Worth Report MR-N-243-1 (NARF-59-22R, 15 September 1959). SRD

4. Bell, J. R., and Miles, J. K., Calibration of Foils for Neutron Flux Measurements. GD/FW Report No. MR-N-279 (NARF-61-18T, 6 June 1961). U

5. Radiation Effects Facility Capabilities. General Dynamics/ Fort Worth Report FZK-9-163A (NARF-61-7T, 1 June 1962). U

6. Brandenberg, W. M., Optical Properties of Thermal-Control Coatings Irradiated with Gamma Rays and Neutrons. GD/Astronautics Report ERR-AN-237 (December 1962). U

7. Kerlin, E. E., and Smith, E. T., Investigation of Combined Effects of Radiation and Vacuum of Engineering Materials. First Quarterly Progress Report, 9 November 1961 through 8 February 1962. GD/FW Report FZK-142 (20 March 1962). U

8. Kerlin, E. E., and Smith, E. T., Investigation of Combined Effects of Radiation and Vacuum on Engineering Materials. Second Quarterly Progress Report, 9 February 1962 through 8 May 1962. GD/FW Report FZK-147 (4 June 1962). U

9. Kerlin, E. E., and Smith, E. T., Investigation of Combined Effects of Radiation and Vacuum and of Radiation and Cryogenic Temperatures on Engineering Materials. Third Quarterly Progress Report, 9 May 1962 through 31 July 1962. GD/FW Report FZK-152 (15 August 1962). U

Preceding page blank